Impact of Thermally Activated Building Systems (TABS) in Office Buildings

by

Lebogang Kagiso Kgaladi (KGLLEB002)

A dissertation submitted to the Faculty of Engineering and Built Environment

in fulfilment of the requirements for the degree of Master of Science in Engineering in Sustainable Energy Engineering

at the University of Cape Town

Supervised by:

Andrew Hibberd and Mascha Moorlach

October 2022

Declaration

I know the meaning of plagiarism and declare that all the work in this document, save for that which is properly acknowledged, is my own. This dissertation has been submitted to the Turnitin module and I confirm that my supervisor has seen my report and that any concerns revealed by such have been resolved with the supervisor.

Document word count: 40 927

Signed by candidate

_____

Lebogang Kgaladi

Abstract

Thermal comfort can be described as the degree to which a person is satisfied with their thermal environment (Yau & Chew, 2014). It is a person's perception of whether they feel warm or cool within their surroundings. The Danish professor, Povl Ole Fanger, developed the Predictive Mean Vote (PMV), a model consisting of physical and personal variables to quantify a person's thermal comfort within a building. The physical variables include air temperature, relative humidity, mean radiant temperature, and air velocity, and the personal variables include activity level and clothing insulation (Yau & Chew, 2014). People control the physical variables using systems that provide heating and cooling to an environment, the earliest of which were found in 9 000-year-old remains from Eastern Turkey (Ma, Wang, & Guo, 2015). The remains consisted of an intermediate space beneath the floor that would have been filled with cold water from Kantara Creek to cool the interior during warm seasons. Personal variables are controlled by changing the individual's activities and clothes.

Today there are various space heating and cooling systems implemented in buildings. This research describes Thermally Activated Building Systems (TABS) and conventional Heating, Ventilation and Air-conditioning (HVAC) systems. Both systems consist of components such as the boiler, chiller and heat pump to condition the fluid used to deliver the heating and cooling. The systems differ and are classified by their heating and cooling transfer processes within the building's interior. HVAC systems use the air to transfer heat by convection, and TABS use the buildings' internal surfaces to transfer heat by radiation (Rhee, Olesen, & Kim, 2012). HVAC systems include Air Handling Units (AHUs) to deliver the conditioned air and provide dehumidification. In contrast, TABS consists of conditioned water pumped through pipes embedded within the building's floor, walls, and ceilings to transfer heat between internal wall surfaces. The combination of water and building material has a higher thermal capacity than air, making TABS more energy-efficient at transferring heat than HVAC systems. This research presents case studies to determine the magnitude by which TABS is more energy-efficient by analysing and comparing both systems' energy consumption as they deliver thermal comfort.

The first case study consisted of an office building located in Cape Town, South Africa, with a TABS installation. The pipe layout in the building's floors was designed and optimised using LoopCAD for its construction between November 2018 and September 2020. The office building was modelled, and the heat load was simulated in EnergyPlus to determine the cooling needed to achieve thermal comfort. The cooling required was used as input into a modified TABS calculator, derived from the calculator given in ISO 11855, to predict the energy usage of the chiller. The electricity consumption determined by the TABS calculator was consistent with the actual chiller's electricity consumption. The mean difference between actual and calculated results is 2.054. It was determined that the TABS calculator results have an 80% confidence level to be within 1.17 of the actual chiller demand. A PMV calculator, rewritten from the calculator given in ISO 7730 and ASHRAE-55, was used to predict the thermal comfort of the occupants in the building. The calculator was tested, and its results were compared with the standard's. It was determined that the calculator's PMV and PPD results have an 80% confidence level to be within 0.015 and 0.5, respectively, of the ISO 7730 calculator's results. The calculator used the results from the TABS calculator to determine that the occupants were likely satisfied with their thermal environment.

The second case study consisted of an office building similar to the first case study, located in Cape Town, South Africa, except with a conventional HVAC installation. Its HVAC system was optimised by installing Variable Speed Drives (VSDs) at the pumps and fans. A simplified building model was developed in SketchUp Pro and imported into EnergyPlus to model and simulate the HVAC system. As with the first case study, the chiller's energy consumption determined by the simulation was consistent with the actual chiller energy consumption. It was determined that EnergyPlus results have an 80%

confidence level to be within 0.57 of the actual chiller demand. The simulation also determined that the occupants were likely satisfied with their thermal environment.

The case studies showed that the TABS calculator and EnergyPlus could accurately simulate the energy usage of TABS and conventional HVAC systems. The buildings in which the systems were installed had different cooling loads, occupancy levels and thermal insulation making it challenging to compare the systems. Therefore, the systems were modelled and simulated in the same building to prove the research hypothesis. The third case study, involving a simple office building, was modelled in SketchUp Pro and imported into EnergyPlus. As with the first case study, the cooling load determined from EnergyPlus simulations were used as inputs into the TABS calculator to determine the energy consumption of the chiller. A Variable Air Volume (VAV) HVAC system was modelled on the building, and the chiller energy consumption was simulated. When comparing the sensible energy consumption of both systems, the simulations show that TABS consumes 41.62% of the HVAC chiller's energy to provide the same neutral thermal experience.

TABS' reduced energy consumption presented an opportunity for a business case of installing the system into an Eskom building with an HVAC system that had reached its end of life. The installed HVAC system used in the business case consumed 8 056 961 kWh annually and, using Eskom's 2018/19 electricity tariff, cost R5 858 518 to operate. Using an annual tariff increase of 6% (the South African Reserve Bank's maximum CPI target) and Eskom's discount rate of 10.4%, the business case resulted in the following options:

1. Replace the HVAC system with an energy-efficient HVAC system would cost R20 360 000 to install, consume 4 212 129 kWh annually and cost R3 062 797 to operate in the initial year. Compared to the current HVAC installation, the proposed installation would have a simple payback period of seven years and a discounted payback of ten years.
2. Install a more expensive TABS installation at a proposed cost of R29 581 440. Although installing TABS costs more than an energy-efficient HVAC system, the TABS would consume less electricity and cost less to operate. The system was estimated to consume 2 384 908 kWh annually and cost R 1 734 156 to operate in the initial year. Similar to the HVAC option, the TABS installation would have a simple payback period of seven years and a discounted payback of ten years.

At first glance, it seems that there is no business case to opt for the TABS instead of the HVAC installation. However, the average increase in the electricity tariff has been 12.17% annually for Eskom's 2019/20 and 2020/21 financial years. The average tariff increase gives the TABS installation a simple and discounted payback period of 7 and 12 years, while the replacement HVAC system has a simple payback period of 9 years and no discounted payback period. TABS also has the added advantages of a consistent temperature gradient and mitigating cold draughts resulting from excessive air movements (Rhee, Olesen, & Kim, 2012)

Acknowledgements
Firstly, I would like to thank God for all He has done and will continue to do for me. I do not believe I would have made it as far as I have without Him, and I am forever grateful.

Secondly, I would like to thank my supervisors from the University of Cape Town (Mascha Moorlach and Andrew Hibberd) and Stellenbosch University (Dr Bernard Bekker) for their efforts that enabled me to pursue and work towards my studies. Your advice, comments and patience when I could not meet the deadline were greatly appreciated.

My colleagues at PJC and Partners (Paul Carew, Yogesh Gooljar, Dolf Bakker, Lesego Tsatsimpe, Sikelelwa Mkhize and Marlene Senne), your insights and advice regarding TABS were invaluable. I consider you all my friends.

Thank you to Matt Rich from Brickfield Group for allowing me access to your building and the TABS installation for analysis. The data received from the system contributed significantly to understanding how the system works.

To my colleagues from Eskom (Dr Michael Ndlovu, Sibusiso Tshabalala and Sis' Nyadi Mkulisi), this journey started with all of you. I will never forget the hard work put into convincing senior management to allow me into a more suitable space to work on these studies.

To my dad, ma, sister, brother and nephew, my love for you all is immeasurable. Your continued support, especially during those times when I felt that I was too tired, gave me the strength to continue. I hold you all close to my heart

Last but not least, I appreciate the support from the rest of my family and friends, although some may not know how you have supported me.

Table of Contents

List of Figures

List of Tables

Abbreviations

ACCA	Air-Conditioning Contractors of America
AHU	Air-Handling Units
ASHRAE	American Society of Heating, Refrigerating, and Air-Conditioning Engineers
BTO	Building Technologies Office
CAD	Computer-Aided Design
CAPEX	Capital Expenditure
CAV	Constant Air Volume
CDD	Cooling Degree Day
CHT	Convective Heat Transfer
CIHG	Convective Internal Heat Gains
CoCT	City of Cape Town
COP	Coefficient of Performance
CPI	Consumer Price Index
CSA	Canadian Standards Association
DOAS	Dedicated Outdoor Air System
DOE	Department of Energy
DWC	Design Weather Conditions
FDM	Finite Difference Model
FEM	Finite Element Method
HDD	Heating Degree Day
HL	Heat Loss
HVAC	Heating, Ventilation and Air-Conditioning
IAQ	Indoor Air Quality
IHG	Internal Heat Gains
IRR	Internal Rate of Return
ISO	International Organization for Standardization
IW	Internal Wall
IWS	Internal Wall Surface
LEED	Leadership in Energy and Environmental Design
LS	Lower Slab
ML	Material Layers
NPV	Net Present Value
OPEX	Operational Expenditure
PL	Pipe Level
PMV	Predictive Mean Vote
PPD	Predicted Percentage of Dissatisfaction
RH	Relative Humidity
RHC	Radiant Heating and Cooling
RHT	Radiant Heat Transfer
RIHG	Radiant Internal Heat Gains
ROI	Return on Investment
SABS	South Africa Bureau of Standards
SG	Solar Gain
SI	International System of Units
TABS	Thermally Activated Building Systems
TC	Technical Committee
TES	Transmission through External Surfaces
TL	Thermal Layers
TOU	Time of Use
US	Upper Slab
VAV	Variable Air Volume
VSD	Variable Speed Drive

Nomenclature

Symbol	Quantity	Unit
α	Heat exchange coefficient	W/m^2K
α_i	Parameter factors for calculation of characteristic curves	-
α_T	Pipe spacing factor	-
α_U	Covering factor	-
α_D	Pipe external diameter factor	-
A_A	Surface of the occupied area	m^2
A_F	Surface of the heating/cooling surface area	m^2
A_R	Surface of the peripheral area	m^2
b_u	Calculation factor depending on the pipe spacing	-
B, B_G, B_O	System coefficients. The coefficients depend on whether the system is of type A, B or C	W/m^2K
Clo	Clothing insulation	clo
c_W	Specific heat capacity of the heating or cooling fluid	kJ/m^2K
D	Pipe external diameter	m
d_a	External diameter of the pipe	m
d_i	Internal diameter of the pipe	m
d_M	External diameter of sheathing	m
h_t	Total heat exchange coefficient (convection and radiation) between surface and space	W/m^2K
k_H	Equivalent heat transmission coefficient	W/m^2K
k_{WL}	Parameter for heat-conducting devices	-
k_{fin}	Parameter for heat-conducting devices	-
k_{CL}	Parameter for heat conducting layer	-
L	Thermal load defined as the difference between the occupants' internal heat production and heat loss to the environment	
L_{WL}	Width of heat-conducting devices	m
L_{fin}	Width of fin	m
L_R	Length of installed pipes	m
m_T	Exponent for α_T	-
m_U	Exponent for α_U	-
m_D	Exponent for α_D	-
$\dot{m}_{H,sp}$	Specific design heating or cooling fluid mass flow	
M	Metabolic rate	met
n, n_G	Exponents	-
q	Heat flux at the surface	W/m^2
q_A	Heat flux in the occupied area	W/m^2
q_{des}	Design heat flux	W/m^2
q_G	Limit heat flux	W/m^2
q_N	Nominal heat flux	W/m^2
q_R	Heat flux in the peripheral area	W/m^2
q_u	Outward heat flux	W/m^2
R_O	Partial inwards heat transmission resistance of surface structure	m^2K/W
R_u	Partial outwards heat transmission resistance of surface structure	m^2K/W
$R_{\lambda,B}$	Thermal resistance of surface covering	m^2K/W
$R_{\lambda,ins}$	Thermal resistance of thermal insulation	m^2K/W
R_w	Resistance between the fluid and the pipe wall	m^2K/W
R_r	Resistance of the pipe wall	m^2K/W
R_x	Resistance between the pipe outside wall temperature and the average temperature of the conductive layer	m^2K/W
s_h	Thickness of thermal insulation from the outward edge of the insulation to the inward edge of the pipes in type B systems	m
s_l	Thickness of thermal insulation from the outward edge of the insulation to the outward edge of the pipes in type B systems	m

Symbol	Quantity	Unit
s_{ins}	Thickness of thermal insulation	m
s_R	Pipe wall thickness	m
s_U	Thickness of the wall above pipe	m
s_{WL}	Thickness of the heat-conducting device	m
S	Thickness of the screed (excluding the pipes in type A systems)	m
T_{op}		
T_{globe}		
U_i	Heat transfer coefficient between the conductive layer and the space side	
v	Velocity	$m.s^{-1}$
W	Space between pipes	m
$\theta_{s,max}$	Maximum surface temperature	°C
$\theta_{s,min}$	Minimum surface temperature	°C
θ_i	Design indoor temperature	°C
θ_m	Temperature of heating/cooling medium	°C
θ_R	Return temperature of heating/cooling medium	°C
θ_V	Supply temperature of heating/cooling medium	°C
θ_u	Indoor temperature in the adjacent space	°C
$\Delta\theta_H$	Heating/cooling medium differential medium	K
$\Delta\theta_{H,des}$	Design heating/cooling medium differential medium	K
$\Delta\theta_{H,G}$	Limit of heating/cooling medium differential medium	K
$\Delta\theta_N$	Nominal heating/cooling medium differential medium	K
$\Delta\theta_V$	Heating/cooling medium differential supply temperature	K
$\Delta\theta_{V,des}$	Design heating/cooling medium differential supply temperature	K
λ	Thermal conductivity	W/mK
σ	Temperature drop	K
φ	Conversion factor for temperatures	-
ψ	Content by volume of the attached burrs in the screed	-

Units of Measurement

W	Watt
K	Kelvin
m	meter
Pa	Pascal
Clo	clothing insulation
met	metabolic rate
°C	degrees Celcius
s	second

1 Introduction

1.1 Background

The objective of space heating and cooling systems is to ensure thermal comfort for occupants within a building. Occupants express thermal comfort when satisfied with their local temperature, humidity and air velocity, i.e. their thermal environment. Space heating and cooling are also essential as they affect occupants' productivity (Yau & Chew, 2014). The earliest evidence of interior space conditioning has been found in 9 000-year-old remains from Eastern Turkey. The remains consisted of an intermediate space beneath the floor that would have been filled with cold water from Kantara Creek to cool the interior during warm seasons (Ma, Wang, & Guo, 2015).

Since then, there have been more developments, such as in the 1990s R Meierhans, a Swiss engineer, published research papers on a cooling system for a building where the water is cooled by flowing through a heat exchanger at night-time. The cooled water would flow through the building to keep the building's temperature within the thermal comfort range. Later, this innovation became known as Thermally Activated Building Systems (TABS) (Ma, Wang, & Guo, 2015). Today, TABS consists of plastic pipes embedded within the concrete slab of the office building's floors, walls, and ceilings. Water from the boiler, chiller or heat pumps flows through the pipes to provide heating and cooling to the offices. Figure 1-1 below shows a cross-section of the pipes embedded between the ground office's ceiling and the top office's floor.

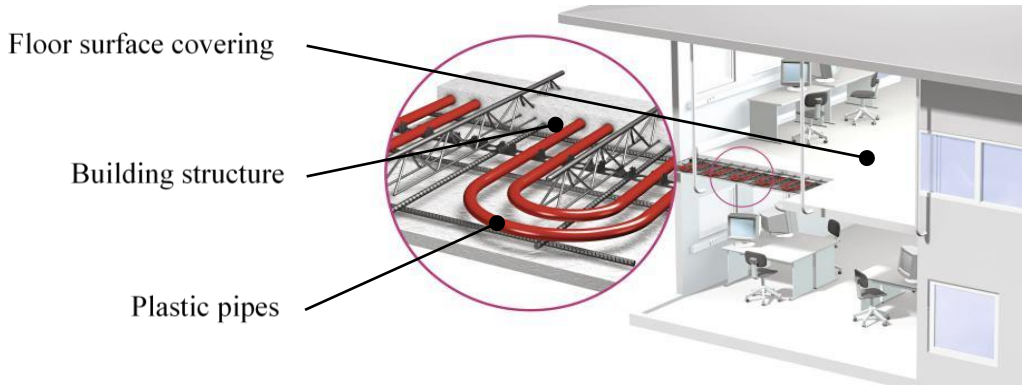

Figure 1-1: Cross Section of the TABS System (REHAU, 2012)

In Europe, the installation of TABS in buildings has since become state-of-the-art in space heating and cooling systems. In other parts of the world, TABS is not as well known, such that in 2007, the American Institute of Architects mentioned only one building in America that uses this form of cooling (American Institute of Architects, 2007). In America, the preferred space heating system has been the Heating, Ventilation and Air-Conditioning (HVAC) system, invented by WH Carrier in 1911. The invention enabled the construction of high-rise buildings as these systems could regulate the air within their interiors (Ma, Wang, & Guo, 2015).

Space heating and cooling systems are affected by weather, occupancy levels and office usage, making it challenging to predict their energy usage. The challenge has led to a reluctance to invest in improved energy-efficient systems even as the cost of electricity increases (Ma, Wang, & Guo, 2015).

1.2 Objectives

The primary aim of the research is to determine potential energy savings that can be achieved from TABS compared to conventional HVAC systems while ensuring that the occupants experience the same

level of thermal comfort. The aim includes understanding how TABS and HVAC systems operate, how they can be modelled and simulated and how they are influenced by weather conditions, occupancy levels and building use. The secondary aim of the research is to develop a business case based on potential savings that can be achieved from a TABS installation. The research hypothesis can be summarised as follows:

Thermally Activated Building Systems (TABS) consume 30% less energy than conventional Heating, Ventilation and Air-Conditioning (HVAC) systems while maintaining the same thermal comfort.

Validating the research hypothesis requires that the following questions are answered:

1. What is thermal comfort, and which variables need to be influenced to achieve occupants' thermal comfort?
2. How do space heating and cooling systems operate, and how do they achieve thermal comfort?
3. Which systems and tools can determine the space heating and cooling systems' demand profile and energy usage?
4. What industry standards should be considered when designing space heating and cooling systems?
5. What is the business case for installing TABS within office buildings?

1.3 Scope and Limitations

The scope of this research is limited to office buildings in South Africa. These buildings were considered since thermal comfort is essential for occupants' productivity (Ma, Wang, & Guo, 2015). An office building with TABS was also identified to be used as a case study in this research. Other industrial facilities, such as warehouses and mining facilities, such as compressor houses, have not been considered since thermal comfort is typically not as high a priority (Ma, Wang, & Guo, 2015). Residential buildings were not considered as well since an actual TABS installation was not identified to develop a case study. Outside Europe, TABS is not widely installed in residential buildings (Ma, Wang, & Guo, 2015).

1.4 Chapters Outline

The chapters in the document are outlined as follows:

Chapter 2: Literature Review

This chapter involves researching and understanding thermal comfort and the Predictive Mean Vote (PMV) model. The chapter details and explains TABS and conventional HVAC systems; and how they achieve thermal comfort.

Chapter 3: Research Methodology

This chapter explains the process followed to validate the research hypothesis and gives a justification for the process followed.

Chapter 4: Tools used for Analysis

This chapter details the tools used to model and simulate the demand and energy consumption of space heating and cooling systems.

Chapter 5: Case Study of Office Building with TABS

This chapter details the development and construction of an actual TABS system. The designs were developed for an office building in Cape Town, South Africa. Once constructed and commissioned, the electrical usage of the chiller was recorded. The TABS calculators described in Chapter 4 were used to

estimate the chiller's electrical usage and compare it with the recorded electrical usage. The PMV and PPD calculator was used to determine the number of occupants satisfied with their thermal environment.

Chapter 6: Case Study of Office Building with Conventional HVAC System
Similarly, as in Chapter 5, the electrical usage of a chiller in an office building with Variable Air Volume (VAV) HVAC installation was recorded. The HVAC was modelled and simulated in EnergyPlus and compared with the recorded electrical use of the building. EnergyPlus also calculated PMV and Predicted Percentage of Dissatisfaction (PPD) to determine the number of occupants satisfied with their thermal environment.

Chapter 7: Systems Comparison by Simulations
The case studies showed that the tools described in Chapter 4 could accurately simulate space heating systems' demand and energy profile. This chapter presents a simplified office building simulated with TABS and an HVAC system to compare their energy usage when the cooling loads, occupancy levels and building thermal insulation are equal.

Chapter 8: The Business Case for a TABS Installation
A financial analysis of a TABS installation is compared with a conventional HVAC installation. The analysis included determining each system's required Captial Expenditure (CAPEX), Operational Expenditure (OPEX), simple and discounted payback period, Net Present Value (NPV) and Internal Rate of Return (IRR).

Chapter 9: Conclusion
This chapter summarises the lessons learnt from the research and validates the hypothesis made in Chapter 1.

Chapter 10: Recommendations
This chapter proposes additional research to expand the understanding of TABS and its potential benefits.

2 Literature Review

This chapter begins by introducing and detailing the concept of thermal comfort, the factors influencing it and how people perceive it. After which, Thermally Activated Building Systems (TABS) and Heating, Ventilation and Air-Conditioning (HVAC) systems are discussed as systems used to improve thermal comfort. The chapter concludes by discussing the refrigeration system, the most significant energy consumer in both systems.

2.1 Thermal Comfort

The American Society of Heating, Refrigerating, and Air-Conditioning Engineers (ASHRAE) produced the standard "Thermal Environmental Conditions for Human Occupancy", which describes thermal comfort as the degree to which a person feels comfortable with their surrounding environment. Occupants are believed to become more efficient and productive once thermal comfort is achieved (Yau & Chew, 2014). Therefore, it is essential to understand how to quantify occupants' thermal comfort.

2.1.1 Predictive Mean Vote (PMV)

In the late 1960s, Danish professor Povl Ole Fanger developed the Predictive Mean Vote (PMV), a model used to determine the thermal comfort of occupants in office and residential buildings (Yau & Chew, 2014). The model relates the heat transferred between the environment (physical variables) and the body (personal variables) to quantify the occupants' perception of their environment. The variables are given in Table 2-1. Important to note the difference between Air Temperature, the measure of the heat content in the air; and Mean Radiant Temperature, the measure of the average temperature of surfaces surrounding a particular body with which it will exchange thermal radiation (DesigningBuildings, 2020). The average of these temperatures is termed the operative temperature. In an office building where indoor surfaces have uniform temperatures and radiation fluxes, Air Temperature and Mean Radiant Temperature are assumed to be equal since their differences are negligible. (Walikewitz, Jänicke, Langner, Meier, & Endlicher, 2014).

Table 2-1: PMV Variables (Yau & Chew, 2014)

Physical Variables	Personal Variables
Air Temperature	Activity Level (Metabolic Rate)
Mean Radiant Temperature	Clothing Insulation
Relative Humidity	
Air Velocity	

Fanger's model is given as (ASHRAE, 2010):

$$PMV = [0.303e^{(-0.036M)} + 0.028] \times [(M - W) - \text{heat flux}] \quad (2.1)$$

Where M refers to metabolic rate [W/m^2], i.e. the amount of energy that the body requires to function at rest (Khan Academy, n.d.) (determined using Table 2-2);

W refers to effective mechanical power [W/m^2], i.e. the heat loss rate from external work such as exercising. The heat loss results from the body increasing blood flow to the skin to dissipate heat (SUNY Cortland, n.d.). It is typically zero for most office-based activities;

the heat flux consists of heat transfer between the body and the environment [W/m^2].

The model can only be used when the variables fall within the following constraints:

- Air temperature is between 10°C to 30°C;
- The mean radiant temperature is between 10°C to 40°C;
- Air velocity is between 0m/s to 1m/s;

- Air pressure is between 0 Pa to 2 700 Pa; and
- Metabolic rate must be between 46 W/m^2 to 232 W/m^2 (0,8 met to 4 met); and
- Clothing insulation is between 0 m^{2}K/W to 0,310 m^{2}K/W (0 clo to 2 clo);

The heat flux in Equation 2.1 is the sum of six heat losses (and gains), classified as evaporative and non-evaporative processes, that the occupant may experience. The heat losses by evaporative processes occur through the skin (sweating) and the respiratory system (latent and dry respiration) (Luginbuehl, Bissonnette, & Davis, 2011); and are determined as follows:

1. **Heat loss by sweating (*HL1*)** (ASHRAE, 2010):

$$HL1 = 0.42[(M - W) - 58.15] \quad | \quad 2.2$$

2. **The heat loss by latent respiration (*HL2*)** (ASHRAE, 2010):

$$HL2 = 1.7 \times 10^{-5} M(5867 - p_a) \quad | \quad 2.3$$

Where p_a is the water vapour partial pressure, [Pa]

3. **The heat loss by dry respiration (*HL3*)** (ASHRAE, 2010):

$$HL3 = 0.0014M(34 - t_a) \quad | \quad 2.4$$

Where t_a is the air temperature, [°C]

The non-evaporative processes include conduction, convection and radiation (Whittow, 1971).

4. **Heat loss by skin contact (*HL4*)** refers to the heat transfer of the body having physical contact with another object or body, i.e. conduction (Vella & Kravitz, n.d.). The physical contact could include the chair that the occupant is sitting on and is calculated as follows (ASHRAE, 2010):

$$HL4 = 3.05 \times 10^{-3} [5733 - 6.99(M - W) - p_a] \quad | \quad 2.5$$

5. **Heat loss by convection (*HL5*)** refers to the heat transfer from the movement of water or air molecules across the skin and is calculated as follows (ASHRAE, 2010):

$$HL5 = f_{cl} h_c (t_{cl} - t_a) \quad | \quad 2.6$$

Where f_{cl} is the clothing surface area factor;
h_c is the convective heat transfer coefficient, [W/(m^{2}K)]; and
t_{cl} is the clothing surface temperature, [°C]

6. **Heat loss by radiation (*HL6*)** refers to heat transfer by infrared rays and is calculated as follows (ASHRAE, 2010):

$$HL6 = -3.96 \times 10^{-8} f_{cl} [(t_{cl} + 273.15)^4 - (t_r + 273.15)^4] \quad | \quad 2.7$$

Where t_r is the mean radiant temperature, [°C]

Heat loss by conduction, convection, and radiation account for most heat transfer because the energy is not required to convert water into vapour as in evaporative processes (Romanovsky, 2018). Under neutral thermal conditions, evaporative processes account for between 10% and 25% of heat losses (Luginbuehl, Bissonnette, & Davis, 2011).

The clothing surface area factor f_{cl}; required for Equations 2.6 and 2.7 is calculated as follows (ASHRAE, 2010):

$$f_{cl} = \begin{cases} 1.00 + 1.290I_{cl} \text{ for } I_{cl} \leq 0.078\text{m}^2 \text{ K/M} \\ 1.05 + 0.645I_{cl} \text{ for } I_{cl} > 0.078\text{m}^2 \text{ K/M} \end{cases} \quad 2.8$$

Where I_{cl} is the clothing insulation, [m²K/W] (determined using Table 2-3); and

The clothing surface temperature t_{cl} also required for Equations 2.6 and 2.7 is calculated as follows (ASHRAE, 2010):

$$t_{cl} = 35.7 - 0.028\,(M - W) - I_{cl}\,\{3.96 \times 10^{-8} f_{cl}\,[(t_{cl} + 273.15)^4 - (t_r + 273.15)^4] + f_{cl}h_c\,(t_{cl} - t_a)\} \quad 2.9$$

It should be noted that Equation 2.9 has the clothing surface temperature term, t_{cl}, on both sides of the equation. It is typically determined by an iterative process using a computer programme. The convective heat transfer coefficient h_c used in equation 2.9 is calculated as follows (ASHRAE, 2010):

$$h_c = \begin{cases} 2.38|t_{cl} - t_a|^{0.25} \text{ for } 2.38|t_{cl} - t_a|^{0.25} > 12.1\sqrt{v_{ar}} \\ 12.1\sqrt{v_{ar}} \text{ for } 2.38|t_{cl} - t_a|^{0.25} < 12.1\sqrt{v_{ar}} \end{cases} \quad 2.10$$

Where v_{ar} is the relative air velocity, [m/s]

Equations 2.1 to 2.5 require that metabolic rate be determined. Table 2-3 below includes various metabolic rates for typical activities in offices and gives the relation between its standard unit, met, and the units used in the equations, W/m², where 1 met = 58,2 W/m². Other activities have been included in Appendix B: Thermal Comfort Tables and Calculators.

Table 2-2: Metabolic Rates for Typical Office Activities (ASHRAE, 2010)

Activity	**Metabolic Rate**	
	Met Units	W/m²
Reading, seated	~1.0	55
Writing	~1.0	60
Typing	~1.1	65
Filing, seated	~1.2	70
Filing, standing	~1.4	80
Walking about	~1.7	100
Lifting/packing	~2.1	120

Equation 2.8 requires the occupants' clothing insulation to be determined. Table 2-3 gives a list of clothes and their associated insulation value. Clothing insulation is determined by summing the insulation of all the clothes by each occupant. It should be noted that 1 clothing unit = 1 clo = 0,155 m² °C/W.

Table 2-3: Clothing Insulation Values for Typical Ensembles (ASHRAE, 2010)

Clothing Description	**Garments Included**	I_{cl} **[clo]**
Trousers	1. Trousers, short-sleeve shirt	0.57
	2. Trousers, long-sleeve shirt	0.61
	3. 2. + suit jacket	0.96
	4. 2. + suit jacket, vest, T-shirt	1.14
	5. 2. + long-sleeve sweater, T-shirt	1.01
	6. 5. + suit jacket, long underwear bottoms	1.30
Skirts/Dresses	Knee-length skirt, short-sleeve shirt (sandals)	0.54

	Knee-length skirt, long-sleeve shirt, full slip	0.67
	Knee-length skirt, long-sleeve shirt, half-slip, long-sleeve sweater	1.10
	Knee-length skirt, long-sleeve shirt, half-slip, suit jacket	1.04
	Ankle-length skirt, long-sleeve shirt, suit jacket	1.10
Shorts	Walking shorts, short-sleeve shirt	0.36
Overalls/Coveralls	Long-sleeve coveralls, T-shirt	0.72
	Overalls, long-sleeve shirt, T-shirt	0.89
	Insulated coveralls, long-sleeve thermal underwear tops and bottoms	1.37
Athletic	Sweat pants, long-sleeve sweatshirt	0.74
Sleepwear	Long-sleeve pyjama tops, long pyjama trousers, short 3/4 length robe (slippers, no socks)	0.96

Determining the heat losses and gains that people experience is a complex and iterative process. For this reason, PMV is usually determined by software tools. An example of a computer programme is provided in ISO 7730 and ASHRAE 55 and is discussed in Chapter 4.1.

The result from the model (Equation 2.1) can then be mapped to a sensational scale (Table 2-4), which describes a mean thermal sensation for a group of occupants.

Table 2-4: Predicted Mean Vote (PMV) Sensation Scale (Nicol & Roaf, 2017)

Cold	Cool	Slightly Cool	Neutral	Slightly Warm	Warm	Hot
-3	-2	-1	0	1	2	3

In a group of occupants, some will not be satisfied with their thermal sensation. The Predicted Percentage of Dissatisfaction (PPD) describes the percentage of dissatisfied occupants.

2.1.2 Predicted Percentage of Dissatisfaction (PPD)

The Predicted Percentage of Dissatisfaction (PPD) measures the number of occupants that will not have a satisfactory thermal experience. PPD is closely associated with PMV and is calculated as follows (ASHRAE, 2010):

$$PPD = 100 - 95\ exp(-0.03353PMV^4 - 0.2179PMV^2) \quad | \ 2.11$$

Equation 2.11 can be shown graphically, as in Figure 2-1. From the graph, it can be seen that not all occupants will experience thermal comfort. There will be at least 5% of occupants who experience discomfort.

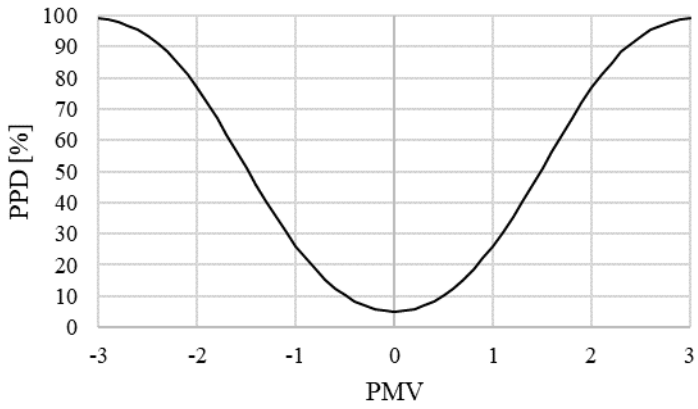

Figure 2-1: Predicted Mean Vote (PMV)/Predicted Percentage Dissatisfied (PPD) Graph (ASHRAE, 2010)

There are discrepancies with the PMV model when comparing actual and predicted thermal sensations developed from laboratory studies. More information on how the PMV model improved in given in Appendix A-1: Adaptive Approach. The following two sections describe technologies, namely TABS and the conventional HVAC system, that improve thermal comfort.

2.2 Radiant Heating and Cooling (RHC) Systems and Thermally Activated Building Systems (TABS)

2.2.1 Defining Radiant Heating and Cooling Systems

Radiant heating and cooling (RHC) systems are systems where over 50% of heat is transferred by radiation (Rhee, Olesen, & Kim, 2012). This heat transfer method differs from a conventional all-air system which transfers heat by convection. RHC systems can be classified by the position of the piping in the building (Rhee, Olesen, & Kim, 2012):

a. **Embedded Surface Systems:** pipes are located within a building layer but are separated from the main building structure;
b. **Thermally Activated Building Systems (TABS):** consists of pipes embedded in buildings' concrete floors, with water flowing through them (Saelens, Parys, & Baetens, 2011), forming part of the thermal mass of the building's HVAC installation (Rijksen, Wisse, & van Schijndel, 2010); and
c. **Radiant Panel Systems:** pipes form part of lightweight panels attached to the building with an open-air gap.

Figure 2-2 below illustrates three RHC systems as classified above.

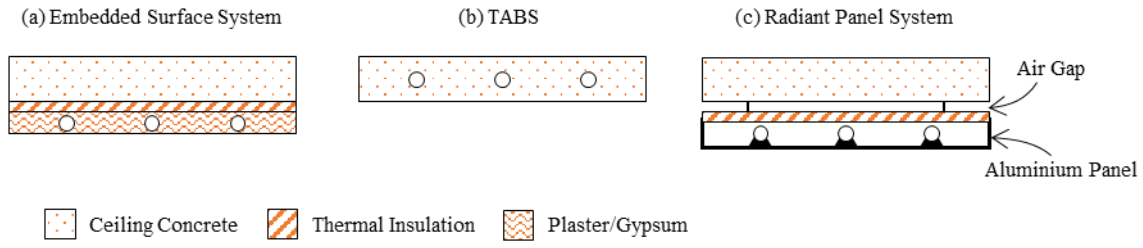

Figure 2-2: Classification of Radiant Heating and Cooling Systems (Rhee, Olesen, & Kim, 2012)

2.2.2 Thermal Comfort from RHC Systems Compared to Conventional Air Systems

ISO 7730 and ASHRAE 55 recommend floor surface temperatures between 17°C and 29°C, although this is dependent on floor surface materials and whether the occupants are wearing shoes or are barefooted. Figure 2-3 is an example taken from ISO 11855-4, showing surface temperatures for ceiling and floor throughout a typical day where TABS has been installed in the building. The figure shows that the difference between the operative and surface temperatures is less than 1.5°C and that in the example, PMV remains between 0.5 and -0.5, i.e. neutral thermal comfort.

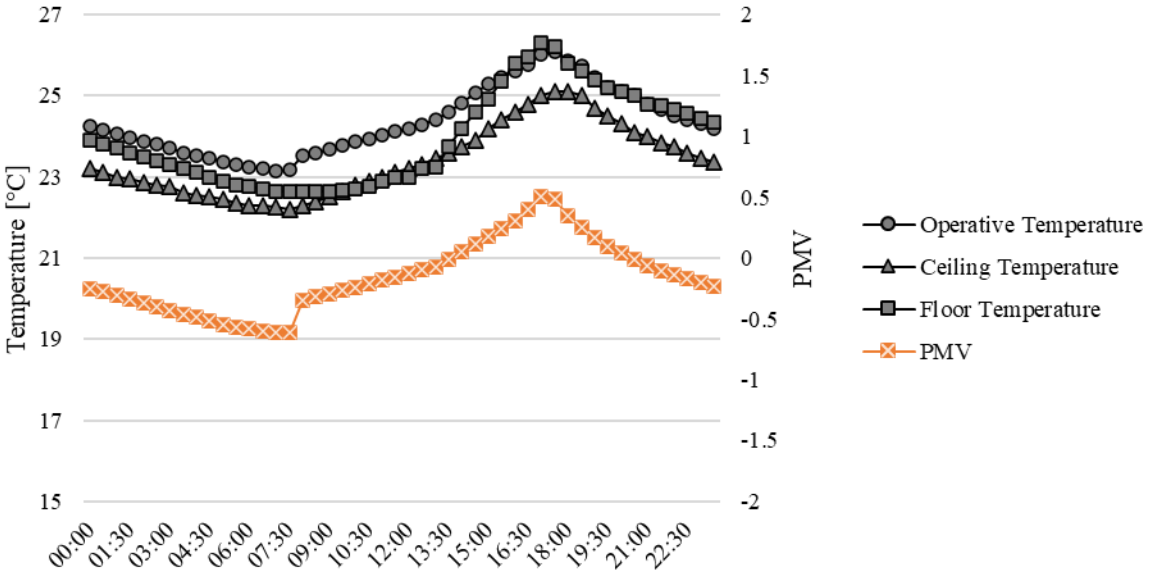

Figure 2-3: Example Temperature Profiles and PMV Values over a 24hr Period (ISO, 2012)

Air systems introduce temperature gradients, where the operative temperature is different at different heights (Rhee, Olesen, & Kim, 2012). Figure 2-4 shows the temperature gradients of a space heated by different heating systems. The figure shows that radiant floor and panels provide a temperature gradient approaching an ideal vertical line. The slight temperature difference is consistent with Figure 2-3, where the difference between the ceiling and floor temperature is less than 0.5°C. Ceiling panels, baseboards and backwalls introduce excessive air movements and cold draughts illustrated by the significant temperature differences. When there is little temperature difference between the levels, the temperature gradient approaches a vertical straight line, which, although not represented in the PMV model, contributes to improving thermal comfort (Rhee, Olesen, & Kim, 2012).

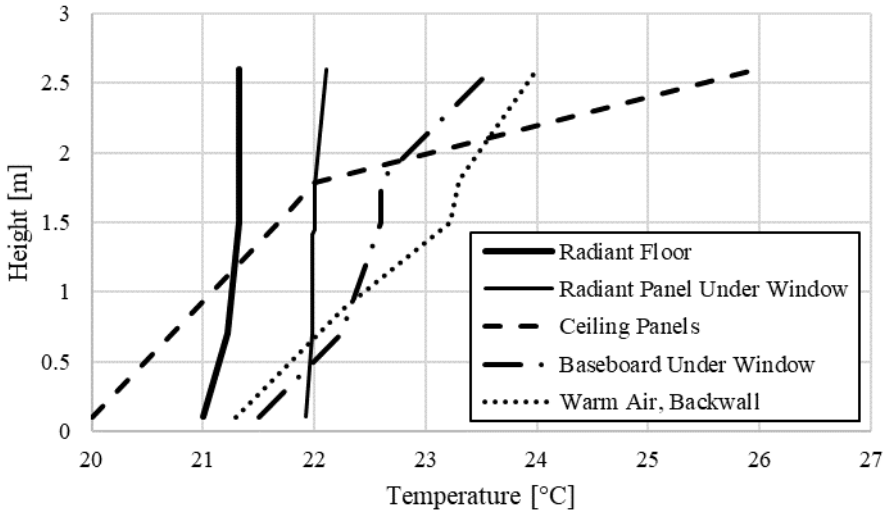

Figure 2-4: Vertical Air Temperature Differences Measured in a Test Space for Different Heating Systems (Rhee, Olesen, & Kim, 2012)

RHC systems operate at lower air flows to deliver the same thermal comfort level as conventional air systems, mitigating cold draughts resulting from excessive air movements (Rhee, Olesen, & Kim, 2012). It has been shown that a chilled ceiling with displacement ventilation and a heat transfer of 100 W/m^2 completely removes any draught risks. It should be noted that RHC systems require appropriate air movement or ventilation to avoid a sensation of stagnant air.

In another research (Sastry & Rumsey, 2014), occupants in adjacent buildings, the first with an RHC system and the second with an air system, were required to complete a survey stating how satisfied they were with their thermal environment. Figure 2-6 shows the survey results of occupants. The figure shows that the occupants in the RHC building have fewer "very to slightly dissatisfied" responses and more "slightly to very satisfied" responses than those in the building with the air system.

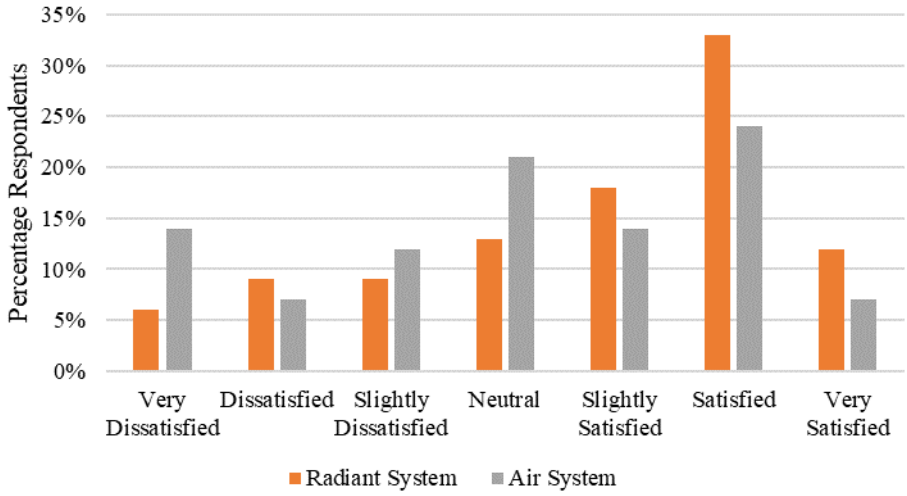

Figure 2-5: Occupant Survey Results from Comparison between Radiant and Air Systems (Sastry & Rumsey, 2014)

2.2.3 Heat Transfer of RHC Systems

The heat transfer medium used in RHC systems is typically water, which has a specific heat of 4.187 kJ/kg.K. In contrast, conventional air systems use air as the heat transfer medium, which has a specific heat of 1.0 kJ/kg.K. Water's higher specific heat enables it to transfer more heat than air at the same volume. (Rhee, Olesen, & Kim, 2012).

2.2.4 TABS Types

The International Standards Organisation Technical Committee 205 (ISO/TC 205) developed the standard on building environment design (ISO 11855), which gives best practices for the installation and operation of TABS. The standard describes the types of TABS as characterised by the position of the pipes within the floor, walls, and ceilings (ISO, 2012):

- Type A: The pipes are embedded within the concrete
- Type B: The pipes are embedded within the thermal insulation and connected to heat diffusion material
- Type C: The pipes are embedded within the screed
- Type D: Consists of a collection of tightly packed pipes between the screed and thermal insulation layer

These system types are illustrated in Figure 2-6 below. The figure gives a cross-sectional area of the floor construction, although the pipes can be embedded within the walls and ceiling.

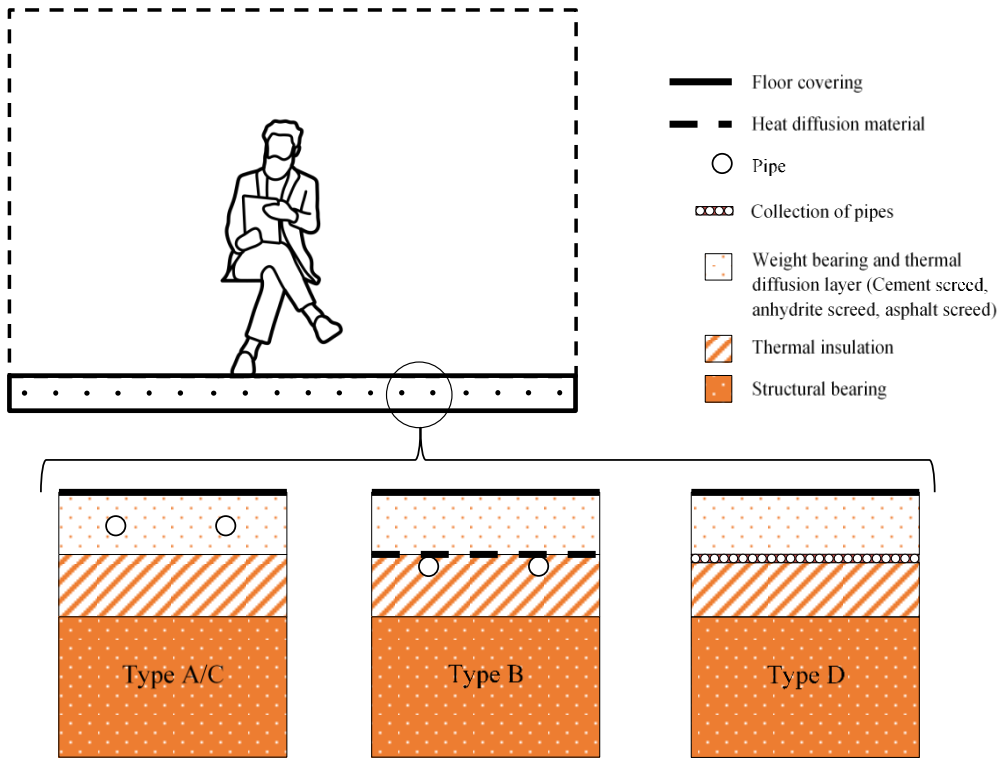

Figure 2-6: Systems Types A/C, B, and D (ISO, 2012)

Other types of TABS consist of pipes within a structure that allows energy transfer between two spaces (ISO, 2012). The spaces could be separated by a floor, i.e., an upper and lower floor, or between two rooms separated by a wall. The types are described as follows:

- Type E: embedded within a concrete slab between floors; and
- Type F: embedded in a layer at the inner surface between floors

Figure 2-7 shows an example where the TABS is installed between an upper and lower space, although the pipes can be embedded within the walls separating different areas.

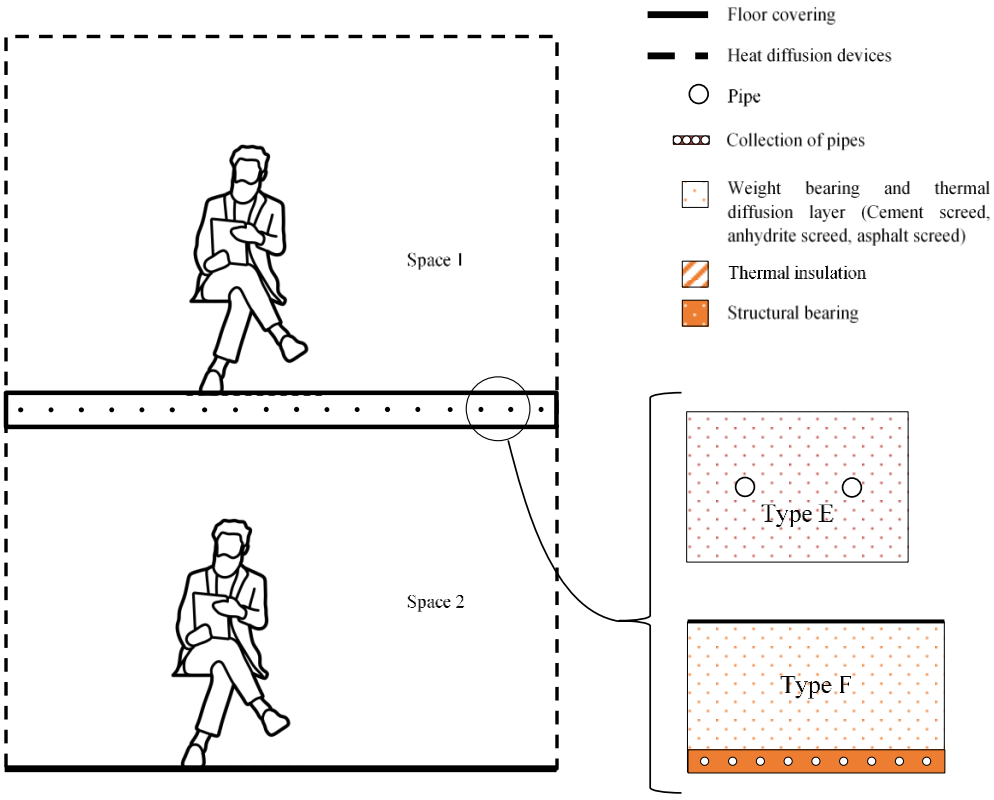

Figure 2-7: System Types E, F and G (ISO, 2012)

The final system type, Type G, consists of pipes embedded within wooden joist floor structures and other similar lightweight structures (ISO, 2012). These structures are made from layers of materials with relatively low thermal conductivity. The heat is distributed horizontally (or vertically, in walls) mainly by thermal conducting metal sheets or fins (heat diffusion devices) with high thermal conductivity.

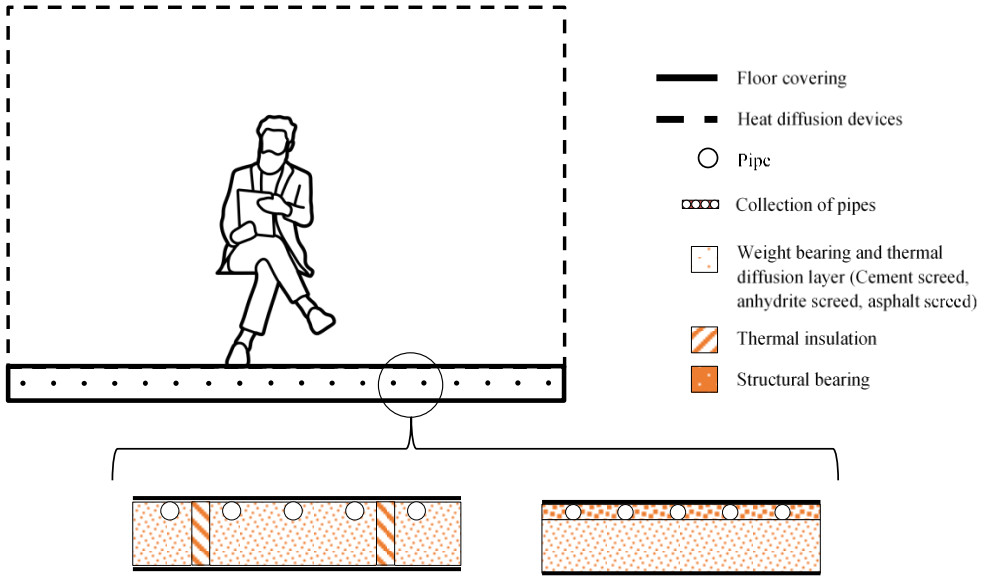

Figure 2-8: System Type G (ISO, 2012)

The following section describes TABS's heating and cooling capacity, which depends on the system type.

2.2.5 TABS Heating and Cooling Capacity

The heating and cooling capacity of TABS refers to the amount of heat that can be transferred between the system and the office space. It can be further described as the relationship between heat transferred between the system and the environment (heat flux) and its effect on indoor and heating (or cooling) medium temperatures. Depending on the installed system type, the capacity can be determined using either of the calculation methods, namely (ISO, 2012):

1. The Universal Single Power Method; or
2. The General Resistance Method

2.2.5.1 The Universal Single Power Method

The Universal Single Power Method was developed from the Finite Element Method (FEM) and is applied to TABS Types A, B, C and D. The heat flux for these systems is given as (ISO, 2012):

$$q = B \prod_i \alpha_i^{m_i} \Delta\theta_H \qquad 2.12$$

Where B is a system-dependent coefficient [W/m^{2}K]

$\prod_i \alpha_i^{m_i}$ is the product of the characteristic curves (i.e. the equation that describes the relationship between the heat flux and the difference between average surface temperature and nominal indoor operative temperature); and

$\Delta\theta_H$ is the temperature difference between the heating medium and the room temperature. Subscript "$_H$" denotes the system when it is in heating mode.

The system-dependent coefficient $B = B_0 = 6.7$ W/m^{2}K when:

Pipe thermal conductivity $\lambda_R = \lambda_{R,0} = 0.35$ W/mK; and

Pipe wall thickness $s_R = s_{R,0} = (d_a - d_i)/2 = 0.002$ m.

The subscript "$_0$" refers to a reference system used to derive other system factors. For other cases, B is calculated using the following equation:

$$\frac{1}{B} = \frac{1}{B_o} + \frac{1.1}{\pi} \prod_i \left(a_i^{m_i}\right) W \left[\frac{1}{2\lambda_R} ln \frac{d_a}{d_a - 2s_R} - \frac{1}{2\lambda_{R,0}} ln \frac{d_a}{d_a - 2s_{R,0}} \right] \quad 2.13$$

If the pipe has additional sheathing, the following equation is used:

$$\frac{1}{B} = \frac{1}{B_o} + \frac{1.1}{\pi} \prod_i a_i^{m_i} W \left[\frac{1}{2\lambda_M} ln \frac{d_M}{d_a} + \frac{1}{2\lambda_R} ln \frac{d_a}{d_a - 2s_R} - \frac{1}{2\lambda_{R,0}} ln \frac{d_M}{d_M - 2s_{R,0}} \right] \quad 2.14$$

The product of the characteristic curves is given as (ISO, 2012):

$$\prod_i \alpha_i^{m_i} = \alpha_B \alpha_W^{m_W} \alpha_U^{m_U} \alpha_D^{m_D} \quad 2.15$$

Where α_B is the surface covering characteristic curve;
$\alpha_W^{m_W}$ is the pipe's spacing characteristic curve;
$\alpha_U^{m_U}$ is the pipe's to floor covering characteristic curve; and
$\alpha_D^{m_D}$ is the pipe's external diameter characteristic curve;

Therefore, Equation 2.12 can be written as:

$$q = B \alpha_B \alpha_W^{m_W} \alpha_U^{m_U} \alpha_D^{m_D} \Delta\theta_H \quad 2.16$$

The surface covering characteristic curve, α_B, is calculated using the following equation:

$$\alpha_B = \frac{\frac{1}{\alpha} + \frac{s_{u,0}}{\lambda_{u,0}}}{\frac{1}{\alpha} + \frac{s_{u,0}}{\lambda_E} + R_{\lambda,B}} \quad 2.17$$

Where α is the constant factor = 10.8 W/m^{2}K;
$s_{u,0}$ is the space between the pipe and the floor covering in the reference system = 0,045m;
$\lambda_{u,0}$ is the heat conductivity of floor covering in the reference system = 1W/mK;
λ_E is the heat conductivity of the screed [W/mK]; and
$R_{\lambda,B}$ is the heat conduction resistance of the floor covering [m^{2}K/W]

The pipe spacing characteristic curve $\alpha_W^{m_W}$ consists of the factor α_W, which is determined using Table 2-5 below:

Table 2-5: Pipe Spacing Factor for Type A and C Systems (ISO, 2012)

$R_{\lambda,B}$	0	0,05	0,1	0,15
α_W	1,23	1,188	1,156	1,134

and its associated exponent is determined using the following equation:

$$m_W = 1 - \frac{W}{0.075} \quad 2.18$$

Where W is the space between the pipes.

The floor covering characteristic curve $\alpha_U^{m_U}$ consists of the factor α_U, which is determined using Table 2-6 below:

Table 2-6: Covering Factors for Type A and C Systems (ISO, 2012)

$R_{\lambda,B}$	0	0,05	0,1	0,15
W	Covering factor α_U			
0,05	1,069	1,065	1,043	1,037
0,075	1,066	1,053	1,041	1,035
0,1	1,063	1,05	1,039	1,0335
0,15	1,057	1,046	1,035	1,0305
0,2	1,051	1,041	1,0315	1,0275
0,225	1,048	1,038	1,0295	1,026
0,3	1,0395	1,031	1,024	1,021
0,375	1,03	1,0221	1,018	1,015

and its associated exponent is determined using the following equation:

$$m_U = 100(0.045 - s_U) \quad (2.19)$$

Where s_u is the space between the pipe and the floor covering

The pipe's external diameter characteristic curve $\alpha_D^{m_D}$ consists of the factor α_D, which is determined using Table 2-7 below:

Table 2-7: Pipe External Diameter Factor for Type A and C Systems (ISO, 2012)

$R_{\lambda,B}$	0	0,05	0,1	0,15
W	Pipe External Diameter Factor α_D			
0,05	1,013	1,013	1,012	1,011
0,075	1,021	1,019	1,016	1,014
0,1	1,029	1,025	1,022	1,018
0,15	1,04	1,034	1,029	1,024
0,2	1,046	1,04	1,035	1,03
0,225	1,049	1,043	1,038	1,033
0,3	1,053	1,049	1,044	1,039
0,375	1,056	1,051	1,046	1,042

and its associated power is determined using the following equation:

$$m_D = 250(D - 0.020) \quad (2.20)$$

The temperature difference between the heating medium and the room temperature $\Delta\theta_H$ is determined using the following equation:

$$\Delta\theta_H = \frac{\theta_V - \theta_R}{ln\frac{\theta_V - \theta_i}{\theta_R - \theta_i}} \quad (2.21)$$

Where θ_V is the supply temperature of the medium
θ_R is the return temperature of the medium
θ_i is the indoor design temperature

The Universal Single Power method used to determine the heating and cooling capacity for TABS Types A, B, C and D can only be used within boundary conditions, summarised in Table 2-8 below.

Table 2-8: System Type Summary (ISO, 2012)

System Type	Description by Pipe Location	Boundary Conditions
A and C	Pipes are located within the screed, separated from the structural bearing by thermal insulation.	$W \geq 0.05$m $s_u \geq 0.01$m $0.008\text{m} \leq d \leq 0.03\text{m}$ $s_u/\lambda_e \geq 0.01$
B	Pipes are located in the thermal insulation layer.	$0.05\text{m} \leq W \leq 0.45\text{m}$ $0.014\text{m} \leq d \leq 0.022\text{m}$ $0.01\text{m} \leq s_u/\lambda_e \leq 0.18\text{m}$
D	Systems with surface elements (plane section systems)	None

2.2.5.1.1 Capacity Conversion for Walls and Ceilings

The Universal Single Power method described so far determines the heating capacity when TABS is embedded in the floor. When TABS is installed in the walls and ceilings, the heating and cooling capacity of the installation is determined by converting the results using the following equation (ISO, 2012):

$$q = K_H \Delta\theta_H \qquad 2.22$$

Where K_H is the equivalent heat transmission coefficient and determined using the following equation (ISO, 2012):

$$K_H = K_H\left(\Delta R_\alpha, R_{\lambda,B}\right) = \frac{K_{H,floor}}{1 + \frac{\Delta R_\alpha + R_{\lambda,B}}{R^*_{\lambda,B}}\left(\frac{K_{H,floor}}{K^*_{H,floor}} - 1\right)} \qquad 2.23$$

Where $K_{H,floor}$ is the heat transmission coefficient determined for the floor;
ΔR_α is the change in the surface thermal resistance [m^2K/W]; and
$R_{\lambda,B}$ is the thermal resistance of the surface covering

The change in the surface thermal resistance ΔR_α is determined using the following equation (ISO, 2012):

$$\Delta R_\alpha = \frac{1}{\alpha} - \frac{1}{10.8} \qquad 2.24$$

Where α is the constant factor [$W/(m^2K)$]

The constant factor and change in surface thermal resistance are given in Table 2-9 below.

Table 2-9: Additional Thermal Transfer Resistance (ISO, 2012)

Case of Application	α	ΔR_α
Floor heating	10,8	0
Floor cooling	6,5	0,0613
Wall heating	8	0,0324
Wall cooling	8	0,0324
Ceiling heating	6,5	0,0613
Ceiling cooling	10,8	0

The heating and cooling capacity for Types E and F are determined using the General Resistance Method, discussed in the next section.

2.2.5.2 The General Resistance Method

The General Resistance Method is applied to TABS Types E and F, where the pipes are embedded within floors and walls, allowing energy transfer between two spaces. The heat flux equation for these systems is given as follows (ISO, 2012):

$$q = K_H \Delta\theta_H \quad (2.25)$$

Where q is the heat flux;
K_H is the equivalent heat transmission coefficient; and
$\Delta\theta_H$ is the temperature difference between the heating medium and the room temperature.

The equivalent heat transmission coefficient is given as follows:

$$K_H = \frac{1}{R_w + R_r + R_x + R_i} \quad (2.26)$$

Therefore the heat flux can be written as:

$$q = \frac{\Delta\theta_H}{R_w + R_r + R_x + R_i} \quad (2.27)$$

Where R_w is the resistance between the fluid and the pipe wall
R_r is the resistance of the pipe wall
R_x is the resistance between the outside pipe wall and the conductive layer
R_i is the resistance from either surface, $i = 1$ or $i = 2$, into the space

The resistance between the fluid and the pipe wall R_w is determined using the following equation:

$$R_w = \frac{W^{0.13}}{8\pi}\left(\frac{d_a - 2s_r}{\dot{m}_{H,sp} l}\right)^{0.87} \quad (2.28)$$

Where W is the pipe spacing;
d_a is the pipe diameter;
s_r is the pipe wall thickness;
$\dot{m}_{H,sp}$ is the fluid mass flow rate; and
l is the length of the pipe

The resistance of pipe wall R_r is determined using the following equation:

$$R_r = \frac{W \ln\left(\frac{d_a}{d_a - 2s_r}\right)}{2\pi\lambda_r} \quad (2.29)$$

Where λ_r is the pipe thermal conductivity

The resistance between the outside pipe wall and the conductive layer R_x can be approximated to:

$$R_x \approx \frac{W \ln\left(\frac{W}{\pi d_a}\right)}{2\pi\lambda_b} \quad (2.30)$$

Where λ_b is the screed thermal conductivity;
The values of R_x is valid when $s_i/W > 0.3$ and $d_a/W < 0.2$

The resistance from either surface, $i = 1$ or $i = 2$, into the space R_i is determined using the following equation:

$$R_i = \frac{1}{U_i} \quad 2.31$$

Where U_i is the heat transfer coefficient between the conductive layer and the space side, calculated using the following equation:

$$U_i = \frac{1}{\frac{1}{h_i} + \frac{s_i}{\lambda_b}} \quad 2.32$$

Where h_i is the heat transfer coefficient
s_i is the thickness of the layer above/below the pipe
λ_b is the conductivity of the concrete;

The heat transfer coefficient is determined using the following equation (Holman, 2010):

$$h_i = \frac{q_{s,i}}{T_{s,i} - T_{a,i}} \quad 2.33$$

Where $q_{s,i}$ is the heat flux between the surface i and space i;
$T_{s,i}$ is the surface temperature of surface i; and
$T_{a,i}$ is the air temperature in space i

The methods used to determine the heating and cooling capacity of TABS for system types E, F, and G can only be used within the boundary conditions, summarised in Table 2-10 below.

Table 2-10: System Type Summary (ISO, 2012)

System Type	Description by Pipe Location	Boundary Conditions
E	Pipes are located within the concrete slab	$s_T/W \geq 0.3$
F	Capillary tubes are located on the concrete surface.	$d_a/W \leq 0.2$
G	Pipes are embedded in or under the subfloor and use heat emission plates to increase heat transfer.	$\lambda_{wl} \geq 10\lambda_{surrounding\_material}$ $s_{wl}\ \lambda \geq 0.01$

TABS' heating and cooling capacity calculations described in this chapter are used to determine the potential heat transferred between the building and the system. Once the heating and cooling capacity is determined, the chiller size is calculated to determine the energy consumption.

2.2.6 Chiller Sizing using The Simplified Model

Where TABS heating and cooling capacity describes the amount of heat that can be transferred between the system and the office space, chiller sizing refers to the heat required to be transferred. The sizing of chillers is determined using mathematical models based on the relationship between the pipe surface and the room surfaces (i.e. floor, walls and ceiling). ISO 11855-4 gives four calculation methods for calculating the relationship:

1. Rough Sizing Method
2. Simplified Method
3. Simplified model based on Finite Difference Model (FDM)
4. Detailed Simulation Models

The section focuses on the simplified method, the other methods are described in Appendix A-2: Additional Methods for Chiller Sizing.

The simplified method performs dynamic simulations predicting the heat transfers between the slab and the environment using the Finite Difference Model (FDM). This method has a typical error variance between 10% and 15%; and requires that the variable cooling loads for each hour in the environment are known. The slab consists of multiple material layers, ML_i, which constitutes thermal layers, TN_i. Some thermal nodes have pre-defined names, as given in Figure 2-9 below.

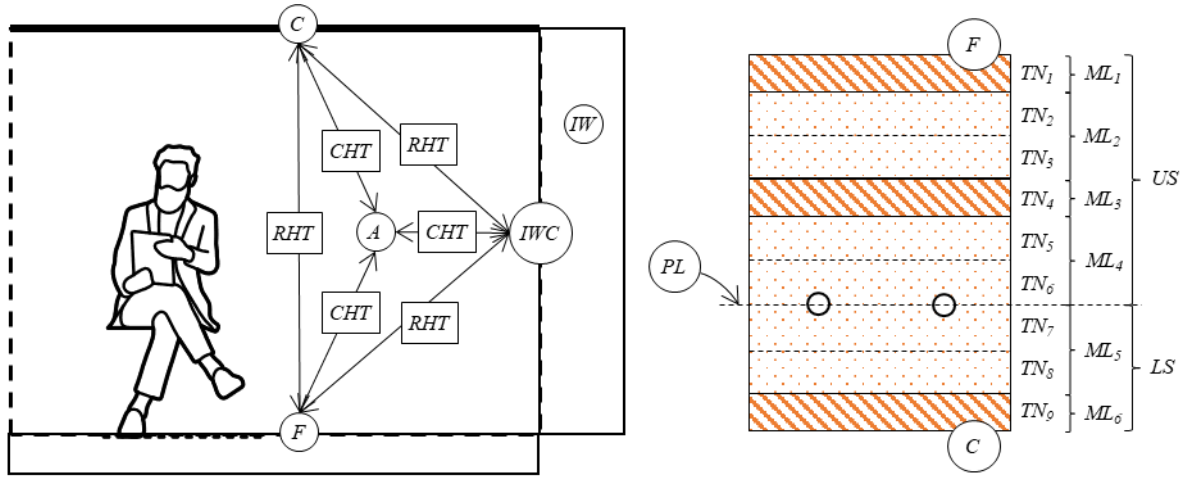

Thermal Nodes						Heat Transfer	
A	Air	*C*	Ceiling Surface	*F*	Floor Surface	*CHT*	Convective Heat Transfer
IW	Internal Wall	*IWS*	Internal Wall Surface	*PL*	Pipe Level	*RHT*	Radiant Heat Transfer
TN_i	i^{th} Thermal Node	ML_i	i^{th} Material Layer	*US*	Upper Slab		
				LS	Lower Slab		

Figure 2-9: Thermal Nodes in Simplified Model (ISO, 2012)

Thermal nodes defined within the slab and environment are used in heat balance calculations. The thermal nodes are related and depend on each other and vary depending on the time of the day. To perform the heat transfer calculations, the physical properties of the following thermal nodes need to be known:

- The thermal inertia C_p of the p^{th} thermal node;
- The thermal resistance RU_p connects the p^{th} thermal node with the boundary of the previous thermal node [$(m^2K)/W$]; and
- The thermal resistance RD_p which connects the p^{th} thermal node with the boundary of the following thermal node [$(m^2K)/W$]

The properties can be determined using the equations in Table 2-11 below.

Table 2-11: Thermal Node Physical Properties

Thermal Node	Thermal Inertia, C_p	Thermal Resistance, RU_p	Thermal Resistance, RD_p
A	0	0	0
C	0	R_{AddC}	0
F	0	0	R_{AddF}

TN_i	$\rho_i c_i \frac{\delta_i}{m_i}$	$\frac{\delta_i}{2m_i\lambda_i}$	$\frac{\delta_i}{2m_i\lambda_i}$
IW	C_w	R_{Walls}	0
IWS	0	0	R_{Walls}
PL	0	0	0

Where R_{AddC} is the additional thermal resistance covering the lower side of the slab [(m^{2}K)/W];
R_{AddF} is the additional thermal resistance covering the upper side of the slab [(m^{2}K)/W];
ρ_i is the density of the material [kg/m^3];
c_i is the specific heat of the material [J/(kgK)];
δ_i is the thickness of the layer [m]
m_i is the number of partitions in the layer
λ_i is the thermal conductivity of the material [W/(mK)]
C_w is the average specific thermal inertia of the internal walls [J/(m^{2}K)]
R_{Walls} is the Wall surface thermal resistance [(m^{2}K)/W]

The heat gains acting in the office space must be determined and depend on the people, equipment, possible air supply, and infiltration. The heat gains contribute to the total convective and radiant heat gains, as shown in Figure 2-10 below.

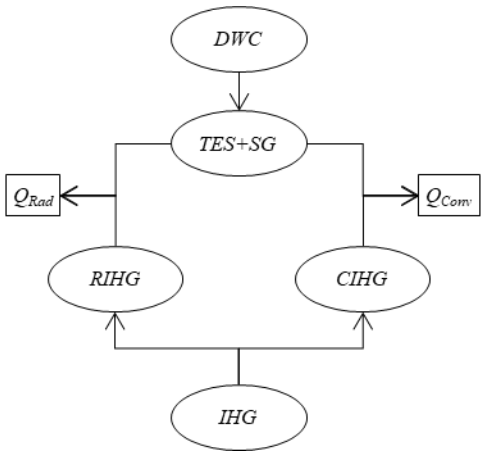

CIHG	Convective Internal Heat Gains
DWC	Design Weather Conditions
IHG	Internal Heat Gains
RIHG	Radiant Internal Heat Gains
Q_{Conv}	Total Convective Heat Gains
Q_{Rad}	Total Radiant Heat Gains
SG	Solar Gain
TES	Transmission through External Surfaces

Figure 2-10: Heat Loads Acting in the Office Space (ISO, 2012)

The assumption is that 15% of the heat gains passing through the external wall (*TES*) contribute to convective heat load. Therefore, the total convective heat gain is determined as follows:

$$Q^h_{conv} = 0.15Q^h_{transm} + Q^h_{IntConv} + Q^h_{PrimAir} \quad | \quad 2.34$$

Where Q^h_{transm} is the Transmission Heat Gains through External Surfaces (*TES*) for each h^{th} hour [W];
$Q^h_{IntConv}$ is Convective Internal Heat Gains (*CIHG*) for each h^{th} hour [W];
$Q^h_{PrimAir}$ is the primary air convective heat gains for each h^{th} hour [W];

The remaining 85% of the heat gains passing through the external wall is considered the radiant heat load. Therefore, the total radiant heat gain is determined as follows:

$$Q^h_{rad} = 0.85Q^h_{transm} + Q^h_{IntRad} + Q^h_{Sun} \quad | \quad 2.35$$

Where Q^h_{IntRad} is the Radiant Internal Heat Gains (*RIHG*) for each h^{th} hour [W]; and
Q^h_{Sun} is the solar heat gains in the room for each h^{th} hour [W]

The values for Q^h_{conv} and Q^h_{rad} are used as inputs for each iteration when calculating the following:

1. The water supply temperature;
2. The temperature of each thermal node; and
3. The actual tolerance at the current iteration

2.2.6.1 Calculating the Water Supply Temperature

The inlet water temperature, $\theta^h_{water,\,in}$, is calculated using the following formula:

$$\theta^h_{water,\,in} = \max\left(\theta^{set\text{-}point,h}_{water,\,in}, \theta^h_{water,\,in} + \frac{Q^h_{circuit} - P^{max,h}_{circuit}}{\dot{m}^h_{H,sp} A_F c_w}\right) \quad 2.36$$

Where $\theta^{set\text{-}point,h}_{water,\,in}$ is the water inlet set-point temperature at the h^{th} hour [°C];
$Q^h_{circuit}$ is the heat flow extracted by the circuit in the h^{th} hour [W];
$P^{max,h}_{circuit}$ is the maximum cooling power in the h^{th} hour [W];
$\dot{m}^h_{H,sp}$ is the specific water mass flow in the circuit in the h^{th} hour, [kg/sm^2];
A_F is the area of the heating/cooling surface [m^2]; and
c_W is the specific heat of the fluid flowing in the circuit [J/kgK]

2.2.6.2 Calculating the Temperature of Each Thermal Node

The temperature for each node in the current iteration, θ^h_p, is determined using the following equation:

$$\theta^h_p = \frac{\begin{pmatrix} H_A\theta^h_A + H_{IWS}\theta^h_{IWS} + H_F\theta^h_F + H_C\theta^h_C + H_{Rad}Q^h_{Rad} + H_{Conv}Q^h_{Conv} + \\ H_{CondUp}\theta^h_{p-1} + H_{CondDown}\theta^h_{p+1} + H_{Inertia}\theta^{h-1}_p + H_{Circuit}\theta^h_{Water,in}f^h_{rm} \end{pmatrix}}{H_A + H_{IWS} + H_F + H_C + H_{CondUp} + H_{CondDown} + H_{Inertia} + H_{Circuit}f^h_{rm}} \quad 2.37$$

Where H_A is the coefficient summarizing the heat transfer coefficient between the p^{th} thermal node and the air thermal node [W/K];
H_{IWS} is the coefficient summarizing the heat transfer coefficient between the p^{th} thermal node and the internal wall surface thermal node [W/K];
H_F is the coefficient summarizing the heat transfer coefficient between the p^{th} thermal node and the floor thermal node [W/K];
H_C is the coefficient summarizing the heat transfer coefficient between the p^{th} thermal node and thermal node "ceiling" [W/K];
H_{Rad} is the fraction of room radiant heat loads impinging on the p^{th} thermal node
H_{Conv} is the fraction of room convective heat loads acting on the p^{th} thermal node
H_{CondUp} is the coefficient summarizing the thermal conduction connection between the p^{th} thermal node and the previous thermal node, i.e. the $(p\text{-}1)^{th}$ thermal node [W/K];
$H_{CondDown}$ is the coefficient summarizing the thermal conduction connection between the p^{th} thermal node and the next thermal node, i.e. the $(p+1)^{th}$ thermal node [W/K];
$H_{Inertia}$ is the coefficient summarizing the inertia contribution at the p^{th} thermal node [W/K]; and
$H_{Circuit}$ is the coefficient summarizing the heat transfer coefficient between the p^{th} thermal node and the water inlet temperature [W/K].

The coefficients for each thermal node are given in Table 2-12 below:

Table 2-12: Coefficients for the Calculation of the Temperature at each Thermal Node

	F	I	PL	C	IWS	IW	A
H_A	$h_{A\text{-}F}A_F$	0	0	$h_{A\text{-}C}A_F$	$h_{A\text{-}W}A_W$	0	0
H_{IWS}	$h_{F\text{-}W}A_F$	0	0	$h_{F\text{-}W}A_F$	0	0	$h_{A\text{-}W}A_W$
H_F	0	0	0	$h_{F\text{-}C}A_F$	$h_{F\text{-}W}A_F$	0	$h_{A\text{-}F}A_F$
H_C	$h_{F\text{-}C}A_F$	0	0	0	$h_{F\text{-}W}A_F$	0	$h_{A\text{-}C}A_F$
H_{Rad}	$\frac{A_F}{2A_FA_W}$	0	0	$\frac{A_F}{2A_FA_W}$	$\frac{A_W}{2A_FA_W}$	0	0
H_{Conv}	0	0	0	0	0	0	1
H_{CondUp}	0	$\frac{A_F}{RU_p + RD_{p\text{-}1}}$	$\frac{A_F}{RU_p + RD_{p\text{-}1}}$	$\frac{A_F}{RU_p + RD_{p\text{-}1}}$	0	$\frac{A_W}{RU_p + RD_{p\text{-}1}}$	0
$H_{CondDown}$	$\frac{A_F}{RD_p + RU_{p+1}}$	$\frac{A_F}{RD_p + RU_{p+1}}$	$\frac{A_F}{RD_p + RU_{p+1}}$	0	$\frac{A_W}{RD_p + RU_{p+1}}$	0	0
$H_{Inertia}$	0	$\frac{c_pA_F}{\Delta t}$	0	0	0	$\frac{c_pA_W}{\Delta t}$	0
$H_{Circuit}$	0	0	$\frac{A_F}{R_t}$	0	0	0	0

Where $h_{A\text{-}C}$ is the convective heat transfer coefficient between the air and the ceiling [W/(m^{2}K)];
$h_{A\text{-}F}$ is the convective heat transfer coefficient between the air and the floor [W/(m^{2}K)];
$h_{A\text{-}W}$ is the convective heat transfer coefficient between the air and the internal walls [W/(m^{2}K)];
$h_{F\text{-}C}$ is the radiant heat transfer coefficient between the floor and the ceiling [W/(m^{2}K)];
$h_{F\text{-}W}$ is the radiant heat transfer coefficient between the floor and the internal walls [W/(m^{2}K)];
A_F is the total floor area [m^2];
A_W is the total area of internal vertical walls [m^2];
RU_p is the conduction thermal resistance of the p^{th} thermal node with the boundary of the $(p-1)^{th}$ thermal node [(m^{2}K)/W];
RU_{p+1} is the conduction thermal resistance of the $(p+1)^{th}$ thermal node with the boundary of the p^{th} thermal node [(m^{2}K)/W];
RD_p is the conduction thermal resistance of the p^{th} thermal node with the boundary of the $(p+1)^{th}$ thermal node [(m^{2}K)/W];
$RD_{p\text{-}1}$ is the conduction thermal resistance of the $(p\text{-}1)^{th}$ thermal node with the boundary of the p^{th} thermal node [(m^{2}K)/W];
c_p is the thermal capacity of the thermal node;
Δt is the calculation time step [s], i.e. for hourly time steps: Δt = 3 600s; and
R_t is the circuit's total thermal resistance

The radiant heat transfer coefficient $h_{F\text{-}C}$ is calculated using the following equation (Holman, 2010):

$$h_{F\text{-}C} = 5.5F_{vF\text{-}C} \qquad 2.38$$

Where $F_{vF\text{-}C}$ is the view factor between the floor and ceiling, determined from Figure 2-11 or Equation 2.39 below.

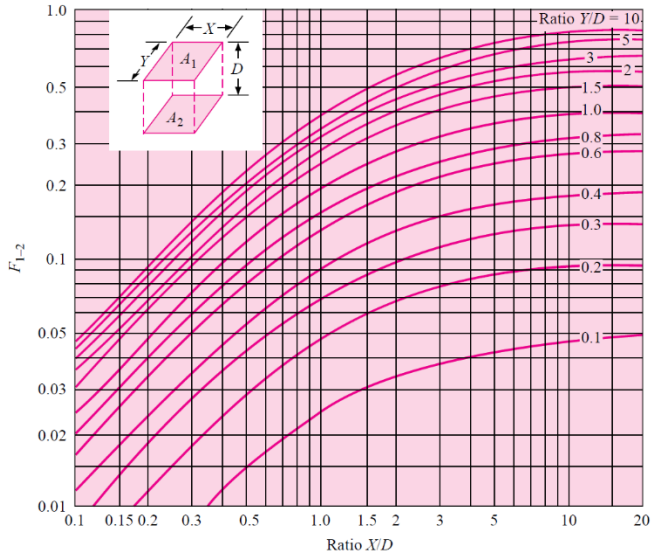

Figure 2-11: Radiation shape factor for Radiation between Parallel Surfaces (Holman, 2010)

$$F_{1\text{-}2}=(2/\pi xy)\left\{\begin{array}{c} ln[(1+x^2)(1+y^2)/(1+x^2+y^2)]^{1/2} \\ +x(1+y^2)^{1/2}\ tan^{-1}[x/(1+y^2)^{1/2}] \\ +y(1+x^2)^{1/2}\ tan^{-1}[y/(1+x^2)^{1/2}] \\ -x tan^{-1}x \\ -y tan^{-1}y \end{array}\right\} \text{ where } x = X/D \text{ and } y = Y/D \qquad 2.39$$

The radiant heat transfer coefficient $h_{F\text{-}W}$ is calculated using the following equation (Holman, 2010):

$$h_{F\text{-}W} = 5.5F_{vF\text{-}W} \qquad 2.40$$

Where $F_{vF\text{-}W}$ is the view factor between the floor and the wall, determined from Figure 2-12 or Equation 2.41 below:

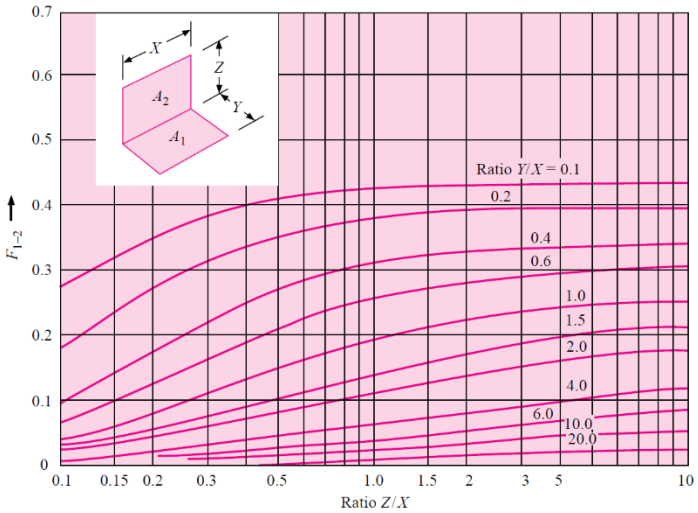

Figure 2-12: Radiation Shape Factor for Radiation between Perpendicular Rectangles with a Common Edge (Holman, 2010)

$$F_{1\text{-}2}=\frac{1}{\pi W}\left(\begin{array}{l} W\tan^{-1}\left(\frac{1}{W}\right)+H\tan^{-1}\left(\frac{1}{H}\right) \\ -\left(H^2+W^2\right)^{\frac{1}{2}}\tan^{-1}\left[\frac{1}{\left(H^2+W^2\right)^{\frac{1}{2}}}\right] \\ +\frac{1}{4}\ln\left\{\begin{array}{l}\left[\frac{\left(1+W^2\right)\left(1+H^2\right)}{\left(1+W^2+H^2\right)}\right] \\ \times\left[\frac{W^2\left(1+W^2+H^2\right)}{\left(1+W^2\right)\left(W^2+H^2\right)}\right]^{W^2} \\ \times\left[\frac{H^2\left(1+H^2+W^2\right)}{\left(1+H^2\right)\left(H^2+W^2\right)}\right]^{H^2}\end{array}\right.\end{array}\right) \quad \text{where } H = Z/X \text{ and } W = Y/X \qquad 2.41$$

2.2.6.3 Calculating the Actual Tolerance at each Iteration

The actual tolerance for each iteration ξ is determined using the following equation:

$$\xi = \sum_{\mathrm{p}}\left(\theta_p^h - \theta_p^{h'}\right) \text{ [K]} \qquad 2.42$$

Where $\theta_p^{h'}$ is the temperature for each node calculated from the previous iteration.

A solution is reached when the number of allowed iterations is less than the maximum iterations ($n < n_{max}$) and the current tolerance is less than the maximum permitted tolerance ($\xi < \xi_{max}$). A higher value for n_{max} and ξ_{max} can be used if a lower degree of accuracy is acceptable and a solution is not reached.

2.2.6.4 Finalising the Solution

Once the solution is reached, system heat transfers and temperatures can be determined using the following equations:

Heat transfer at the circuit, on the h^{th}-hour, is calculated using the following equation:

$$Q_{circuit}^h = \frac{\theta_{PL}^h - \theta_{Water,in}^h}{R_t} f_{rm}^h A_F \qquad 2.43$$

Heat transfer at the floor, on the h^{th}-hour, is calculated using the following equation:

$$Q_F^h = h_{A\text{-}F}A_F\left(\theta_A^h - \theta_F^h\right) + h_{F\text{-}C}A_F\left(\theta_C^h - \theta_F^h\right) + h_{F\text{-}W}A_F\left(\theta_{IWS}^h - \theta_F^h\right) + \frac{A_F}{2A_F + A_W}Q_{Rad}^h \qquad 2.44$$

Heat transfer at the ceiling, on the h^{th}-hour, is calculated using the following equation:

$$Q_C^h = h_{A\text{-}C}A_F\left(\theta_A^h - \theta_C^h\right) + h_{F\text{-}C}A_F\left(\theta_F^h - \theta_C^h\right) + h_{F\text{-}W}A_F\left(\theta_{IWS}^h - \theta_C^h\right) + \frac{A_F}{2A_F + A_W}Q_{Rad}^h \qquad 2.45$$

Heat transfer at the wall surface, on the h^{th}-hour, is calculated using the following equation:

$$Q_{IWS}^h = h_{A\text{-}W}A_W\left(\theta_A^h - \theta_{IWS}^h\right) + h_{F\text{-}W}A_F\left(\theta_F^h - \theta_{IWS}^h\right) + h_{F\text{-}W}A_F\left(\theta_C^h - \theta_{IWS}^h\right) + \frac{A_W}{2A_F + A_W}Q_{Rad}^h \qquad 2.46$$

Mean radiant temperature, on the h^{th}-hour, is calculated using the following equation:

$$\theta_{MR}^{h} = \frac{A_F\theta_F^h + A_F\theta_C^h + A_W\theta_{IWS}^h}{2A_F + A_W} \quad 2.47$$

Operative temperature, on the h^{th}-hour, is calculated using the following equation:

$$\theta_{Op}^{h} = \frac{\theta_A^h + \theta_{MR}^h}{2} \quad 2.48$$

Water outlet temperature, on the h^{th}-hour, is calculated using the following equation:

$$\theta_{water,\,out}^{h} = \theta_{water,\,in}^{h} + \frac{Q_{circuit}^{h}}{\dot{m}_{H,sp}A_F c_w} \quad 2.49$$

Once the water supply and return temperatures are determined, the chiller size can be determined using the refrigeration cycle discussed in Appendix A-5: The Chiller Plant and the Refrigeration Cycle.

2.3 Conventional Heating, Ventilation and Air Conditioning (HVAC) Systems

HVAC systems condition and distribute air throughout a building. Its main component, the Air Handling Unit (AHU), processes the air by heating, cooling, dehumidifying and filtering (McQuiston, Parker, & Spitler, 2005). The outside air can be cooled (or heated) in the AHU as it passes through the cooling (or heating) coils. The coil is a heat exchanger that transfers heat between the air and chilled or heated water (McQuiston, Parker, & Spitler, 2005). Heat is removed or added from the water by chillers and boilers and recirculated back to the AHU. The AHU is categorised by how it distributes energy, ventilation air, and its arrangement of components (McQuiston, Parker, & Spitler, 2005).

2.3.1 Variable Air Volume (VAV) System

A building with multiple zones with different heating and cooling requirements can be met by a Variable Air Volume (VAV) system. A damper adjusts the volume of air entering each zone (McQuiston, Parker, & Spitler, 2005). A single-duct (VAV) system, shown in Figure 2-23, shows outside air passing through the heating and cooling coils before being supplied through a single duct to a zone.

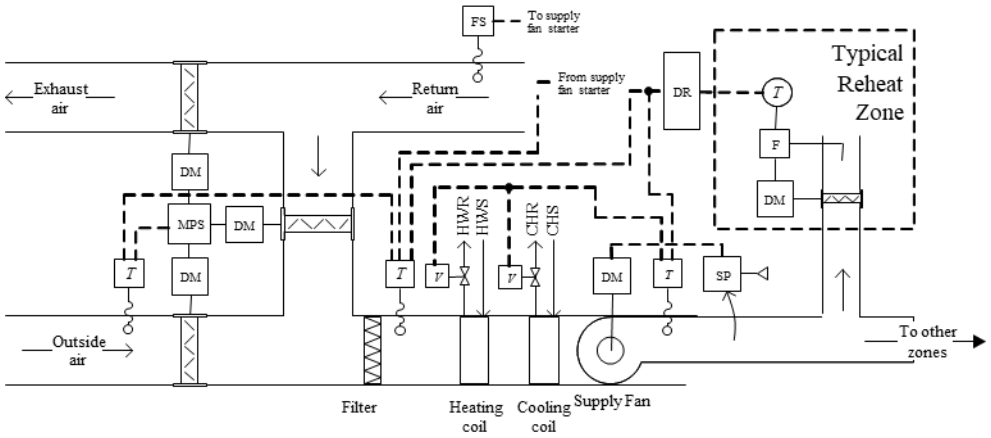

Figure 2-13: Schematic of a Single-duct Variable Air Volume (VAV) System (McQuiston, Parker, & Spitler, 2005)

Other types of AHUs include, Constant Air Volume (CAV) System; Constant Air Volume, Reheat System; Dual Duct (Double Duct) System and the Multi-Zone System which are described in Appendix A-3: Types of Air-Handling Units (AHU). The heating and cooling coil process and refrigeration cycle used by AHUs are covered in Appendix A-4: The Heating and Cooling Coil Process and Appendix A-5: The Chiller Plant and the Refrigeration Cycle.

2.4 Systems' Operational Control Strategies

The difference between TABS and conventional air systems can also be seen in their operational control strategies. The following section describes load shifting and thermal comfort considerations as control strategies for each system.

2.4.1 Control by Load Shifting

A typical control strategy for TABS includes shifting the chiller (or boiler) demand outside of working hours while the conventional air system operates during working hours (Rijksen, Wisse, & van Schijndel, 2010). Load shifting as a control strategy for TABS reduces peak load, meaning a smaller chiller size can be used, and the cost of electricity is reduced since some of the electricity would be consumed during periods when electricity is cheaper. The control strategy is shown in Figure 2-14, where the chiller in a TABS installation operates during the non-occupational periods instead of during occupational periods as in a conventional air system. The power required by the Air Handling Unit (AHU), highlighted in grey, is needed to provide air movement and dehumidification. It cannot be moved and remains the same in both strategies.

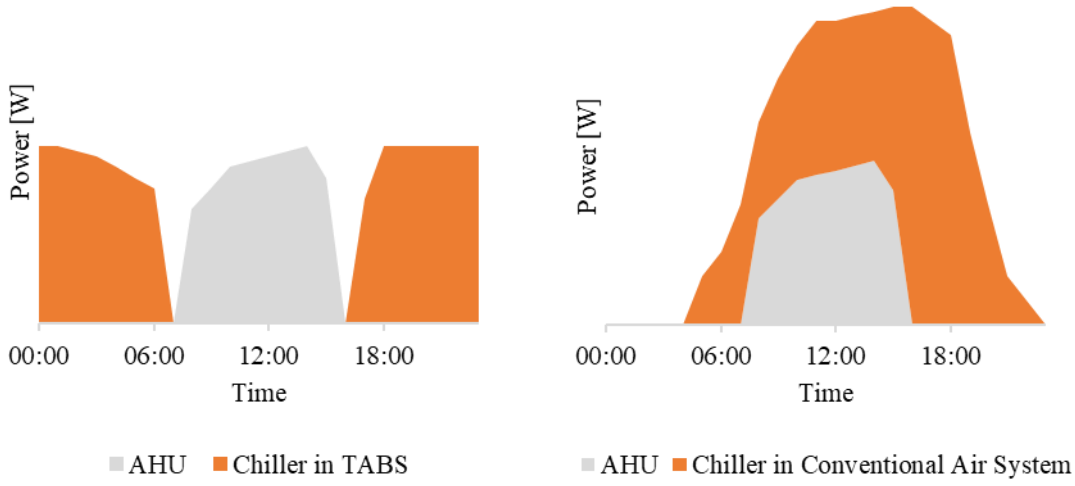

Figure 2-14: Load Shifting in TABS and HVAC Systems (Rijksen, Wisse, & van Schijndel, 2010)

2.4.2 Control by Thermal Comfort Considerations

The physical variables, namely air temperature, relative humidity and air velocity in Fanger's Predictive Mean Vote model, are attributes that a conventional air system can control. The process by which the physical attributes are managed to suit the occupants can be described in a psychrometric chart. The chart gives air's physical and thermodynamic properties at constant pressure (ASHRAE, 1992). The chart can be highly detailed; however, a simplified diagram is shown in Figure 2-15. The *x*-axis represents the dry-bulb temperature, which refers to ambient air temperature, and the curved grey lines represent the relative humidity. A more detailed chart is given in Appendix B-2: Psychrometric Chart.

The psychrometric chart determines how to condition the air to fall within the shaded comfort zones. In winter, when the outside air varies from "extreme cold" to "less cold", TABS transfers sensible heat into the building, increasing the air temperature. When the outside air temperature and humidity ratio falls in H1, H2, H3-2 or H4-2, the conventional air system humidifies the air. In summer, when the outside air varies from "hot and humid" to "moderate and dry", TABS extracts heat from the building,

decreasing the dry-bulb temperature. The HVAC dehumidifies the air when the outside temperature falls in C1-1 and C2-1. The figure shows the annual minimum and maximum temperatures (T_{o_min} and T_{o_max}). The intermediate period between $T_{limit\_heating}$ and $T_{limit\_cooling}$ is when no heating or cooling is required.

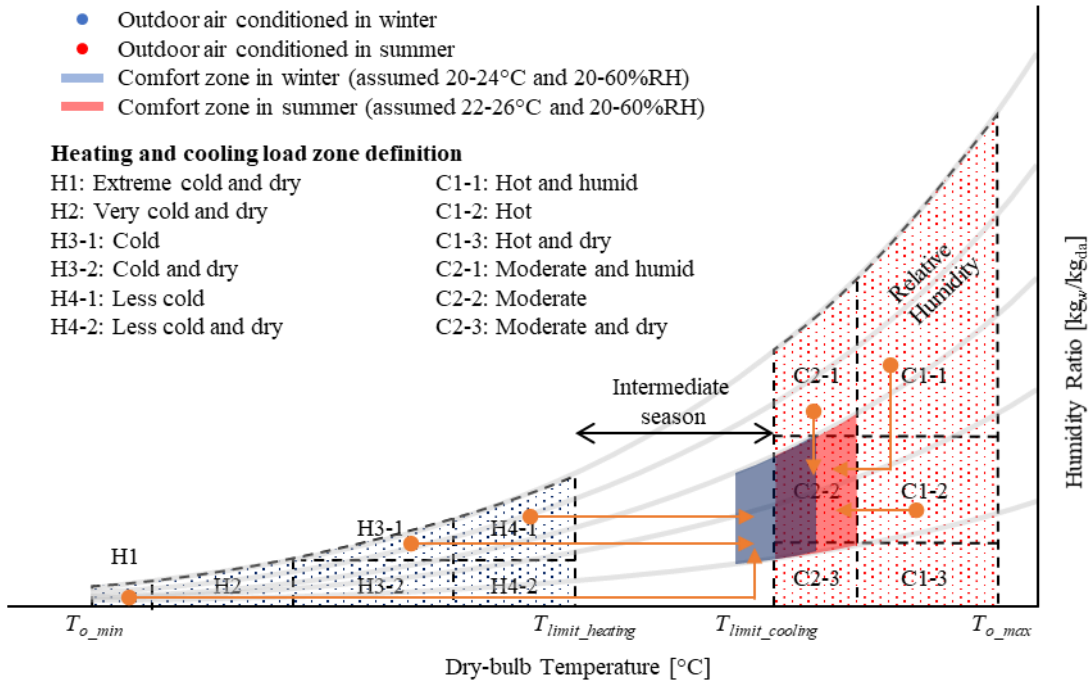

Figure 2-15: Heating and Cooling Load Zones (Lim, Song, & Song, 2014)

The heating and cooling zones can then be mapped to their respective loads. These loads are characterised by internal heat gains such as occupancy rate and activity level. Figure 2-16 shows that the heat load increases as the outside air temperature decreases from $T_{limit\_heating}$ to the annual minimum temperature T_{o_min}. The bar graph represents TABS's heating and cooling output, which is proportional to the heating and cooling load lines. The loads' slope depends on the building's degree of insulation and its internal heat gain characteristics (Lim, Song, & Song, 2014). The figure also shows that the heat load increases as the outside air temperature increases from $T_{limit\_cooling}$ to the annual maximum temperature T_{o_max}. T_{sf} represents the surface temperature of the ceiling or floor where the TABS pipelines are installed. The maximum surface temperature T_{sf_max}, as stated in ISO 7730, recommends that TABS should not operate at higher outputs than P1 when in heating mode. The standard recommends that TABS should not operate at higher outputs than P2 and P3 in cooling mode to prevent condensation. At P2 and P3, the return water temperature T_{wr} and surface temperature equal the dew point temperature T_{dew}. When the outside air temperature is higher than P2 and P3, the air must be cooled using AHU.

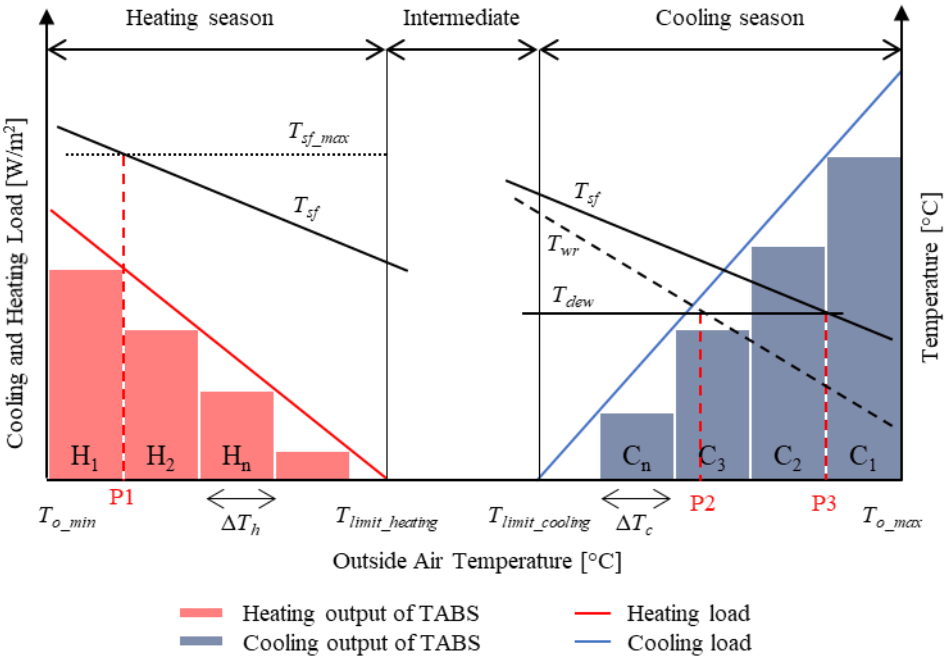

Figure 2-16: Conceptual Operational Strategy for TABS (Lim, Song, & Song, 2014)

A study by Saelens, Parys, & Baetens compared the energy usage of TABS with conventional HVAC systems in buildings located in Belgium. The research focused on the systems' energy usage as the occupants' behaviour changed. The occupants' behaviour, termed the "user profile", includes changes in the following parameters:

- **Occupancy Rate:** an indication of the occupancy levels of the building;
- **Mobility:** an indication of how often users move between office spaces; and
- **User Type:** an indication of how active or passive users are at switching lights and using shading devices such as automated curtains. Simulations of this user type did not include intermediate shading positions.

The researchers used the software package TRNSYS to simulate the energy flow within an environment. For thermal comfort, the temperatures were set between 21°C and 25°C. The slab would be cooled at night, and the control algorithm would ensure that the morning temperatures are never below 21°C. Using different user profiles, the simulations showed that the temperatures within the offices exceeded a temperature of 25°C only 2.2% of the time during office hours for the south-facing offices and 1.2% of the time during office hours for the north-facing offices. The researchers performed simulations to determine the influence of occupancy behaviour on the systems using fixed user profiles (i.e. fixed user type, occupancy rate and mobility). Analysis of different user profiles showed that the occupancy rate mainly influences the cooling demand. On average, the cooling demand increases by 18% for one of the user types used in the simulation and could even go up to 36% as the occupancy rate increases. The simulations also showed a vulnerability with TABS, that immediate control is challenging. HVAC systems address the immediate control vulnerability and the inability of TABS to provide dehumidification and filtering.

2.5 Concluding Remarks

This chapter explained thermal comfort and how it can be measured using the Predictive Mean Vote (PMV) and PPD (Predicted Percentage of Dissatisfaction). It was discussed that thermal comfort might

have to be adjusted for a region. Thermal comfort can be achieved by space heating systems such as Thermally Activated Building Systems (TABS) and HVAC systems. Various TABS and HVAC systems were presented, and the methods used to determine their respective energy consumption were also discussed. Either system's most significant energy consumer is the chiller, boiler and heat pump. The research hypothesis in Chapter 1.2 was validated using the research methodology described in the next chapter.

3 Research Methodology

In Chapter 1, the research aim was explained as determining the magnitude by which Thermally Activated Building Systems (TABS) consume less energy than conventional Heating, Ventilation and Air-Conditioning (HVAC) systems while ensuring thermal comfort for occupants in an office building. The approach to validating the research hypothesis and answering respective questions was similar to (Rijksen, Wisse, & van Schijndel, 2010), where the chiller energy consumption of TABS and HVAC systems were simulated and compared with actual installations in an office building. Their research used the software package, TRNSYS, to simulate the cooling power of the systems in Dutch climate conditions. The results showed that the TABS' demand and energy consumption are significantly less than the HVAC system. The results also showed that the software package accurately simulated TABS' cooling power and the rooms' operative temperature.

In this research, the systems' chiller demand and energy consumption were simulated using the software package EnergyPlus and the TABS calculator in ISO 11855. Each system's chiller was simulated, and its results were compared with actual metered energy consumption to determine the tools' accuracy. In each simulation, the thermal comfort of the occupants was determined using Fanger's Predictive Mean Vote (PMV) model given in ISO 7730 and ASHRAE 55. Fanger's PMV model has been used in other research and is widely accepted in describing thermal comfort (Rhee, Olesen, & Kim, 2012). Although the office buildings' sizes were similar, they differed in thermal load, occupancy levels and insulation. Therefore, once the tools were determined to accurately simulate the system's chiller demand and energy consumption, the hypothesis was validated by modelling and simulating the systems in the same office building. The series of simulations were presented as case studies and are further described in the following sections:

3.1 Case Study 1: Simulating TABS' Energy Consumption

The first case study aimed to determine the accuracy of the TABS calculator given in ISO 11855 by comparing its results with the demand and energy consumption of an actual TABS installation. This case study required the design and construction of TABS and included the following steps:

a. Developed the pipe layout in LoopCAD, a software tool used to develop circuit layout designs for radiant heating systems, and employed HVAC contractors for installation
b. Once the building was operational, data loggers with valid calibration certificates were installed on the chiller to collect hourly energy consumption. A sanity check was performed to ensure that there was no missing data and that it was within reasonable parameters, i.e. the energy consumed should not have negative values and be greater than its rated nameplate.
c. Computed a linear regression on the chiller energy consumption using the online tool from degreedays.net to determine the building's base temperature. This tool is further described in chapter 4.5.
d. Collected hourly weather data from the Cape Town International Airport weather station and reformatted it so it could be used in OpenStudio and EnergyPlus, software tools used to model and quantify building designs' energy performance.
e. Imported the office building's model into OpenStudio and EnergyPlus. Modelled the occupation, lighting, and electrical load of the building in OpenStudio, set the building's base temperature as determined in step c, and simulated to determine the required cooling load to achieve thermal comfort.
f. Inputted the resultant cooling load into the TABS calculator, given in ISO 11855, to determine the systems' hourly energy consumption. The process of rewriting the calculator from the standard is described in the next chapter.

g. The chiller's actual hourly energy consumption was compared with the TABS calculator results to determine its accuracy.
h. Used the PMV calculator in ISO 7730 and ASHRAE 55 to quantify occupants' thermal comfort. The process of rewriting the calculator from the standard is described in the next chapter.

3.2 Case Study 2: Simulating HVAC's Energy Consumption

The second case study aimed to determine the accuracy of the EnergyPlus simulations by comparing the results with the actual chiller demand and energy consumption of a conventional HVAC system. The case study included the following steps:

a. Collected hourly energy consumption from data loggers with valid calibration certificates from an office building with an HVAC installation. The building's size was similar to the building with the TABS installation in the previous case study. A sanity check was performed on the data to ensure that there was no missing data and that the data was within reasonable parameters, i.e. the energy consumed should not have negative values and be greater than its rated nameplate.
b. Computed a linear regression on the hourly energy consumption using the online tool degreedays.net to determine the building's base temperature. This tool is further described in chapter 4.5.
c. Collect hourly weather data from the Cape Town International Airport weather station and reformat it so it can be used in OpenStudio and EnergyPlus.
d. Modelled the office building in SketchUp Pro, a 3D modelling software used for drawing and design applications, and imported it into OpenStudio and EnergyPlus. Modelled the occupation, lighting, and electrical load of the building in OpenStudio, set the building's base temperature as determined in step c, and simulated to determine its energy consumption and thermal comfort variables.
e. Compared the energy consumption of an actual HVAC with the results from the simulation to determine its accuracy.
f. Analysed the PMV and PPD values as determined by EnergyPlus to ensure that the occupants experienced satisfactory thermal comfort.

3.3 Case Study 3: Simulating TABS and HVAC's Energy Consumption in a Simplified Office Building

Once the accuracy of the TABS calculator and EnergyPlus were confirmed, the tools were used to model and simulate TABS and HVAC in the same office building with the same heat loads, occupancy levels and thermal insulation. This case study would confirm the research hypothesis and included the following steps:

a. Modelled a simple office building in SketchUp Pro and imported it into OpenStudio. The occupation, lighting, and electrical loads were modelled in OpenStudio and EnergyPlus and simulated to determine the required cooling load to achieve thermal comfort.
b. An HVAC system was modelled on the office building model in OpenStudio and simulated to determine the HVAC's cooling load and energy consumption.
c. Various percentages of the cooling load were input into the TABS calculator to determine which would result in satisfactory thermal comfort. The calculator would also determine the hourly energy consumption of the TABS.
d. The simulated energy consumption of the TABS and HVAC was compared with each other.
e. Determined and compared the thermal comfort achieved in both TABS and HVAC.

f. Confirmed that the research hypothesis is valid.

3.4 Developing a Business Case for TABS

After validating the research hypothesis, this business case was developed to emphasise the impact of a TABS compared to the conventional HVAC system. The business case was based on an office building with an HVAC system that had reached its end of life and had a proposal to replace it with an energy-efficient HVAC system. The business case included the following steps:

a. Collected half-hourly energy consumption of the entire building since the HVAC did not have meters installed. The HVAC system was assumed to consume 26% of the total energy consumption, as given in literature studies.
b. Determined the energy usage of the proposed HVAC installation. The usage was based on comparing the capacity of the old and proposed chillers and boilers.
c. Determine the energy usage of the TABS and the costs of the installation.
d. Compared the energy consumption from both systems and applied an electricity tariff to determine the annual cost of the electricity, assuming a 6% annual increase per the maximum CPI target set by the South African Reserve Bank.
e. Determined and compared the simple and discounted payback period achieved from both systems.

3.5 Concluding Remarks

This chapter described the methodology used to validate the research hypothesis given in Chapter 1.2. The approach mentioned the software tools used in the research (i.e. the PMV and TABS calculators, EnergyPlus and OpenStudio, LoopCAD and DegreeDays). These tools are further described in the following chapter.

4 Tools used for Analysis

ISO 11855 and ASHRAE 55 provide computer programmes that calculate PMV, the heating and cooling capacity of TABS and chiller sizing. The calculators were written in the BASIC and FORTRAN programming languages, so the calculators were rewritten in the Python programming language for the following reasons:

- It would allow the calculators to be on a single code base, allowing them to be integrated; and
- The code could be modified to make it applicable to the case studies in the research;

The standards provide expected results from running the calculator and simulation, given specific inputs. The following section describes the implementation of the calculators in Python and compares its output with the expected results in the standards. A description of OpenStudio, EnergyPlus, LoopCAD and DegreeDays is also provided.

4.1 The Predictive Mean Vote (PMV) Calculator

As stated in 2.1.1, determining the PMV is an iterative process and can be calculated using computer programming. ISO 7730 and ASHRAE 55 include a PMV calculator developed in the BASIC programming language. The calculator uses equations 2.1 to 2.10 to determine PMV. The inputs required to perform the calculation are the four physical and two personal variables listed in Table 2-1.

The inputs and results from the calculators and ISO 7730 are given in Table 4-1. The standard does not give a rationale behind the selected inputs besides being used to validate the results when the calculator is being tested. The table shows that the PMV and PPD values given in ISO 7730 and those determined by the Python calculator have a mean difference of -0.0246 and 0.0769, respectively. Therefore, it was determined that the Python calculator's PMV and PPD results have an 80% confidence to be within 0.015 and 0.5, respectively, of the results in ISO 7730. The small confidence interval means that the calculator, included in Appendix A: Thermal Comfort Tables and Calculators, can determine PMV and PPD accurately.

Table 4-1: Input Values used to Test the PMV Calculator

	Inputs						**Results from ISO 7730**		**Results from Python Calculator**		**Difference**	
	Air Temp [°C]	RH [%]	Radiant Temp [°C]	Air Vel [m/s]	Met	CLO	PMV	PPD [%]	PMV	PPD [%]	PMV	PPD [%]
1	22	60	22	0.1	1.2	0.5	-0.75	17	-0.7	15	-0.05	2
2	27	60	27	0.1	1.2	0.5	0.77	17	0.81	19	-0.04	-2
3	27	60	27	0.3	1.2	0.5	0.44	9	0.48	10	-0.04	-1
4	23.5	60	25.5	0.1	1.2	0.5	-0.01	5	0.03	5	-0.04	0
5	23.5	60	25.5	0.3	1.2	0.5	-0.55	11	-0.51	10	-0.04	1
6	19	40	19	0.1	1.2	1	-0.6	13	-0.57	12	-0.03	1
7	23.5	40	23.5	0.1	1.2	1	0.5	10	0.39	8	0.11	2
8	23.5	40	23.5	0.3	1.2	1	0.12	5	0.15	5	-0.03	0
9	23	40	21	0.1	1.2	1	0.05	5	0.08	5	-0.03	0
10	23	40	21	0.3	1.2	1	-0.16	6	-0.13	5	-0.03	1
11	22	60	22	0.1	1.6	0.5	0.05	5	0.08	5	-0.03	0
12	27	60	27	0.1	1.6	0.5	1.17	34	1.2	35	-0.03	-1
13	27	60	27	0.3	1.6	0.5	0.95	24	0.99	26	-0.04	-2
										Average PMV Difference:	-0.0246	
										Average PPD Difference:	0.0769	

The Python PMV calculator was modified to output the heat losses for the 13 calculations performed; the results are given in Table 4-2 below. The table shows that the heat losses from the occupants are primarily caused by the heat difference through the skin, radiation and convection, consistent with the literature (Romanovsky, 2018). The heat loss by sweating remained the same for the first ten calculations because it was influenced by the metabolic rate, which did not change in their respective scenarios.

Table 4-2: Heat Loss and Gains determined by PMV Calculator

	Results from Python Calculator		**Heat loss difference through the skin**	**Heat loss by sweating**	**Latent respiration heat loss**	**Dry respiration heat loss**	**Heat loss by radiation**	**Heat loss by convection**	**Total**
	PMV	PPD							
		[%]	[W/m^2]	[W/m^2]	[W/m^2]	[W/m^2]	[W/m^2]	[W/m^2]	[W/m^2]
1	-0.7	15	11.16	4.88	5.08	1.17	31.92	28.96	83.17
2	0.81	19	9.47	4.88	4.42	0.68	18.64	16.34	54.43
3	0.48	10	9.47	4.88	4.42	0.68	16.32	24.82	60.59
4	0.03	5	10.7	4.88	4.9	1.03	20.87	26.93	69.31
5	-0.51	10	10.7	4.88	4.9	1.03	17.04	40.87	79.42
6	-0.57	12	13.32	4.88	5.92	1.47	28.4	26.67	80.66
7	0.39	8	12.47	4.88	5.59	1.03	20.15	18.26	62.38
8	0.15	5	12.47	4.88	5.59	1.03	16.67	26.26	66.9
9	0.08	5	12.57	4.88	5.63	1.07	27.52	16.57	68.24
10	-0.13	5	12.57	4.88	5.63	1.07	24.38	23.8	72.33
11	0.08	5	10.67	14.65	6.77	1.56	30.08	27.35	91.08
12	1.2	35	8.98	14.65	5.9	0.91	16.78	14.73	61.95
13	0.99	26	8.98	14.65	5.9	0.91	14.68	22.37	67.49

The occupants' heat losses for the first calculation in Table 4-2 are illustrated in Figure 4-1. It can be seen that the occupant loses most heat losses by radiation and convection, accounting for 38.38% and 34.82%, respectively. Table 2-2, which gives metabolic rates for typical office activities, gives that the metabolic rate of 1.2 equals 70W/m^2. Therefore, as occupants' total heat loss is 83.17W/m^2; the heat balance is 70W/m^2 – 83.17W/m^2 = –13.17 W/m^2. The negative heat balance means the occupant releases energy into the environment, making the occupant approach a slightly cool thermal experience, consistent with the sensation scale in Table 2-4 with a PMV of -0.7.

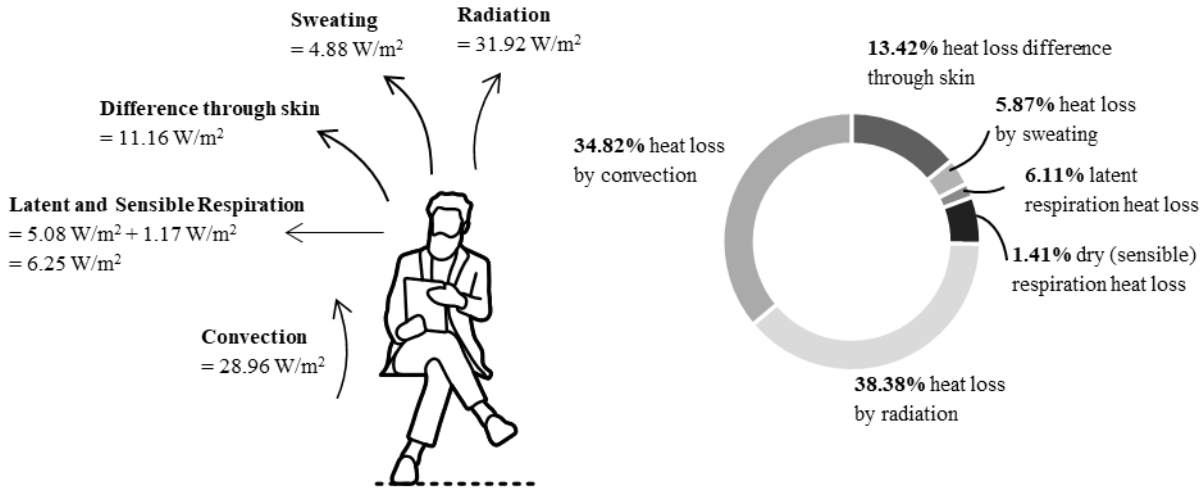

Figure 4-1: Illustration of Heat Gains (Losses) of Occupant

This section showed that the PMV calculator, rewritten in Python, produced results consistent with the results given in ISO 7730. The results have also confirmed that most heat losses and gains occur by convection and radiation.

4.2 The TABS Calculator

The TABS calculator, rewritten from ISO 11855-4, can output various information about TABS, such as air and surface temperatures, heat flows and chiller demand and energy consumption. The calculator, written in FORTRAN, is derived from the Simplified Model described in Chapter 2.2.6. As with the PMV calculator, the calculator was rewritten in Python and tested with input from the ISO standard. The characteristics of the test slab are shown in Table 4-3 below.

Table 4-3: Test Slab Characteristics (ISO, 2012)

Layer no.	Layer side	Layer Thickness, δ [m]	No. of Partitions	Thermal Conductivity, λ [W/(mK)]	Density, ρ [kg/m^3]	Specific Heat, c [J/(kgK)]
1	Upper	0.02	2	0.17	700	2300
2	Upper	0.07	3	1.1	1900	850
3	Upper	0.1	4	1.9	2000	880
4	Lower	0.1	4	1.9	2000	880

Each layer in the slab represents a thermal node. Other thermal nodes in the space, including the air, ceiling, floor and wall, have the characteristics given in Table 4-4 below.

Table 4-4: Test Space Characteristics (ISO, 2012)

Floor Area, A_F	30	[m^2]
Wall Area, A_W	48	[m^2]
Convective Heat Transfer Coefficient between Air and Floor, $h_{A\text{-}F}$	1.5	[W/(m^{2}K)]
Convective Heat Transfer Coefficient between Air and Ceiling, $h_{A\text{-}C}$	5.5	[W/(m^{2}K)]
Convective Heat Transfer Coefficient between Air and Internal Walls, $h_{A\text{-}W}$	2.5	[W/(m^{2}K)]
View Factor between Floor and External Wall, $F_{v\ F\text{-}EW}$	0.21	
View Factor between Floor and Ceiling, $F_{vF\text{-}C}$	0.35	
Additional Floor Thermal Resistance, R_{addF}	0.1	[(m^{2}K)/W]
Additional Ceiling Thermal Resistance, R_{addC}	0	[(m^{2}K)/W]
Wall Surface Thermal Resistance, R_{walls}	0.05	[(m^{2}K)/W]
Specific Thermal Capacity of Internal Walls, c_w	25600	[J/(m^{2}K)]

Table 4-5 below includes the total thermal resistance and water characteristics required by the calculator. The thermal resistance can be determined from TABS' heating and cooling capacity calculations described in Chapter 2.2.5. TABS Type E was used in the test, meaning that the total thermal resistance was determined using the General Resistance Method described in Chapter 2.2.5.2. Its calculator is included in Appendix C-3: Type E Calculator.

Table 4-5: Test Fluid Characteristics (ISO, 2012)

Total Thermal Resistance, R_t [(m^{2}K)/W]	Specific Heat Capacity, c_w [J/(kgK)]	Mass Flow, $\dot{m}_{Hspm}$ [kg/(m^{2}s)]
0.073	4187	0.01

The TABS calculator goes through an iterative process to balance the cooling load and the heat that flows through the ceiling, floor and walls. The convective and radiant cooling load over 24 hours are given in Table 4-6. Running mode indicates when the chiller is switched on (1) or off (0). In the example, the chiller is on in the morning and evening.

Table 4-6: Test Input Cooling load and Energy

Time	Convective Cooling Load, Q_{conv} [W]	Radiant Cooling Load, Q_{rad} [W]	Total Cooling Load [W]	Running Mode
00:00 – 07:59	30	10	40	1
08:00 – 18:59	400	300	700	0
19:00 – 23:59	150	100	350	1
Total Cooling Energy	**5390 Wh**	**3880 Wh**	**9270 Wh**	

The standard (ISO) and Python calculator (Sim) results are illustrated in Figure 4-2 below and tabulated in Appendix C-5: Hourly Boundary Conditions and Results. The figure shows that the respective heat flows are almost identical and that the total heat flows equal the total cooling load for each hour. The figure also shows that most heat flows through the ceiling and floor. A positive heat flow represents cooling, and a negative heat flow represents heating. The heat flow through the floor and walls is negative in the morning and evening, meaning that heat would flow into the space through the floor and exit through the ceiling.

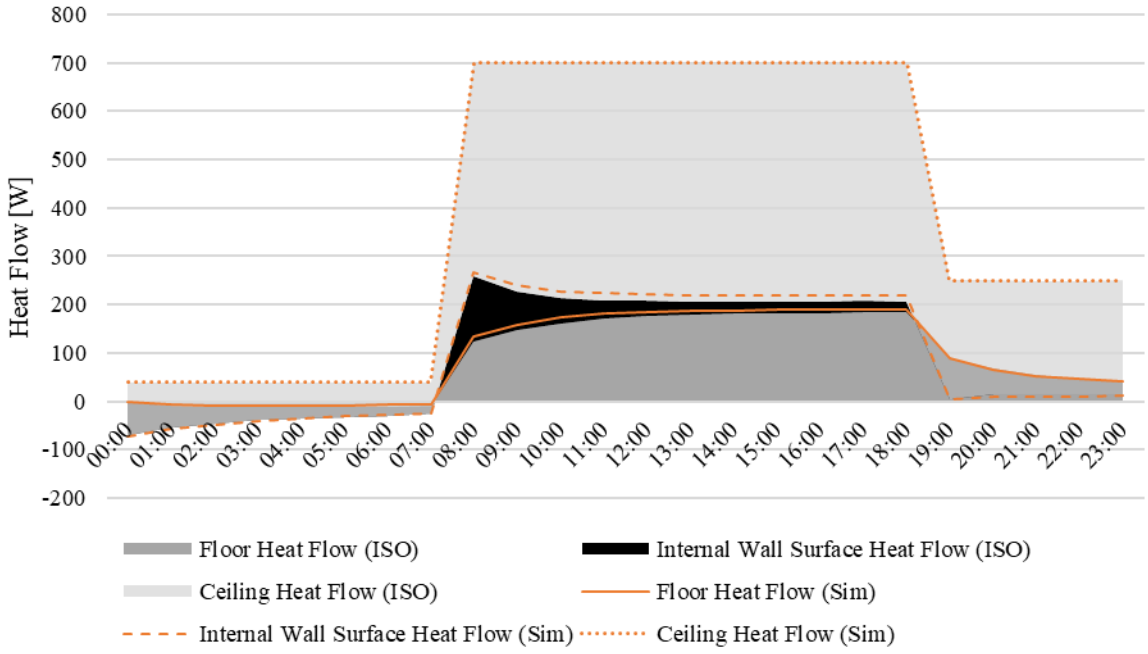

Figure 4-2: Heat Flow through Surfaces in Room

Figure 4-3 below shows the air temperature and heat extracted by the system. A breakdown of the values that make the figure is tabulated in Appendix C-5: Hourly Boundary Conditions and Results. The figure shows that the air and surface temperatures vary between 21 and 26°C throughout the day. When the chiller is off, the air temperature rises slightly but does not exceed 26°C. The ability of the system to provide cooling during the day, even when the chiller is off, is an example of TABS' load-shifting control strategy described in Chapter 2.4.1.

The cooling energy equals the sum of the heat flow through the floor, walls and ceiling. The energy is also equal to the heat flow through the circuit to the evaporator in the chiller. Therefore, chiller demand can be determined using Equation **12.13** when the Coefficient of Performance (CoP) is known.

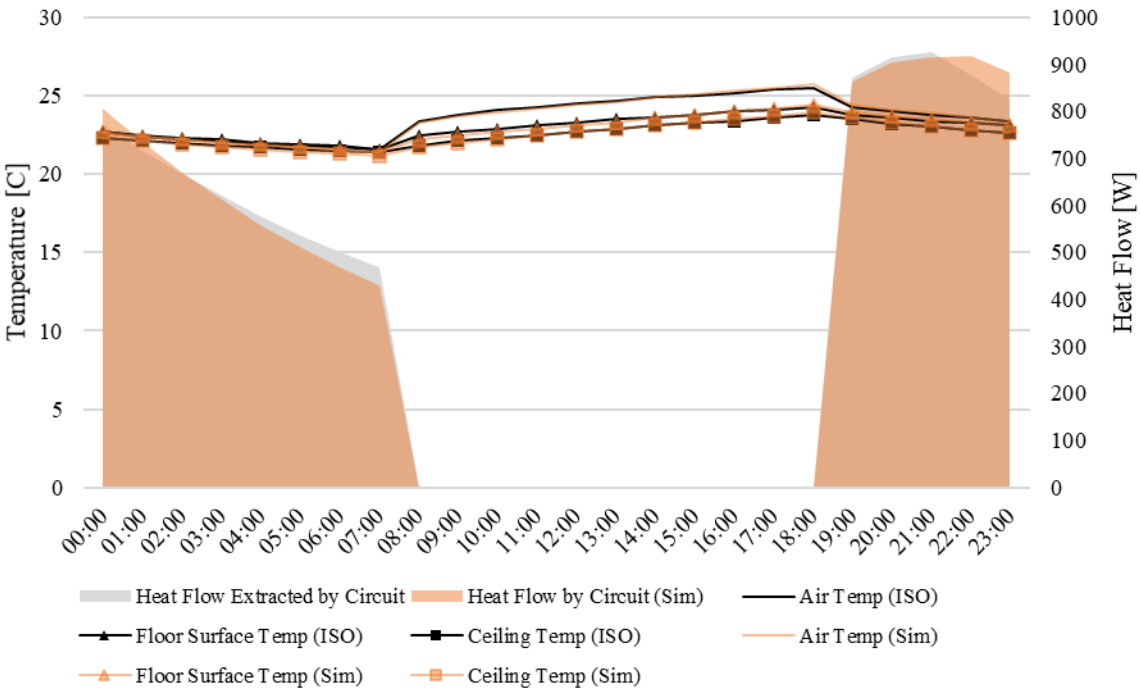

Figure 4-3: Surface Temperatures and Heat Flow through Circuit

This section showed that rewriting the TABS calculator into the Python programming language resulted in similar outputs to the ISO standard results. The calculator can then be modified to work with the PMV calculator described in Chapter 4.1.

4.3 EnergyPlus and OpenStudio

EnergyPlus is a console-based software tool architects, engineers, and researchers use to model and quantify building designs' energy performance (OpenStudio, 2020). The tools provide methods for simulating HVAC, natural ventilation and Leadership in Energy and Environmental Design (LEED) calculations. At the design stages, the model assists architects and engineers to optimise the balance between thermal comfort, the initial capital cost of construction, ongoing operational costs and environmental footprint while complying with building regulations (DesignBuilder Software Ltd, 2021). The development of EnergyPlus is funded by the U.S. Department of Energy's (DOE) Building Technologies Office (BTO) (EnergyPlus, 2021). Figure 4-4 below shows screenshots of EnergyPlus' interface. OpenStudio is a more user-friendly and free interface to EnergyPlus; see Figure 4-5 below.

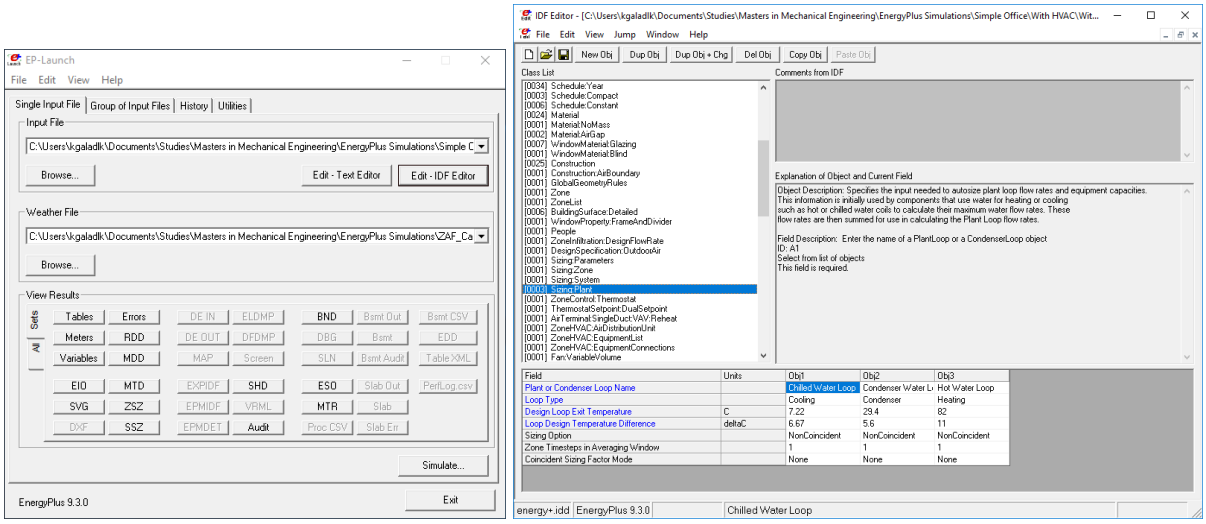

Figure 4-4: Interface to Input EnergyPlus Files and Initiate Simulations (left) Interface to Edit EnergyPlus File (right)

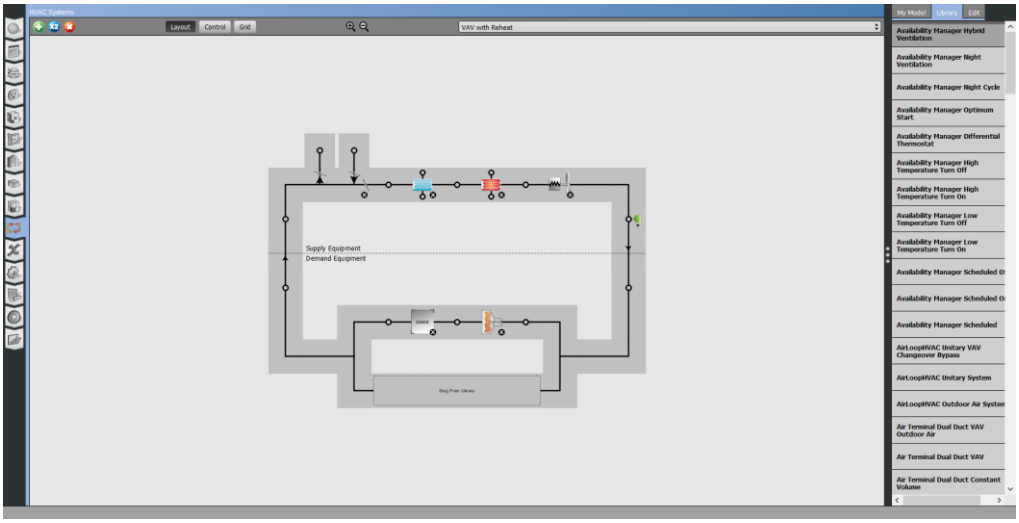

Figure 4-5: OpenStudio Interface for Designing HVAC System

4.3.1 Simulation Inputs

Running a simulation requires specific input, and this research required occupancy levels, lighting load, electrical load and weather data.

4.3.1.1 Occupancy Levels, Lighting Load and Electrical Load

Where metered data for occupancy levels, lighting, and electrical loads were unavailable, minimum safety values were taken from SANS 10400. Minimum occupancy levels for space types are given in Appendix B-3: Occupancy or Building Classification . The metabolic rate for each person in an office was taken as the maximum heat for office activities, i.e. 2met (120W/m^2) per person.

4.3.1.2 Weather Data

OpenStudio can download the weather file required for the simulation based on the building's location (EnergyPlus, 2021). The file may not include weather data for a particular simulation period but can be used to determine chiller and boiler sizes required for thermal comfort. The file did not have the data for the simulation periods needed for this research. However, the data was retrieved from the closest weather station to the buildings at Cape Town International Airport (airport code: FACT). EnergyPlus

is bundled with the tool Weather Statistics and Conversions (Figure 4-6), which converts the downloaded file into a CSV file that can be updated with the relevant weather data. The CSV file can then be saved with the .epw extension, i.e. the EnergyPlus weather file extension that can then be used in EnergyPlus. The data to be updated includes air temperature, dew point, humidity and air pressure.

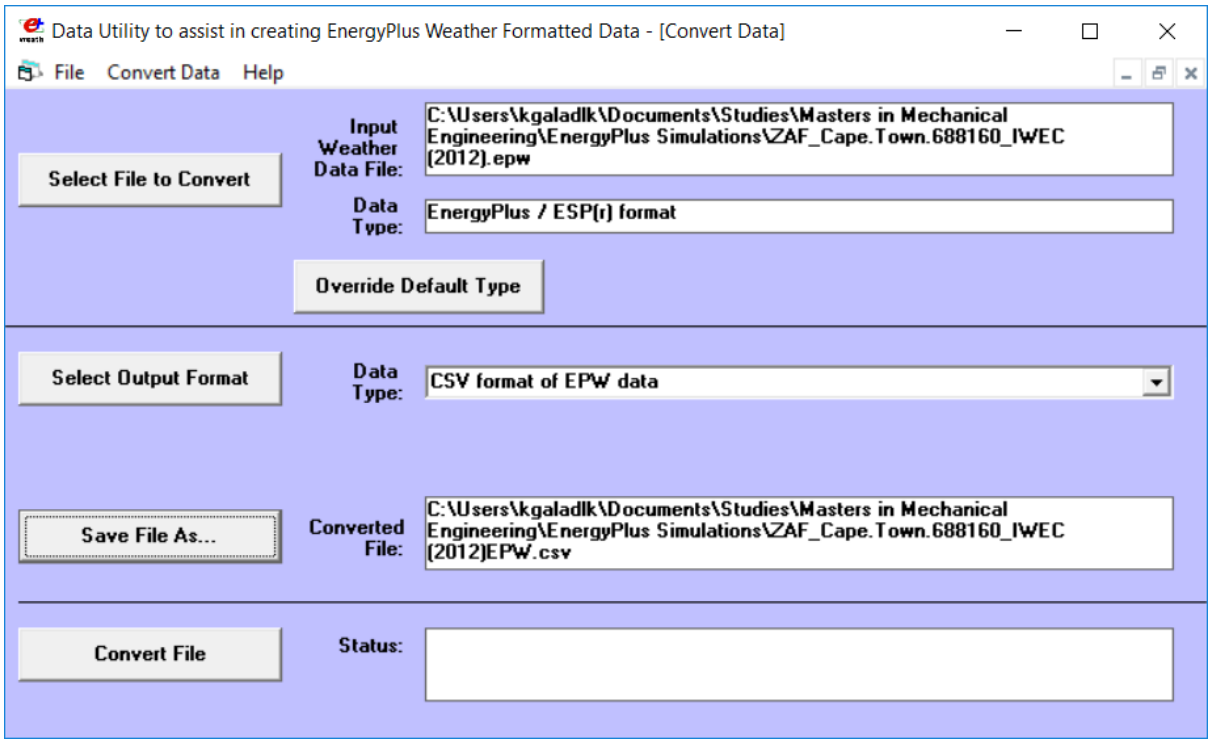

Figure 4-6: Weather Statistics and Conversions Screenshot

4.3.2 Simulation Outputs

EnergyPlus simulations aim to determine the HVAC's energy consumption required to optimise occupants' thermal comfort. The tool can output different results, including air, radiant and operative temperature, and relative humidity necessary to compute PMV and PPD. Other outputs essential for this research include the total cooling load resulting in satisfactory thermal comfort. The cooling load is heat removed from the office building and is a combination of sensible and latent load (Liu, Wang, & Xu, 2021), where:

- The sensible cooling load is a measure of the amount of energy required to change air temperature; and
- The latent cooling load is a measure of the amount of energy required to dehumidify the air

4.4 LoopCAD

LoopCAD is a software tool primarily used to develop circuit layout designs for radiant heating systems (RHS). Additionally, it can perform radiant heating and cooling calculations (Avenir, 2019). Hydronics refers to fluids as the medium for heating and cooling systems. Typically water is the medium used in RHS; however, glycol and oil can be used. LoopCAD performs hydronic calculations using water as the medium. The calculations comply with various standards such as ASHRAE 2013, CSA F280-12 and the Air-Conditioning Contractors of America (ACCA) approved Manual J. Figure 4-7 are screenshots from the software when (a) selecting the radiant floor panel and (b) an example of a circuit layout. The example circuit is included for illustrative purposes only.

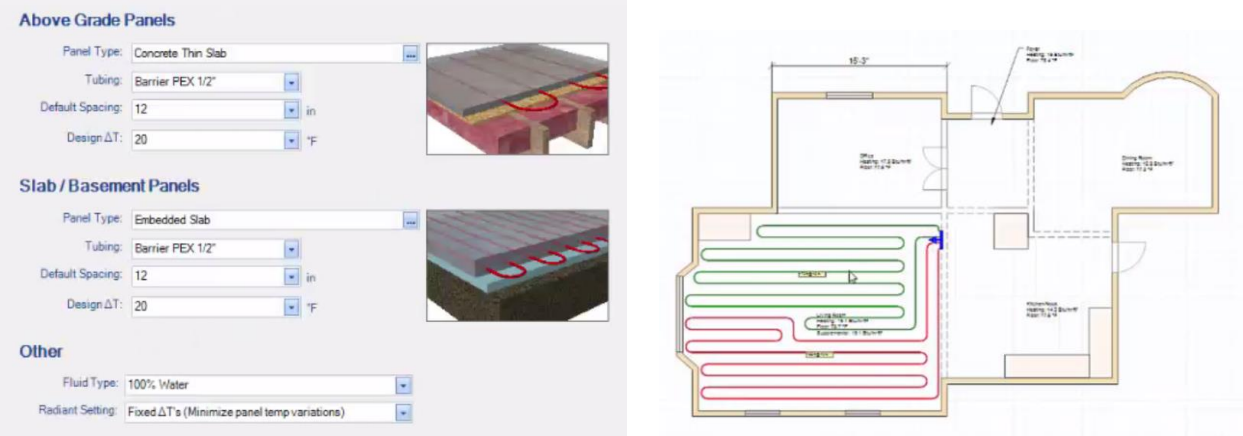

(a) (b)

Figure 4-7: Screenshots from LoopCAD for (a) Radiant Panels Selection and (b) Circuit Drawing Example

4.5 Linear Regression and DegreeDays

Linear regression refers to mathematically determining the relationship between two or more variables. It is characterised by two types of variables (Chatterjee & Simonoff, 2013):

1. The dependent variable y, also called the target or response variable; and
2. A set of independent variable(s) x_n, called the predicting variable, potentially predicts or models the dependent variable.

The simplest linear model consists of a dependent variable that changes at a constant rate of a single independent variable. Their relationship can be equated to a straight line (Rawlings, Pantula, & Dickey, 1998):

$$y = \beta_0 + \beta_1 x \quad | \quad 4.1$$

Where β_0 is the y-intercept when $x = 0$;
β_1 is the slope (i.e. the rate of change) of the line;

For data that consists of multiple independent variables $\{x_1, x_2, \ldots, x_i\}$, the equation is generalised to a multiple linear regression:

$$y = \beta_0 + \beta_1 x_1 + \cdots + \beta_n x_n + \varepsilon \quad | \quad 4.2$$

Where ε is the error term that represents the deviation from the population mean; and
the subscript n denotes the number of independent variables.

In this thesis, linear regression was used to determine the relationship between the space cooling system's energy consumption (i.e. the dependent variable y) and outside air temperature (i.e. the independent variable x). The system provides cooling when the outside air temperature exceeds the building's base temperature, i.e. the outside air temperature when the system is not required to provide cooling (Bromley, 2022). The system consumes the least energy and may only provide ventilation at this temperature. The measure of the system's energy usage when the outside air temperature is above the building's base temperature is called Cooling Degree Day and is calculated as follows (Bromley, 2022):

$$CDD(T_b) = \sum_{t=0}^{n} [(T_{o,t} - T_b) \times \frac{1}{n} \text{days}] \qquad 4.3$$

Where T_b is the building's base temperature [°C];
t is the time in the day when the data is recorded;
n is the number of data recordings in a day;
$T_{o,t}$ is the outside air temperature at time t when greater than T_b [°C];

The degree-days website gives an example of a building with a base temperature of 21°C. For illustrative purposes, a similar example is created for Figure 4-8, Figure 4-10 and Figure 4-11, showing the Cooling Degree Days (CDD) as a function of the outside temperature.

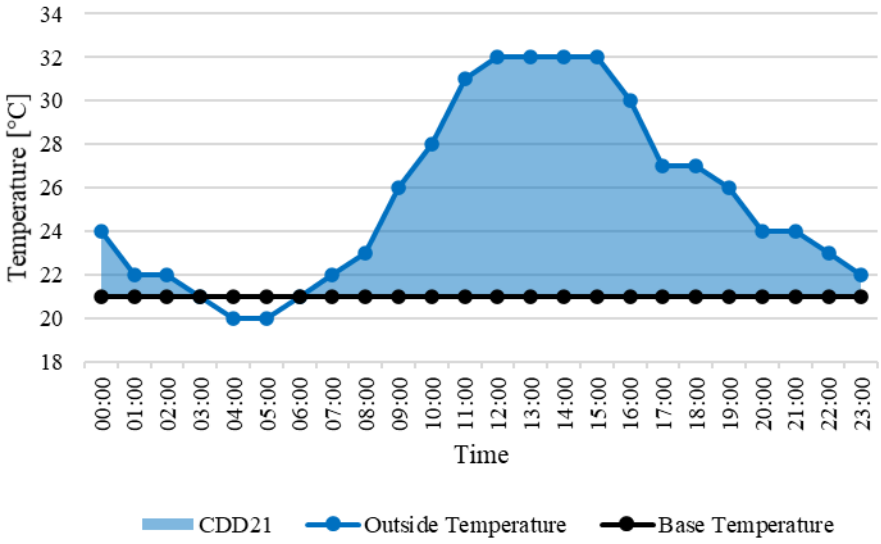

Figure 4-8: Example Building Baseline and Actual Temperature

The CDD with the building at a base temperature of 21°C, i.e. CDD21, for the day given in Figure 4-8 will be calculated as follows:

$$\begin{aligned}
\text{CDD21} &= [(T_o - T_b)_{00:00} \times 1/24 \text{ days}] + \ldots + [(T_o - T_b)_{23:00} \times 1/24 \text{ days}] \\
&= [(24 - 21)_{00:00} \times 1/24 \text{ days}] + \ldots + [(22 - 21)_{23:00} \times 1/24 \text{ days}] \\
&= [3 + 1 + 1 + 0 + 0 + 0 + 0 + 1 + 2 + 5 + 7 + 10 + 11 + 11 + 11 + 11 + 9 + 6 + 6 + 5 + \\
&\quad 3 + 3 + 2 + 1] \times 1/24 \text{ days} \\
&= 109°\text{C} \times 1/24 \text{ days} \\
&= 4.54 \text{ cooling degree days}
\end{aligned}$$

Likewise, the measure of the space heating system's energy usage when the outside air temperature is less than the building's base temperature can be determined and is called Heating Degree Days (HDD) (Bromley, 2022).

DegreeDays also provides an online tool that uses linear regression to determine the relationship between energy and degree days. A screenshot of the tool is given in Figure 4-9 below.

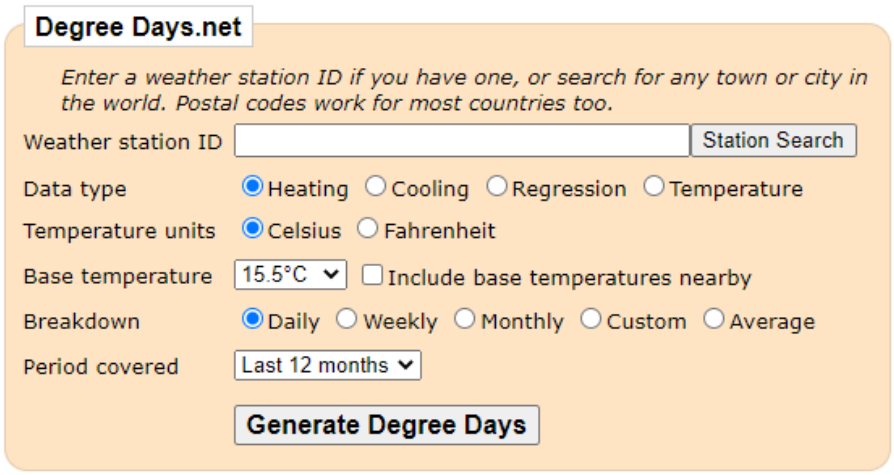

Figure 4-9: Screenshot of DegreeDays Online Tool (Bromley, 2022)

The tool retrieves weather data from the weather station closest to the building and the space heating and cooling system's energy consumption to perform the analysis. The user indicates that the energy consumption data is for heating or cooling operations or a combination of the two. Multiple base temperatures are used if the base temperature is unknown until the best-fitting relationship is found. Extending on the example from the degree-days website, the linear relationship can be plotted. Figure 4-10 below shows that the cooling system's energy consumption increases as the outside air temperature increases above the base temperature. The example illustrates that energy consumption increases at 20.8kWh/CDD21 and that, at a minimum, 3.6kWh is used for ventilation.

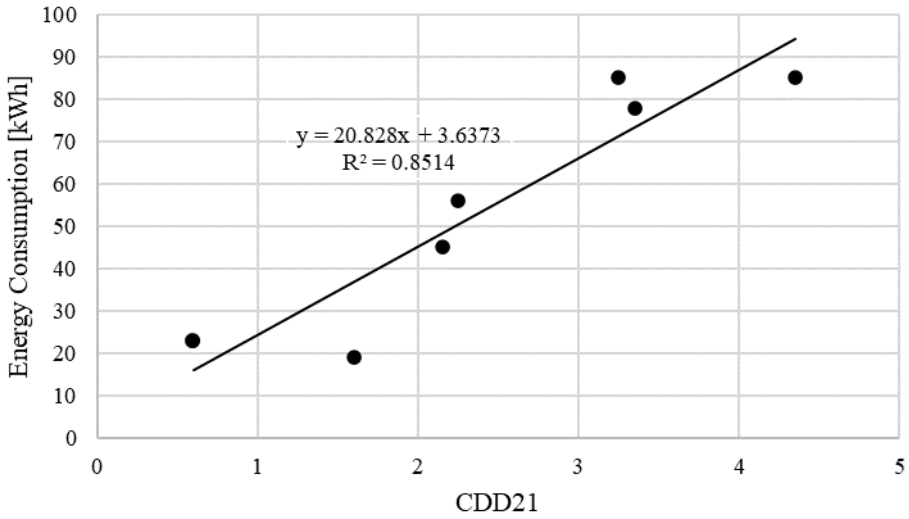

Figure 4-10: Linear Relationship between Energy Consumption and CDD21

A similar plot can be developed if the system provides both heating and cooling. An example is given in Figure 4-11. Note that the base temperature may be different for cooling and heating operations. For this example, the base temperature for cooling is 21°C, and for heating, it is 17°C.

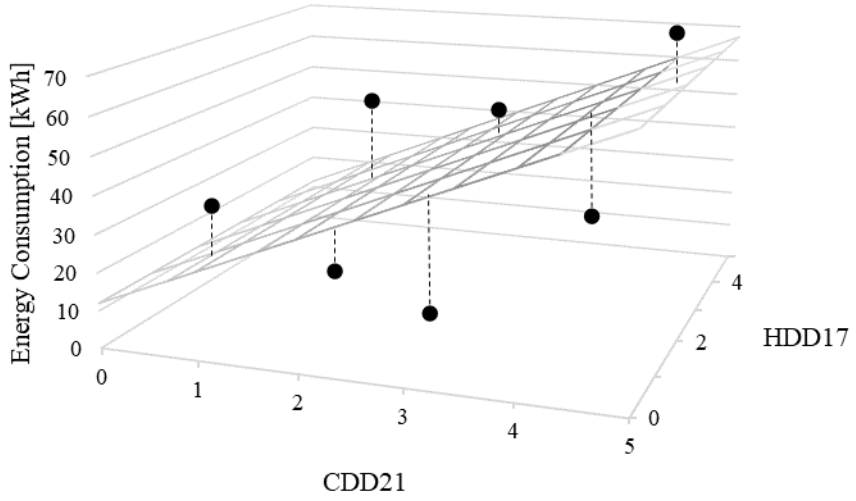

Figure 4-11: Linear Relationship between Energy Consumption and CDD21 and HDD17

4.6 Concluding Remarks

The tools described in this chapter are used in this research. The Predictive Mean Vote (PMV) calculator was used to determine whether the occupants were experiencing thermal comfort in their office spaces. The TABS calculator was used to determine heat flows, air and surface temperatures and the energy consumed by the TABS installation. OpenStudio and EnergyPlus were used to model the buildings and the heat gains/losses in the buildings. Once the energy consumed by the space heating/cooling systems was determined, the online tool DegreeDays was used to determine the relationship between the energy consumed and the outside air temperature.

5 Case Study of Office Building with TABS

The following chapter presents a case study showing that the demand and energy consumption of TABS installations can be accurately simulated using EnergyPlus and the TABS calculator presented in Chapter 4. This is done by comparing the simulation results with actual metered consumption data. The case study included partnering with PJC and Partners, a consulting company that specialises in evaluating and designing strategies for improving the environmental performance of buildings, to design and construct the TABS installation at an office building in Cape Town, South Africa. Designing the pipe layouts involved collaborating with architects and engineers to turn a structure consisting of the roof, walls and pillars into a three-story office building. The architects designed a 3D model (Figure 5-1) of the building, and structural engineers developed the steelwork supporting the floors. The floor details wherein the pipes would be embedded are given in Table 5-1 below.

Table 5-1: Floor Details

Floor	Area No.	Floor Area [m^2]	Perimeter [m]	Length [m]	Width [m]
Ground	Main	2540.92	242.19	53.49	47.5
Ground	2	217.45	64.98	10.42	20.87
Ground	3	314.58	78.07	17.39	18.09
1	Main	2539.45	242.35	53.46	47.5
1	2	248.32	65.84	11.82	21
2	Main	2452.15	251.06	51.62	47.5
2	2	195.5	63.91	8.34	23.45
		8508.37		**206.54**	**225.91**

5.1 Circuit (Pipework) Design

The pipes embedded within the floors are called circuits. Each circuit is connected to a manifold to transfer heat into sections of floors and ceilings called thermal zones. Designing the circuits depended on architectural and structural designs. This design process lasted about eight months as the structural engineers had to finalise the support steelwork, and the architects had to complete the building aesthetics. Designing the circuits had additional constraints, such as the maximum pipe length available from the local supplier was 150m. Therefore, each circuit was designed to be shorter than 150m to avoid joining pipes and risking water leaking into the floors and ceilings. The manifolds available could only connect up to ten circuits which restricted the size of each thermal zone.

The application LoopCAD, described in 4.3, was used to develop the circuit layouts, summarised in Table 5-2. The table shows that 25 030m of pipe was used for the circuits. While designing the circuits, it was learnt that they must be as simple as possible to minimise errors during construction. It was acknowledged that the pipes were not as flexible as the circuits designed in LoopCAD. Lastly, in a multi-story building, efforts should be made to align the manifolds connected from one floor to another to avoid bends in the pipes that deliver water from the chiller. The pipe layouts are included in Appendix D-2: Pipe Details and Circuit Diagrams.

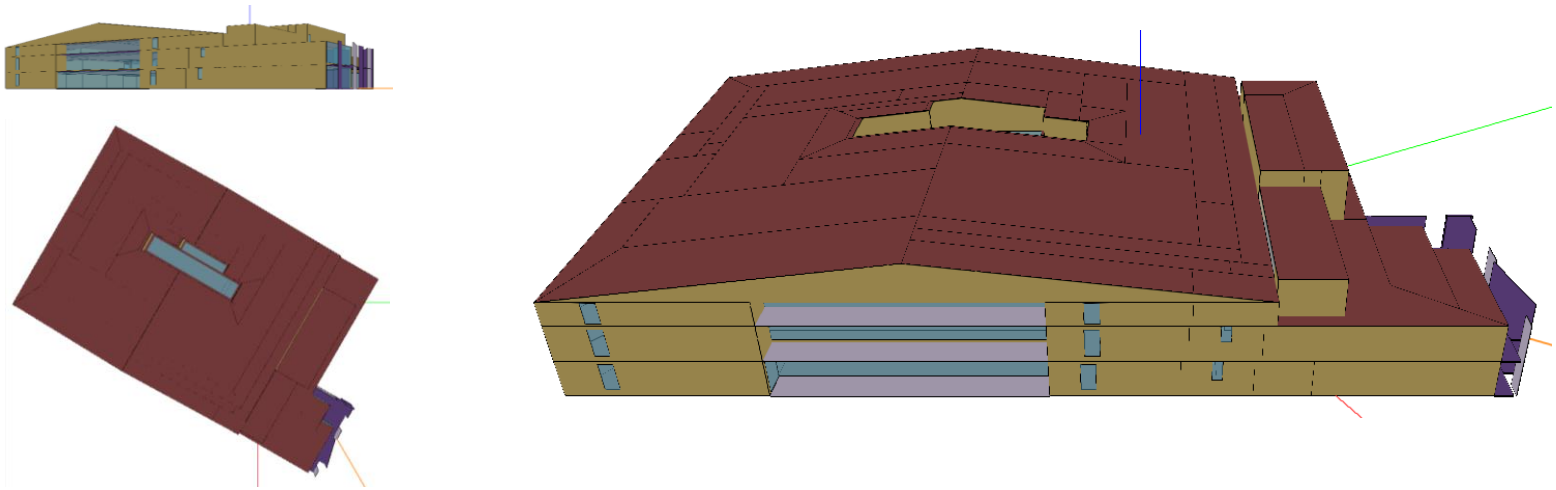

Figure 5-1: 3D Model of Case Study Building with TABS Installation

Table 5-2: Circuit Details

Ground Floor				**First Floor**				**Second Floor**			
Manifold Name	**No. of Circuits**	**Pipe Length [m]**	**Circuit Area [m2]**	**Manifold Name**	**No. of Circuits**	**Pipe Length [m]**	**Circuit Area [m2]**	**Manifold Name**	**No. of Circuits**	**Pipe Length [m]**	**Circuit Area [m2]**
GS1	8	940	275.28	1S1	9	916.3	303.76	2S1	8	896.4	315.43
GS2	6	662.7	195.2	1S2	9	847	271.39	2S2	6	695.4	198.36
GS3	9	1225.5	365.38	1S3	10	990.9	279.64	2S3	9	1219.5	378.19
GS4	9	1191.5	362.98	1S4	10	1080.2	339.95	2S4	9	933.9	313.66
GC1	9	802.5	232.65	1C1	9	802.7	265.7	2C1	9	765.2	244.79
GC2	6	649.8	198.3	1C2	10	1051.2	310.55	2C2	7	578.1	175.02
GC3	9	1222	365.19	1C3	10	1118.6	313.35	2C3	8	1031	361.21
GC4	8	999.7	341.9	1C4	10	940.9	291.12	2C4	7	714.5	255.12
GN1	6	710.5	215.76	1N1	5	575.9	224.92	2N1	4	440.1	194.04
GN2	9	1028.4	312.93								
	79	**9432.6**	**2865.57**		**82**	**8323.7**	**2600.38**		**67**	**7274.1**	**2435.82**

Figure 5-2 below shows the TABS types for the building, i.e. Type A for the ground floor and Type E for the first and second floors. Therefore, the cooling capacity for the system would be determined using the Universal Single Power method (Chapter 2.2.5.1) for the ground floor and the General Resistance method (Chapter 2.2.5.2) for the first and second floors. Details of the pipes are given in Appendix D-1: Technical Details of Pexal Multilayer Pipe.

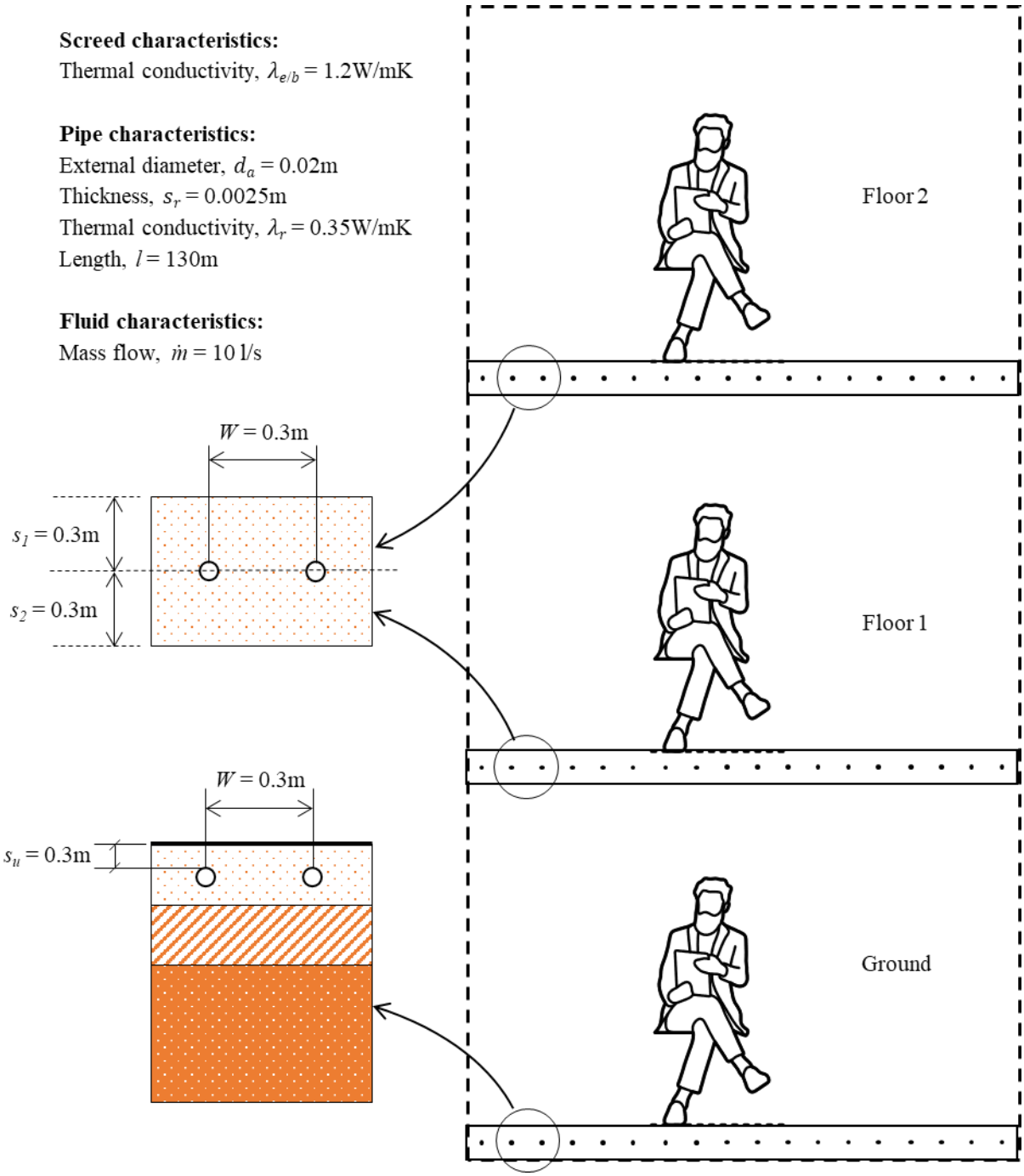

Figure 5-2: Simplified TABS with Ventilation Configuration

5.2 Construction

Contractors had to install the pipes and pour cement onto the floors to cover the pipework. The pipes were tested to ensure no leaks by pumping water into the circuit up to a pressure of 600kPa. The high pressure ensured that a puncture would be quickly identified if the pipes were punctured during

installation. The water pumped from the chiller was also expected not to exceed this pressure. Figure 5-3 shows the steelwork construction on which the pipework was installed, the plastic manifold and the pressure gauge indicating that the water pressure was raised to 600kPa during the testing procedure.

(a)

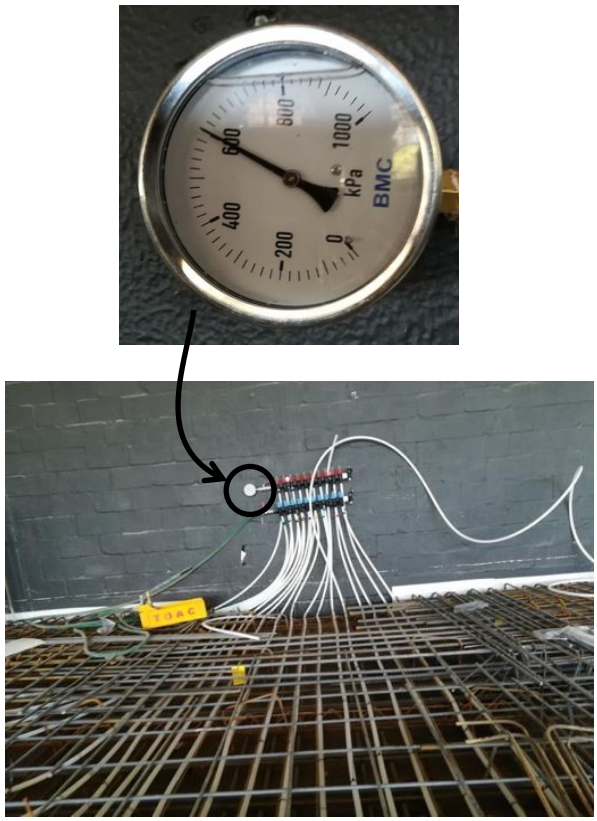

(b)

Figure 5-3: Constructing Circuits (a) Steel Work, (b) Monitoring Pressure at Manifold

Plastic manifolds were used for testing since, during construction, the manifolds could get damaged. The manifolds would be replaced with steel manifolds once construction was complete. As the cement was poured over the pipes, the water pressure was monitored to ensure no leakage into the cement. An incident occurred where a pipe was pierced, and the pressure in the circuit started to decrease. Unfortunately, the steelwork around the perforated pipe made it challenging to replace. Hence, the pipe was disconnected from the manifold, slightly reducing the thermal capacity of that zone. The cement was allowed to settle for two days while the pipes remained pressurised. Figure 5-4 shows zones where the pipes were installed and cement poured, making the office floor.

Figure 5-4: Pipe Installation and Poured Cement

The water would be chilled by Climaveneta's NECS-N/CA/S 2416 heat pump, shown in Figure 5-5. The heat pump has a cooling and heating capacity of 624.8kW and 673.6kW and a cooling and heating demand of 215kW and 209.9kW, respectively. The selection of the heat pump was not covered in this research, but further details on its specifications are included in Appendix E: Heat Pump Specifications

Figure 5-5: Installed Heat Pump (Climaveneta, 2020)

5.3 Analysis of Actual TABS Installation

5.3.1 Energy Analysis of Actual TABS Installation

The building was completed and occupied in July 2019. Meters were installed at the chiller from October 2020 to June 2021 to measure its electricity usage. The chiller's average weekday electricity demand for each month is given in Figure 5-6 below. The figure shows that electricity demand is most significant during the hotter months of the year (January and February) and least in the cooler months (May and June). The installation was scheduled to operate between 02:00 – 06:00 and 10:00 – 17:00, but as shown in the figure, there are some deviations. Around 20:30, there is a surge in energy consumption; in January and February, the chiller operates throughout the day. The building's facilities manager explained that the issues result from the thermostat, which measured the internal operative temperature to be high as though the building was fully occupied.

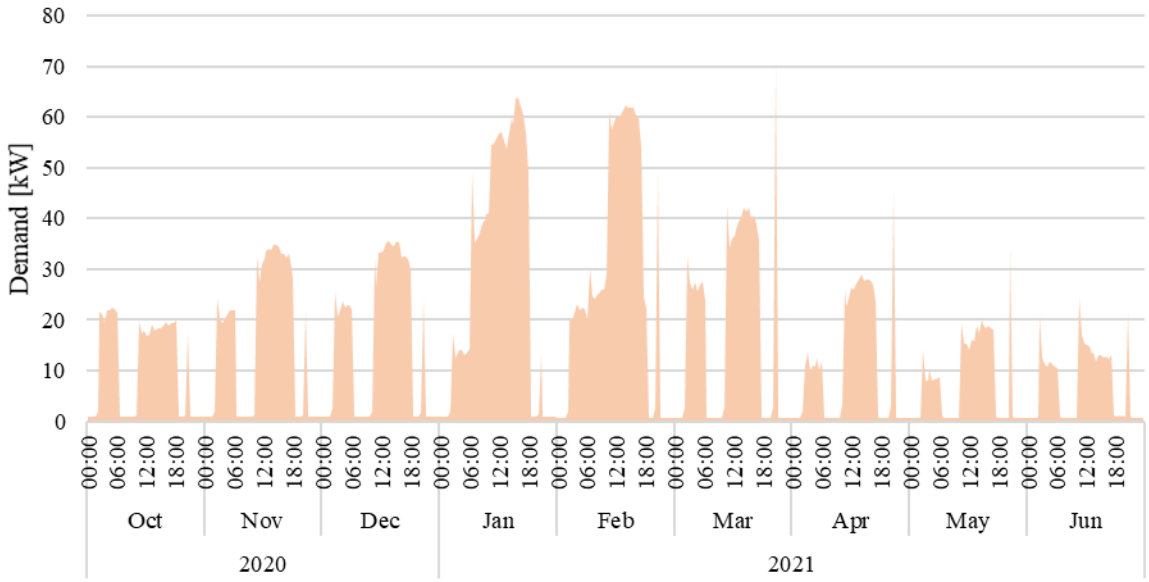

Figure 5-6: Actual Chiller Demand for TABS

Table 5-3 gives the chiller's monthly energy consumption by Eskom's low and high demand seasons. Over the period that the chiller was metered, the chiller consumed 72 045.20 kWh.

Table 5-3: Monthly Electricity Consumption for the period Oct 2020 – Jun 2021

Low Demand Season (September to May)						**High Demand Season (June to August)**	
Sep 20	-	Dec 20	8 877.29	Mar 21	9 716.06	Jun 21	3 503.91
Oct 20	4 209.98	Jan 21	14 523.53	Apr 21	5 917.41	Jul 21	-
Nov 20	7 857.48	Feb 21	13 372.05	May 21	4 067.50	Aug 21	-
					Total for Low Demand Season:		68 541.30 kWh
					Total for High Demand Season:		3 503.91 kWh
					Total:		**72 045.20 kWh**

The online tool degreedays.net was used to perform a regression analysis on the chiller's energy consumption data. It was determined that the TABS energy consumption significantly correlated with a Cooling Degree Day of 22°C (i.e. CDD22). The correlation, illustrated in Figure 5-7 below, can be interpreted as CDD22 being the building's base temperature, meaning that the TABS installation starts cooling when the outside air temperature rises above 22°C. Each point in the graph is the HVAC's total monthly energy consumption.

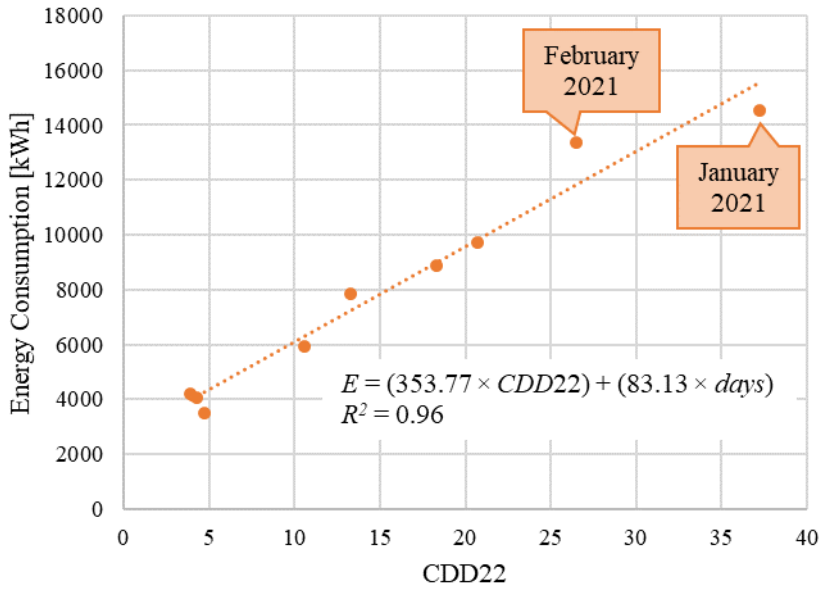

Figure 5-7: Cooling Degree Days

5.3.2 Financial Analysis of Actual TABS Installation

The electricity tariff for the analysed period is given in Table 5-4 below. The tariff is used with the tariff wheel (Figure 5-8) to determine the monthly electricity costs to operate the TABS installation.

Table 5-4: City of Cape Town Electricity Tariff for Large User, Low Voltage 2020/21 (City of Cape Town, 2021)

	High Demand Season (June to August) [c/kWh]	Low Demand Season (September to May) [c/kWh]
Peak	388.75	129.4
Standard	120.44	90.28
Off Peak	67.18	58.67

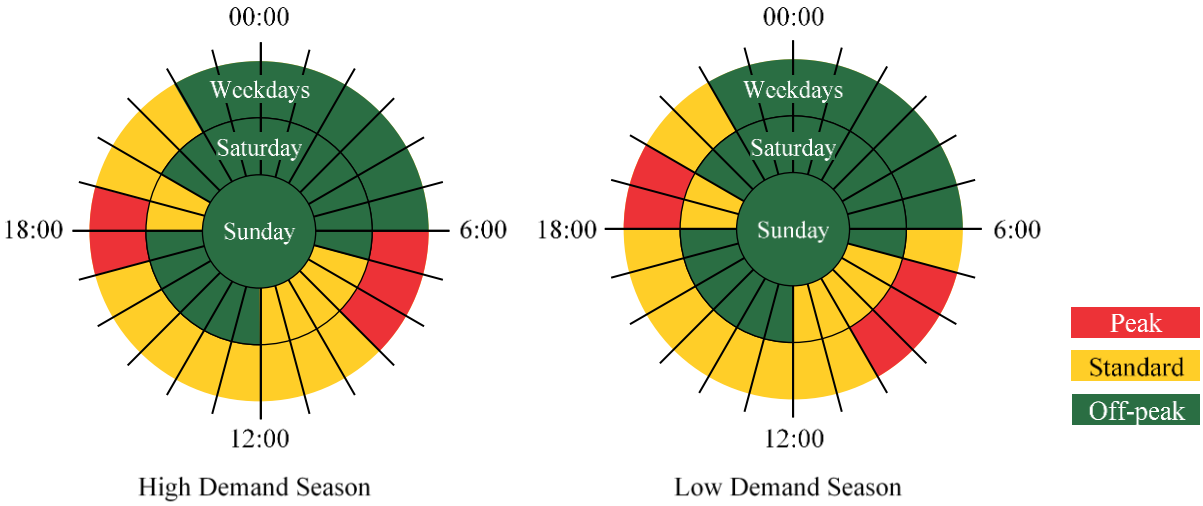

Figure 5-8: Time of Use (TOU) (Eskom, 2018)

Figure 5-9 shows the chiller's monthly electricity consumption and associated costs. The figure shows that the most electricity was consumed during the standard periods; and that the highest monthly cost occurred in January and February when the chiller's electricity consumption peaked.

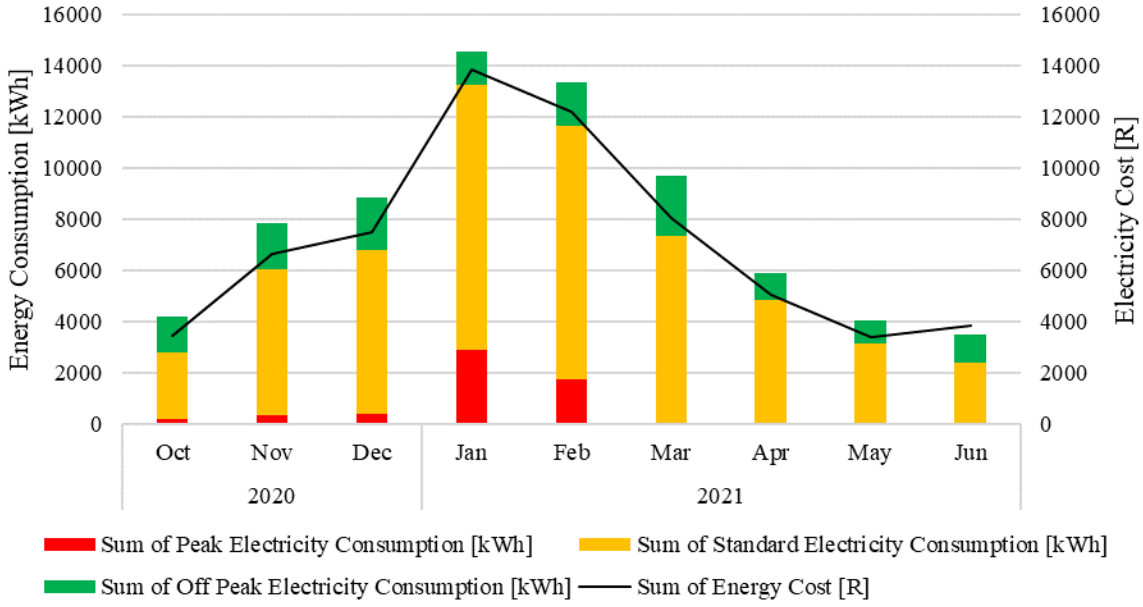

Figure 5-9: Monthly Electricity Consumption and Cost of Case Study Building

The TABS' electricity consumption and costs are given in Table 5-5 below. The table shows that for the nine months that the chiller was metered, its total electricity cost was R64 090.72.

Table 5-5: Monthly Energy Consumption and Cost of Case Study Building for the period Oct 2020 – Jun 2021

	Peak [kWh]	Standard [kWh]	Off Peak [kWh]	Monthly Total [kWh]	Energy Cost [R]
Oct 2020	222.64	2 587.94	1 399.39	4 209.98	3 445.52
Nov 2020	374.99	5 672.01	1 810.48	7 857.48	6 668.13
Dec 2020	431.36	6 362.59	2 083.34	8 877.29	7 524.62
Jan 2021	2 932.63	10 336.76	1 254.14	14 523.53	13 862.65
Feb 2021	1 738.57	9 926.01	1 707.47	13 372.05	12 212.69
Mar 2021	80.62	7 255.94	2 379.50	9 716.06	8 051.04
Apr 2021	79.83	4 769.40	1 068.18	5 917.41	5 035.81
May 2021	75.78	3 091.55	900.17	4 067.50	3 417.24
Jun 2021	85.80	2 334.18	1 083.93	3 503.91	3 873.02
Period Total	**6 022.21**	**52 336.39**	**13 686.60**	**72 045.20**	**64 090.72**

5.4 Analysis of Simulated TABS Installation

These steps were followed when performing the simulations:

1. Downloading and formatting the weather data;
2. Modelling and simulating the heat loads in the office building;
3. Determining the required cooling capacity;
4. Comparing TABS' actual and simulated demand and energy consumption; and
5. Analysing occupants' thermal comfort

5.4.1 Weather Data Download and Formatting

Simulations in EnergyPlus required a weather file to be created for the simulation period. The weather file included data downloaded from the Cape Town International weather station, which consisted of air temperature, dew point, relative humidity, and air pressure. Figure 5-10 shows the average weekday weather data from the Cape Town International weather station for July 2020 to June 2021.

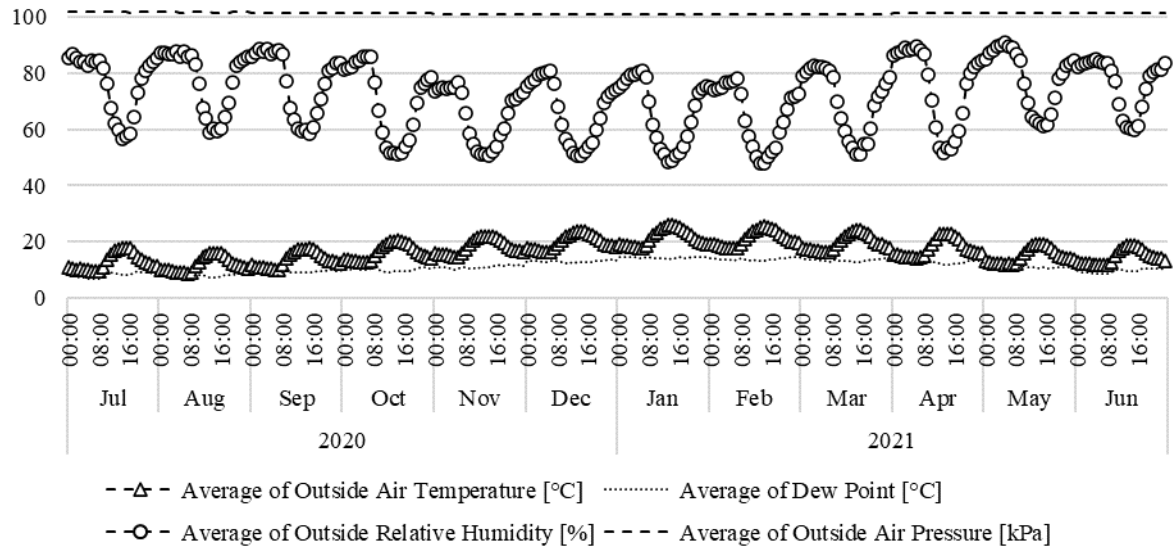

Figure 5-10: Average Outside Air, Relative Humidity, Dew Point and Air Pressure

The weather data was formatted into an EnergyPlus weather file described in Chapter 4.3.1.2.

5.4.2 Heat Load Modelling and Simulation

The heat loads used in the simulations included lighting, electrical appliances and the occupants radiating heat into the office space. According to SANS 10400: The Application of the National Building Regulations, an office building should be designed to have an occupancy of 1 person per 15m^2. During the analysed period, South Africa was under lockdown due to COVID-19 regulations, and the building had varied occupancy. However, from January to February 2021, the thermostat measured the internal operative temperature to be high as though the building was fully occupied. The simulations were adjusted to have full occupancy to account for the glitch. Table 5-6 gives the occupancy levels, and Figure 5-11 provides a screenshot from EnergyPlus showing the occupancy levels modelled for the analysed period.

Table 5-6: Occupancy Levels

Oct-20	80%	**Mar-21**	30%
Nov-20	80%	**Apr-21**	10%
Dec-20	80%	**May-21**	30%
Jan-21	100%	**Jun-21**	60%
Feb-21	100%		

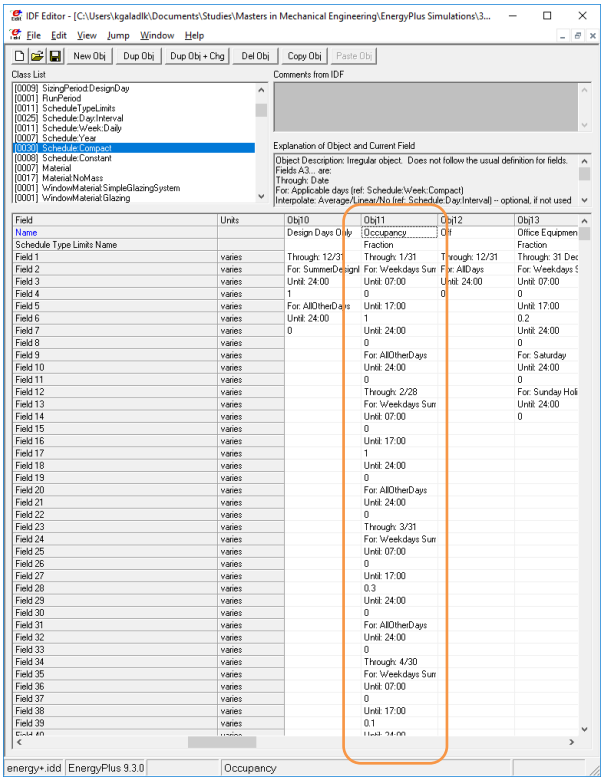

Figure 5-11: Screenshot from EnergyPlus Showing Occupancy Levels

Other thermal comfort factors used in the simulations are given in Table 5-7 below. The heat load from lights and electrical equipment was set to zero since the LED lights and laptops used in the building radiate an insignificant amount of heat.

Table 5-7: Design Heat Loads and Thermal Comfort Factors

	Cooling season	**Heating season**
Metabolic rate [met]	2 (using Table 2-2)	
Clothing insulation [clo]	0.5 (using Table 2-3)	1 (using Table 2-3)
Air velocity [m.s^{-1}]	0.1	
Lights [W/m^2]	0	
Electric Equipment [W/m^2]	0	

To determine TABS' influence on the occupants' thermal comfort, EnergyPlus simulated the heat loads as though there was no space heating system in the building. Figure 5-12 shows the average weekday inside operative temperature and relative humidity for each month of the period. The figure shows that the inside operative temperature would vary between 19°C in the winter mornings to 33°C in the summer midday. The relative humidity ranges between 50% and 70%.

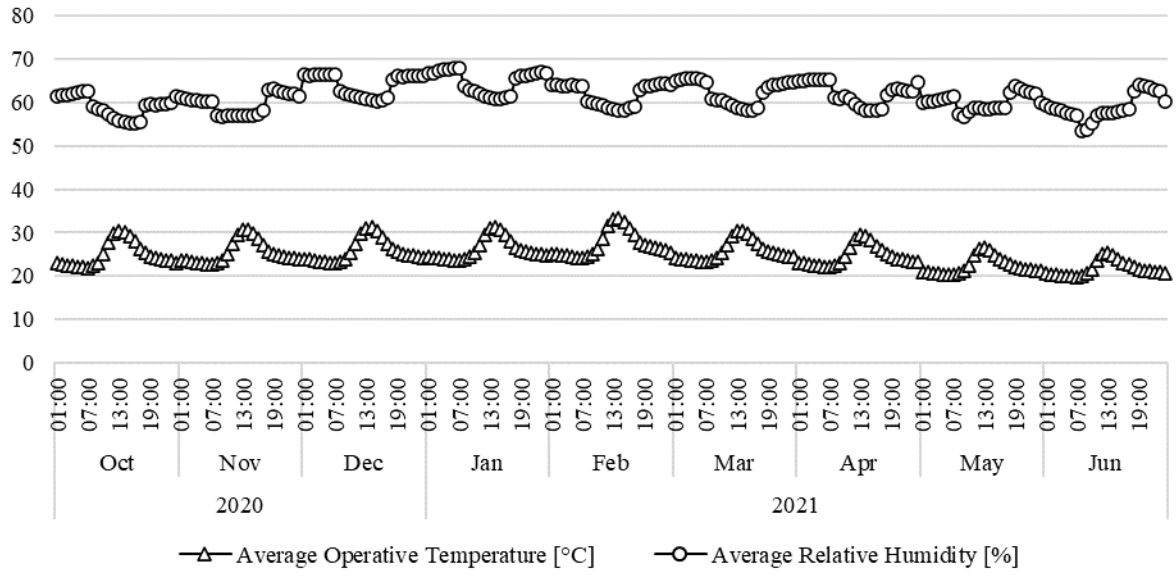

Figure 5-12: Average Weekday Inside Operative Temperature and Relative Humidity for the Simulation Period

EnergyPlus also determined the occupant's thermal comfort. Figure 5-13 shows a graph of the PMV/PPD (Predictive Mean Vote/Predicted Percentage of Dissatisfaction) graph and PPD over 24 hours for the warmest and coldest months as though a space heating system was not installed for the analysed period.

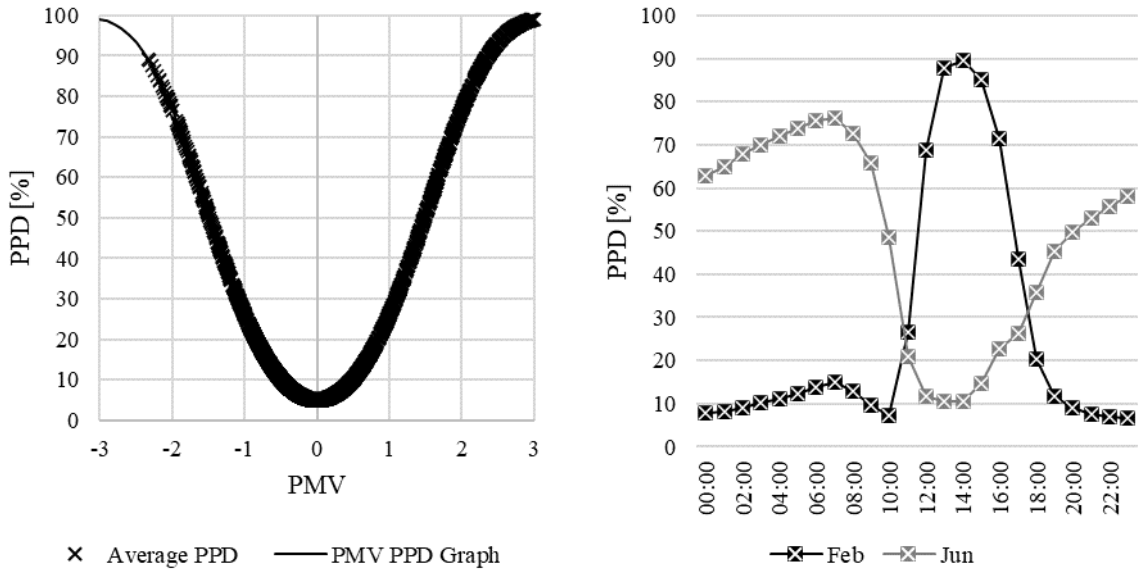

Figure 5-13: Occupants' Thermal Comfort with no Space Heating System Installed. PMV/PPD for the Office Building (left) and Average PPD over 24 hours for Warmest and Coolest Months (right)

The figure on the left shows that if no space heating system were installed, the occupants' thermal discomfort would vary between -3 (cold) and +3 (hot). On the right, the figure shows that the occupants' thermal dissatisfaction is low in February because of the warmer mornings and evenings. During the day, the occupants' dissatisfaction increases because the air and mean radiant temperature is too high

as they radiate heat into the office space. In the cooler month (June), the occupants' dissatisfaction is inversed. The occupants in the mornings and evenings are highly dissatisfied because the environment is too cold with little heat input. When the building begins to be occupied, the heat radiating from the occupants reduces their thermal dissatisfaction. The sum of data points from the PMV/PPD graph is tabulated in Table 5-8 below. Each data point from the PMV/PPD graph represents the occupants' thermal sensation for every hour. Over the simulated period, the building is occupied for 1950 hours (195 weekdays between October 2020 to June 2021 × 10 hours). The table shows that 29.9% of the time, the occupants experience a neutral thermal sensation. Most of the time (70.1%), the occupants experience increasing thermal discomfort. The high rate of thermal discomfort indicates the need to install a space heating/cooling system in the building.

Table 5-8: PMV Scale for Office Building without TABS

	-3 Cold	-2 Cool	-1 Slightly Cool	0 Neutral	1 Slightly Warm	2 Warm	3 Hot
No. of hours	0	100	464	583	366	321	116
No. of hours [%]	0.00%	5.13%	23.79%	29.90%	18.77%	16.46%	5.95%

5.4.3 Required Cooling Capacity

The EnergyPlus simulations determined the average weekday sensible cooling demand and energy required to achieve thermal comfort. Figure 5-14 shows the required sensible cooling demand profile, which shows that the peak cooling demand would be 85kW.

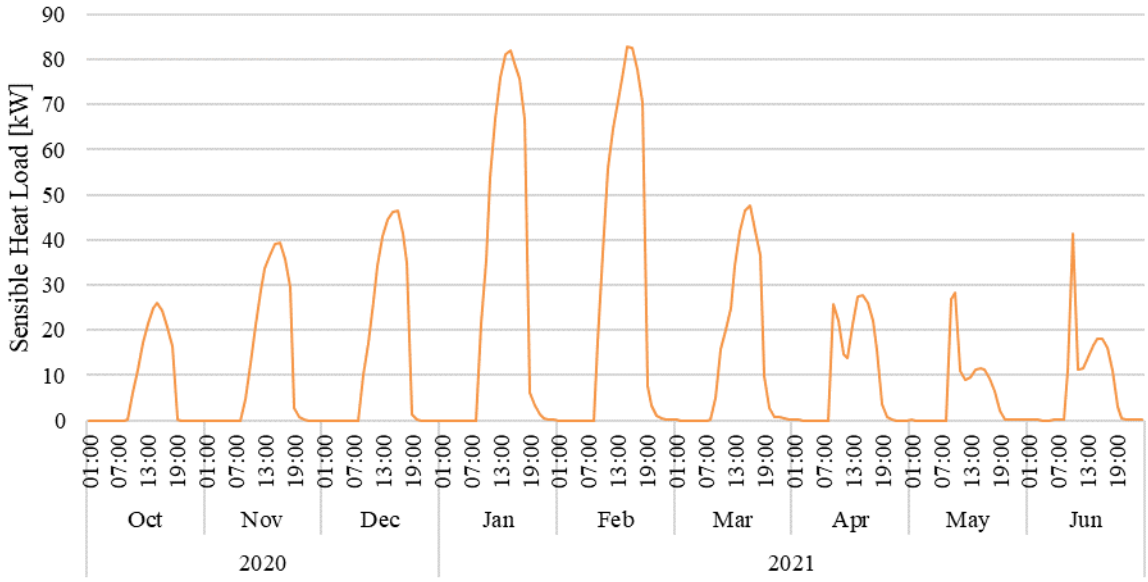

Figure 5-14: Required Cooling Demand Profile

The sensible cooling energy for each weekday for each month in the analysed period is given in Table 5-9 below. The table shows that the most significant energy consumption occurred in January and February.

Table 5-9: Required Weekday Cooling Energy for each Month (Oct 2020 – Jun 2021)

Oct 20	169.02 kWh	**Jan 21**	650.25 kWh	**Apr 21**	220.97 kWh
Nov 20	285.41 kWh	**Feb 21**	649.45 kWh	**May 21**	137.00 kWh

Dec 20	344.33 kWh	**Mar 21**	328.78 kWh	**Jun 21**	173.89 kWh

5.4.4 Actual and Simulated Demand and Energy Consumption

The chiller was scheduled to operate daily for 11 hours, 02:00 to 06:00 and 10:00 to 17:00. The operating hours, maximum cooling demand and profile were input into the TABS calculator to determine the chiller's demand profile. Figure 5-15 below includes the calculated demand profile and the actual chiller's demand profile, as given in Figure 5-6. The calculators' results have also been included in Appendix F: Results of the Case Study of Office Building with TABS. The Appendix table shows that the mean difference between actual and calculated results is 2.054. Therefore, it was determined that the TABS calculator results have an 80% confidence level to be within 1.17 of the actual chiller demand. The magnitude in the morning demand profile is smaller than the midday/evening profile. The TABS calculator seems to make the demand consistent throughout the day when TABS is on.

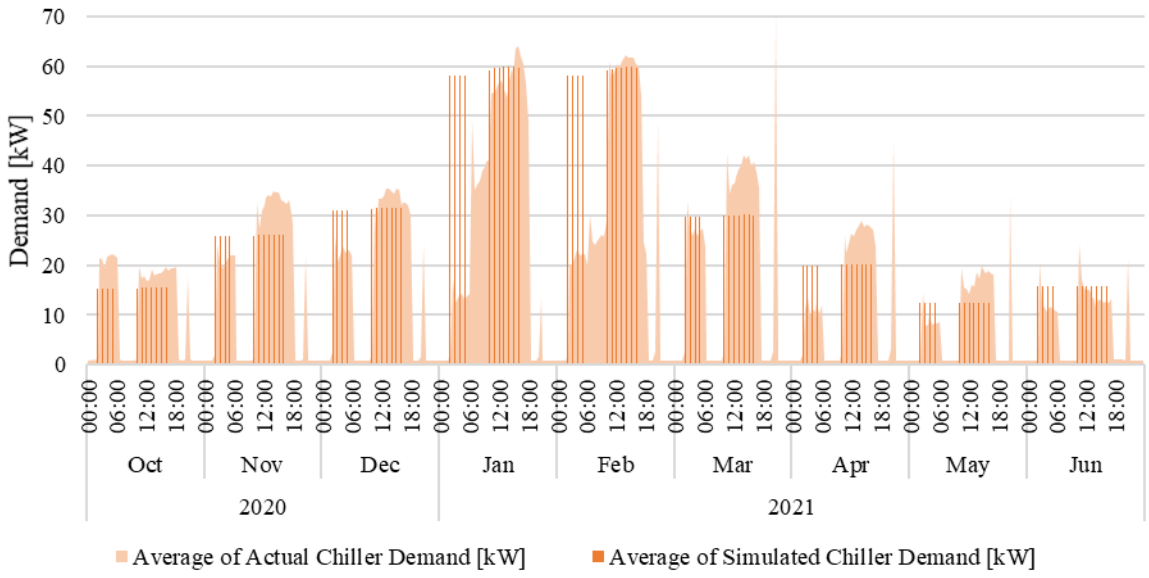

Figure 5-15: Simulated and Actual Chiller Demand for the Simulation Period

The chiller's actual and calculated energy consumption are compared in Figure 5-16. The trendline gives the relationship between the two as $y = 0.9998x$. This relationship approaches the dotted line ($y = x$), representing an exact correlation. The slope of the x term almost equals one, and the high R^2 value indicates a high correlation between the actual and calculated monthly energy consumption.

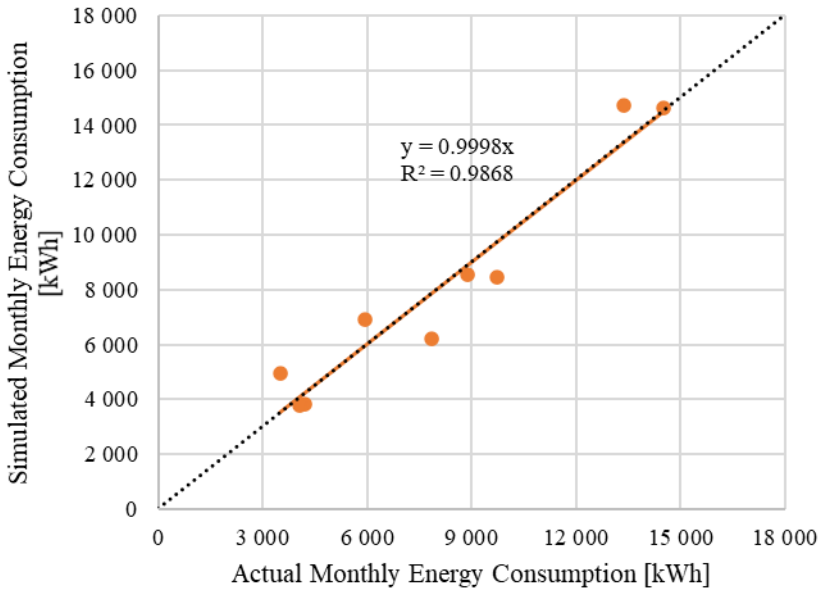

Figure 5-16: Simulated and Actual Energy Consumption

5.4.5 Occupants' Thermal Comfort

The Python TABS Calculator also gives the resultant operative temperature and relative humidity for the office building when TABS is installed. Figure 5-17 shows the monthly weekday averages and EnergyPlus simulation results as presented in Figure 5-12 when the building does not have a space cooling system installed. The figure shows that when the building has a TABS installation, the operative temperature approach 24°C, and relative humidity increases since the TABS calculator does not include calculations for dehumidification.

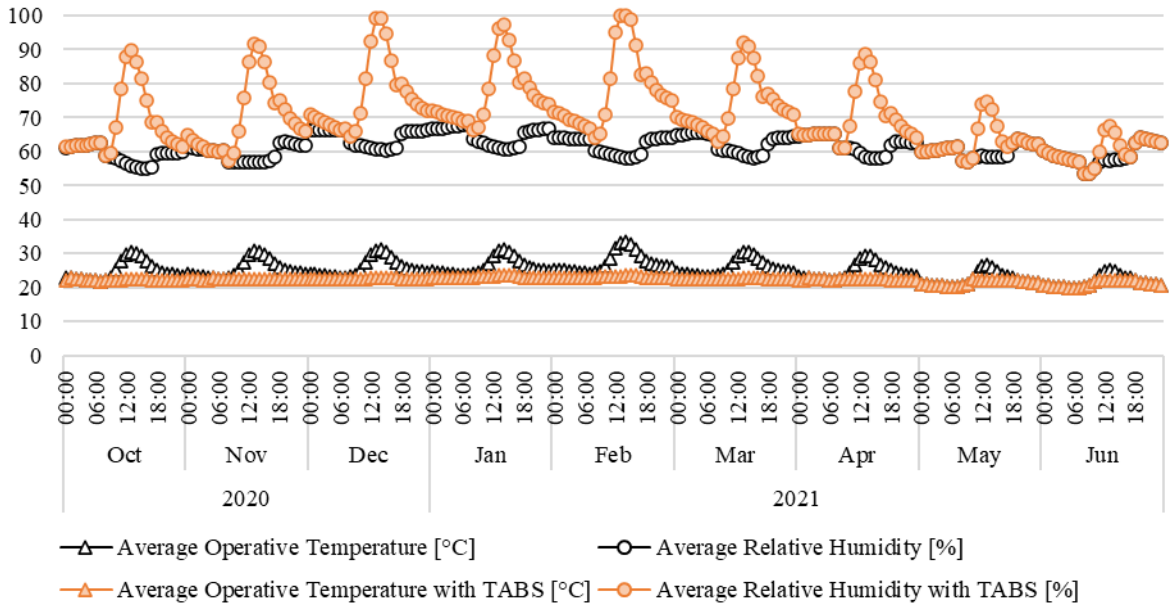

Figure 5-17: Average Operative Temperature and Relative Humidity with and without TABS Installation

Figure 5-18 includes the PMV/PPD relation and weekday PPD profile over 24 hours for the simulations where the building is with and without a TABS installation.

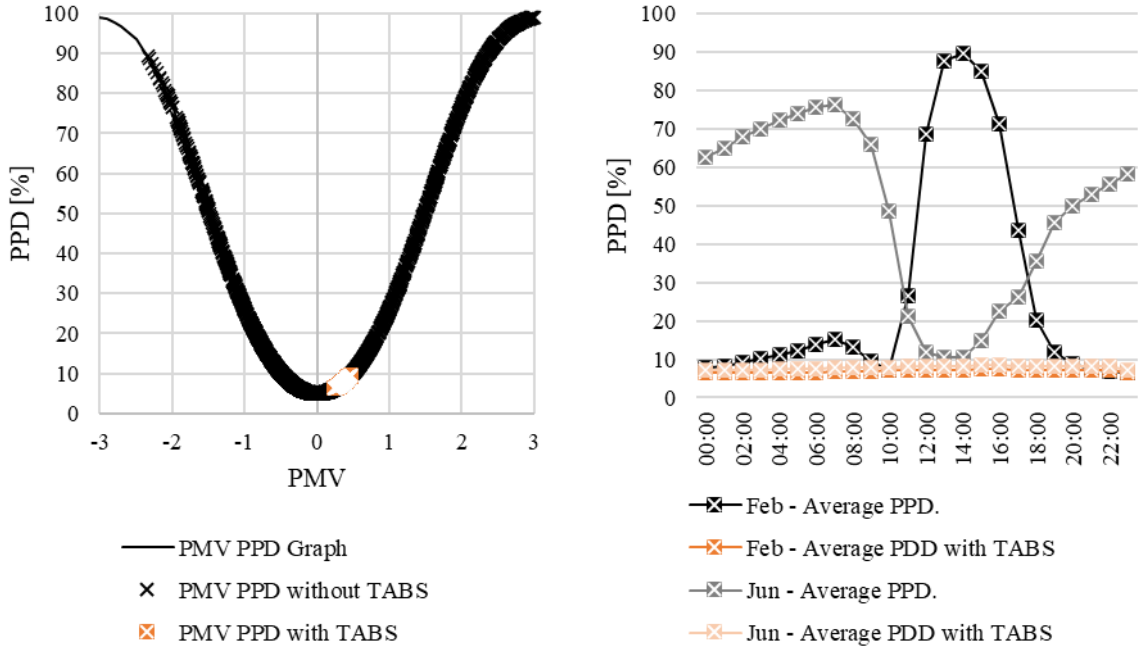

Figure 5-18: Occupants' Thermal Comfort for Building with and without TABS Installation. PMV/PPD for the Office Building (left) and Average PPD over 24 hours for Warmest and Coolest Months (right)

The figure above shows that PMV remains between 0 and 1, and PPD is less than 10% when TABS is installed. The sum of data points from the PMV/PPD graph is tabulated in Table 5-10. Each data point from the PMV/PPD graph represents the occupants' thermal sensation for every hour. Over the simulated period, the building is occupied for 1950 hours (195 weekdays between October 2020 to June 2021 × 10 hours). The table shows that the occupants' thermal sensation would be neutral throughout the time the building is occupied.

Table 5-10: PMV Scale for Office Building with TABS

	-3 Cold	-2 Cool	-1 Slightly Cool	0 Neutral	1 Slightly Warm	2 Warm	3 Hot
No. of hours	0	0	0	1950	0	0	0
No. of hours [%]	0.00%	0.00%	0.00%	100.00%	0.00%	0.00%	0.00%

5.5 Concluding Remarks

The purpose of the case study presented in this chapter was to show that the energy consumption of actual TABS installations can be simulated using EnergyPlus and the TABS calculator given in ISO standards. The case study began by showing the design and construction of TABS in a building located in Cape Town, South Africa. The construction was completed in July 2019, and the chiller's energy consumption was measured from October 2020 to June 2021. The system's energy consumption was simulated by downloading and formatting the weather data from the closest weather station at CapeTown International Airport. The weather file was imported into EnergyPlus, and the heat gains were modelled and simulated. The simulation showed that the occupants would experience thermal discomfort unless a space heating system was installed. EnergyPlus also determined the cooling load

required to improve thermal comfort, to be used as input into the TABS calculator. The TABS calculator simulated the chiller's demand and energy consumption. Compared with the actual chiller readings, the simulated demand is consistent. The TABS calculator determined the air temperature, mean radiant temperature and relative humidity. These variables were inputs into the PMV calculator and showed that the occupants had a neutral thermal experience since TABS was installed.

6 Case Study of Office Building with Conventional HVAC System

The following chapter presents a case study showing that the demand and energy consumption of actual HVAC installations can be accurately modelled and simulated in OpenStudio and EnergyPlus. The simulation results will also show how effectively the system ensures thermal comfort in the office building.

6.1 Description of Conventional HVAC System

The seven-floor building used in the case study is located in Cape Town, South Africa. The bottom three floors were used for parking, and the top four as office space. The first two office floors consist of four Air Handling Units (AHUs), and the top two floors consist of two AHUs each. The HVAC system mainly provides cooling by pumping chilled water to the AHUs to cool the air that flows into the office floors through the Variable Air Volume (VAV) system. Figure 6-1 shows a schematic diagram of the VAV-type HVAC system installed in the building.

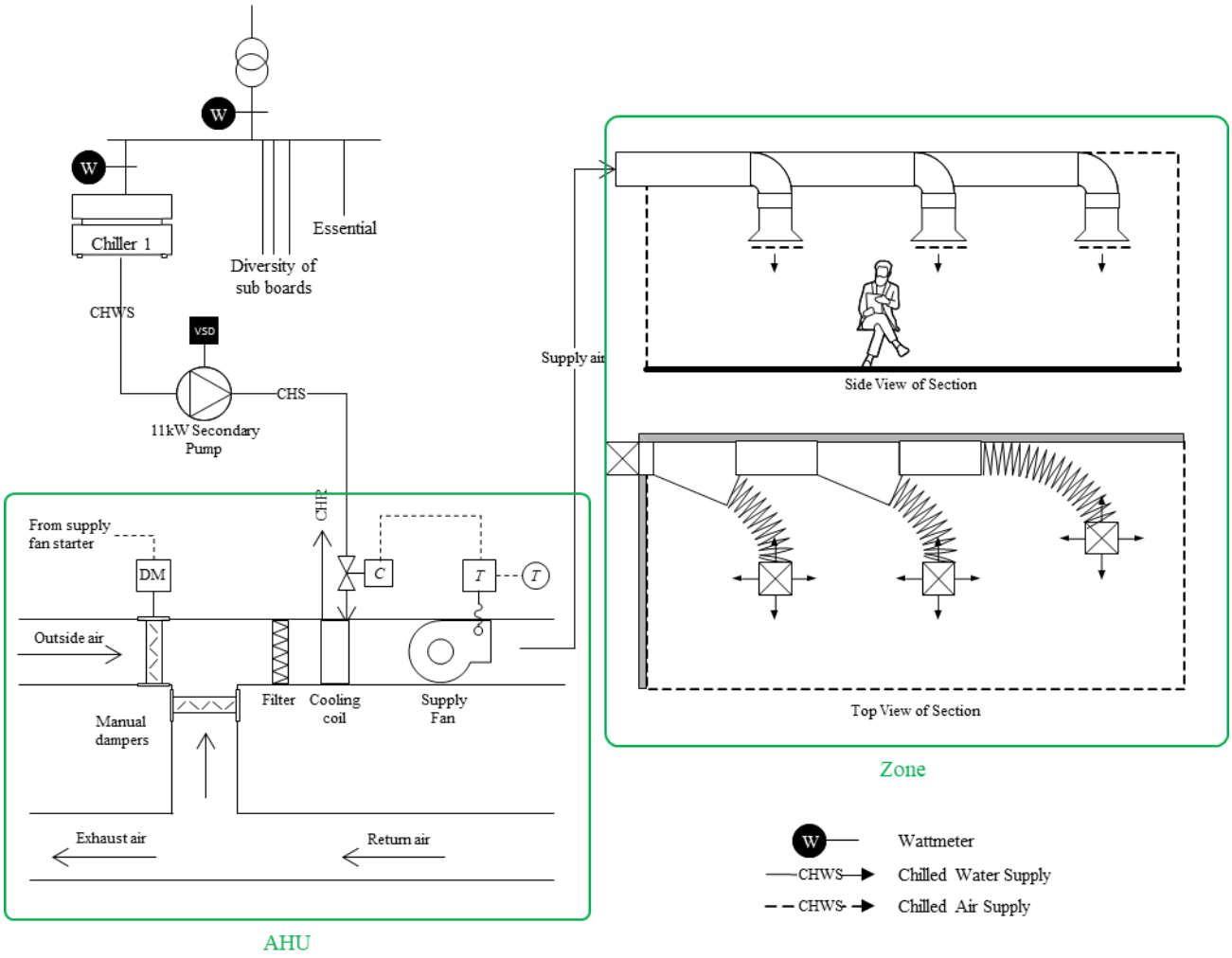

Figure 6-1: Simplified Reticulation Diagram and HVAC Layout

The figure shows two points where watt meters are installed to measure demand for the whole building and another to measure the HVAC system. The demand was recorded at 30min intervals. The secondary pumps in the AHUs and axial flow fans serving the condensers and parking ventilation are rated at 11kW and have Variable Speed Drives (VSDs) installed. Unfortunately, the number of pumps and fans in the HVAC and their operational times were unknown. Software systems have been implemented to

automatically switch off parts of the HVAC system after business hours when the building is less occupied.

6.2 Energy Analysis of Actual Conventional HVAC System

The electricity consumed by the HVAC system was recorded from 2008 to 2013 at 30-minute intervals. The year 2012 was the chosen period for analysis since the data for that year had minor errors compared to other periods with more missing data. Figure 6-2 shows the average weekday demand profile for each month in the analysed period. The figure shows that since the HVAC system mainly provides cooling, it is consistent with the higher chiller demand in summer (January, February and December). The lowest cooling demand is in winter (June, July and August).

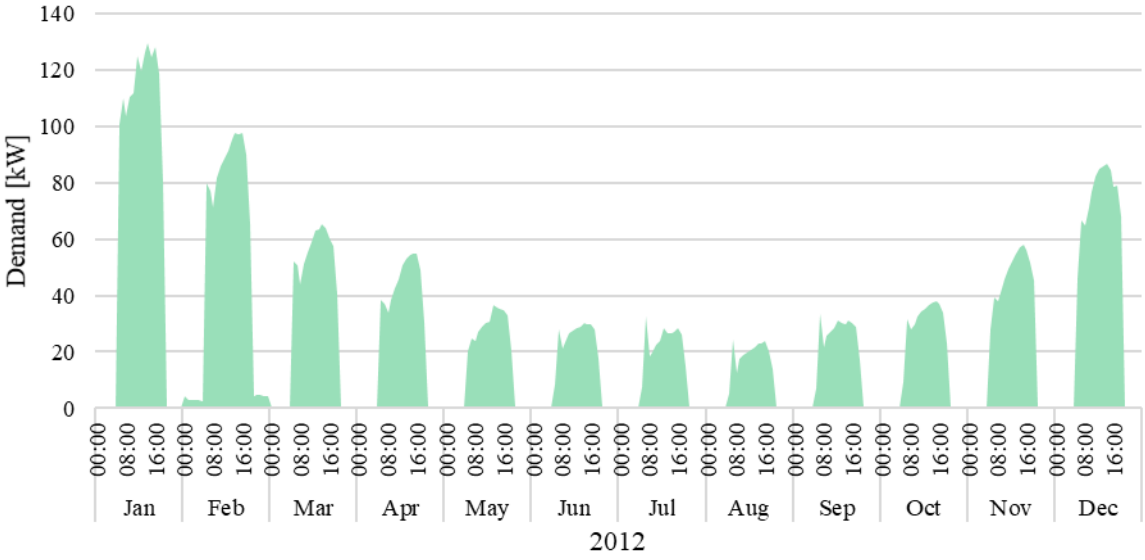

Figure 6-2: HVAC's Actual Average Weekday Demand Profile for Each Month in 2012

The monthly energy consumption for the period is given in Table 6-1 below. Consistent with the demand profiles, the table shows that the most energy was consumed in Summer and the least in Winter. The total electricity consumption was 182 518 kWh.

Table 6-1: Actual HVAC's Monthly Energy Consumption for the period Jan – Dec 2012

Jan	37 451 kWh	Apr	14 025 kWh	Jul	6 811 kWh	Oct	10 247 kWh
Feb	27 360 kWh	May	10 294 kWh	Aug	5 838 kWh	Nov	15 014 kWh
Mar	18 183 kWh	Jun	7 857 kWh	Sep	7 519 kWh	Dec	21 921 kWh

Understanding that the total monthly energy consumption of the HVAC system is proportional to Cooling Degree Days, regression analysis was performed using the online tool DegreeDays.net and graphed in Figure 6-3. Each point in the graph is the HVAC's total monthly energy consumption. The online tool performed multiple regressions on the monthly electricity consumption data and determined that the HVAC's energy consumption significantly correlated with a Cooling Degree Day of 26°C (i.e. CDD26). At this base temperature, the R^2-value is 0.9181, and the monthly energy consumed by the HVAC can therefore be determined using the formula $(1678.37 \times CDD26) + (269.85 \times days)$

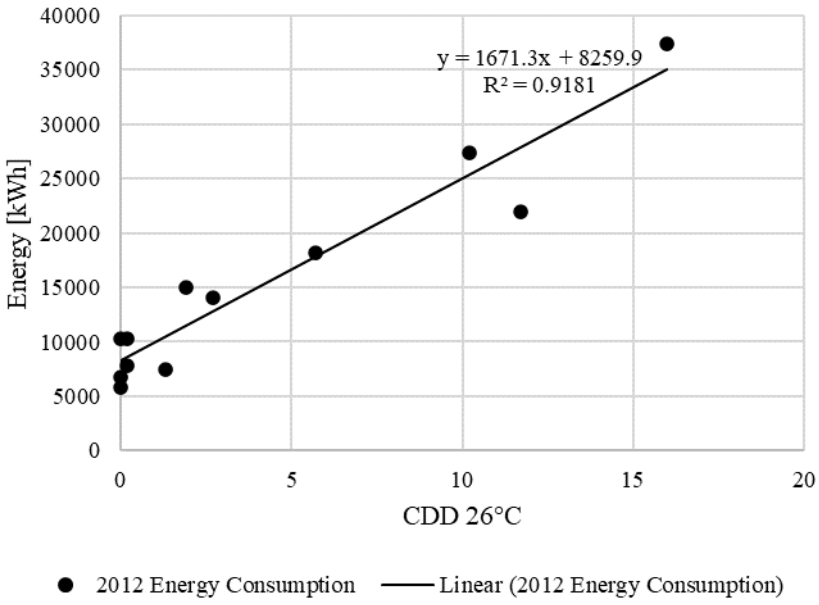

Figure 6-3: Cooling Degree Days for Office Building with Conventional HVAC System

6.3 Analysis of Simulated Conventional HVAC System

These steps were followed when performing the simulations:

1. Downloading and formatting the weather data;
2. Modelling the office building;
3. Modelling the heat loads in the office building;
4. Comparing the HVAC's actual and simulated demand and energy consumption; and
5. Analysing occupants' thermal comfort

6.3.1 Weather Data Download and Formatting

The weather file was created from data downloaded from the weather station located at Cape Town International Airport (FACT). Figure 6-4 illustrates the average air temperature, relative humidity, dew point temperature and air pressure for 2012.

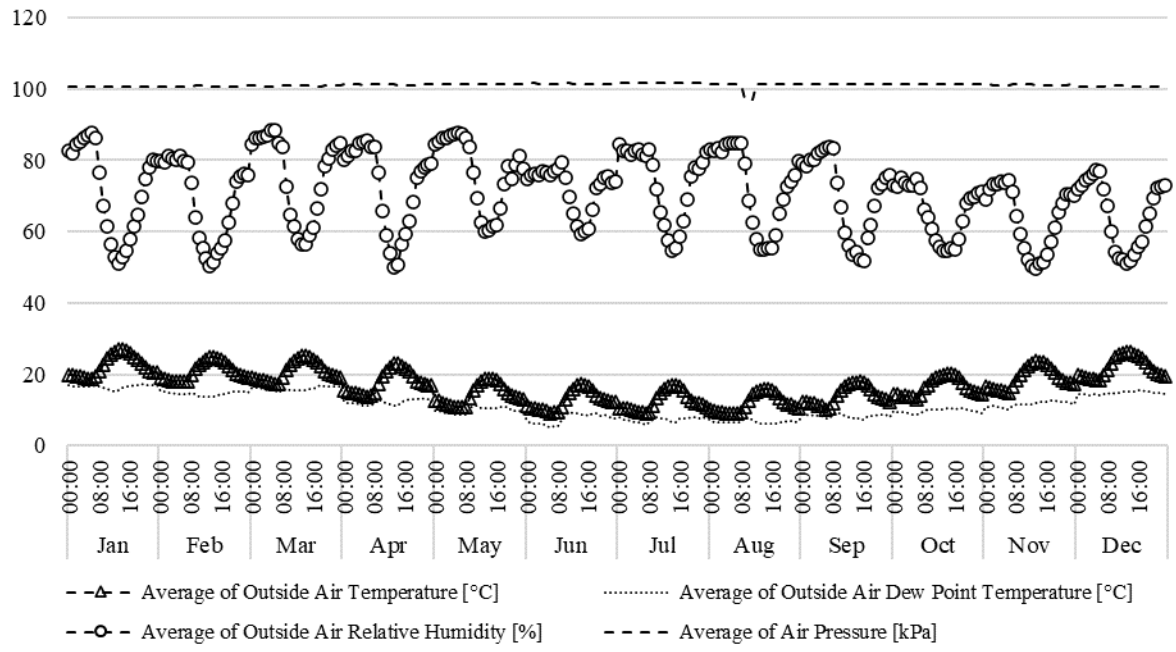

Figure 6-4: 2012 Average Outside Air Temperature, Relative Humidity, Dew Point and Air Pressure in Cape Town for the period Jan-Dec 2012

The weather data was formatted into an EnergyPlus weather file using tools bundled with EnergyPlus.

6.3.2 Office Building Model

The architectural designs of the building were not available; however, a simplified model of the building was developed in SketchUp Pro.

6.3.2.1 Creating Office Building with HVAC Model

The architectural plans for the office building were unavailable. Therefore, the office building was modelled based on map data and information about each floor. SketchUp Pro can import the satellite and street map into the model, as shown in Figure 6-5 below.

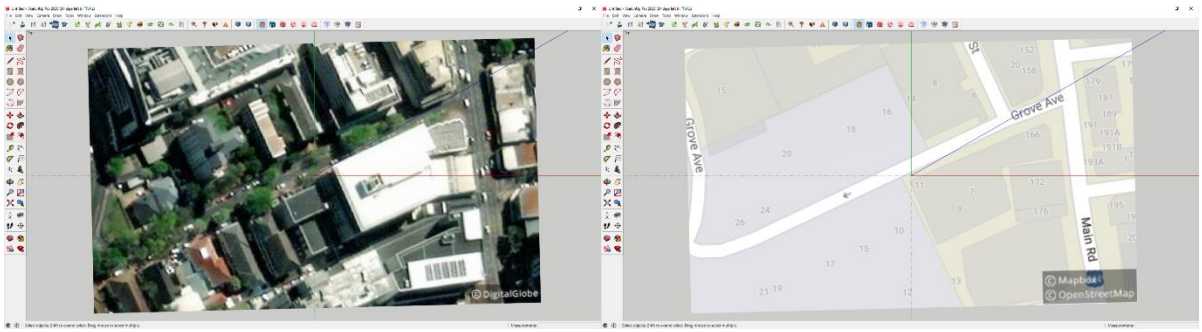

Figure 6-5: Satellite and Street Map of Office Building

The guidelines outlining the floor area and the first floor were drawn. Figure 6-6 below shows the guidelines and a top view of the first floor.

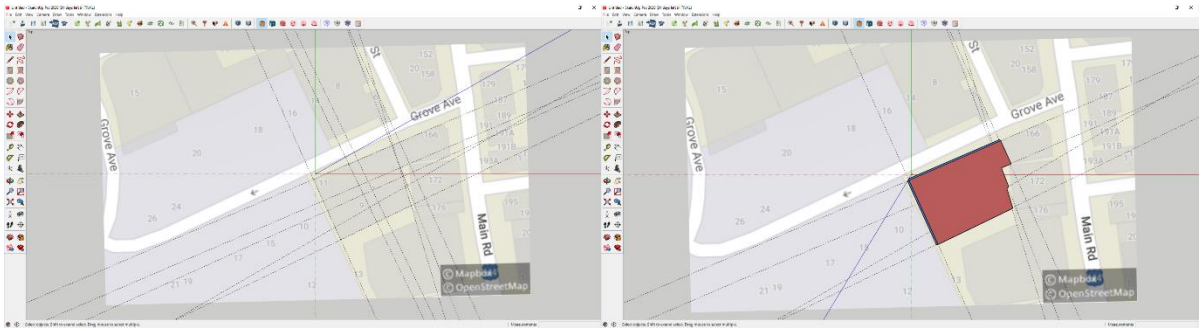

Figure 6-6: Gridlines on Street Map and Top View of First Floor

The three floors were used for parking and would not be included in determining the HVAC demand and energy consumption. Figure 6-7 below shows the three parking floors and the next two floors, which consist of four thermal zones. The thermal zone sizes were created by dividing along the midpoints across the length and width of the building.

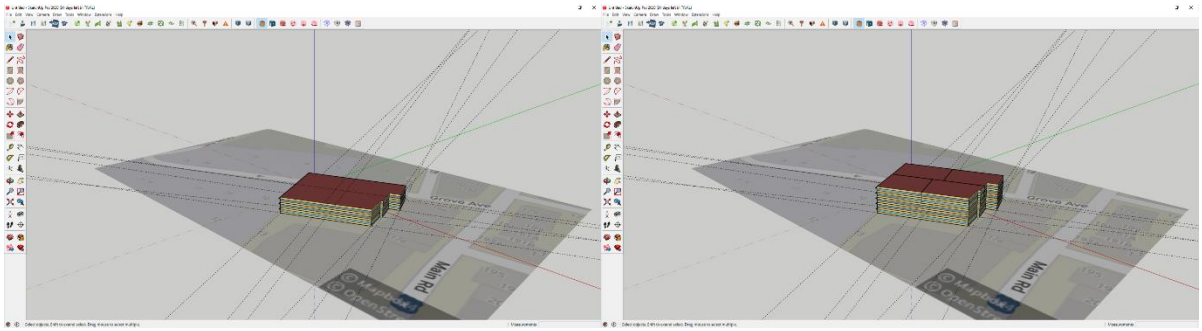

Figure 6-7: Isometric View of Parking Floors and Office Floors

Floors 6 and 7 consisted of two thermal zones and were drawn to create the final building, as shown in Figure 6-8 below.

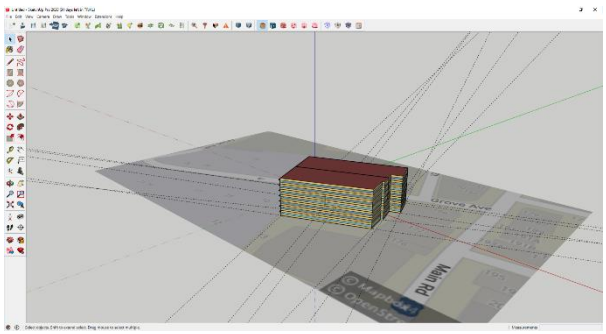

Figure 6-8: Office Building Model with all Seven Floors

The model was imported into OpenStudio, where the HVAC was modelled. A model of the building is given in Figure 6-9 below.

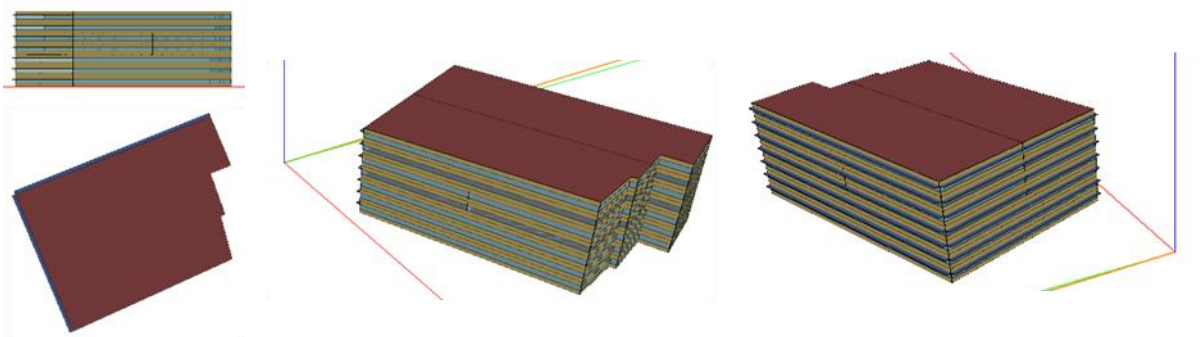

Figure 6-9: 3D Model of Case Study Building with HVAC Installation

The thermal zones on each floor were colour coded and given in Figure 6-10

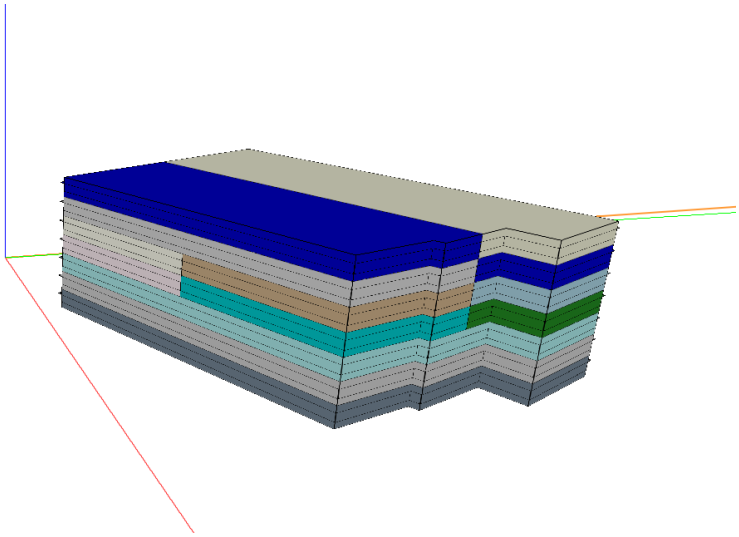

Figure 6-10: Building Thermal Zones as Modelled in SketchUp and Imported into OpenStudio

In OpenStudio, the thermal zones were connected to the VAV HVAC system, similar to Figure 4-5.

6.3.2.2 Heat Load Modelling and Simulation

The heat loads used in the simulations included lighting, electrical appliances and the occupants radiating heat into the office space. The heat loads are based on SANS 10400 and ASHRAE 189.1-2009 and summarised in Table 6-2 below.

Table 6-2: Design Heat Loads and Thermal Comfort Factors

	Cooling season	Heating season
People [m^2/person]	15	
Metabolic rate [met]	2 (using Table 2-2)	
Clothing insulation [clo]	0.5 (using Table 2-3)	1 (using Table 2-3)
Air velocity [$m.s^{-1}$]	0.1	
Lights [W/m^2]	10	
Electric Equipment [W/m^2]	6	

The chiller was scheduled to turn on when the outside air temperature was equivalent to the building's base temperature of 26°C, as was determined in Chapter 6.2. The software used to control the pumps and fans was unavailable, although assumptions based on the required cooling demand were

determined. Table 6-5 below gives an assumption of the number of pumps and fans operating each month, and Figure 6-11 shows their sizes modelled in EnergyPlus.

Table 6-3: Pump and Fans Operations

	No. of Pumps Operating	Equivalent Pump Demand	No. of Fans Operating	Equivalent Fan Demand
Jan and Dec	8	8 × 11 = 88kW	4	4 × 11 = 44kW
Feb and Nov	4	4 × 11 = 44kW	4	4 × 11 = 44kW
Mar to Oct	4	4 × 11 = 44kW	2	2 × 11 = 22kW

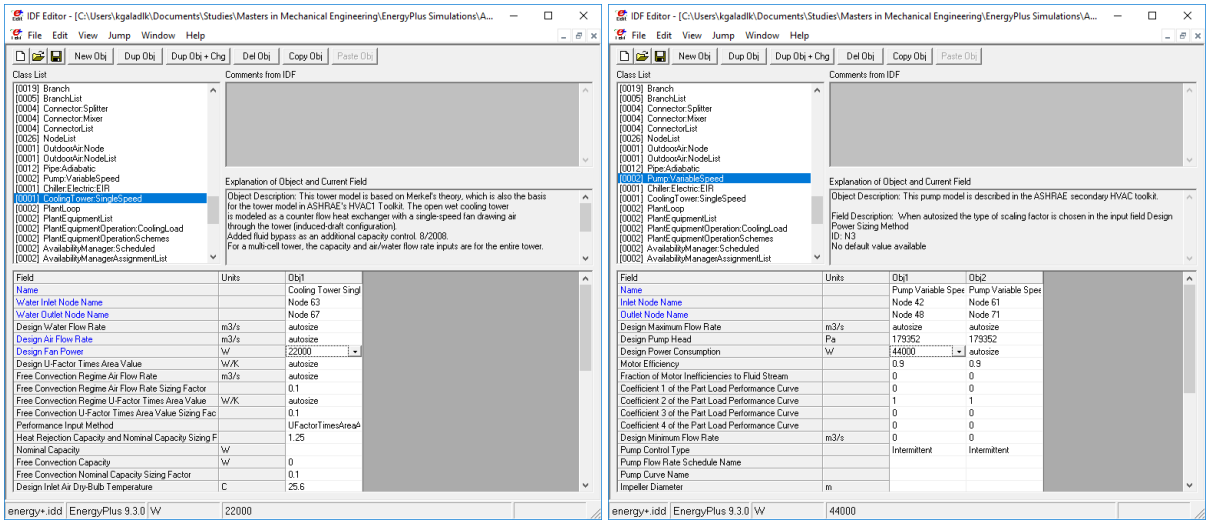

Figure 6-11: Screenshots from EnergyPlus Showing Pump and Fan Sizes

6.3.3 Actual and Simulated Demand and Energy Consumption

The resultant average simulated and actual demand profiles for the HVAC are shown in Figure 6-12 below. The calculators' results have also been included in Appendix G: Results of the Case Study of the Conventional HVAC System. The mean difference between actual and simulated results is 0.47. Therefore, it was calculated that EnergyPlus results have an 80% confidence level to be within 0.57 of the actual chiller demand.

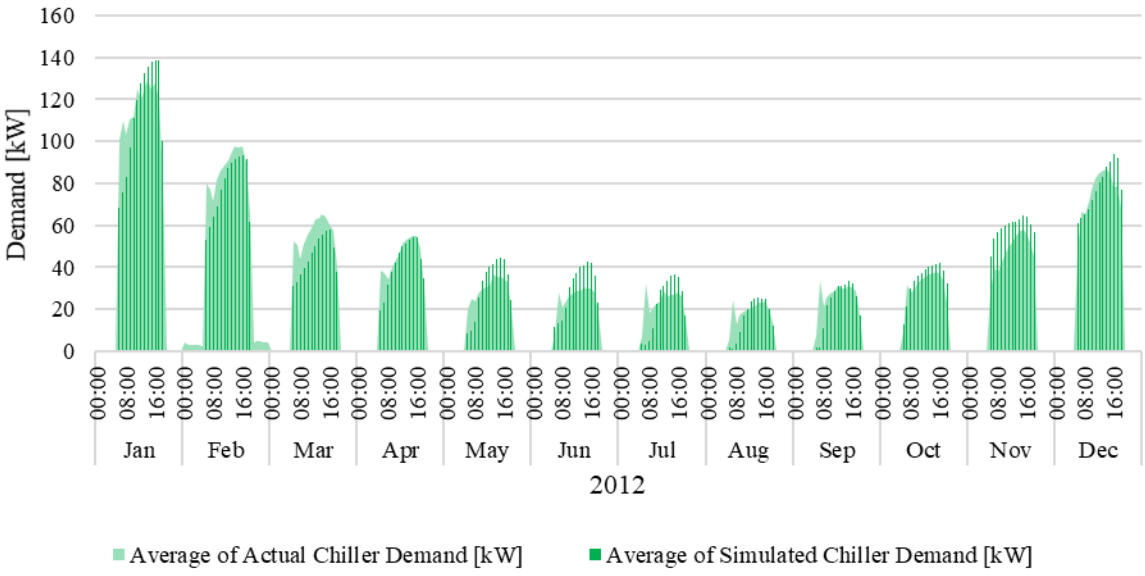

Figure 6-12: Simulated and Actual Chiller Demand

The chiller's actual and calculated energy consumption are compared in Figure 6-13 below. The trendline gives the relationship between the two as $y = 0.9725x$. This relationship approaches the dotted line ($y = x$), representing an exact correlation. The slope of the x term almost equals one, and the R^2 value is high (equal to 0.9887), indicating a high correlation between the actual and calculated energy consumption.

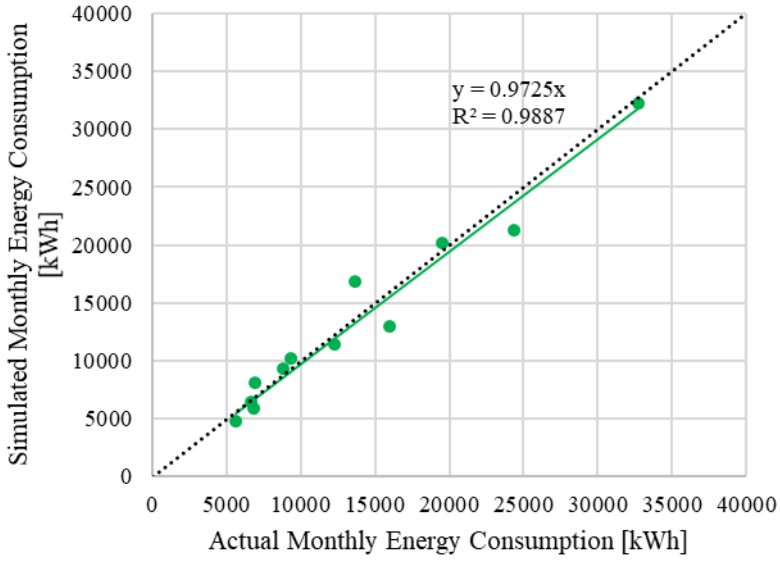

Figure 6-13: Simulated and Actual Energy Consumption

The minor differences between the actual and simulated energy consumption could result from the following reasons:

- **A low U-value for the walls, windows and roof:** The U-value (thermal transmittance) of the building refers to a measure of the heat that can transfer through the building's walls, windows

and roof. A lower U-value increases the cooling load. Therefore, a lower simulated U-value means that the simulated chiller energy consumption would be higher than the actual chiller.

- **The heat loads could be overstated:** The simulation may have a higher demand profile from overstated heat loads. The actual heat loads could be lesser than those modelled.

6.3.4 Occupants' Thermal Comfort

The simulated weekday average inside operative temperature and relative humidity for the analysed period are given in Figure 6-14 below. The outside air temperature and relative humidity were included in the figure to show how they changed after passing through the HVAC system. The figure shows that, on average, the HVAC increased the temperature during the colder months. Throughout all months, the average relative humidity was reduced.

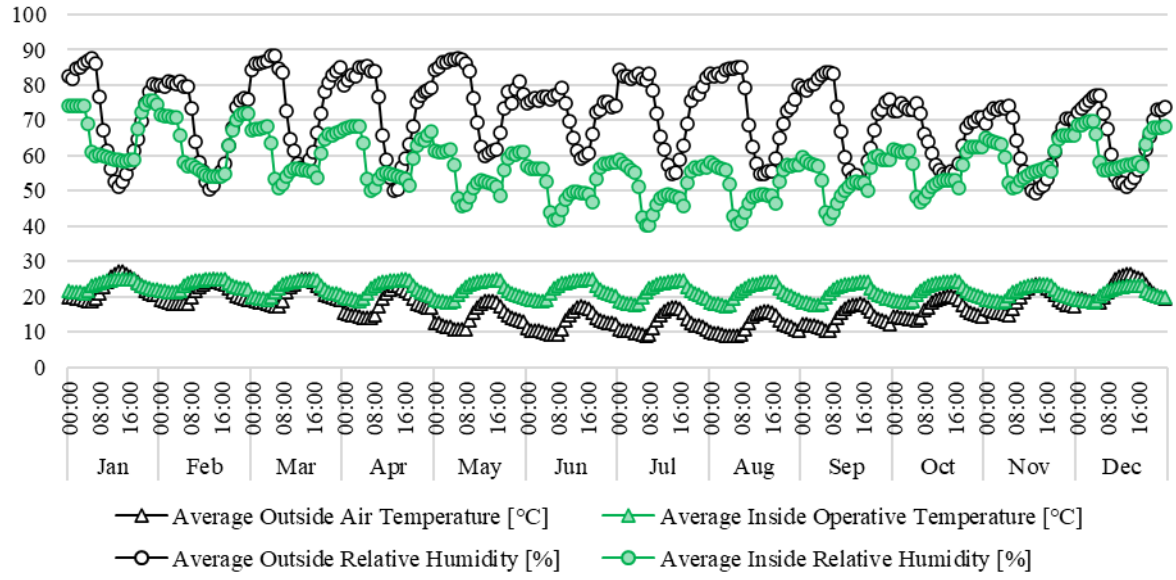

Figure 6-14: Average Outside Air Temperature and Relative Humidity, and Inside Operative Temperature and Relative Humidity

The resultant operative temperature and relative humidity improved the occupants' thermal comfort. Figure 6-15 below gives the PMV/PPD (Predictive Mean Vote/Predicted Percentage of Dissatisfaction) graph and the weekday PPD over 24 hours for the warmest month (February) and coldest month (July).

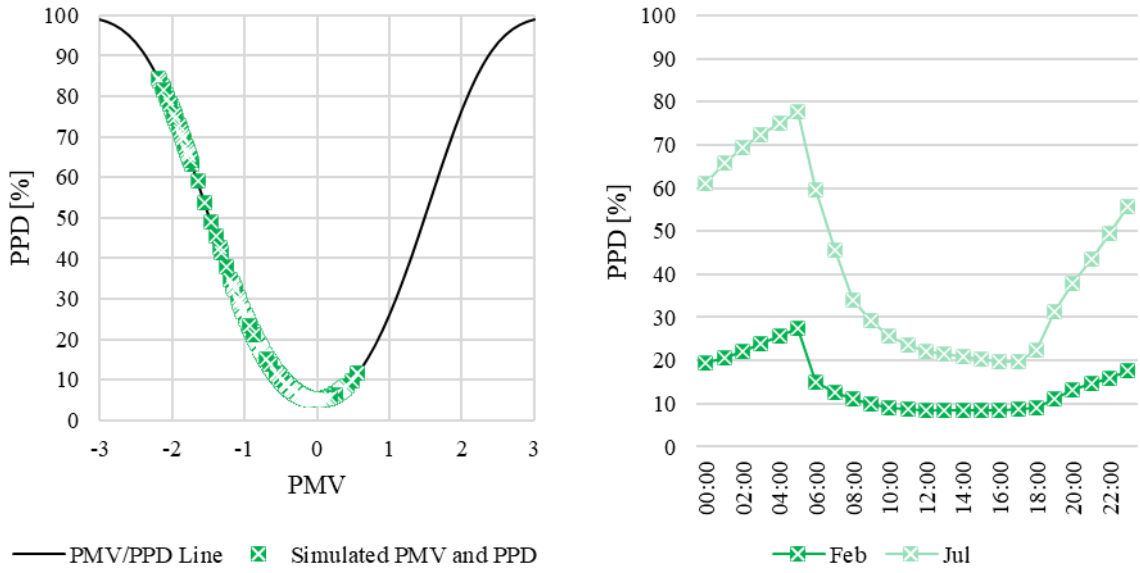

Figure 6-15: Occupants' Thermal Comfort for Building with Conventional HVAC Installation. PMV/PPD for the Office Building (left) and Average PPD over 24 hours for Warmest and Coolest Months (right)

The PMV/PPD graph shows that the data points are prominent on the negative side of the scale, meaning that the occupants experience a neutral to slightly cooler thermal sensation. The weekday PPD is highest in the mornings and evenings and reduces during the day as the building is occupied. The February PPD profile is improved during the day because the chiller provided the required cooling load. In July, the cooling load was significantly less, meaning that PPD was reduced mainly from the heat radiating from the lights, electrical load and occupants. The HVAC may not have provided additional heating in the cooler months. The occupants' thermal comfort, however, was not confirmed. The sum of the data points from the graph is tabulated in Table 6-4. Each data point from the PMV/PPD graph represents the occupants' thermal sensation for every hour. Over the simulated period, the building is occupied for 2088 hours (261 weekdays in 2012 × 8 hours). Therefore table shows that the occupants' thermal sensation would be neutral most of the time (84.48%) and slightly cool for 12.55% of when they occupy the building.

Table 6-4: PMV for Simulated Office Building with HVAC

	-3 Cold	-2 Cool	-1 Slightly Cool	0 Neutral	1 Slightly Warm	2 Warm	3 Hot
No. of hours	0	60	262	1764	2	0	0
No. of hours [%]	0.00%	2.87%	12.55%	84.48%	0.10%	0.00%	0.00%

6.4 Concluding Remarks

This case study aimed to show that the energy consumption of actual HVAC installations can be simulated using EnergyPlus, as presented in Chapter 4. A building with an HVAC installation used for the case study had been optimised by installing Variable Speed Drives (VSDs) at the pumps and fans. Although the building's architectural drawings and exact chiller sizes were unavailable, the simulations correlated with the actual demand and energy consumption. The simulated and actual energy consumption differences could result from modelling a very low U-value for the building construction and overstating heat loads.

7 Systems Comparison by Simulations

The case studies in Chapters 5 and 6 showed how accurately the TABS calculator and EnergyPlus determined TABS' and HVAC's demand and energy consumption. The buildings used in the case studies had different thermal loads, occupancy levels and thermal insulation, making it difficult to compare the systems' performances. Therefore, the following chapter presents a case study where TABS and the conventional HVAC system are modelled and simulated on the same office building with the same thermal load, occupancy levels and thermal insulation. The office building was also simulated with the space cooling system switched off to highlight the dissatisfaction in thermal comfort that occupants would experience when the systems are unavailable. The case study compares the systems' performances and ability to ensure thermal comfort to validate the hypothesis given in chapter 1.2, which states:

TABS consume 30% less energy than conventional HVAC systems while maintaining the same thermal comfort level.

7.1 Office Building Description

Figure 7-1 shows the simple office building model used in this case study. The building was modelled in SketchUp Pro and imported into EnergyPlus to model and simulate the heat loads.

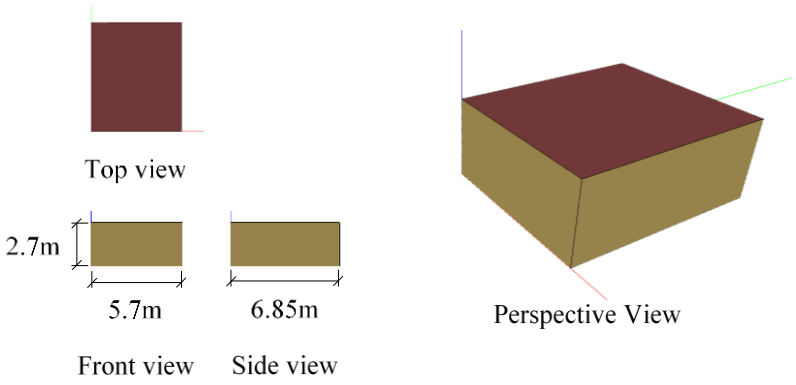

Figure 7-1: 3D Model of Simple Office Space

7.1.1 Weather Data Download and Formatting

The weather data used was for the year from July 2020 to June 2021. The period's average outside air temperature, relative humidity, dew point and air pressure were given in Figure 5-10.

7.1.2 Heat Load Modelling and Simulation

The office building was modelled with an overcapacity of people to ensure that the building only requires cooling, as has been the focus in previous case studies presented in Chapters 5 and 6. The heat loads used in the simulations are summarised in Table 6-2 below.

Table 7-1: Design Heat Loads and Thermal Comfort Factors

	Cooling season	Heating season
People [m^2/person]	1	
Metabolic rate [met]	2 (using Table 2-2)	
Clothing insulation [clo]	0.5 (using Table 2-3)	1 (using Table 2-3)
Occupational hours	06:00 – 18:00 (12 hours)	
Air velocity [$m.s^{-1}$]	0.1	
Lights [W/m^2]	0	
Electric Equipment [W/m^2]	0	

7.1.3 Occupants' Thermal Comfort

The heat loads were modelled and simulated in EnergyPlus. Figure 7-2 shows the average weekday operative temperature and relative humidity when a space cooling technology is not installed. The lack of space cooling raises the operative temperature to approach 30°C and relative humidity between 65% and 80% when the office building is occupied.

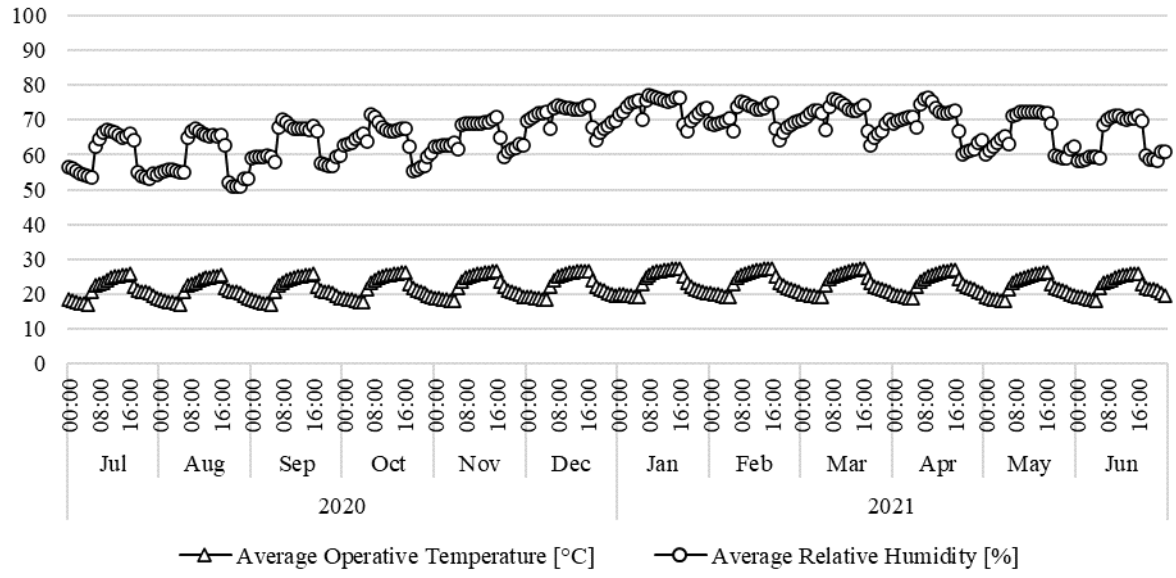

Figure 7-2: Average Inside Operative Temperature and Relative Humidity for Simulation with no TABS or HVAC Installation

Figure 7-3 shows charts indicating the relationship between Predicted Mean Vote (PMV) and Percentage of Predicted Dissatisfaction (PPD) when no space cooling system is installed. The chart on the left shows that PMV values range between -1 (slightly cool) and 2 (warm), and PPD approaches 50% when the office building is occupied. The chart on the right shows the average PPD throughout the weekday for the warmest and coolest months of the year, i.e. February and July. Three periods in the day should be noted:

- In both months before 06:00, when the office building is not occupied, the outside weather is cold, and the heat load inside is minimal, resulting in a low operative temperature. The occupants would have experienced an unsatisfying thermal sensation, hence the high PPD. In July and other cooler months, PPD is higher because of the colder mornings.
- From 06:00, when the building starts to be occupied, the occupants radiate heat into the office space raising the operative temperature and reducing PPD to around 10%. The occupants continue to radiate heat throughout the day, increasing the operative temperature and raising PPD. PPD increases faster in February and other warmer months, and the occupants experience a slightly warm thermal sensation. From around 16:00, PPD in February drops as the outside temperature decreases. PPD in July remains at 15%, and the occupants experience a neutral thermal sensation.
- Once the building is vacated from 18:00, PPD increases in both months since the heat load is minimal and the operative temperature decreases. In July, PPD in the evening is again more significant than in February because of the colder evening. During these periods, occupants would have experienced a slightly cool thermal sensation.

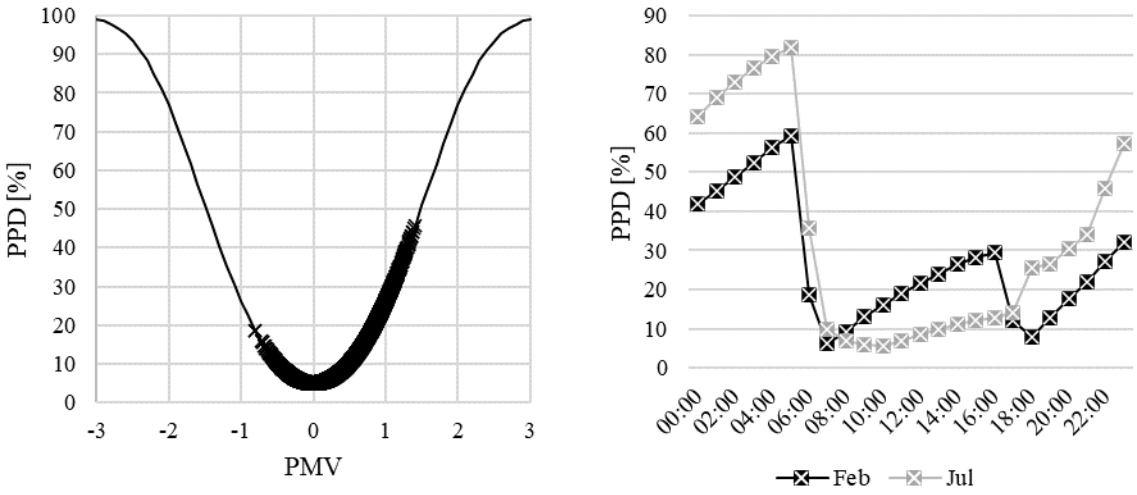

Figure 7-3: PMV and PPD for Simulation of Office Building without Space Cooling Installation

The PMV/PPD chart was mapped to the PMV sensational scale in Table 7-2. Each data point in the PMV/PPD scale represents an hour when the office building is occupied. Over the simulated period, the building is occupied for 3132 hours. Therefore, the table shows that when the building is occupied, the occupants' thermal experience is slightly warm 48.88%of the time and neutral 49.78% of the time.

Table 7-2: PMV for Simulated Office Building with no Space Cooling Installation

	-3 Cold	-2 Cool	-1 Slightly Cool	0 Neutral	1 Slightly Warm	2 Warm	3 Hot
No. of hours	0	0	42	1559	1531	0	0
No. of hours [%]	0.00%	0.00%	1.34%	49.78%	48.88%	0.00%	0.00%

7.2 HVAC Simulations

7.2.1 Simulated Demand Energy Consumption

The office building was modelled and simulated with a VAV HVAC system in EnergyPlus and a chiller Coefficient of Performance (COP) of 4. Figure 7-4 shows the average weekday demand profile for each month resulting from the simulation. The figure shows that the total demand, which consists of sensible and latent demand, is highest in the warmer months (January and February) and lowest in the cooler months (July and August). The peak sensible demand is around 400W.

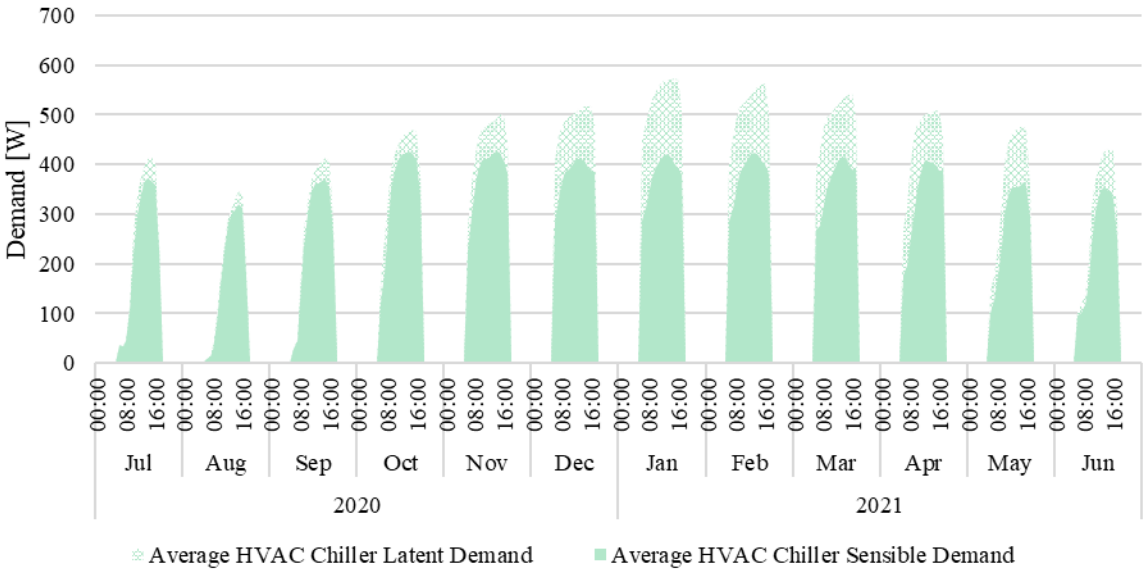

Figure 7-4: Average Weekday HVAC Chiller Demand for Each Month

Table 7-3 shows the average weekday cooling demand the HVAC system delivers to meet thermal comfort.

Table 7-3: Chiller's Average Weekday Sensible and Total Cooling Energy Consumption

2020	Sensible	Total	2021	Sensible	Total
Jul	6 644.37 Wh	7 386.64 Wh	**Jan**	19 960.93 Wh	29 017.33 Wh
Aug	4 661.56 Wh	5 036.85 Wh	**Feb**	18 674.37 Wh	26 335.97 Wh
Sep	7 366.84 Wh	8 195.42 Wh	**Mar**	16 985.70 Wh	23 418.09 Wh
Oct	10 776.18 Wh	12 405.91 Wh	**Apr**	13 606.36 Wh	18 336.70 Wh
Nov	14 246.85 Wh	17 109.32 Wh	**May**	9 123.36 Wh	12 212.70 Wh
Dec	15 919.23 Wh	21 185.45 Wh	**Jun**	7 961.11 Wh	9 764.68 Wh

Table 7-4 shows the chiller's monthly sensible and total energy consumption in the simulated period.

Table 7-4: Chiller's Monthly Sensible and Total Cooling Energy Consumption

2020	Sensible	Total	2021	Sensible	Total
Jul	66 297.46 Wh	70 773.06 Wh	**Jan**	96 329.80 Wh	135 431.10 Wh
Aug	47 510.58 Wh	49 642.52 Wh	**Feb**	92 220.99 Wh	123 963.65 Wh
Sep	71 285.71 Wh	76 067.34 Wh	**Mar**	103 468.92 Wh	137 064.38 Wh
Oct	94 332.68 Wh	103 321.03 Wh	**Apr**	93 961.68 Wh	118 925.05 Wh
Nov	98 268.99 Wh	112 387.18 Wh	**May**	76 516.47 Wh	92 964.12 Wh
Dec	107 684.65 Wh	135 322.98 Wh	**Jun**	70 244.25 Wh	80 422.24 Wh

7.2.2 Occupants' Thermal Comfort

The average weekday operative temperature and relative humidity when the building is with and without an HVAC installation are shown in Figure 7-5. The figure shows that when the HVAC system is off, in the early mornings and late evenings, the operative temperature and relative humidity are the same as when there is no HVAC installation. During the day, when the office building is occupied, and the HVAC system is on, both operative temperature and relative humidity are reduced. The figure shows that the HVAC system provides cooling and dehumidification to meet thermal comfort.

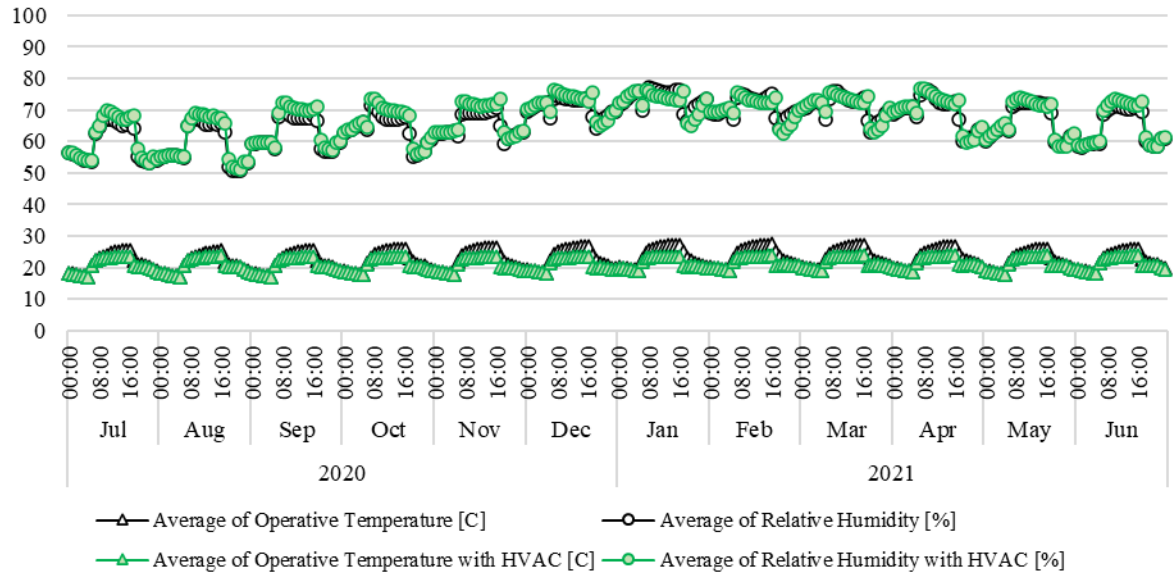

Figure 7-5: Average Inside Operative Temperature and Relative Humidity with and without the Conventional HVAC Installation

Figure 7-6 shows charts indicating the relationship between PMV/PPD when the office building is with and without an HVAC system. The chart on the left shows the occupants' thermal experience when the building is occupied. The simulations show that the occupants' thermal experience is mostly neutral when an HVAC system is installed. The chart on the right shows the average PPD throughout the weekday for the warmest and coolest months of the year, i.e. February and July. Three periods in the day should be noted:

- In the early mornings before 06:00, the office building is not occupied, the HVAC system is off, and PPD is the same as when there is no space cooling system. The cooler month results in a cooler operative temperature and hence a higher PPD than in February.
- From 06:00, when the office building is occupied, occupants radiate heat into the space, and the HVAC system is on. The system controls the air temperature and relative humidity such that PPD is reduced and remains below 10%.
- From 18:00, the office building is no longer occupied, and the operative temperature starts to cool, increasing PPD. During this period, PPD is higher than when no HVAC is installed because the occupants' thermal experience would start from neutral to slightly cool. Therefore PPD begins from a minimum and continues to rise. In contrast, when no cooling system is installed, the occupants' thermal experience starts from slightly warm, shifts to neutral, and then moves to slightly cool. Therefore, PPD begins at a higher level and then reduces to a minimum before rising again.

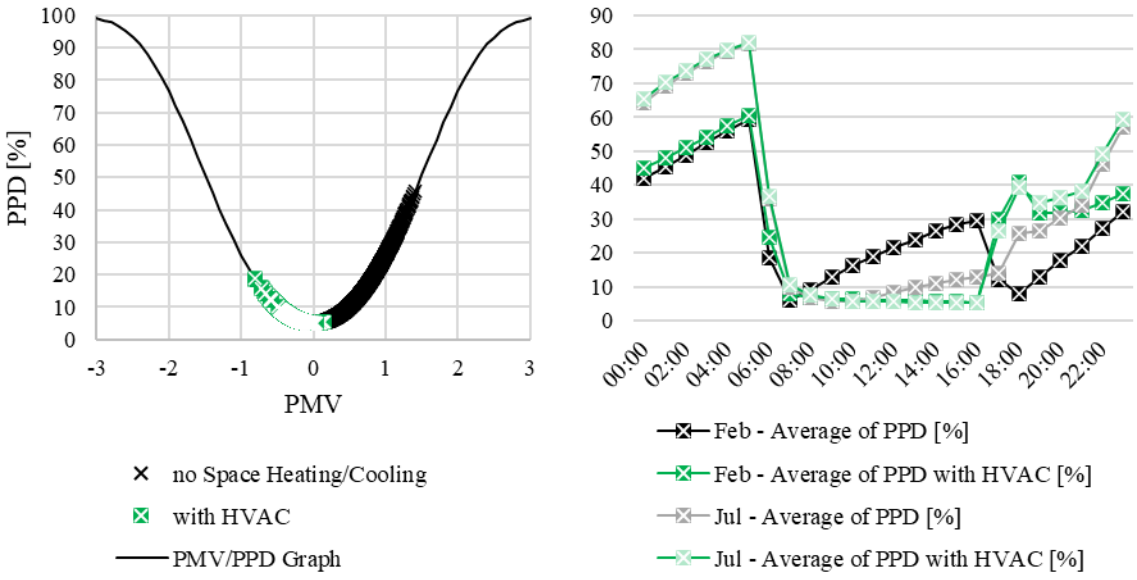

Figure 7-6: Simulated PMV and PPD for Conventional HVAC Installation

The PMV/PPD chart was mapped to the PMV sensational scale, as given in Table 7-5 below. Over the simulated period, the building is occupied for 3132 hours. Therefore, the table shows that 97.25% of the time, when the building is occupied, the occupants' thermal experience is neutral.

Table 7-5: PMV for Simulated Office Building with Conventional HVAC Installation

	-3 Cold	-2 Cool	-1 Slightly Cool	0 Neutral	1 Slightly Warm	2 Warm	3 Hot
No. of hours	0	0	86	3046	0	0	0
No. of hours [%]	0.00%	0.00%	2.75%	97.25%	0.00%	0.00%	0.00%

7.3 TABS Simulations

7.3.1 Circuit Description

The schematic of TABS used in the TABS calculator is given in Figure 7-7 below. The screed and pipe characteristics are shown in the figure. Further pipe details are provided in Appendix D-1: Technical Details of Pexal Multilayer Pipe.

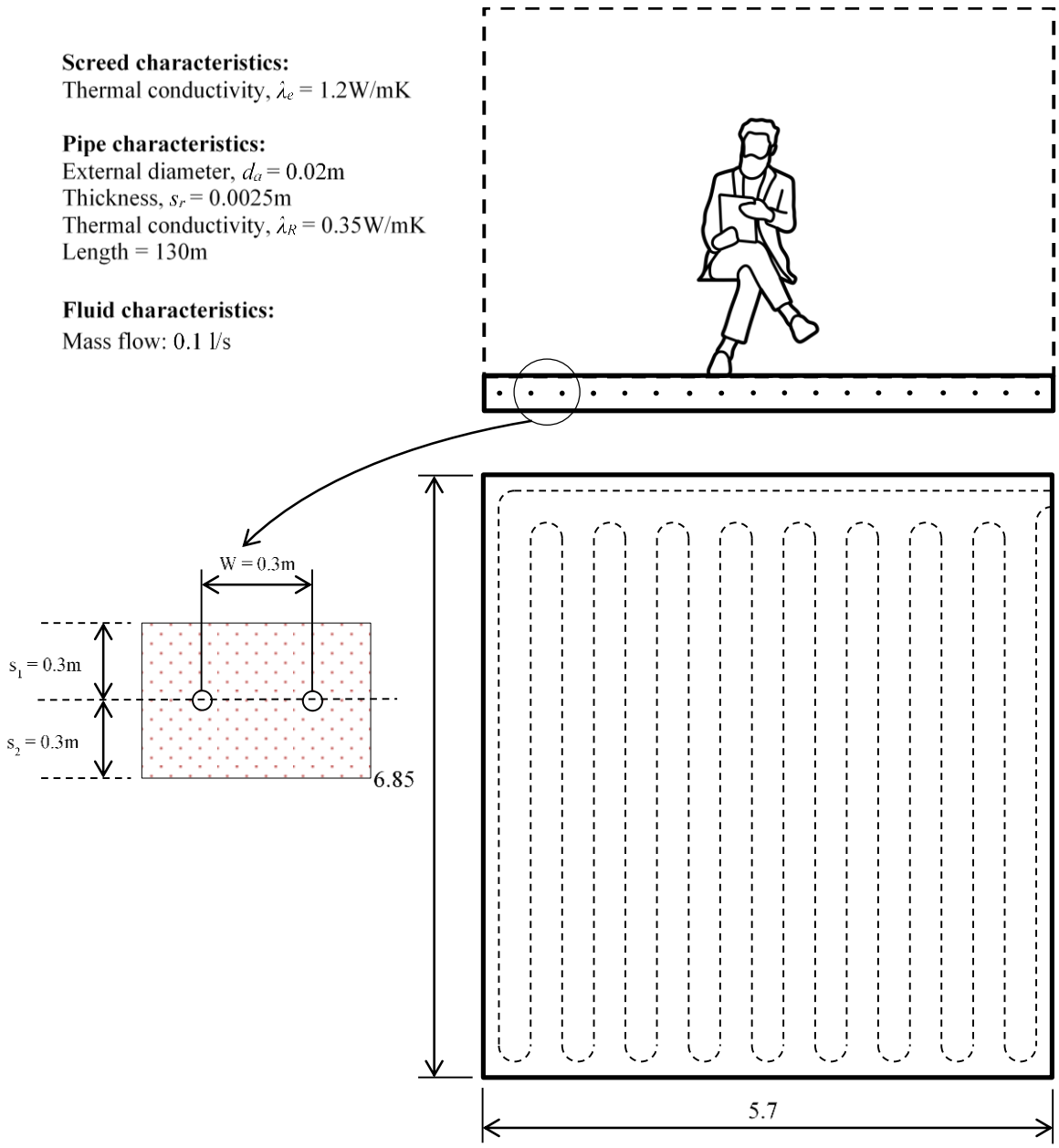

Figure 7-7: Schematic for TABS

7.3.2 Required Cooling Capacity

As explained in Chapter 4.3, EnergyPlus simulations aim to determine the HVAC's energy consumption required to optimise occupants' thermal comfort. The TABS calculator requires that the cooling energy should already be determined. Therefore, choosing the required cooling capacity was an iterative process. It is derived from the cooling demand determined by the HVAC simulations shown in Figure 7-4 and Table 7-3. Various percentages of the HVAC sensible demand were input into the TABS calculator, and the thermal comfort was analysed. The percentage of HVAC sensible demand that achieved the best thermal comfort would determine the cooling capacity.

Figure 7-8 gives the PMV/PDD graph determined by the TABS calculator at various percentages of the HVAC sensible demand. The figure shows that at 100%, the occupants are slightly cool, and at 25%, they are slightly warm. At 50%, the occupants seem to have a neutral thermal experience.

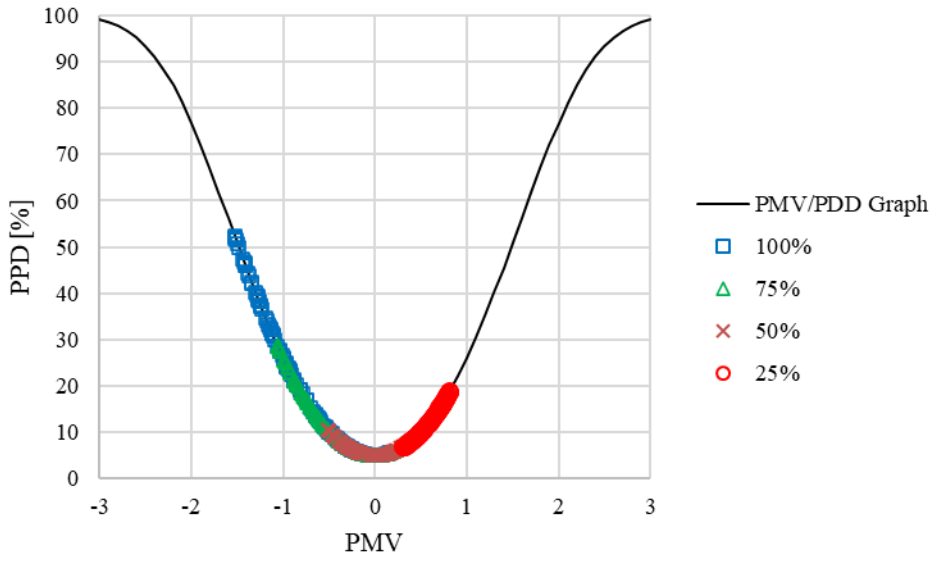

Figure 7-8: PMV and PPD Values of TABS Operating at 100%, 75%, 50% and 25% of HVAC Sensible Energy

The PMV/PPD values chart was mapped to the PMV sensational scale and given in Table 7-6 below. The table confirms that the occupants would experience the most neutral thermal experience when TABS's sensible energy is 50% of HVAC's sensible energy. As with the HVAC simulation, the building is occupied for 3132 hours and 97.25% of the time, the occupants' thermal experience is neutral.

Table 7-6: PMV for Simulated Office Building with TABS Installation at Various Sensible Energy of HVAC Simulations

	-3 Cold	-2 Cool	-1 Slightly Cool	0 Neutral	1 Slightly Warm	2 Warm	3 Hot
100% Sensible Energy							
No. of hours	0	84	1693	1355	0	0	0
No. of hours [%]	0.00%	2.68%	54.05%	43.26%	0.00%	0.00%	0.00%
75% Sensible Energy							
No. of hours	0	0	1365	1767	0	0	0
No. of hours [%]	0.00%	0.00%	43.58%	56.42%	0.00%	0.00%	0.00%
50% Sensible Energy							
No. of hours	0	0	84	3048	0	0	0
No. of hours [%]	0.00%	0.00%	2.68%	97.32%	0.00%	0.00%	0.00%
25% Sensible Energy							
No. of hours	0	0	0	1191	1941	0	0
No. of hours [%]	0.00%	0.00%	0.00%	38.03%	61.97%	0.00%	0.00%

7.3.3 Simulated Demand and Energy Consumption

As with the HVAC simulations, the chiller's COP was set to 4. Therefore, the TABS calculator determined the average weekday chiller demand profile for all months, as shown in Figure 7-9. The figure shows that the chiller begins with a spike and tapers down throughout the day.

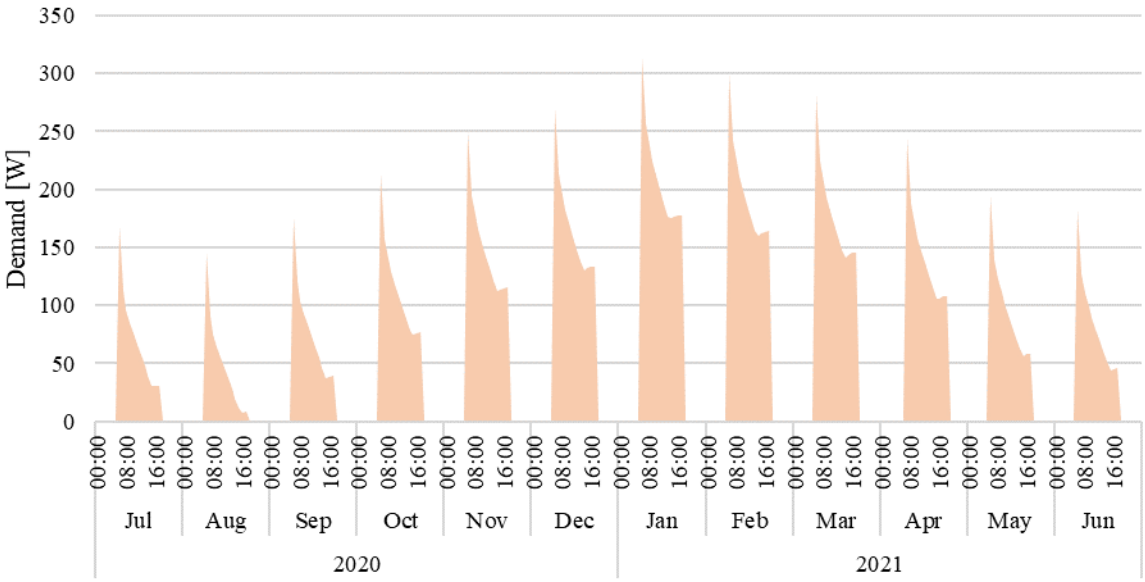

Figure 7-9: Average TABS Chiller Demand

The weekday and monthly chiller energy consumption are given in Table 7-7. The table shows that the most significant energy consumption occurred in January.

Table 7-7: Weekday and Monthly Cooling Energy Consumption

	2020		2021		
Month	**Weekday**	**Month**	**Month**	**Weekday**	**Total**
Jul	3322.19 Wh	19 211.30 Wh	**Jan**	9980.47 Wh	52 695.86 Wh
Aug	2330.78 Wh	12 306.13 Wh	**Feb**	9337.18 Wh	46 951.85 Wh
Sep	3683.42 Wh	20 374.00 Wh	**Mar**	8492.85 Wh	49 112.00 Wh
Oct	5388.09 Wh	29 803.13 Wh	**Apr**	6803.18 Wh	37 630.60 Wh
Nov	7123.43 Wh	37 610.90 Wh	**May**	4561.68 Wh	24 085.01 Wh
Dec	7959.61 Wh	46 028.39 Wh	**Jun**	3980.56 Wh	22 017.70 Wh

7.3.4 Occupants' Thermal Comfort

Figure 7-10 shows the average weekday operative temperature and relative humidity for each month as determined by the TABS calculator. The figure also included the average weekday operative temperature and relative humidity from Figure 7-2. The calculator determined that the operative temperature would be decreased to 22°C, and the relative humidity would rise to 100%. Therefore, as the temperature decreases, office space would realise even more condensation. The results show that TABS needs to include a system for dehumidification to operate successfully.

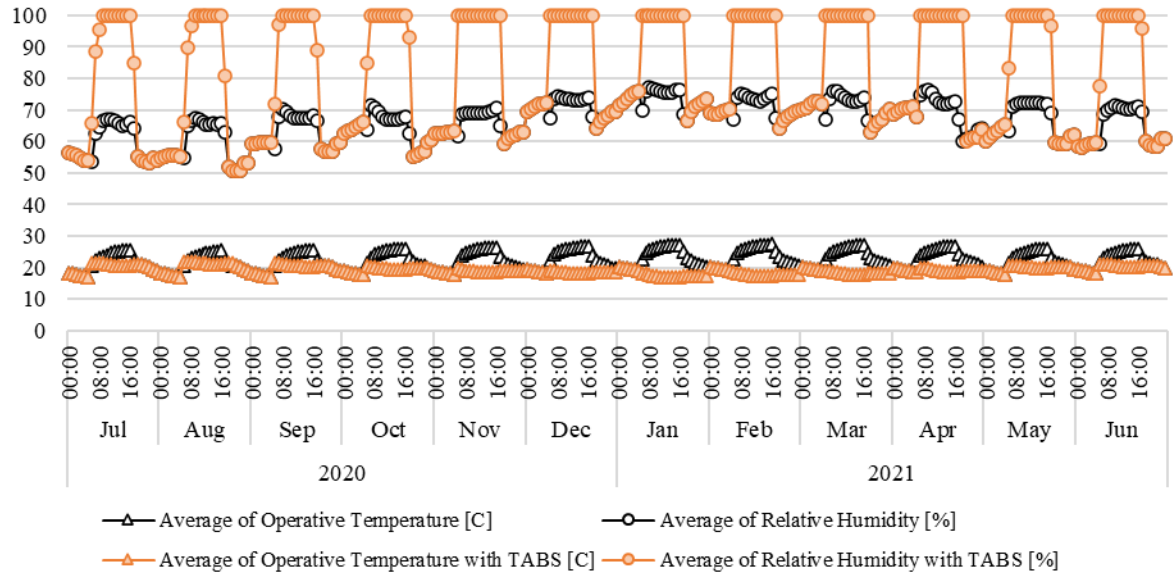

Figure 7-10: Average Inside Operative Temperature and Relative Humidity for Simulations with and without TABS Installation

Figure 7-11 shows the PMV/PPD relationship when the office building is with and without TABS. The graph on the left indicates that when the office has TABS installed, the occupants' thermal experience would mostly be neutral. The graph on the right shows the average PPD throughout the weekday for the warmest and coolest months of the year, i.e. February and July. Three periods in the day should be noted:

- In the early mornings before 06:00, the office building is not occupied, TABS is off, and PPD is similar to when there is no space cooling system. The cooler month results in a cooler operative temperature and hence a higher PPD than in February.
- From 06:00, when the office building is occupied, occupants radiate heat into the space, and TABS is on. The system controls the air temperature such that PPD is reduced and remains below 10%.
- After 18:00, when the office building is no longer occupied, PPD is similar to when there is no space cooling system.

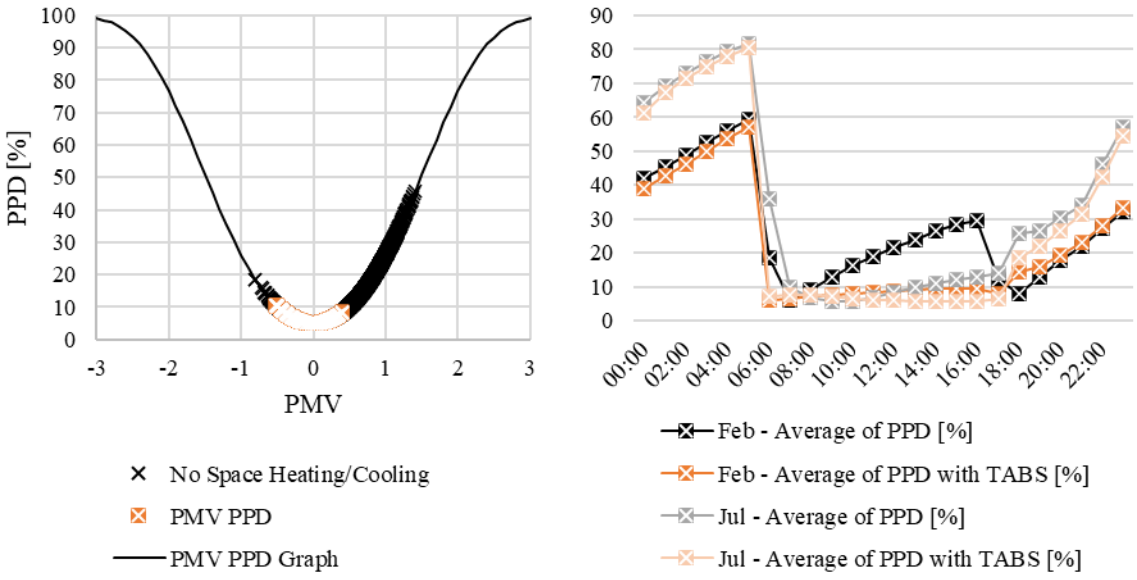

Figure 7-11: Simulated PMV and PPD for Occupants in Office Building with TABS Installation

7.4 Comparing TABS and Conventional HVAC Simulations

Figure 7-12 shows each month's average weekday operative temperature and relative humidity from the TABS and conventional HVAC simulations. The figure shows that the operative temperature for both systems is mostly similar. The figure also shows that the HVAC simulation reduces relative humidity to avoid condensation. Unfortunately, the TABS calculator does not make provision for dehumidification hence the rise in relative humidity. Turning off dehumidification in the HVAC simulation to make a fair comparison was also not possible. Therefore the only comparison that can be deduced from the simulation should be focused on the sensible demand and energy.

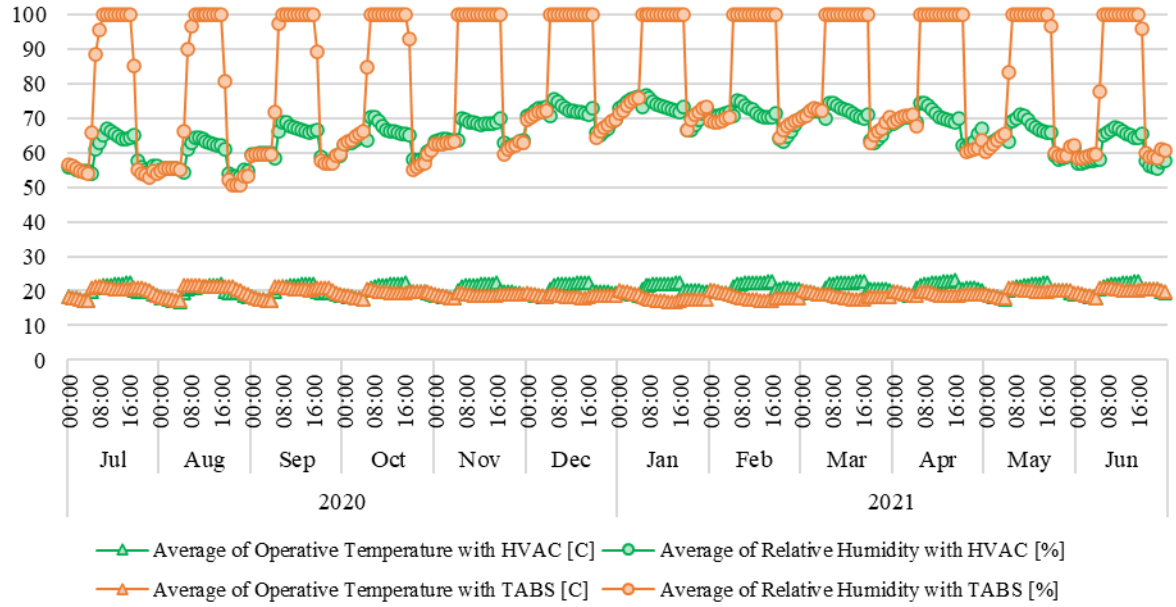

Figure 7-12: Operative Temperature and Relative Humidity for TABS and Conventional HVAC Simulation

Figure 7-13 shows the PMV/PPD relationship and PPD over the weekday for both TABS and HVAC simulations. The figure shows that although TABS does not provide dehumidification, the system can improve PMD and PPD similarly to the conventional HVAC system. Unless dehumidification is considered with a TABS installation, it may result in condensation. Condensation would lead to mould growth, unpleasant damp smells and damage to decorations and fabrics.

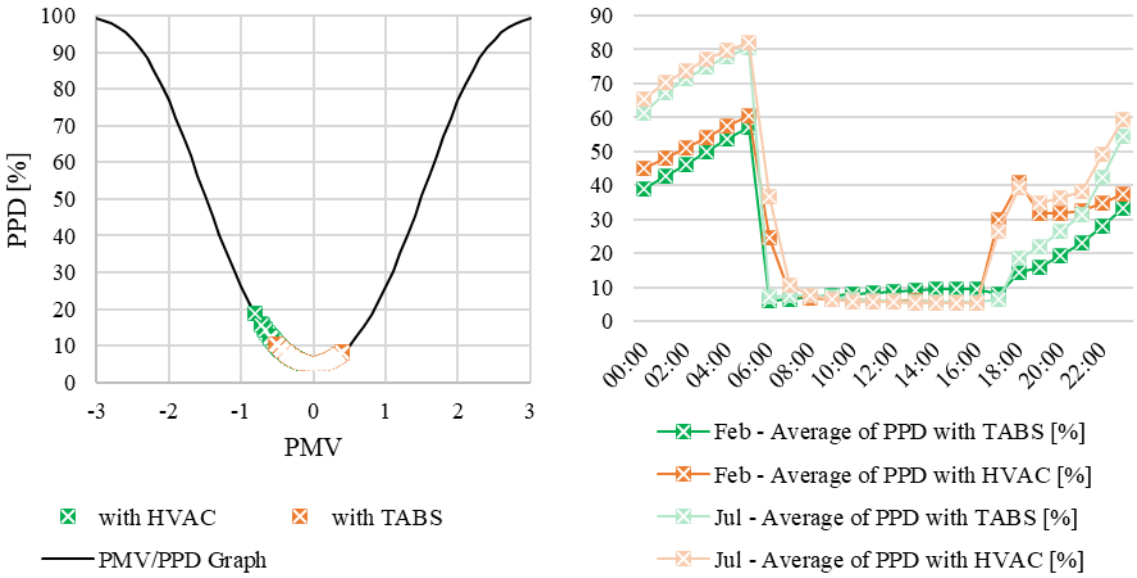

Figure 7-13: PMV/PPD graph and PPD for the weekday for TABS and Conventional HVAC Simulation

Figure 7-14 shows the chiller sensible demand profile for both systems. The figure shows that the sensible chiller demand in TABS is less than the sensible demand for the HVAC system. However, the chiller demand in the HVAC system avoids the TABS starting peak demand.

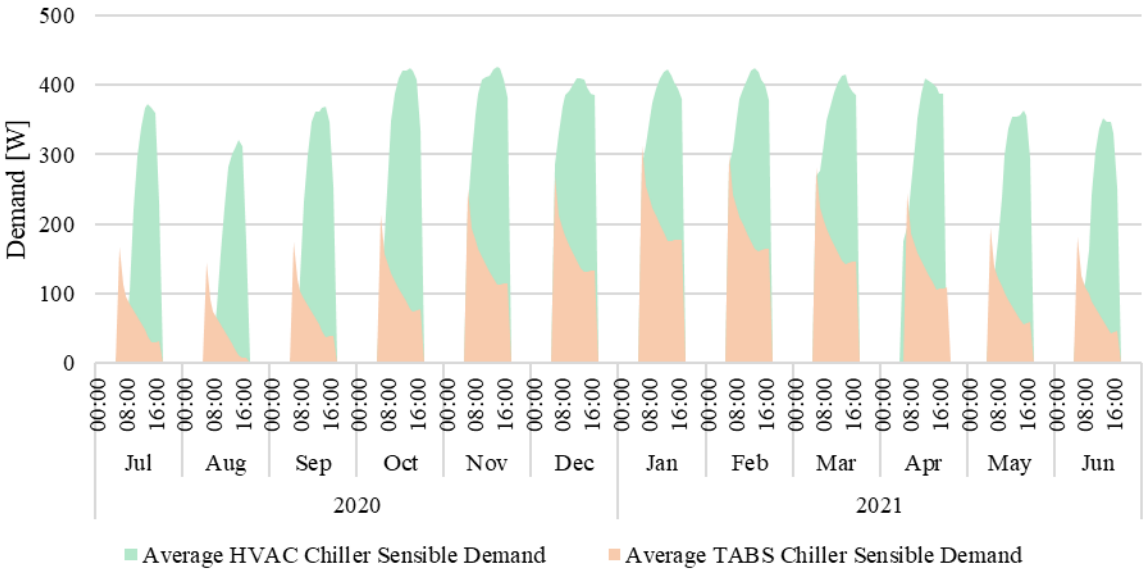

Figure 7-14: Average Weekday TABS and Conventional HVAC Demand

A comparison of the monthly chiller energy consumption for TABS and the conventional HVAC system is given in Figure 7-15 below. The figure includes a linear regression that shows that TABS consumes 41.62% of the HVAC chiller's monthly sensible energy consumption. The high R2 value indicates a high correlation between the chiller's energy consumption.

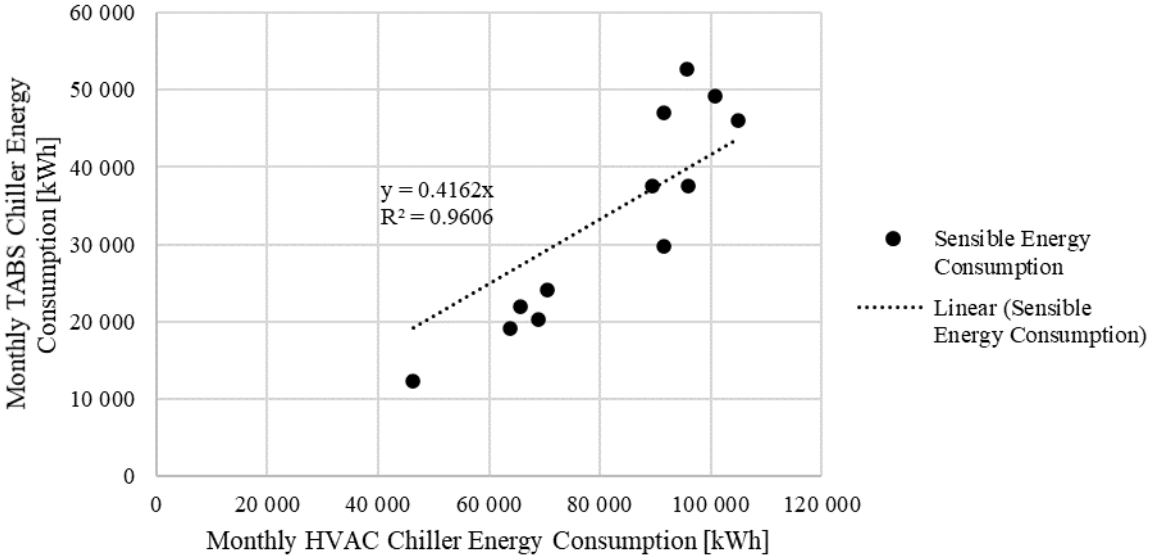

Figure 7-15: Monthly TABS and Conventional HVAC Chiller Energy Consumption

7.5 Concluding Remarks

The chapter compared occupants' thermal comfort, chiller demand and energy consumption from simulations of TABS and the conventional HVAC system. The systems were modelled and simulated in the same office building with the heat load mainly from its occupants. Weather data was sourced from Cape Town International Airport and formatted to be used in EnergyPlus. Initially, the occupants were simulated without a space cooling system which showed that they would mostly have a slightly warm thermal experience. The occupants' thermal satisfaction improved when the building was modelled and simulated with the HVAC system. The simulation results showed that 97.25% of the time when the building is occupied, the occupants' thermal experience would be neutral.

For the TABS calculator, it was determined that when half of the sensible energy consumption of an HVAC system was used as input into the TABS calculator, the occupants would have a neutral thermal experience. When comparing the sensible energy consumption of both systems, the simulations show that TABS consumes 41.62% of the HVAC chiller's energy to provide the same neutral thermal experience. Once again, it should be noted that the TABS calculator does not make provision for dehumidification; therefore, the calculator can only determine the sensible chiller demand and energy consumption.

8 The Business Case for a TABS Installation

The following chapter presents a business case for installing TABS instead of an HVAC system at Eskom's office building. The business case is based on the reduced demand and energy consumption of TABS compared to the HVAC system, as determined in Chapter 7. In making the business case, the following investment terms need to be understood (Firer, Ross, Westerfield, & Jordan, 2012):

- **Net Present Value (NPV):** refers to the difference between an investment's discounted cash flows and cost. NPV can be calculated using Microsoft's Excel function *=NPV(rate, value1, [value2],…)*. In this research, the same result can be using the following formula:

  NPV = Investment Amount + Discounted Cash Flow

- **Discount Rate:** refers to the interest rate used to determine the present value of future cash flows.
- **Net Cash Flow**: refers to the gain or loss of funds after all costs have been paid.
- **Discounted Cash Flow (DCF):** refers to the valuation of an investment by discounting its expected future cash flows.
- **Simple Payback Period:** refers to the amount of time for an investment's cash flows to recover the cost of an investment.
- **Discounted Payback Period:** refers to the amount of time for an investment's discounted cash flows to recover the cost of an investment.
- **Internal Rate of Return (IRR):** refers to a discount rate that makes all cash flows' net present value (NPV) equal to zero. In this research, NPV was calculated using Microsoft's Excel function *=IRR(values, [guess])*.

The following business case used Eskom's official discount rate of 10.4%.

8.1 Analysis of Current HVAC Installation

The building used in this business case was Eskom's Megawatt Park since its existing HVAC system had reached its end of life and needed to be replaced. The three-floor building is in Johannesburg, South Africa and consists mainly of open office spaces separated into Blocks A, B, C and D, Link and Centre Core. The HVAC system to be replaced supplies heating and cooling to Blocks C, D and Centre Core, illustrated in Figure 8-1. The Centre Core is composed mainly of an open courtyard, elevators, escalators and a few offices, which do not contribute significantly to the overall HVAC demand.

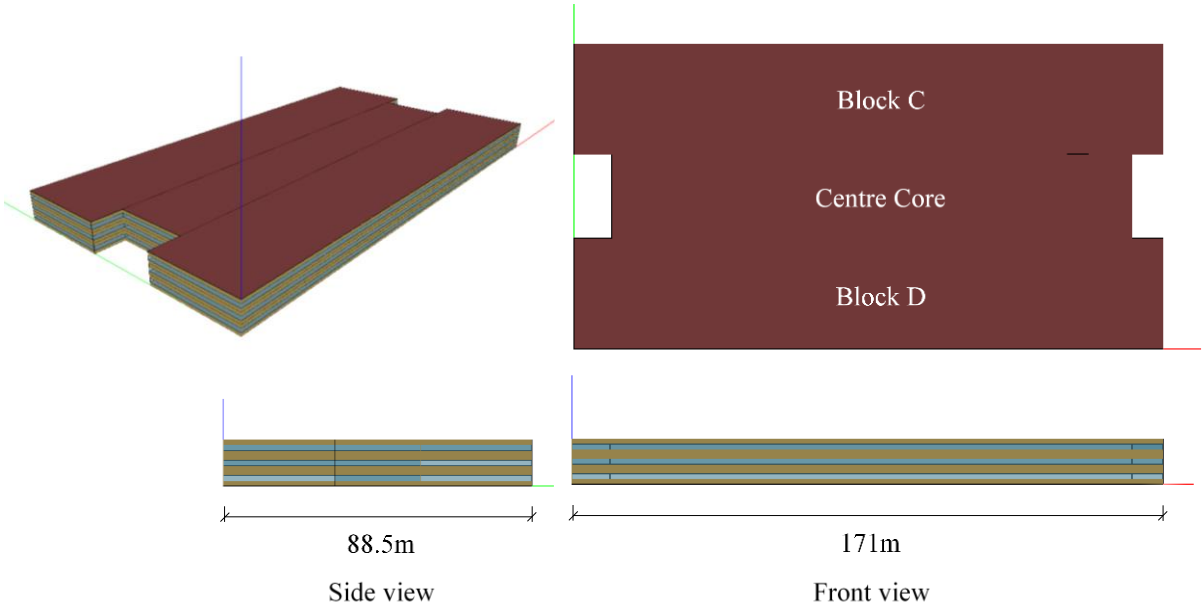

Figure 8-1: Megawatt Park Model

A contractor was appointed to compile a proposal to replace the HVAC system that would meet the criteria given in Table 8-1. The table includes thermal comfort variables, operative temperature, relative humidity and air velocity. The maximum noise level refers to the noise made by the fans and motors moving the air in and out of the office space.

Table 8-1: Desired Indoor Criteria

Max Summer / Min Winter Temp [°C]	**Relative Humidity** [%]	**Max Noise Level** [dBA]	**Min Filter Efficiency** [%]	**Air velocity** [L/s/person]
22±2°C	30-60	35	35%	7.5

8.1.1 Energy Analysis of the HVAC System

The capacity of the chillers and boilers that supply heating and cooling at Block C and D are given in Table 8-2 below.

Table 8-2: Capacities of Chillers and Boilers at Megawatt Park

Chillers	**Capacity [kW]**	**Boiler**	**Capacity [kW]**
Chiller 1	1 107	Electrode Boiler 1	1 500
Chiller 2	453	Electrode Boiler 2	1 500
Chiller 3	222		
	1 782		**3 000**

Unfortunately, no meters or data loggers were installed at the chillers and boilers, making it difficult to accurately determine the HVAC's demand and energy consumption. Therefore for the business case, the demand profile was estimated as a percentage of the total building energy consumption. Figure 8-2 gives averages of the energy consumed by each technology in a commercial building. The figure shows that energy consumed by an HVAC system in a commercial building is, on average, 26% of the total energy (Eskom, 2014). The energy consumed is potentially a conservative percentage as other studies have estimated more significant usage, i.e. 30.4% (Tamasauskas, Kegel, & Sunye, 2013) and 55% (Liu Y. , 2012).

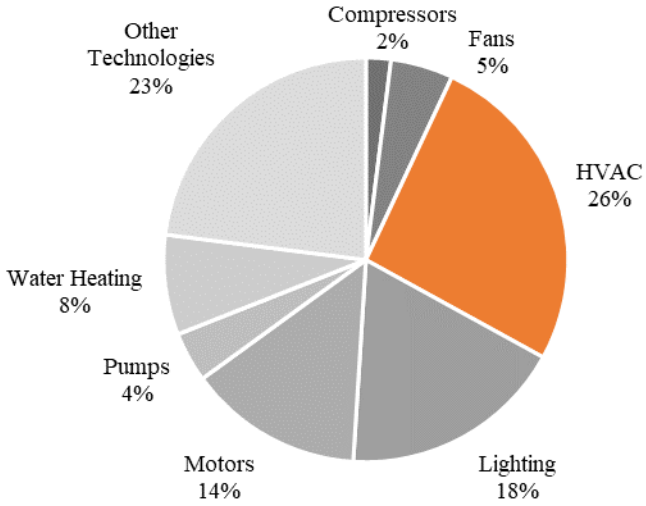

Figure 8-2: Energy Consumption in Typical Commercial Building by Technology (Eskom, 2014)

Megawatt Park's half-hourly energy consumption between April 2018 and March 2019 was used to make this business case. The tariff for Eskom's direct customers increases on 1 April every year, so the period was chosen to avoid analysing electricity costs using multiple tariffs. This date is also the beginning of Eskom's financial year. Assuming that the HVAC consumes 26% of the total energy, the average weekday demand profile for each month is given in Figure 8-3. The figure shows increased electricity demand between 04:30 and 19:30, consistent with the scheduling of the HVAC system.

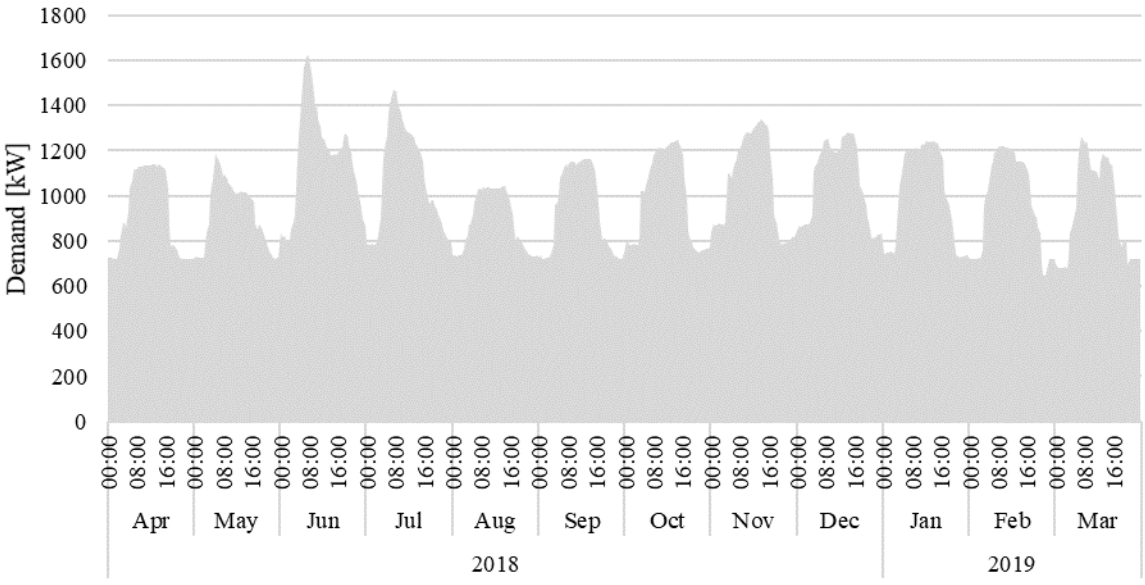

Figure 8-3: Current HVAC Demand

The HVAC monthly energy consumption by Time-of-Use for the period is given in Table 8-3 below. The total annual electricity consumption was 8 056 961.08 kWh.

Table 8-3: HVAC's Monthly Energy Consumption

Year	Month	Off Peak [kWh]	Standard [kWh]	Peak [kWh]	Total [kWh]
2018	**Apr**	257 294.82	253 359.58	102 827.35	613 481.76
	May	265 992.06	265 162.05	114 697.21	645 851.31
	Jun	325 154.53	323 183.83	149 484.32	797 822.67
	Jul	303 363.08	300 366.99	136 717.25	740 447.31
	Aug	252 497.33	249 288.06	103 553.92	605 339.31
	Sep	266 563.61	251 236.28	100 467.06	618 266.95
	Oct	273 128.17	294 973.60	117 226.08	685 327.84
	Nov	286 982.01	301 416.32	117 124.86	705 523.20
	Dec	320 675.67	290 269.54	118 130.10	729 075.31
2019	**Jan**	263 333.51	298 409.64	125 054.51	686 797.66
	Feb	239 150.00	250 285.93	107 829.76	597 265.69
	Mar	259 666.37	261 878.54	110 217.15	631 762.06
		3 313 801.16	**3 339 830.36**	**1 403 329.56**	**8 056 961.08**

8.1.2 Financial Analysis of the HVAC System

Megawatt Park is on the MegaFlex tariff, and the 2018/19 electricity tariff is given in Table 8-4 below.

Table 8-4: MegaFlex Non-local Authority Tariff for 2018/19 (Eskom, 2018)

	High Season (June – August)	Low Season (September – May)
Peak	288.29	94.03
Standard	87.34	64.73
Off-Peak	47.43	41.06

Therefore the electricity cost for the period was determined. Figure 8-4 below shows the total energy consumed per TOU, and the line shows the monthly electricity cost. The monthly electricity costs during the low-demand season averaged R400 000; however, in the high-demand season, the cost approached R900 000. The higher cost results from the higher seasonal tariff and the slightly higher electricity consumption.

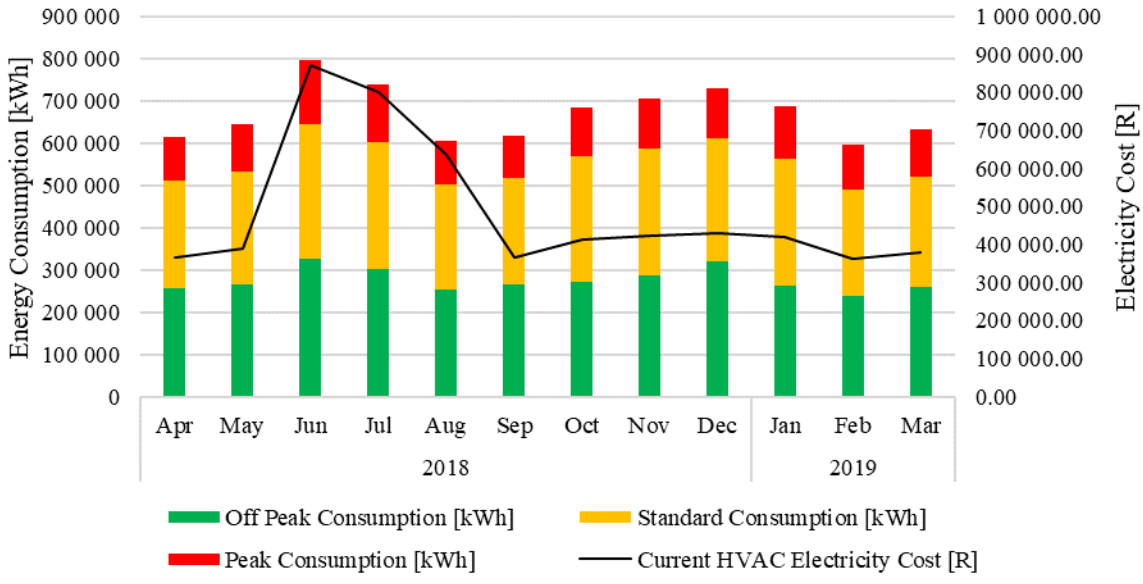

Figure 8-4: Monthly Electricity Consumption and Cost

A breakdown of the electricity consumption and costs is given in Table 8-5 below. The total electricity cost was R5 858 517.74 for the analysed period.

Table 8-5: HVAC Electricity Cost

Month Year	Cost [R]	Month Year	Cost [R]
Apr 2018	366 333.47	**Oct 2018**	413 310.52
May 2018	388 705.51	**Nov 2018**	423 074.11
Jun 2018	872 230.80	**Dec 2018**	430 638.64
Jul 2018	801 590.61	**Jan 2019**	418 874.06
Aug 2018	635 847.01	**Feb 2019**	361 597.39
Sep 2018	366 545.44	**Mar 2019**	379 770.18
		Total	**5 858 517.74**

Assuming that the HVAC electricity consumption remains consistent and the annual cost of electricity increases by 6%, the maximum CPI target by the South African Reserve Bank (South African Reserve Bank, 2020) over 15 years, Figure 8-5 was drawn. This is a conservative tariff increases because the recent actual increase has been greater than 6%. The graph shows that the cost of operating the HVAC system after 15 years will have risen to R13 245 546 annually. It should be noted that the annual increase in electricity tariff for the commercial sector, which includes office buildings, has been 14.36% and 9.97% for Eskom's financial year 2019/20 and 2020/21, respectively (Eskom, 2022). The increases represent an average increase of 12.17%, more than double the maximum CPI target.

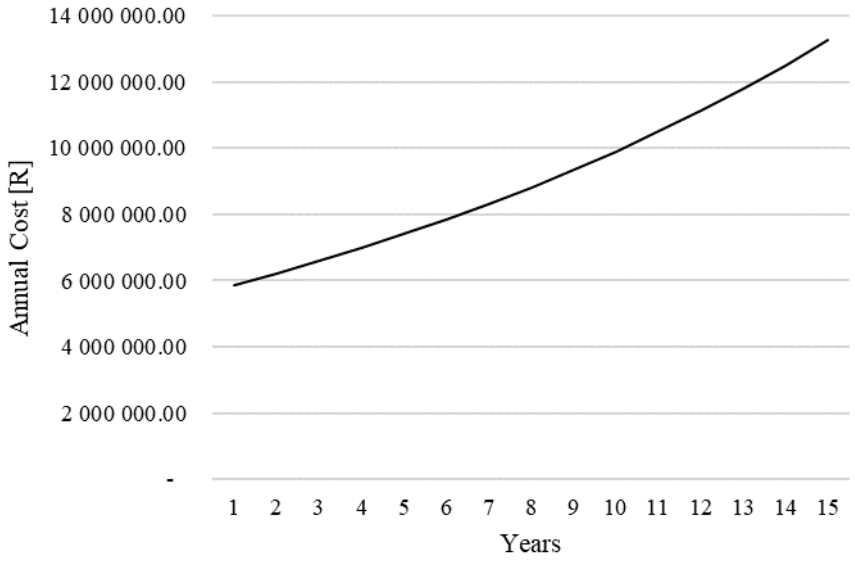

Figure 8-5: Electricity Cost for HVAC System Over 15 Years

8.2 Analysis of the HVAC Replacement

8.2.1 Energy Analysis of HVAC Replacement

The proposal for replacing the HVAC system includes the installation of chillers and boilers with energy-efficient chillers, some of which can reverse their cycle to operate as heat pumps. The respective capacities are given in Table 8-6 below. The table shows that the current installed capacity of boilers and chillers would be reduced from 4782kW to 2500kW, representing a reduction of 48%.

Table 8-6: Capacity of Replacement Chillers and Heatpumps

Currently Installed Items	Total Capacity [kW]	Replacement Items	Total Capacity [kW]
Chiller	1 782	3 x Energy Efficient Chiller	1 000
Boiler	3 000	3 x Energy Efficient Chiller and Heatpump Combination	1 500
	4 782		**2 500**

Table 8-7 shows that assuming that the reduced boiler and chiller capacity would result in a similar reduction in annual electricity consumption, the electricity consumption and cost would be 4 212 129 kWh and R3 062 797, respectively.

Table 8-7: Current, Proposed and Saved Electricity Consumption and Cost

	Current System	Proposed HVAC system	Saving
Electricity consumption	8 056 961 kWh	4 212 129 kWh	3 844 832 kWh
Electricity Cost	R5 858 518	R3 062 797	R2 795 721

8.2.2 Financial Analysis of Replacement HVAC

The contractor quoted that the cost of installing the energy-efficient HVAC installation would be R20 360 000.00. A breakdown of the costs is given in Table 8-8 below.

Table 8-8: Chiller Plant Cost Breakdown

Item(s)	Unit Price [R]	Quantity	Cost [R]
Air-cooled chillers	2 150 000.00	3	6 450 000.00
Air-cooled chillers + Heat pumps	3 000 000.00	3	9 000 000.00
15000L Buffer water tanks	150 000.00	2	300 000.00
Booster pump system (Feeder tank & pumps)	240 000.00	1	240 000.00
Chilled water pumps	435 000.00	2	870 000.00
Valves and strainers	1 500 000.00	1	1 500 000.00
BMS for chiller plant control	650 000.00	1	650 000.00
Piping in the plant area	350 000.00	1	350 000.00
Distribution board in chiller plant	1 000 000.00	1	1 000 000.00
			20 360 000.00

The annual electricity cost savings of R2 795 721 shown in Table 8-7 were then used to determine the time it would take to recoup the investment, i.e. the payback period.

Table 8-9: Electricity Consumption and Costs for Current and Replacement HVAC Systems

	Current HVAC System	Replacement HVAC System	Savings
Electricity Consumption [kWh]	8 056 961	4 212 129	3 844 832
Electricity Cost [R]	5 858 518	3 062 797	2 795 721

Assuming that the electricity consumption remains consistent and an annual cost of electricity increase by 6% (at the maximum CPI) over 15 years and using Eskom's discount rate of 10.4%, the reduced electricity cost and payback periods are given in Figure 8-6 below. The graph on the right shows the cumulative cash flows from the electricity savings. The investment would have been paid back when the cumulative cash flows crossed the dashed line. The figure shows that the simple payback period is seven years, and the discounted payback is ten years.

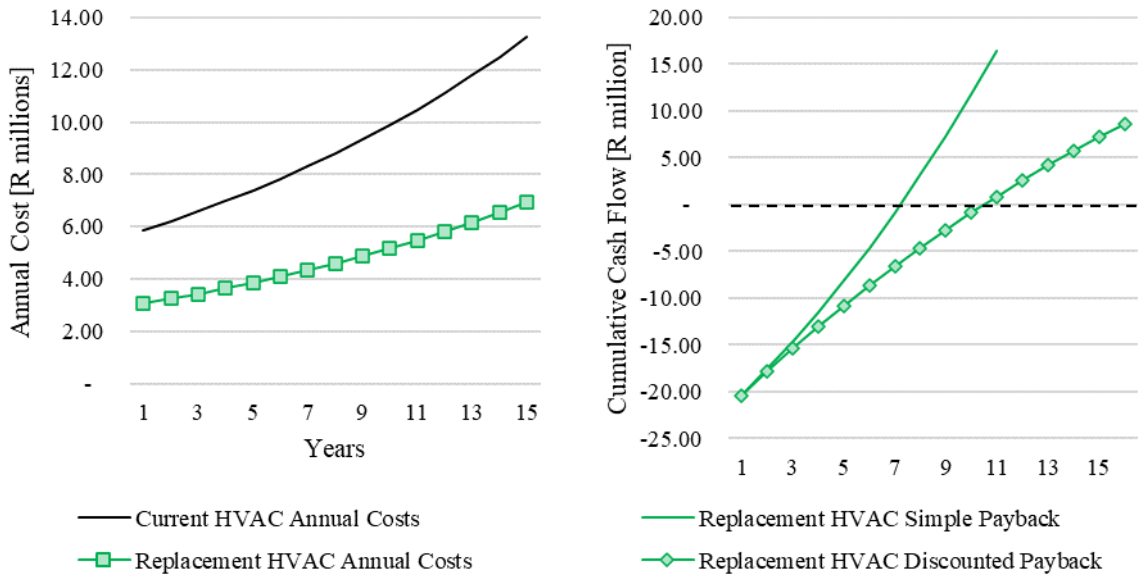

Figure 8-6: Electricity Cost and Net Cash Flow for HVAC Replacement Business Case

The Net Present Value (NPV) over the 15 years can be determined as investment amount + discounted savings, i.e.:

–R20 360 000 + R29 017 345 = **R8 657 345**

The Internal Rate of Return (IRR) was 16%. An IRR higher than the discount rate means the project would add value to the business. The electricity costs, savings and cumulative cash savings are given in Table 8-10 below.

Table 8-10: Net cashflow for HVAC Replacement Case

Year	Current HVAC Annual Costs [R]	HVAC Replacement Annual Costs [R]	Savings [R] (Difference in Costs)	Net Payback [R] (Investment – Savings)	Discounted Savings [R]	Net Discounted Payback [R]
0				-20 360 000		-20 360 000
1	5 858 518	3 062 797	2 795 721	-17 564 279	2 532 356	-17 827 644
2	6 210 029	3 246 565	2 963 464	-14 600 815	2 431 429	-15 396 215
3	6 582 631	3 441 358	3 141 272	-11 459 543	2 334 524	-13 061 691
4	6 977 588	3 647 840	3 329 748	-8 129 794	2 241 481	-10 820 210
5	7 396 244	3 866 710	3 529 533	-4 600 261	2 152 147	-8 668 063
6	7 840 018	4 098 713	3 741 305	-858 956	2 066 373	-6 601 690
7	8 310 419	4 344 636	3 965 784	3 106 828	1 984 017	-4 617 673
8	8 809 045	4 605 314	4 203 731	7 310 558	1 904 944	-2 712 729
9	9 337 587	4 881 633	4 455 954	11 766 513	1 829 023	-883 706
10	9 897 842	5 174 531	4 723 312	16 489 824	1 756 127	872 421
11	10 491 713	5 485 003	5 006 710	21 496 535	1 686 136	2 558 557
12	11 121 216	5 814 103	5 307 113	26 803 648	1 618 935	4 177 492
13	11 788 489	6 162 949	5 625 540	32 429 187	1 554 412	5 731 905
14	12 495 798	6 532 726	5 963 072	38 392 260	1 492 461	7 224 366
15	13 245 546	6 924 689	6 320 857	44 713 116	1 432 979	**8 657 345**
			65 073 116		**29 017 345**	

8.3 Analysis of a TABS Installation and HVAC Comparison

As determined in Chapter 7.4, TABS electricity consumption is 41.62% of the conventional HVAC system. For the business case, the error variance of 15% in the TABS calculator discussed in Chapter 4.2 was included as a safety factor. The safety factor also ensures that the savings from TABS are conservative. Therefore, for the business case, TABS energy consumption was 41.62 + 15 = 56.62% of the replacement HVAC system. A breakdown of the additional costs is given in Table 8-9. Therefore, the total cost would be R29 581 440, assuming that the equipment used in the replacement HVAC system would remain the same for the TABS installation. The TABS installation would include additional costs for materials such as pipework and its associated labour.

Table 8-11: Additional Costs for TABS Breakdown

Item(s)	Unit Price [R]	Quantity	Cost [R]
Replacement HVAC			20 360 000
20-diameter pex pipe	30	109 440	3 283 200
10 port supply manifolds	12 000	84	1 008 000
20% Contingency for Miscellaneous Items (e.g. Pipe fixing mesh, screed and supply piping)			4 930 240
		Total	**29 581 440**

The TABS installation would result in reduced annual electricity consumption of 2 384 908 kWh, and the electricity cost would be R1 734 156 compared to the current HVAC installation, as shown in Table 8-12 below.

Table 8-12: Electricity Consumption and Costs for Current HVAC and TABS Systems

	Current HVAC System	TABS System	Savings
Electricity Consumption [kWh]	8 056 961	2 384 908	5 672 053
Electricity Cost [R]	5 858 518	1 734 156	4 124 362

The more significant cost savings were then used to determine the time it would take to recoup the investment, i.e. determine the payback period. The reduced electricity costs and payback periods for the replacement HVAC and TABS installation are given in Figure 8-7. The graph on the left shows that TABS's electricity costs would be less than for the replacement HVAC. The graph on the right shows the cumulative cash flows from the electricity savings. The investment would have been paid back when the cumulative cash flows crossed the dashed line. The figure shows that a simple payback period is seven years, and the discounted payback is ten years for both systems.

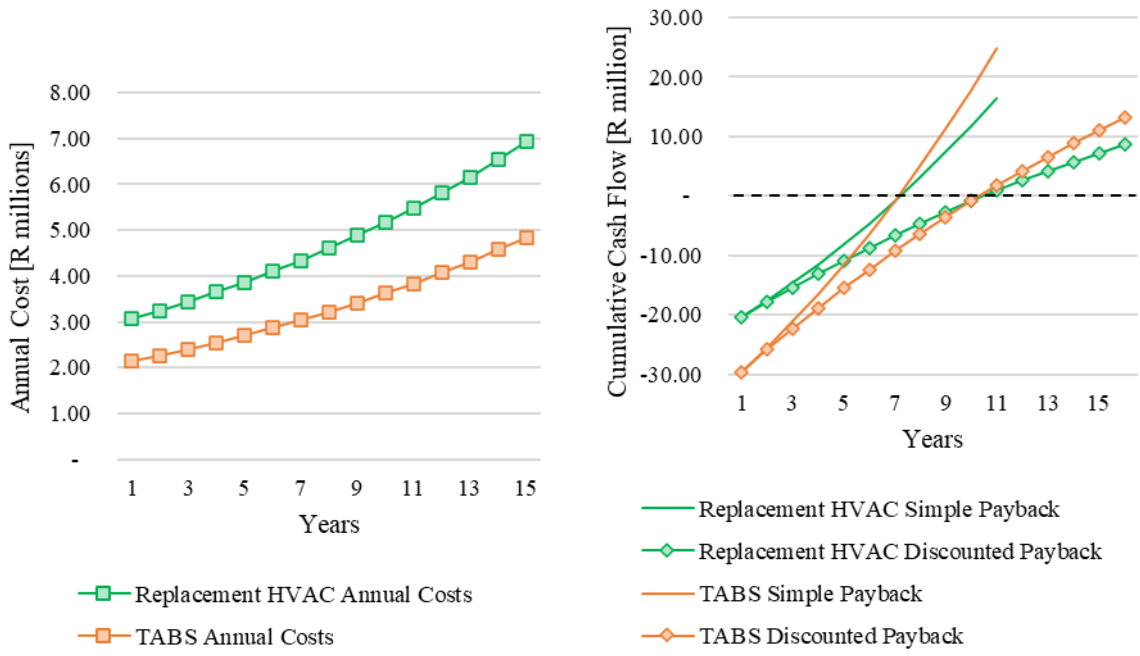

Figure 8-7: Electricity Cost and Net Cash flow for Business Cases

The Net Present Value (NPV) for the TABS installation over the 15 years can be determined as investment amount + discounted savings, i.e.:

-R29 581 440 + R42 807 577 = **R13 226 137**

The Internal Rate of Return (IRR) is 17%. An IRR higher than the discount rate means the project would add value to the business. The electricity costs, savings and cumulative cash savings are given in Table 8-13 below.

Table 8-13: Net Cash flow for TABS Installation

Year	Current HVAC Annual Costs [R]	TABS Replacement Annual Costs [R]	Savings [R] (Difference in Costs)	Net Payback [R] (Investment – Savings)	Discounted Savings [R]	Net Discounted Payback [R]
0				-29 581 440		-29 581 440
1	5 858 518	1 734 156	4 124 362	-25 457 078	3 735 835	-25 845 605
2	6 210 029	1 838 205	4 371 824	-21 085 254	3 586 943	-22 258 661
3	6 582 631	1 948 497	4 634 133	-16 451 121	3 443 985	-18 814 676
4	6 977 588	2 065 407	4 912 181	-11 538 939	3 306 725	-15 507 951
5	7 396 244	2 189 331	5 206 912	-6 332 027	3 174 935	-12 333 015
6	7 840 018	2 320 691	5 519 327	-812 700	3 048 398	-9 284 617
7	8 310 419	2 459 933	5 850 487	5 037 787	2 926 904	-6 357 713
8	8 809 045	2 607 529	6 201 516	11 239 302	2 810 252	-3 547 461
9	9 337 587	2 763 980	6 573 607	17 812 909	2 698 249	-849 212
10	9 897 842	2 929 819	6 968 023	24 780 932	2 590 710	1 741 498
11	10 491 713	3 105 608	7 386 105	32 167 037	2 487 457	4 228 956
12	11 121 216	3 291 945	7 829 271	39 996 308	2 388 320	6 617 275
13	11 788 489	3 489 462	8 299 027	48 295 335	2 293 133	8 910 408
14	12 495 798	3 698 829	8 796 969	57 092 303	2 201 740	11 112 148
15	13 245 546	3 920 759	9 324 787	66 417 090	2 113 989	**13 226 137**
			95 998 530		**42 807 577**	

As explained earlier, the average increase in the electricity tariff has been 12.17% annually for Eskom's 2019/20 and 2020/21 financial years. The average tariff increase emphasises the TABS business case, as shown in Figure 8-8. The figure shows that TABS has a simple and discounted payback period of 7 and 12 years, while the replacement HVAC system has a simple payback period of 9 years and no discounted payback period. The figure shows that the higher the electricity tariff increases, the better the business case for TABS.

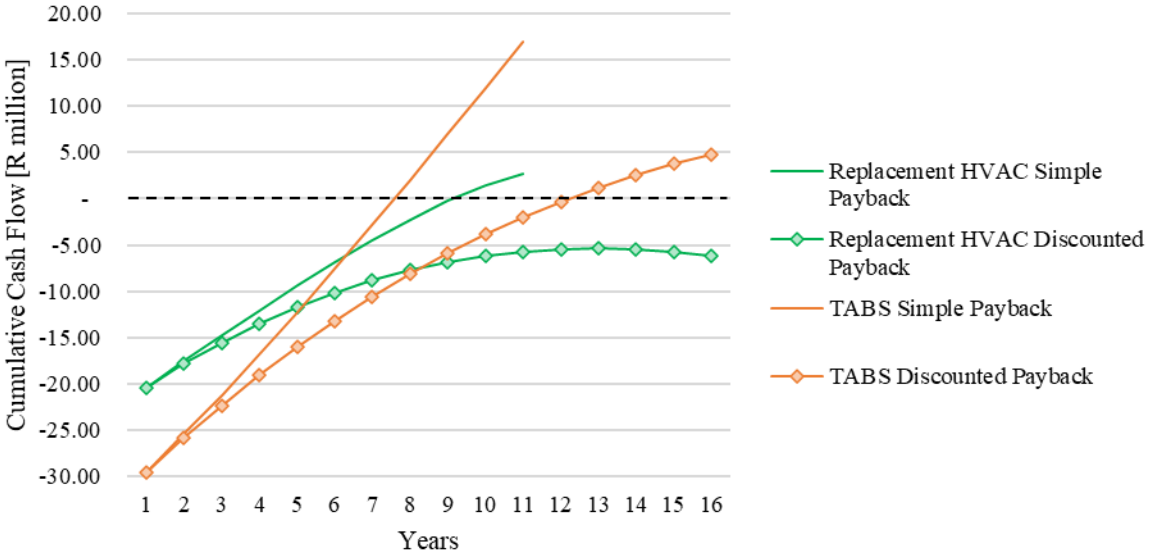

Figure 8-8: Electricity Cost and Net Cash flow for Business Cases Projected using Actual Tariff Increases

8.4 Concluding Remarks

This chapter presented a business case for installing TABS at Eskom's head office, Megawatt Park, in Johannesburg, South Africa. The building was chosen since the installed HVAC system needed to be replaced, and a consultant had been appointed to prepare a proposal for a new system. The HVAC system was estimated to have annual electricity consumption of 8 056 961.08 kWh and cost R5 858 518.

The cost of installing the new HVAC installation was proposed to cost R20 360 000. The replacement HVAC system's reduced chiller capacity would result in an annual electricity consumption of 4 212 129 kWh, and the electricity cost would be R3 062 797. The savings would result in a simple payback period of seven years, and the discounted payback period was ten years.

Alternatively, the TABS system would cost R29 581 440 to install, resulting in an annual electricity consumption of 2 384 908 kWh, and the electricity cost would be R1 734 156. The simple and discounted payback period would be the same as the replacement HVAC system at seven and ten years, respectively. An addendum to the business case showed that higher electricity tariff increases improve the business case for TABS. With higher tariff increases, TABS's simple and discounted payback period is 7 and 12 years, while the replacement HVAC system has a simple payback period of 9 years and no discounted payback period.

9 Conclusion

This research showed that thermal comfort could be achieved by Thermally Activated Building Systems (TABS) and conventional Heating, Ventilation, and Air-Conditioning (HVAC) systems. As modelled by PO Fanger, thermal comfort consists of physical and personal variables. The systems influence physical variables (operative temperature, relative humidity and air velocity), and personal variables include occupants' activity level and clothing insulation. The research aim was to validate the following hypothesis:

*TABS **consume 30% less energy** than conventional HVAC systems while **maintaining the same thermal comfort**.*

The process of validating the hypothesis involved rewriting the PMV/PPD calculator from ISO 7730 and ASHRAE 55. The reasons for rewriting the calculator were to allow for modifications and to integrate it with other tools. Testing the rewritten calculator showed that the mean difference between its PMV and PPD results and those given in ISO 7730 were -0.0246 and 0.0769, respectively. It was also calculated that the rewritten calculator had an 80% confidence level that PMV is within 0.015 and that PPD is within 0.5 of the results from ISO 7730.

The research showed that TABS' chiller demand and energy consumption could be determined using the TABS calculator from ISO 11855. The calculator requires the building and its heat loads to be simulated in EnergyPlus. Where the heat loads are unknown, minimum standards may be derived from SANS 10400. The required cooling demand can then be imported into the TABS calculator to determine the chiller's sensible demand and energy consumption. The results showed that the mean difference between actual and calculated results is 2.054. It was also determined that the results from the TABS calculator had an 80% confidence to be within 1.17 of the actual chiller demand. The research also showed that EnergyPlus accurately simulates a conventional HVAC's demand and energy consumption. Results show that the mean difference between actual and simulated results is 0.47. It was also determined that EnergyPlus results have an 80% confidence to be within 0.57 of the actual chiller demand. The tools show that they can accurately determine the chiller energy consumption.

The TABS calculator does not make provision for dehumidification; hence the calculator could only be used to determine a chiller's sensible demand and energy consumption. The simulations presented in Chapter 7 showed that the higher thermal capacity of TABS results in the chiller's sensible energy consumption being 41.62% of a conventional HVAC system. Literature also stated that the calculator has an error variance between 10 and 15%, meaning that, at most, TABS could consume up to 56.62% of the conventional HVAC system. The results show that the TABS consumes **more than 30% less energy** than the conventional HVAC system.

The case studies assumed that the operative temperature and relative humidity were accurately determined, although they were not recorded and compared with the simulations. Given that the TABS calculator and EnergyPlus have been used and tested throughout the built environment, we can assume that the operative temperature and relative humidity are accurately determined. The operative temperature and relative humidity show that TABS **maintains the same thermal comfort** as an HVAC system. The two points highlighted in bold font validate the hypothesis; however, the percentage reduction of energy consumption is a conservative estimate.

The business case for replacing an old HVAC system with energy-efficient HVAC or TABS was developed using this knowledge. The business case assumed that the rise in electricity tariff is at the maximum CPI target set by the South African Reserve Bank and Eskom's discount rate of 10.4%. Using

these assumptions showed that both systems would have a simple payback period of seven years and a discounted payback of ten years. The actual increase in electricity tariff was more than double the maximum CPI target during Eskom's 2019/20 and 2020/21 financial years, improving the business case for TABS. Projecting the actual electricity tariff meant that TABS would have a simple and discounted payback period of seven and twelve years, while the replacement HVAC system would have a simple payback period of nine years and would not have a discounted payback period.

10 Recommendations

The following chapter introduces recommended research studies to enhance the field of knowledge in Thermally Activated Building Systems (TABS).

Recommended measuring the operative temperature, relative humidity, air velocity, and water mass flow in a TABS installation and comparing them with the calculator results to determine its accuracy.

The TABS calculator does not determine dehumidification and does not vary air velocity and water mass flow rate. The calculator could be modified and improve its accuracy in determining TABS' demand profile.

Recommended researching the optimal pipe length, spacing, and diameter in circuits to improve TABS' thermal capacity. The optimisations could result in enhancing the potential demand and energy consumption.

The circuits used in the case study of TABS in an office building (Chapter 5) were embedded in the building's floors. Recommended researching when other surfaces have circuits installed. Depending on whether the system is in cooling or heating, the system may improve performance since circuits in the floor installations perform better in heating operations, and circuits in the ceiling perform better in cooling operations.

The case study where both systems were simulated and compared analysed the systems operating over 12 hours when the office building was occupied. TABS can run throughout the day, and literature shows that the system consumes less energy when operating over an extended period. The recommendation is to determine the potential demand and energy reductions when TABS is operated over an extended period.

11 References

ACCA. (2016). *Manual J - ACCA*. Retrieved May 2020, from ACCA: https://www.acca.org/HigherLogic/System/DownloadDocumentFile.ashx?DocumentFileKey=df4aaf8b-c82b-4337-bb95-081f67444222

American Institute of Architects. (2007). AIA. 50.

ASHRAE. (1992). ASHRAE Psychrometric Chart #1 (SI). Retrieved May 2020, from ASHRAE: https://www.ashrae.org/File%20Library/Technical%20Resources/Bookstore/UP3/SI-1.pdf

ASHRAE. (2007). Energy Standard for Building except Low-Rise Residential Buildings (90.1). Retrieved from ASHRAE: https://www.ashrae.org/technical-resources/bookstore/standard-90-1

ASHRAE. (2010). *Thermal Environmental Conditions for Human Occupancy*. Atlanta, Ga: The Society.

Avenir. (2019). *LoopCAD 2019*. Retrieved May 2020, from Avenir Software - HVAC Software Solutions: https://www.avenir-online.com/AvenirWeb/LoopCAD/LoopCADHome.aspx

Bromley, M. (2022, April 28). *Degree Days - An Introduction*. Retrieved October 2019, from Degree Days: degreedays.net

Chatterjee, S., & Simonoff, J. S. (2013). *Handbook of Regression Analysis.* Hoboken, New Jersey: John Wiley & Sons, Inc.

City of Cape Town. (2021, May). *Electricity Consumption Tariffs.* Retrieved from City of Cape Town.

Climaveneta. (2020). *NECS 1314 - 3218.* Retrieved from Mitsubishi Electric Hydronics & IT Cooling Systems: https://in.climaveneta.com/en/products/1507/chiller-air-source-for-outdoor-installation

CSA. (n.d.). *F280-12 (R2017)*. Retrieved May 2020, from CSA Group: https://store.csagroup.org/ccrz__ProductDetails?viewState=DetailView&cartID=&portalUser=&store=&cclcl=en_US&sku=F280-12

DesignBuilder Software Ltd. (2021, 7 25). *Simulation*. Retrieved from DesignBuilder Software Ltd: https://designbuilder.co.uk/simulation

DesigningBuildings. (2020, September 15). *Temperature in Buildings*. Retrieved from DesigningBuildings: https://www.designingbuildings.co.uk/wiki/Temperature_in_buildings

EnergyPlus. (2021, 7 25). *EnergyPlus*. Retrieved May 2020, from EnergyPlus: https://energyplus.net/

EnergyPlus. (2021, 7 25). *Weather Data by Location | Weather Data Download - Cape Town 688160 (IWEC)*. Retrieved from EnergyPlus: https://energyplus.net/weather-location/africa_wmo_region_1/ZAF/ZAF_Cape.Town.688160_IWEC

Eskom. (2014). Energy Efficiency Opportunities in South Africa: Commercial Sector. Johannesburg, Gauteng, South Africa.

Eskom. (2018). *Tariff History*. Retrieved November 17, 2020, from Eskom: https://www.eskom.co.za/CustomerCare/TariffsAndCharges/Pages/Tariff_History.aspx

Eskom. (2022). *Tariff History*. Retrieved from Eskom: https://www.eskom.co.za/distribution/tariffs-and-charges/tariff-history/

Firer, C., Ross, S. A., Westerfield, R. W., & Jordan, B. D. (2012). *Fundamentals of Corporate Finance: South African Edition.* New York: McGraw-Hill/Irwin.

Fritz, R., & Mcneil, A. (2019, January 04). *About Radiance*. Retrieved May 2020, from Radsite: https://www.radiance-online.org/about

Holman, J. P. (2010). *Heat Transfer*. New York: McGraw-Hill.

ISO. (2012). Building environment design - Design, dimensioning, installation and control of embedded radiant heating and cooling systems Part 2: Determination of the design heating and cooling capacity. *ISO*. ISO.

ISO. (2012). Building environment design - Design, dimensioning, installation and control of embedded radiant heating and cooling systems Part 4: Dimensioning and calculation of the dynamic heating and cooling capacity of Thermo Active Building Systems (TABS). *ISO*.

Khan Academy. (n.d.). *Metabolic Rate*. Retrieved from Khan Academy: https://www.khanacademy.org/science/ap-biology/ecology-ap/energy-flow-through-ecosystems/a/metabolic-rate

Lim, J.-H., Song, J.-H., & Song, S.-Y. (2014). Development of Operational Guidelines for Thermally Activated Building System According to Heating and Cooling Load Characteristics. *Applied Energy, 126*, 123-135.

Liu, Y. (2012). *A Process Model for Heating, Ventilation and Air Conditioning Systems Design for Advanced Energy Retrofit Projects.*

Liu, Z., Wang, Z., & Xu, X. (2021). Climatic division for the design of HVAC systems. *Journal of Cleaner Production, 323*.

Luginbuehl, I., Bissonnette, B., & Davis, P. J. (2011). Chapter 6 - Thermoregulation: Physiology and Perioperative Disturbances. *Smith's Anesthesia for Infants and Children*, 157-178.

Ma, P., Wang, L.-S., & Guo, N. (2015). Energy Storage and Heat Extraction from Thermally Activated Building Systems (TABS) to Thermally Homeostatic Buildings. *Renewable and Sustainable Energy Reviews, 45*, 677-685.

McQuiston, F. C., Parker, J. D., & Spitler, J. D. (2005). *Heating, Ventilation and Air Conditioning: Analysis and Design* (6th ed.). New York: John Wiley & Sons.

Nicol, J. F., & Roaf, S. (2017). Rethinking Thermal Comfort. *Building Research and Information, 45*(7), 711-716.

OpenStudio. (2020). *OpenStudio*. Retrieved May 2020, from OpenStudio: https://openstudio.net/

Rawlings, J. O., Pantula, S. G., & Dickey, D. A. (1998). *Applied Regression Analysis: A Research Tool.* New York: Springer-Verlag New York, Inc.

REHAU. (2012, March 28). *Energy Efficient Building Solutions from REHAU*. Retrieved September 20, 2017, from Specifile: https://www.specifile.co.za/news/2012-03-28-rehau-promotes-energy-efficient-building-solutions/

Rhee, K.-N., Olesen, B. W., & Kim, K. W. (2012). Ten questions about radiant heating and cooling systems. *Building and Environment*(112), 367-381.

Rijksen, D. O., Wisse, C. J., & van Schijndel, A. W. (2010). Reducing Peak Requirements for Cooling by using Thermally Activated Building Systems. *Energy and Buildings, 42*, 298-304.

Romanovsky, A. A. (2018). Chapter 1 - The thermoregulation system and how it works. *Handbook of Clinical Neurology*, 4-43.

SABS. (2022). SANS 10400: The Application of the National Building Regulations.

Saelens, D., Parys, W., & Baetens, R. (2011). Energy and Comfort Performance of Thermally Activated Building Systems including Occupant Behaviour. *Building and Environment, 46*, 835 - 848.

Sastry, G., & Rumsey, P. (2014). VAV vs. Radiant Side-by-Side Comparison. *ASHRAE Journal*, 16-24.

Simscale. (n.d.). *Computational Fluid Dynamics Software*. Retrieved May 2020, from Simscale: https://www.simscale.com/product/cfd/

South African Reserve Bank. (2020). *Monetary Policy*. Retrieved from South African Reserve Bank: https://www.resbank.co.za/en/home/what-we-do/monetary-policy

SUNY Cortland. (n.d.). *Thermoregulation and Exercise: Thermoregulation and the Body's Limits*. Retrieved from SUNY (State University of New York) Cortland: https://web.cortland.edu/buckenmeyerp/Lecture13.html

Tamasauskas, J., Kegel, M., & Sunye, R. (2013). Development of Canadian Building Archetypes in TRNSYS for NZEB Analysis. *EIC Climate Change Technology Conference.*

University of Toronto. (n.d.). *0000Psych 11x17US SI*. Retrieved May 2020, from StuDocu: https://www.studocu.com/en-ca/document/university-of-toronto/environmental-engineering/lecture-notes/0000psych-11x17us-si/3841927/view

Valsir-Uneeq. (2013). *Pexal.* Retrieved June 18, 2019, from https://valsir-uneeq.co.za/EN/pexal.htm

Vella, C. A., & Kravitz, L. (n.d.). *Staying Cool When Your Body is Hot*. Retrieved July 7, 2020, from University of New Mexico: https://www.unm.edu/~lkravitz/Article%20folder/thermoregulation.html

Walikewitz, N., Jänicke, B., Langner, M., Meier, F., & Endlicher, W. (2014). The difference between the mean radiant temperature and the air temperature within indoor environments: A case study during summer conditions. *Building and Environment*, 151-161.

Whittow, G. C. (1971). *Mammals.* Academic Press.

Yau, Y. H., & Chew, B. T. (2014). A Review on Predicted Mean Vote and Adaptive Thermal Comfort Models. *Building Services Engineering Research and Technology, 35*(1), 23-35.

12 Appendix A: Additional Literature

Appendix A-1: Adaptive Approach

There are discrepancies with the PMV model when comparing actual and predicted thermal sensations developed from laboratory studies (Yau & Chew, 2014). Field studies showed that the PMV equations do not adequately express thermal comfort. The cause of these errors is a result of incorrect assumptions made regarding the thermal sensation given by the steady-state heat balance approach, occupants' adaptive behaviours and limitations in the Fanger equation (Yau & Chew, 2014). The literature unfortunately does not give examples of these assumptions. Moreover, the neutral feeling on the thermal sensation scale is relative. Occupants in hot climates prefer a slightly cooler sensation, while occupants in cooler climates prefer a slightly warmer than neutral (Yau & Chew, 2014). The adaptive approach suggests that individuals adjust their thermal environment to meet their desired thermal comfort. These measures (adaptations) can be categorised as follows (Yau & Chew, 2014):

- **Physiological Adaptation** refers to the individual's body reaching comfort levels through perspiration, vasoconstriction, and vasodilatation.
- **Psychological Adaptation** refers to the feeling of thermal perception based on past experiences.
- **Behavioural Adjustments** refer to activities that the individual takes to achieve thermal comfort. Actions in behavioural adjustments include:
  - **Personal Adjustments:** the individual changes their activity, clothing, posture, consuming hot or cold food or drinks and moving to different locations;
  - **Technological Adjustments:** modifying the environment by adjusting the air-conditioner and opening or closing windows and doors; and
  - **Cultural Adjustments:** includes siesta on a hot day.

Research by R de Dear and GS Brager regarding occupants in buildings throughout the world; and by KWH Mui and WTD Chan regarding occupants in buildings located in Hong Kong showed the correlation between personal adjustments and operative temperature. These adjustments would influence Equation 2.8. Figure 12-1 shows that the operative temperature inversely correlates to clothing insulation. As the operative temperature decreases, the occupants wear more clothes (increasing clothing insulation), and as the operative temperature increases, the occupants wear fewer clothes (decreasing clothing insulation). The operative temperature/clothing insulation correlation for occupants worldwide and humid sub-tropical Hong Kong are similar, indicating that the correlation may not be dependent on climate.

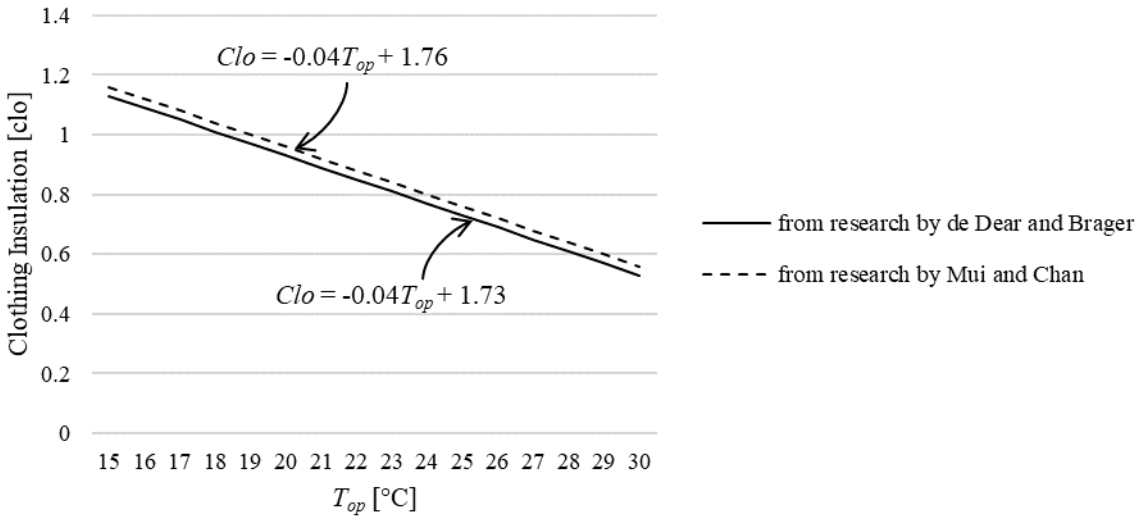

Figure 12-1: Relationship between Clothing Insulation and Operative Temperature (Yau & Chew, 2014)

The researchers also studied the correlation between air velocity and operative temperature. Figure 12-2 shows that operative temperature is proportional to air velocity. However, the degree to which air velocity changes may depend on the climate since Hong Kong is humid compared to several parts of the world.

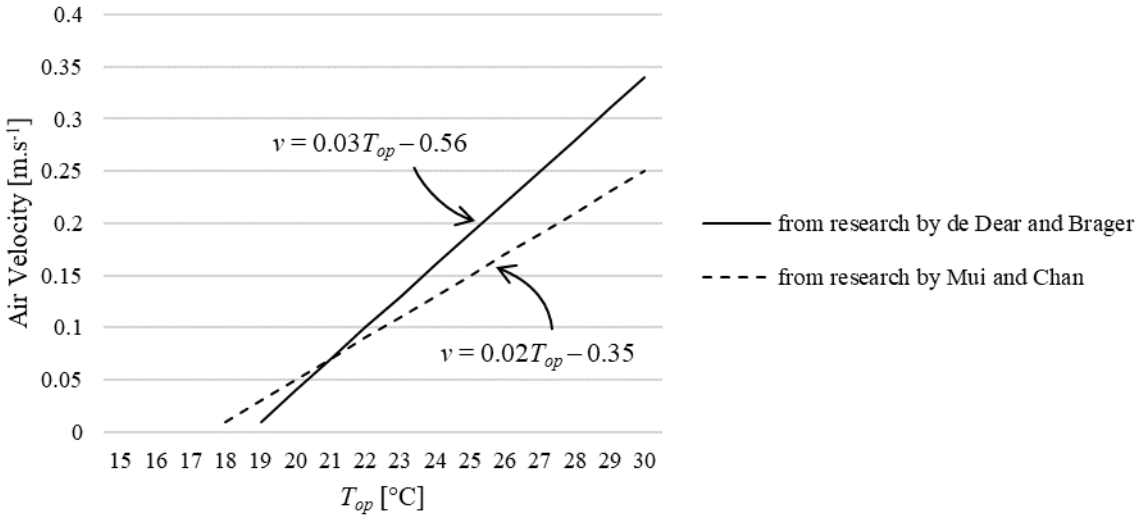

Figure 12-2: Relationship between Air Velocity and Temperature (Yau & Chew, 2014)

Appendix A-2: Additional Methods for Chiller Sizing

Rough Sizing Method

This method uses a simple equation to calculate the heating and cooling power. This method has a typical error variance between 20% and 30%; and is determined using the following equation:

$$P_{circuit,spec}^{max} = 1000 \frac{E_{day}}{n_h} f_s \qquad 12.1$$

Where $P^{max}_{circuit,spec}$ is the maximum specific power, i.e. the maximum power per m^2 [W/m^2];
E_{day} is the specific daily energy gains, i.e. the daily energy gains per m^2 [kWh/m^2];
n_h is the number of operating hours [h]; and
f_s is the safe design factor (usually 1.15)

The equation gives a rough estimate that engineers can use in the initial stages of planning a TABS installation.

Simplified Sizing by Diagrams

This method determines the chiller size by calculating the input and output water temperatures. It has a typical error variance between 15% and 20%. To begin the calculation, the average temperature of the slab θ^{ave}_{slab}, is determined using the equation below:

$$\theta^{ave}_{slab} = \theta^{max}_{comfort} + \omega E_{day} \quad | \quad 12.2$$

Where $\theta^{max}_{comfort}$ is the maximum operative room temperature required for thermal comfort [°C];
ω is a coefficient dependent on daily operational hours, the number of active surfaces and room orientation. The constant's values are given in Table 12-1 and Table 12-2; and
E_{day} is the specific daily energy gains, i.e. the sum of heat gains values acting throughout the design day, divided by the floor area [kWh/m^2]

Table 12-1: Constant internal heat gains from 8:00 to 18:00

Circuit running mode	Number of active surfaces	Orientation of the environment		
		East	South	West
			ω	
Continuous (24 h)	Floor and ceiling (C2)	-4,6816	-5,3696	-5,935
	Only ceiling (C1)	-6,3022	-7,2237	-7,7982
Intermittent (8 h)	Floor and ceiling (I2)	-5,5273	-6,1701	-6,7323
	Only ceiling (I1)	-7,2853	-7,8562	-8,5791

Table 12-2: Constant internal heat gains from 8:00 to 12:00 and from 14:00 to 18:00

Circuit running mode	Number of active surfaces	Orientation of the environment		
		East	South	West
			ω	
Continuous (24 h)	Floor and ceiling (C2)	-6,279	-7,1094	-7,3681
	Only ceiling (C1)	-7,9663	-8,7989	-8,7455
Intermittent (8 h)	Floor and ceiling (I2)	-8,1474	-8,758	-9,3264
	Only ceiling (I1)	-10,029	-10,685	-10,967

The resultant average temperature of the slab is then used to determine the supply water temperature $\theta^{set\text{-}point}_{water,\ in}$ required to ensure thermal comfort. The supply water temperature is determined using the following equation.

$$\theta^{set\text{-}point}_{water,\ in} = \theta^{ave}_{slab} - 1000\left(\frac{E_{day}}{n_h}\right)(R_{int} + R_t) \quad | \quad 12.3$$

Where E_{day} is the specific daily energy gains [kWh/m^2];
n_h is the daily operational hours;
R_{int} is the internal thermal resistance of the slab conductive region [m^2K/W]; and

R_t is the circuit's total thermal resistance determined using the General Resistance Method given in 2.2.5.1.1

Once the supply water temperature is determined, the return temperature is determined using equation 2.21, which gives the temperature difference between the heating medium and the room temperature. The water supply and return temperatures determine the chiller size, as discussed in Chapter 0.

Dynamic Building Simulation Programmes

This method consists of an overall dynamic simulation of the radiant system and the environment using building-system simulation software. This method has a typical error variance between 6% and 10%. A study (Rijksen, Wisse, & van Schijndel, 2010) included on-site measurements of an office with TABS installed. A simulation model in TRNSYS showed that the maximum difference between the measured and simulated cooling power was 4.9W.m^{-2}. The difference between the measured and calculated operative room temperature was 1°C. The study also stated that the differences are within the range of measurements and calculations.

TABS heating and cooling capacity (Chapter 2.2.5) and chiller sizing methods determine TABS' demand and energy consumption. The following section discusses HVAC systems as alternative space heating and cooling system.

Appendix A-3: Types of Air-Handling Units (AHU)

Constant Air Volume (CAV) System

Constant Air Volume (CAV) systems are the simplest form of AHU and typically only serve a single zone. A simple schematic diagram of the AHU is illustrated in Figure 12-3 below. The figure shows that the supply fan delivers a constant airflow when the dampers are open and switches off when the dampers are closed (McQuiston, Parker, & Spitler, 2005). The zone thermostat is used to maintain the temperature in the zone. The discharge thermostat uses the zone thermostat to control the valves on the heating and cooling coils.

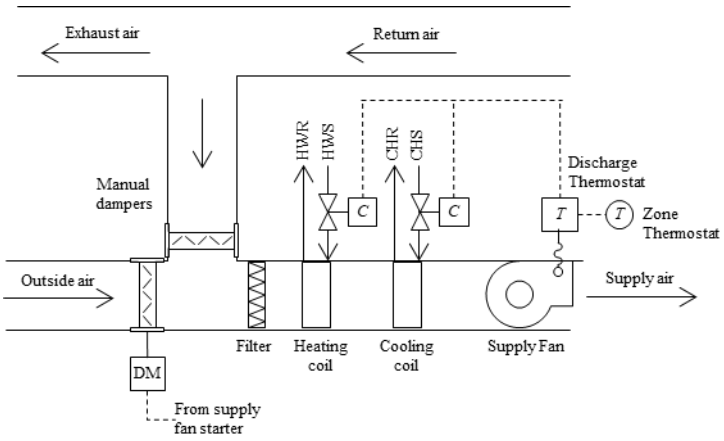

Figure 12-3: Schematic Diagram of a Simple Single-zone Constant Air Volume (CAV) System (McQuiston, Parker, & Spitler, 2005)

Constant Air Volume, Reheat System

The reheat system is a modified constant air volume system that supplies multiple zones with unequal heating and cooling loads. The schematic of the CAV reheat system, given in Figure 12-4, shows that outside air passes through the cooling coil before being delivered at a fixed temperature to the zones

(McQuiston, Parker, & Spitler, 2005). The heating coils placed at the zones would then raise the air's temperature using hot water, steam, or electricity as set by the thermostat (McQuiston, Parker, & Spitler, 2005).

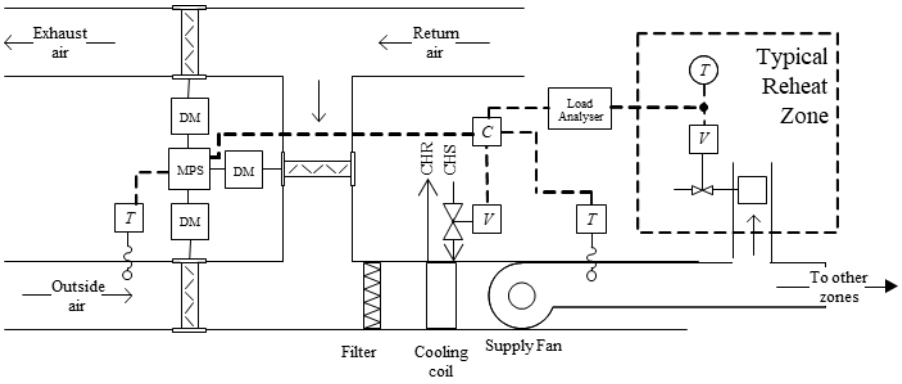

Figure 12-4: Schematic for a Simple Constant Air Volume Reheat System (McQuiston, Parker, & Spitler, 2005)

Dual Duct (Double Duct) System

A dual duct system, shown in Figure 12-5, consists of two ducts, one supplying hot air and another supplying cold air, parallel to each other. The figure shows that the outside air is separated into two ducts, one with the cooling coils installed and the other with heating coils installed. The amount of hot and cold air flowing through each zone is mixed and controlled in the mixing box depending on the zone's heating and cooling requirements (McQuiston, Parker, & Spitler, 2005).

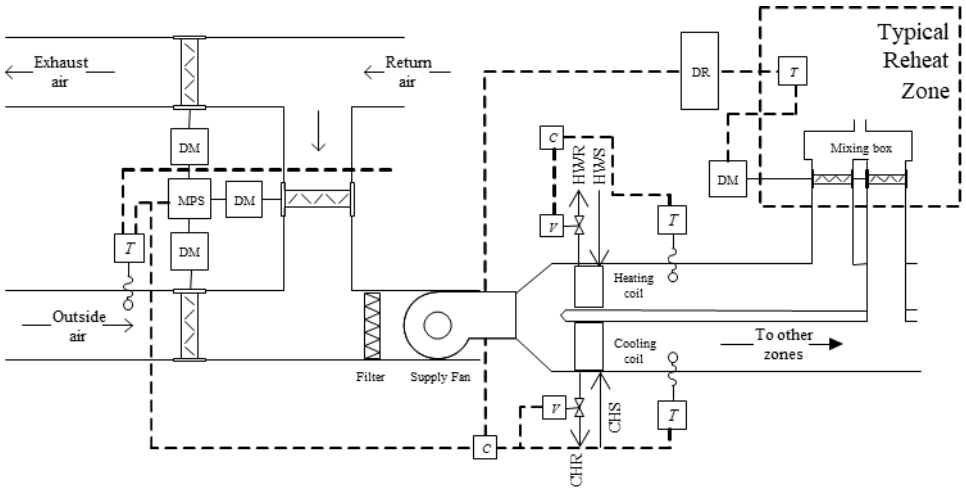

Figure 12-5: Schematic of a Simple Dual-duct System (McQuiston, Parker, & Spitler, 2005)

Multi-Zone System

A multi-zone system resembles a combination of single and dual duct systems. Figure 2-25 shows a schematic of a multi-zone system. The figure shows that the air is mixed before flowing through the single duct to each zone. This approach provides greater flexibility than a single duct system at a lower cost than a dual system (McQuiston, Parker, & Spitler, 2005).

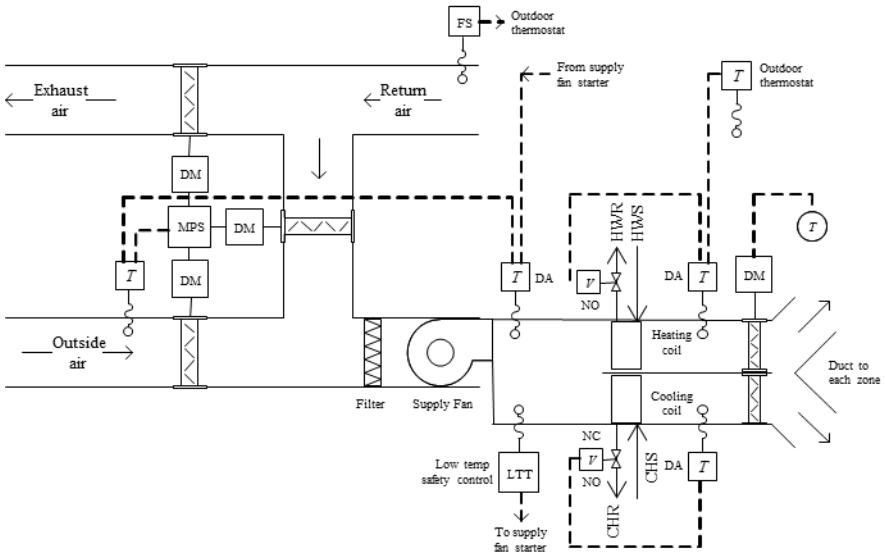

Figure 12-6: Schematic of a Simple Multi-Zone System (McQuiston, Parker, & Spitler, 2005)

Appendix A-4: The Heating and Cooling Coil Process

The AHU has the function of heating, cooling, humidifying and dehumidifying the air. Their processes can be derived from the energy equation, i.e. the first law of thermodynamics for an open system (McQuiston, Parker, & Spitler, 2005):

$$\dot{Q}_{net} - \dot{W}_{net} + \sum \dot{m}_i \left(h_i + \frac{1}{2} V_i^2 + g z_i \right) - \sum \dot{m}_e \left(h_e + \frac{1}{2} V_e^2 + g z_e \right) = \frac{dE_{sys}}{dt} \qquad 12.4$$

Where $\dot{Q}_{net}$ is the net heat transfer [kJ/s or kW];
$\dot{W}_{net}$ is the net work done [kJ/s or kW];
$\dot{m}$ is the mass flow rate [kg/s];
h is enthalpy [kJ/kg];
V is velocity [m/s]
g is gravitational acceleration [m^2]; and
z is height [m];
the subscript i denotes the matter that goes into the system;
the subscript e denotes the matter that exits the system; and
$\frac{dE_{sys}}{dt}$ is the net change in total energy [kJ/s or kW];

In air-conditioning systems, heat is transferred from the air (cooling) or to the air (heating). No work is done, kinetic and potential energy is zero, and there is no net change in total energy. Therefore Equation 12.4 can be simplified to:

$$\dot{Q}_{net} = \sum \dot{m}_e h_e - \sum \dot{m}_i h_i \qquad 12.5$$

A schematic diagram of the air and heating or cooling medium in the coils is given in Figure 12-7.

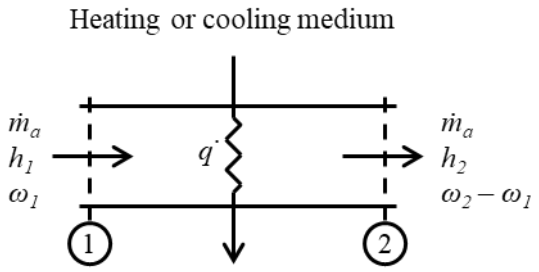

Figure 12-7: Schematic of a Heating or Cooling Device (McQuiston, Parker, & Spitler, 2005)

The thermodynamic properties of the air before passing the heating or cooling coil are denoted by 1. After passing the cooling coil, the thermodynamic properties are denoted with a 2. These thermodynamic properties can be taken from a psychrometric chart such as that was described in 2.4.2. Therefore, Equation 12.5 can be rewritten as:

$$\begin{aligned} \dot{q} &= \dot{m}_a h_2 - \dot{m}_a h_1 \\ &= \dot{m}_a (h_2 - h_1) \end{aligned} \qquad 12.6$$

Alternatively, because the air is considered to be a perfect gas, equation 12.6 can be written as:

$$\dot{q}_s = \dot{m}_a c_p (T_2 - T_1) \qquad 12.7$$

Where subscript *s* is the sensible heat.

The AHU may be required to cool and dehumidify the air. Figure 12-8 shows a schematic of a cooling and dehumidifying device. It is similar to the heating and cooling coil shown in Figure 12-7 and includes the condensate (saturated water, denoted as *w*) leaving the AHU.

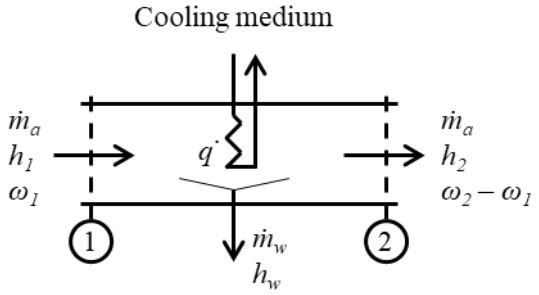

Figure 12-8: Schematic of a Cooling and Dehumidifying Device (McQuiston, Parker, & Spitler, 2005)

For the cooling and dehumidifying process, the energy balance becomes:

$$\begin{aligned} \dot{q} &= \dot{m}_a h_2 - \dot{m}_a h_1 + \dot{m}_v h_v \\ &= \dot{m}_a (h_2 - h_1) + \dot{m}_v h_v \end{aligned} \qquad 12.8$$

The AHU may be required to heat and humidify the air. Figure 12-9 shows a schematic of a heating coil and humidifying device. It is similar to the heating and cooling coil shown in Figure 12-7 and includes the humidifier. The humidifier adds water to the air.

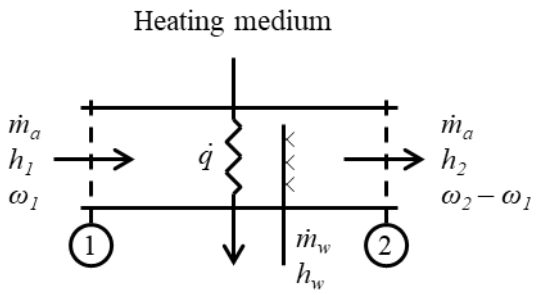

Figure 12-9: Schematic of a Heating and Humidifying Device (McQuiston, Parker, & Spitler, 2005)

For the heating and humidifying process, the energy balance becomes:

$$\begin{aligned}\dot{q} &= \dot{m}_a h_2 - \dot{m}_a h_1 - \dot{m}_v h_v \\ &= \dot{m}_a(h_2 - h_1) - \dot{m}_v h_v\end{aligned} \qquad 12.9$$

Appendix A-5: The Chiller Plant and the Refrigeration Cycle

The majority of the energy usage in TABS and conventional HVAC systems are consumed in the chiller plant, boiler plant and heat pumps. The plant is responsible for transferring energy between the systems and the environment outside the building (McQuiston, Parker, & Spitler, 2005). When the plant transfers heat from the system, the plant is in cooling mode, and when the plant transfers heat to the system, the plant acts as a heat pump and is in heating mode. The simplest form of a chiller plant consists of the following components (McQuiston, Parker, & Spitler, 2005):

1. **The evaporator:** Transfers the energy between the fluid in TABS and HVAC systems with the refrigerant in the chiller plant;
2. **The compressor:** Increases the refrigerant's pressure and pushes it through the plant;
3. **The condenser:** Transfers the energy between the refrigerant in the plant and the environment outside the building; and
4. **The expansion valve:** Decreases the refrigerant's pressure.

The components are arranged in a cycle, the simplest form being the single-stage compression cycle, shown in Figure 12-10. The fluid from a TABS and conventional HVAC system enters the evaporator to transfer heat between the fluid and the refrigerant. When the TABS or conventional HVAC system is in cooling mode, i.e. moving heat from the building, the refrigerant flow in the cycle flows anticlockwise, and energy is transferred from the water to the refrigerant (McQuiston, Parker, & Spitler, 2005).

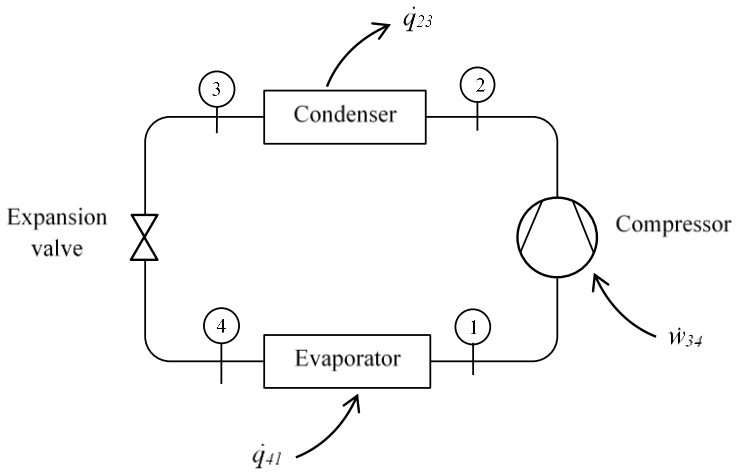

Figure 12-10: Schematic of Single-Stage Compression Cycle (McQuiston, Parker, & Spitler, 2005)

As the refrigerant flows through the chiller plant, its thermodynamic state changes. The bubbles between the components in Figure 12-10 represent the refrigerant's state in the cycle. When the plant is in cooling mode, the refrigerant flows anticlockwise from 1-2-3-4 and its state changes as follows (McQuiston, Parker, & Spitler, 2005):

- **State 1:** the refrigerant leaves the evaporator as a saturated vapour with a low temperature and pressure;
- **State 2:** the compressor increases the refrigerant's temperature and pressure to a super-heated vapour;
- **State 3:** The condenser reduces the refrigerant's temperature to a saturated liquid while its pressure remains high;
- **State 4:** the expansion valve reduces the refrigerant's pressure to a liquid/vapour mixture. The refrigerant flows back into the evaporator, repeating the cycle

Two thermodynamic properties are introduced, entropy (*s*) and enthalpy (*h*). Entropy is a thermodynamic quantity representing the amount of energy unavailable to do work, and enthalpy is equivalent to the sum of internal energy and the product of pressure and volume. The refrigerant states in the cycle can also be represented using *T-s* and *P-h* graphs, as shown in Figure 12-11.

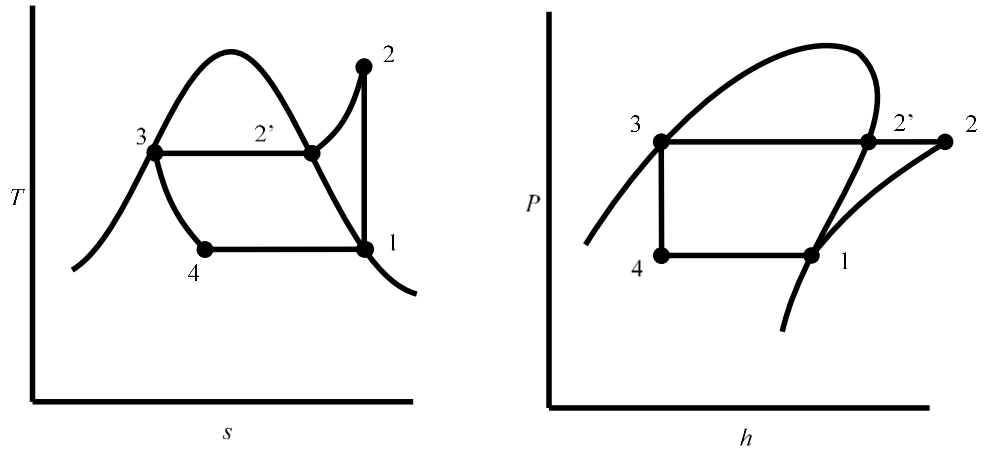

Figure 12-11: T-s and P-h Diagram of an Ideal, Single-Stage Cycle (McQuiston, Parker, & Spitler, 2005)

The cooling load in the evaporator is calculated using the following equation (McQuiston, Parker, & Spitler, 2005):

$$\dot{q}_{41} = (h_1 - h_4)\dot{m} = (h_1 - h_3)\dot{m} \quad | \quad 12.10$$

The work done by the compressor is calculated using the following equation (McQuiston, Parker, & Spitler, 2005):

$$\dot{w}_{12} = (h_2 - h_1)\dot{m} \quad | \quad 12.11$$

The heat rejected by the condenser is calculated using the following equation (McQuiston, Parker, & Spitler, 2005):

$$\dot{q}_{23} = (h_2 - h_3)\dot{m} \quad | \quad 12.12$$

The Coefficient of Performance (COP), the ratio of useful heating or cooling provided to required work, can be calculated using the following equation (McQuiston, Parker, & Spitler, 2005):

$$COP = \frac{useful\ refrigeration/heating\ effect}{net\ energy\ input} = \frac{\dot{q}_{41}}{\dot{w}_{12}} \quad | \quad 12.13$$

The refrigerant's state at stage 4 can be calculated by first determining the quality (x) of the mixture using the following equation (McQuiston, Parker, & Spitler, 2005):

$$x = \frac{h_2 - h_f}{h_g - h_f} \quad | \quad 12.14$$

Where $h_4 = h_3$

h_f is the enthalpy of the refrigerant as a saturated liquid at pressure P; and

h_g is the enthalpy of the refrigerant as a saturated vapour at pressure P

Once the quality of the mixture is determined, the refrigerant's entropy at stage 4 can be determined using the following equation (McQuiston, Parker, & Spitler, 2005):

$$s_4 = s_f + x(s_g - s_f) \quad | \quad 12.15$$

13 Appendix B: Thermal Comfort Tables and Calculators

Appendix B-1: Metabolic Rates for Typical Tasks

Activity	Metabolic Rate	
	Met Units	W/m^2
Resting		
Sleeping		
Reclining	0.8	45
Seated, quiet	1.0	60
Standing, relaxed	1.2	70
Walking (on level surface)		
0.9 m/s, 3.2 km/h, 2.0 mph	2.0	115
1.2 m/s, 4.3 km/h, 2.7 mph	2.6	150
1.8 m/s, 6.8 km/h, 4.2 mph	3.8	220
Office Activities		
Reading, seated	1.0	55
Writing	1.0	60
Typing	1.1	65
Filing, seated	1.2	70
Filing, standing	1.4	80
Walking about	1.7	100
Lifting/packing	2.1	120
Driving/Flying		
Automobile	1.0–2.0	60–115
Aircraft, routine	1.2	70
Aircraft, instrument landing	1.8	105
Aircraft, Combat	2.4	140
Heavy vehicle	3.2	185
Miscellaneous Occupational Activities		
Cooking	1.6–2.0	95–115
House cleaning	2.0–3.4	115–200
Seated, heavy limb movement	2.2	130
Machine work		
sawing (table saw)	1.8	105
light (electrical industry)	2.0–2.4	115–140
heavy	4.0	235
Handling 50 kg (100 lb) bags	4.0	235
Pick and shovel work	4.0–4.8	235–280
Miscellaneous Leisure Activities		
Dancing, Social	2.4–4.4	140–255
Callisthenics/exercise	3.0–4.0	175–235
Tennis, single	3.6–4.0	210–270
Basketball	5.0–7.6	290–440
Wrestling, Competitive	7.0–8.7	410–505

Appendix B-2: Psychrometric Chart

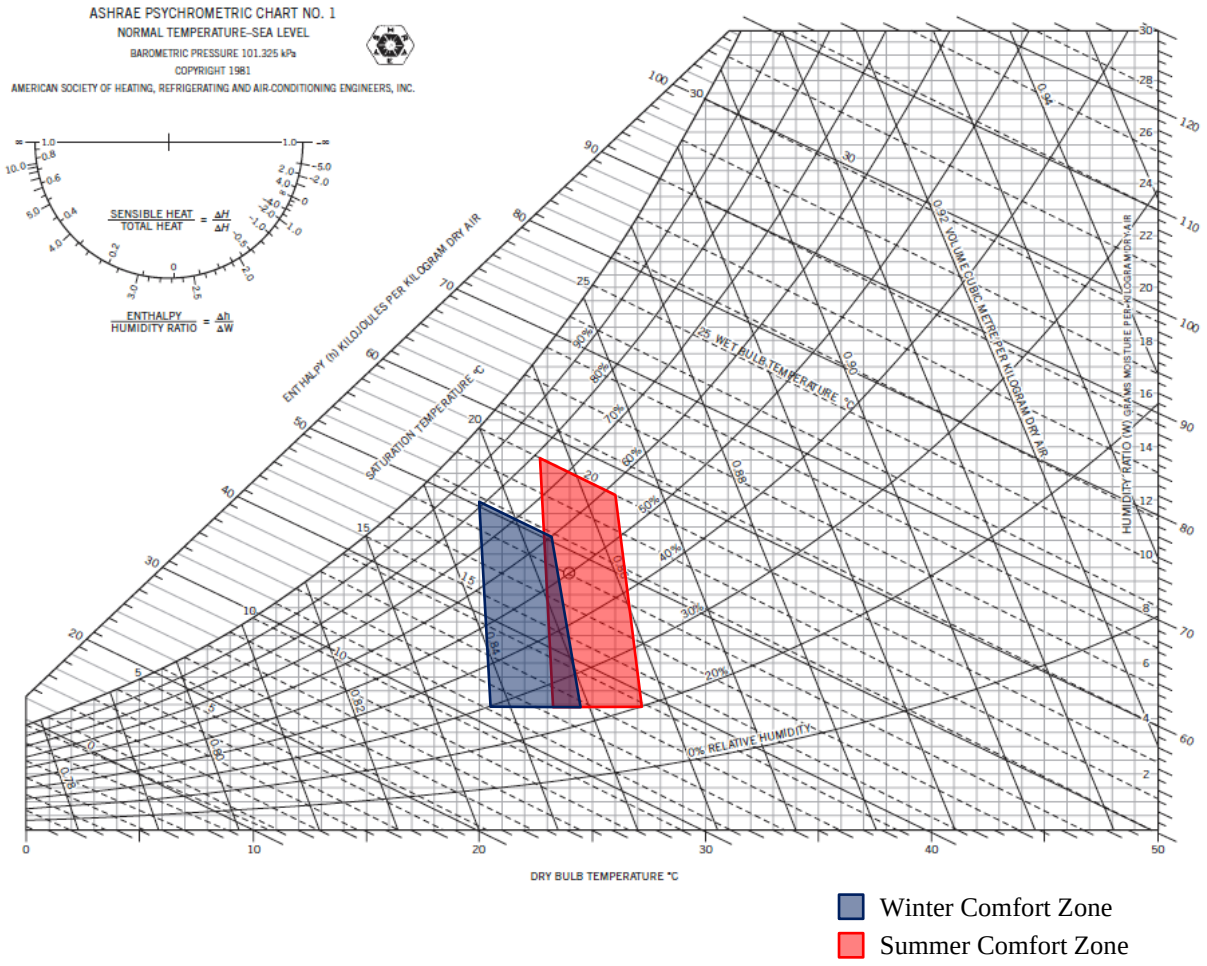

Psychrometric Chart (ASHRAE, 1992) and (University of Toronto, n.d.)

Appendix B-3: Occupancy or Building Classification (SABS, 2022)

Class of occupancy or building	Occupancy
A1	**Entertainment and public assembly** Occupancy where persons gather to eat, drink, dance or participate in other recreation.
A2	**Theatrical and indoor sport** Occupancy where persons gather for the viewing of theatrical, operatic, orchestral, choral, cinematographical or sports performances
A3	**Places of instruction** Occupancy where school children, students or other persons assemble for the purpose of tuition or learning.
A4	**Worship** Occupancy where persons assemble for the purpose of worshipping.
A5	**Outdoor sport** Occupancy where persons view outdoor sports events.
B1	**High-risk commercial service** Occupancy where a non-industrial process is carried out and where either the material handled or the process carried out is liable, in the event of fire, to cause combustion with extreme rapidity or give rise to poisonous fumes, or cause explosions.
B2	**Moderate risk commercial service** Occupancy where a non-industrial process is carried out and where either the material handled or the process carried out is liable, in the event of fire, to cause combustion with moderate rapidity but is not likely to give rise to poisonous fumes, or cause explosions.
B3	**Low risk commercial service** Occupancy where a non-industrial process is carried out and where neither the material handled nor the process carried out falls into the high or moderate risk category.
C1	**Exhibition hall** Occupancy where goods are displayed primarily for viewing by the public.
C2	**Museum** Occupancy comprising a museum, art gallery or library.
D1	**High risk industrial** Occupancy where an industrial process is carried out and where either the material handled or the process carried out is liable, in the event of fire, to cause combustion with extreme rapidity or give rise to poisonous fumes, or cause explosions.
D2	**Moderate risk industrial** Occupancy where an industrial process is carried out and where either the material handled or the process carried out is liable, in the event of fire, to cause combustion with moderate rapidity bulls not likely to give rise to poisonous fumes, or cause explosions.
D3	**Low risk industrial** Occupancy where an industrial process is carried out and where neither the material handled nor the process carried out falls into the high or moderate risk category
D4	**Plant room** Occupancy comprising usually unattended mechanical or electrical services necessary for the running of a building.
E1	**Place of detention** Occupancy where people are detained for punitive or corrective reasons or because of their mental condition.
E2	**Hospital** Occupancy where people are cared for or treated because of physical or mental disabilities and where they are generally bedridden.
E3	**Other institutional (residential)** Occupancy is where groups of people who either are not fully fit, or are restricted in their movements or ability to make decisions, reside and are cared for.
F1	**Large shop**

	Occupancy where merchandise is displayed and offered for sale to the public and the floor area exceeds 250 m².
F2	**Small** Occupancy where merchandise is displayed and offered for sale to the public and the floor area does not exceed 250 m².
F3	**Wholesalers' store** Occupancy where goods are displayed and stored and where only a limited selected group of persons is present at any one time
G1	**Offices** Occupancy comprising offices, banks, consulting rooms and other similar usage.
H1	**Hotel** Occupancy where persons rent furnished rooms, not dwelling units.
H2	**Dormitory** Occupancy where groups of people are accommodated in one room
H3	**Domestic residence** Occupancy consisting of two or more dwelling units on a single site
H4	**Dwelling house** Occupancy consisting of a dwelling unit on its own site, including a garage and other domestic outbuildings. If any.
J1	**High risk storage** Occupancy where material is stored and where the stored material is liable, in the event of fire, to cause combustion with extreme rapidity or give rise to poisonous fumes, or cause explosions.
J2	**Moderate risk storage** Occupancy where material is stored and stored material is liable, in the event of fire, to cause combustion with moderate rapidity but is not likely to give rise to poisonous fumes, or cause explosions.
J3	**Low risk storage** Occupancy where the material stored does not fall into the high or moderate risk category.
J4	**Parking garage** Occupancy used for storing or parking more than 10 motor vehicles

Appendix B-4: Design Population

Class of occupancy of room or storey or portion thereof	Population
A1, A2, A4, A5	Number of fixed seats or 1 person per m² if there are no fixed seats
E1, E3, H1, H3	2 persons per bedroom
G1	1 person per 15 m²
J1, J2, J3, J4	1 person per 50 m²
C1, E2, F1, F2	1 person per 10 m²
B1, B2, B3, D1, D2, D3	1 person per 15 m²
C2, F3	1 person per 20 m²
A3, H2	1 person per 5 m²

14 Appendix C: PMV and TABS Calculator and Results

Appendix C-1: PMV Calculator

```
"""
The following module calculates a space's Predicted Mean Vote (PMV) and
Predicted Percentage of Dissatisfaction (PPD). Module is translated into python
from BASIC program following ISO 7730.

It further determines the air and radiant temperature at which the occupants
will be thermally comfortable.
"""


import math

from air import Air
import units
from units import Temperature

HEAT_LOSSES = {
    'THROUGH_SKIN': 'skin',
    'BY_SWEATING': 'sweating',
    'BY_LATENT_RESPIRATION': 'latent_respiration',
    'BY_DRY_RESPIRATION': 'dry_respiration',
    'BY_RADIATION': 'radiation',
    'BY_CONVECTION': 'convection',
}

class ThermalConditions:
    def __init__(self, air_temperature, relative_humidity,
                 mean_radiant_temperature, relative_air_velocity,
                 metabolic_rate, clothing, external_work=0,
                 water_vapour_pressure=0):
        self._TA = air_temperature   # [°C]
        self._RH = relative_humidity   # [%]
        self._TR = mean_radiant_temperature   # [°C]
        self._VEL = relative_air_velocity   # [m/s]
        self._MET = metabolic_rate   # [met]
        self._CLO = clothing   # Clothing [clo]

        self._WME = external_work   # External work, normally around 0 [met]
        self._PA = water_vapour_pressure    # Water vapour pressure [Pa]

        # Check boundary conditions
        if self._MET < 0.8:
            print('WARNING: MET TOO LOW')
            sys.exit()
        elif self._MET > 4.0:
            print('WARNING: MET TOO HIGH')
            sys.exit()

        if self._CLO is not None:
            if self._CLO < 0.0:
                print('WARING: CLO CANNOT BE NEGATIVE')
                sys.exit()
            elif self._CLO > 2.0:
                print('WARING: CLO IS TOO HIGH')
                sys.exit()
```

```
        if self._TA is not None:
            if self._TA < 10.0:
                print('WARNING: TA TOO LOW')
                sys.exit()
            elif self._TA > 30.0:
                print('WARNING: TA TOO HIGH')
                sys.exit()

        if self._TR is not None:
            if self._TR < 10.0:
                print('WARNING: TR TOO LOW')
                sys.exit()
            elif self._TR > 40.0:
                print('WARNING: TR TOO HIGH')
                sys.exit()

        if self._VEL is not None:
            if self._VEL < 0.0:
                print('WARNING: VEL CANNOT BE NEGATIVE')
                sys.exit()
            elif self._VEL > 1.0:
                print('WARNING: VEL TOO HIGH')
                sys.exit()

        if self._PA == 0.0:
            # Function used to determine saturated vapour pressure [kPa] using
            # Antoine's equation
            sat_vap_press = math.exp(16.6536 - 4030.183/(self._TA+235))
            self._PA = self._RH * 10 * sat_vap_press
        self._ICL = self._CLO * 0.155  # thermal insulation of clothing
        self._M = self._MET * 58.15    # metabolic rate [W/m2]
        self._W = self._WME * 58.15    # external work [W/m2]
        # internal heat production in the human body
        self._MW = self._M - self._W
        if self._ICL <= .078:
            self._FCL = 1 + (1.29 * self._ICL)      # clothing area factor
        else:
            self._FCL = 1.05 + (0.645 * self._ICL)
        # heat transfer coeff. by forced convection
        self._HCF = 12.1 * math.sqrt(self._VEL)
        self._TAA = self._TA + 273.15  # air temperature
        self._TRA = self._TR + 273.15  # radiant mean temperature

        self._heat_loss_components_store = HeatLossComponentsStore()

    def get_heat_loss(self, how):
        # first guess for the surface temperature of clothing
        TCLA = self._TAA + (35.5-self._TA) / (3.5*((6.45*self._ICL)+.1))

        P1 = self._ICL * self._FCL
        P2 = P1 * 3.96
        P3 = P1 * 100
        P4 = P1 * self._TAA
        P5 = 308.7 - (0.028 * self._MW) + (P2 * math.pow((self._TRA/100), 4))
        XN = TCLA / 100.0
        XF = XN
```

```
# XF = TCLA / 50.0

N = 1
AXNNF = 1
EPS = .00015
HC = 0
TCL = 0
while AXNNF > EPS:
    XF = (XF + XN) / 2
    # heat transfer coefficient by natural convection
    HCN = 2.38 * math.pow(abs(100 * (XF-self._TAA)), 0.25)

    if self._HCF < HCN:
        HC = self._HCF
    else:
        HC = HCN
    XN = (P5 + (P4 * HC) - (P2 * math.pow(XF, 4))) / (100 + (P3 * HC))

    AXNNF = abs(XN - XF)
    TCL = (100 * XN) - 273.15

    N = N + 1
    if N > 150:
        PMV = 99999
        PPD = 100
        break

if how == HEAT_LOSSES['THROUGH_SKIN']:
    skin = 3.05 * 0.001 * (5733 - 6.99 * self._MW - self._PA)

    return skin

elif how == HEAT_LOSSES['BY_SWEATING']:
    if self._MW > 58.15:
        sweating = 0.42 * (self._MW - 58.15)
    else:
        sweating = 0

    return sweating

elif how == HEAT_LOSSES['BY_LATENT_RESPIRATION']:
    latent_respiration = 1.7 * 0.00001 * self._M * (5867 - self._PA)

    return latent_respiration

elif how == HEAT_LOSSES['BY_DRY_RESPIRATION']:
    dry_respiration = .0014 * self._M * (34 - self._TA)

    return dry_respiration

elif how == HEAT_LOSSES['BY_RADIATION']:
    radiation = (3.96 * self._FCL *
                 (math.pow(XN, 4.0) - math.pow((self._TRA/100), 4)))

    return radiation

elif how == HEAT_LOSSES['BY_CONVECTION']:
```

```
        convection = self._FCL * HC * (TCL - self._TA)

        return convection

def get_heat_flux(self):
    if '_Q' in self.__dict__:
        return self._Q
    else:
        self._Q = (
            self.get_heat_loss(HEAT_LOSSES['THROUGH_SKIN']) +
            self.get_heat_loss(HEAT_LOSSES['BY_SWEATING']) +
            self.get_heat_loss(HEAT_LOSSES['BY_LATENT_RESPIRATION']) +
            self.get_heat_loss(HEAT_LOSSES['BY_DRY_RESPIRATION']) +
            self.get_heat_loss(HEAT_LOSSES['BY_RADIATION']) +
            self.get_heat_loss(HEAT_LOSSES['BY_CONVECTION'])
        )
        return self._Q

def get_pmv(self):
    if '_PMV' in self.__dict__:
        return self._PMV
    else:
        TS = 0.303 * math.exp(-0.036 * self._M) + 0.028
        self._PMV = TS * (self._MW - self.get_heat_flux())
        return self._PMV

def get_occupant_sensation(self):
    if (self._MW - self.get_heat_flux()) > 0.0:
        return 'warm'
    else:
        return 'cold'

def get_ppd(self):
    if '_PPD' in self.__dict__:
        return self._PPD
    else:
        self._PPD = (
            100 - (95 * math.exp(
                -0.03353 * math.pow(self.get_pmv(), 4.0) -
                0.2179 * math.pow(self.get_pmv(), 2.0)))
        )
        return self._PPD
```

Appendix C-2: Type A Calculator

```
"""
This module uses the Universal Single Power (USP) method for Type A and C
systems to determine the required water supply temperature
"""

import sys, math
from decimal import Decimal
from collections import OrderedDict

# from functions import Functions

PIPE_SPACING_FACTOR = OrderedDict({
    0: {'α_W': 1.23},
    0.05: {'α_W': 1.188},
    0.1: {'α_W': 1.156},
    0.15: {'α_W': 1.134},
})
COVERING_FACTOR = OrderedDict({
    0: {
        0.05: {'α_U': 1.069},
        0.075: {'α_U': 1.066},
        0.1: {'α_U': 1.063},
        0.15: {'α_U': 1.057},
        0.2: {'α_U': 1.051},
        0.225: {'α_U': 1.048},
        0.3: {'α_U': 1.0395},
        0.375: {'α_U': 1.03},
    },
    0.05: {
        0.05: {'α_U': 1.065},
        0.075: {'α_U': 1.053},
        0.1: {'α_U': 1.05},
        0.15: {'α_U': 1.046},
        0.2: {'α_U': 1.041},
        0.225: {'α_U': 1.038},
        0.3: {'α_U': 1.031},
        0.375: {'α_U': 1.0221},
    },
    0.1: {
        0.05: {'α_U': 1.043},
        0.075: {'α_U': 1.041},
        0.1: {'α_U': 1.039},
        0.15: {'α_U': 1.035},
        0.2: {'α_U': 1.0315},
        0.225: {'α_U': 1.0295},
        0.3: {'α_U': 1.024},
        0.375: {'α_U': 1.018},
    },
    0.15: {
        0.05: {'α_U': 1.037},
        0.075: {'α_U': 1.035},
        0.1: {'α_U': 1.0335},
        0.15: {'α_U': 1.0305},
        0.2: {'α_U': 1.0275},
        0.225: {'α_U': 1.026},
        0.3: {'α_U': 1.021},
```

```
        0.375: {'α_U': 1.015},
    },
})
PIPE_EXTERNAL_DIAMETER_FACTOR = OrderedDict({
    0: {
        0.05: {'α_D': 1.013},
        0.075: {'α_D': 1.021},
        0.1: {'α_D': 1.029},
        0.15: {'α_D': 1.04},
        0.2: {'α_D': 1.046},
        0.225: {'α_D': 1.049},
        0.3: {'α_D': 1.053},
        0.375: {'α_D': 1.056},
    },
    0.05: {
        0.05: {'α_D': 1.013},
        0.075: {'α_D': 1.019},
        0.1: {'α_D': 1.025},
        0.15: {'α_D': 1.034},
        0.2: {'α_D': 1.04},
        0.225: {'α_D': 1.043},
        0.3: {'α_D': 1.049},
        0.375: {'α_D': 1.051},
    },
    0.1: {
        0.05: {'α_D': 1.012},
        0.075: {'α_D': 1.016},
        0.1: {'α_D': 1.022},
        0.15: {'α_D': 1.029},
        0.2: {'α_D': 1.035},
        0.225: {'α_D': 1.038},
        0.3: {'α_D': 1.044},
        0.375: {'α_D': 1.046},
    },
    0.15: {
        0.05: {'α_D': 1.011},
        0.075: {'α_D': 1.014},
        0.1: {'α_D': 1.018},
        0.15: {'α_D': 1.024},
        0.2: {'α_D': 1.03},
        0.225: {'α_D': 1.033},
        0.3: {'α_D': 1.039},
        0.375: {'α_D': 1.042},
    },
})

def interpolate(self, x, x1, x2, y1, y2):
        return y1 + ((y2 - y1) / (x2 - x1) * (x - x1))

class TypeA:
    def __init__(self, floor_covering_properties, screed_thickness,
                 screed_properties, pipe_spacing, pipe_length, pipe_properties,
                 heat_conducting_device_properties):
        self.R_λB = floor_covering_properties.THERMAL_RESISTANCE
        self.su = screed_thickness
        self.λ_E = screed_properties.THERMAL_CONDUCTIVITY
        self.W = pipe_spacing
```

```
        self.pipe_length = pipe_length
        self.d = pipe_properties.EXTERNAL_DIAMETER
        self.sr = pipe_properties.THICKNESS
        self.λr = pipe_properties.THERMAL_CONDUCTIVITY
        self.heat_conducting_device_properties = (
            heat_conducting_device_properties)

        self._system_factors_store = SystemFactorsStore()

        # Check boundary conditions
        if self.W < 0.05:
            print('WARNING: Pipe spacing is too small')
            sys.exit()
        if self.su < 0.01:
            print('WARNING: Screed thickness is too small')
            sys.exit()
        if self.d < 0.008 or self.d > 0.03:
            print('WARNING: Pipe thickness is out boundary conditions')
            sys.exit()
        if self.su/self.λ_E < 0.01:
            print('WARNING: Screed thickness to thermal conductivity ratio ' +
                  'is too small')
            sys.exit()

    def get_system_coefficient(self):
        if self.λr == 0.35 and self.sr == 0.002:
            B = 6.7
        else:
            B_0 = 6.7
            λ_r0 = 0.35
            s_r0 = 0.002
            B = math.pow(
                (1/B_0)+(1.1/math.pi) *
                (self.get_pipe_spacing_factor() *
                 self.get_covering_factor() *
                 self.get_pipe_external_diameter_factor()) *
                self.W*(
                    (1/(2*self.λr))*math.log(self.d/(self.d-2*self.sr))
                    - (1/(2*λ_r0))*math.log(self.d/(self.d-2*s_r0))),
                -1)

        self._system_factors_store.store(B=B)

        return B

    def get_surface_covering_factor(self):
        α = 10.8  # [W/m2K]
        λ_u0 = 1.0  # [W/mK]
        s_u0 = 0.045  # [m]

        α_B = ((1/α) + (s_u0/λ_u0)) / ((1/α) + (s_u0/self.λ_E) + self.R_λB)

        self._system_factors_store.store(α_B=α_B)

        return α_B

    def get_pipe_spacing_factor(self):
```

```
    α_W = None

    prev_conduction_resistance = None
    prev_spacing_factor = None
    for conduction_resistance, spacing_factor in PIPE_SPACING_FACTOR.items():
        if (prev_conduction_resistance is not None and
            prev_spacing_factor is not None and
            prev_conduction_resistance <= self.R_λB and
                conduction_resistance >= self.R_λB):
            α_W = interpolate(
                self.R_λB,
                prev_conduction_resistance,
                conduction_resistance,
                prev_spacing_factor['α_W'],
                spacing_factor['α_W'],
            )
        else:
            prev_conduction_resistance = conduction_resistance
            prev_spacing_factor = spacing_factor

    m_W = 1.0 - self.W/0.075

    self._system_factors_store.store(α_W=α_W, m_W=m_W)

    return math.pow(α_W, m_W)

def get_covering_factor(self):
    α_U = None
    prev_conduction_resistance = None
    prev_covering_factor_row = None

    for conduction_resistance, covering_factor_row in COVERING_FACTOR.items():
        if (prev_conduction_resistance is not None and
            prev_covering_factor_row is not None and
            prev_conduction_resistance <= self.R_λB and
                conduction_resistance >= self.R_λB):

            prev_pipe_spacing = None
            prev_covering_factor = None
            for pipe_spacing, covering_factor in covering_factor_row.items():
                if (prev_pipe_spacing is not None and
                    prev_covering_factor is not None and
                    prev_pipe_spacing <= self.W and
                        pipe_spacing >= self.W):

                    covering_factor1 = interpolate(
                        self.W,
                        prev_pipe_spacing,
                        pipe_spacing,
                        prev_covering_factor['α_U'],
                        covering_factor['α_U'],
                    )
                else:
                    prev_pipe_spacing = pipe_spacing
                    prev_covering_factor = covering_factor

            prev_pipe_spacing = None
```

```
                prev_covering_factor = None
                for pipe_spacing, covering_factor in prev_covering_factor_row.items():
                    if (prev_pipe_spacing is not None and
                        prev_covering_factor is not None and
                        prev_pipe_spacing <= self.W and
                            pipe_spacing >= self.W):

                        covering_factor2 = interpolate(
                            self.W,
                            prev_pipe_spacing,
                            pipe_spacing,
                            prev_covering_factor['α_U'],
                            covering_factor['α_U'],
                        )
                    else:
                        prev_pipe_spacing = pipe_spacing
                        prev_covering_factor = covering_factor

                α_U = interpolate(
                    self.R_λB,
                    conduction_resistance,
                    prev_conduction_resistance,
                    covering_factor1,
                    covering_factor2,
                )

            else:
                prev_conduction_resistance = conduction_resistance
                prev_covering_factor_row = covering_factor_row

        m_U = 100.0*(0.045-self.su)

        self._system_factors_store.store(α_U=α_U, m_U=m_U)

        return math.pow(α_U, m_U)

    def get_pipe_external_diameter_factor(self):
        α_D = None
        prev_conduction_resistance = None
        prev_covering_factor_row = None

        for            conduction_resistance,            covering_factor_row            in
PIPE_EXTERNAL_DIAMETER_FACTOR.items():
            if (prev_conduction_resistance is not None and
                prev_covering_factor_row is not None and
                prev_conduction_resistance <= self.R_λB and
                    conduction_resistance >= self.R_λB):

                prev_pipe_spacing = None
                prev_covering_factor = None
                for pipe_spacing, covering_factor in covering_factor_row.items():
                    if (prev_pipe_spacing is not None and
                        prev_covering_factor is not None and
                        prev_pipe_spacing <= self.W and
                            pipe_spacing >= self.W):

                        covering_factor1 = interpolate(
```

```
                    self.W,
                    prev_pipe_spacing,
                    pipe_spacing,
                    prev_covering_factor['α_D'],
                    covering_factor['α_D'],
                )
            else:
                prev_pipe_spacing = pipe_spacing
                prev_covering_factor = covering_factor

        prev_pipe_spacing = None
        prev_covering_factor = None
        for pipe_spacing, covering_factor in prev_covering_factor_row.items():
            if (prev_pipe_spacing is not None and
                prev_covering_factor is not None and
                prev_pipe_spacing <= self.W and
                    pipe_spacing >= self.W):

                covering_factor2 = interpolate(
                    self.W,
                    prev_pipe_spacing,
                    pipe_spacing,
                    prev_covering_factor['α_D'],
                    covering_factor['α_D'],
                )
            else:
                prev_pipe_spacing = pipe_spacing
                prev_covering_factor = covering_factor

        α_D = interpolate(
            self.R_λB,
            conduction_resistance,
            prev_conduction_resistance,
            covering_factor1,
            covering_factor2,
        )

    else:
        prev_conduction_resistance = conduction_resistance
        prev_covering_factor_row = covering_factor_row

m_D = 250*(self.d - 0.02)

self._system_factors_store.store(α_D=α_D, m_D=m_D)

return math.pow(α_D, m_D)
```

Appendix C-3: Type E Calculator

```
"""
The following module uses the General Resistance Method (GRM) to calculate the
heat flux of TABS
"""

import math
from decimal import Decimal

from air import Air
from water import Water

class TypeE:
    def __init__(self, screed_thickness_above_pipes,
                 screed_thickness_below_pipes, screed_properties, pipe_spacing,
                 pipe_length, pipe_properties, parameter, mass_flow,
                 water_temp):
        self.s_1 = screed_thickness_above_pipes
        self.s_2 = screed_thickness_below_pipes
        self.λ_b = screed_properties.THERMAL_CONDUCTIVITY
        self.screed = screed_properties
        self.W = pipe_spacing
        self.length = pipe_length
        self.d_a = pipe_properties.EXTERNAL_DIAMETER
        self.s_r = pipe_properties.THICKNESS
        self.λ_r = pipe_properties.THERMAL_CONDUCTIVITY
        self.parameter = parameter
        self.m_sp = mass_flow  # [kg/s]
        self.T = water_temp

        self._system_resistances_store = SystemResistancesStore()

    def get_water_flow_resistance(self):
        self.c_w = Water(self.T).get('specific_heat')*1000  # [(m2K)/W]
        r_z = 1 / (2*self.m_sp*self.c_w)

        return r_z

    def get_resistance_between_fluid_and_pipe_wall(self):
        r_w = (math.pow(self.W, 0.13))/(8.0*math.pi) * \
            (math.pow((self.d_a-(2*self.s_r)) / (self.m_sp*self.length), 0.87))

        return r_w

    def get_resistance_at_pipe_wall(self):
        r_r = (self.W*math.log(self.d_a/(self.d_a-(2*self.s_r))) /
               (2*math.pi*self.λ_r))

        return r_r

    def get_resistance_between_pipe_wall_and_conductive_layer(self):
        if (self.s_1/self.W > 0.3 and self.s_2/self.W > 0.3 and
                self.d_a/self.W < 0.2):
            r_x = self.W*math.log(
                self.W/(math.pi * self.d_a)) / (2*math.pi*self.λ_b)

            return r_x
```

```
    else:

        return None

def get_total_resistance(self):
    r_z = self.get_water_flow_resistance()
    r_w = self.get_resistance_between_fluid_and_pipe_wall()
    r_r = self.get_resistance_at_pipe_wall()
    r_x = self.get_resistance_between_pipe_wall_and_conductive_layer()

    # if self.m_sp*self.c_w*(r_w + r_r + r_x) < 0.5:
    #     r_z = None

    r_total = r_z + r_w + r_r + r_x

    return r_total
```

Appendix C-4: TABS Calculator

```
# This programme is translated from FORTRAN (programme language) as given in
# ISO 11855-4:2012(E)

import math
from prettytable import PrettyTable

class layer:
    def __init__(self, divisions, thickness, thermal_conductivity, density,
                 specific_heat):
        self.divisions = divisions
        self.thickness = thickness
        self.thermal_conductivity = thermal_conductivity
        self.density = density
        self.specific_heat = specific_heat

class heat_loads_and_circuit:
    def __init__(self, rad_heat_flux, conv_heat_flux, running_mode,
                 max_cooling_power, mass_flow, water_temp, air_temp=None,
                 floor_temp=None, pipe_level_temp=None, ceiling_temp=None,
                 wall_temp=None, floor_heat_flow=None, ceiling_heat_flow=None,
                 wall_heat_flow=None, circuit_heat_flow=None, water_temp_out=None,
                 mean_rad_temp=None, operating_temp=None):
        self.rad_heat_flux = rad_heat_flux
        self.conv_heat_flux = conv_heat_flux
        self.running_mode = running_mode
        self.max_cooling_power = max_cooling_power
        self.mass_flow = mass_flow
        self.air_temp = air_temp
        self.floor_temp = floor_temp
        self.pipe_level_temp = pipe_level_temp
        self.ceiling_temp = ceiling_temp
        self.wall_temp = wall_temp
        self.water_temp = water_temp
        self.floor_heat_flow = floor_heat_flow
        self.ceiling_heat_flow = ceiling_heat_flow
        self.wall_heat_flow = wall_heat_flow
        self.circuit_heat_flow = circuit_heat_flow
        self.water_temp_out = water_temp_out
        self.mean_rad_temp = mean_rad_temp
        self.operating_temp = operating_temp

class node:
    def __init__(self, thermal_inertia, resistance_upper, resistance_lower,
                 position, previous_temp=None, temp=None, air_coeff=None,
                 wall_coeff=None, floor_coeff=None, ceiling_coeff=None,
                 rad_coeff=None, conv_coeff=None, cond_upper_coeff=None,
                 cond_lower_coeff=None, inertia_coeff=None,
                 circuit_coeff=None):
        self.thermal_inertia = thermal_inertia
        self.resistance_upper = resistance_upper
        self.resistance_lower = resistance_lower
        self.previous_temp = previous_temp
        self.temp = temp
        self.position = position
        self.air_coeff = air_coeff
        self.wall_coeff = wall_coeff
```

```
        self.floor_coeff = floor_coeff
        self.ceiling_coeff = ceiling_coeff
        self.rad_coeff = rad_coeff
        self.conv_coeff = conv_coeff
        self.cond_upper_coeff = cond_upper_coeff
        self.cond_lower_coeff = cond_lower_coeff
        self.inertia_coeff = inertia_coeff
        self.circuit_coeff = circuit_coeff

# Main slab input data
layers = [[
    layer(divisions=2, thickness=0.02, thermal_conductivity=0.17,
          specific_heat=2300, density=700),
    layer(divisions=3, thickness=0.07, thermal_conductivity=1.1,
          specific_heat=850, density=1900),
    layer(divisions=4, thickness=0.1, thermal_conductivity=1.9,
          specific_heat=880, density=2000)], [
    layer(divisions=4, thickness=0.1, thermal_conductivity=1.9,
          specific_heat=880, density=2000)]]

# Main room input data
floor_area = 30
wall_area = 48
h_air_to_floor = 1.5
h_air_to_ceiling = 5.5
h_air_to_walls = 2.5
fv_floor_to_ceiling = 0.21
fv_slab_to_external_wall = 0.35
floor_resistance = 0.1
ceiling_resistance = 0.0
wall_resistance = 0.05
c_walls = 10600

# Main circuit input data
total_resistance = 0.073
time_step = 3600
fluid_specific_heat = 4187
mass_flow = 0.3
water_temp_setpoint = 20

# Hourly boundary conditions
boundary = []
for i in range(0, 8):
    boundary.append(
        heat_loads_and_circuit(
            conv_heat_flux=30, rad_heat_flux=10, running_mode=1,
            water_temp=water_temp_setpoint, max_cooling_power=1000,
            mass_flow=mass_flow))
for i in range(8, 19):
    boundary.append(
        heat_loads_and_circuit(
            conv_heat_flux=400, rad_heat_flux=300, running_mode=0,
            water_temp=water_temp_setpoint, max_cooling_power=0,
            mass_flow=mass_flow))
for i in range(19, 24):
    boundary.append(
        heat_loads_and_circuit(
```

```
            conv_heat_flux=150, rad_heat_flux=100, running_mode=1,
            water_temp=water_temp_setpoint, max_cooling_power=1000,
            mass_flow=mass_flow))

h_floor_to_ceiling = ((1 - fv_floor_to_ceiling - fv_slab_to_external_wall)*4 *
                      math.pow(300, 3)*5.67/math.pow(10, 8)*0.9)
h_slab_to_walls = (fv_floor_to_ceiling*4*math.pow(300, 3) *
                   5.67/math.pow(10, 8)*0.9)

thermal_nodes = []
for i in range(len(layers)):  # Upper/lower layers
    for j in range(len(layers[i])):  # Number of layers in upper/lower layers
        # Number of divisions in layer
        for k in range(layers[i][j].divisions):
            if i == 0 and j == 0 and k == 0:
                floor_node = 0
                thermal_nodes.append(
                    node(
                        thermal_inertia=0,
                        resistance_upper=0,
                        resistance_lower=floor_resistance,
                        position='F'))  # floor thermal node
            elif (i == 0 and j == len(layers[i])-1 and
                    k == layers[i][j].divisions-1):
                pipe_level_node = len(thermal_nodes)
                thermal_nodes.append(
                    node(
                        thermal_inertia=0,
                        resistance_upper=0,
                        resistance_lower=0,
                        position='P'))  # pipe level thermal node
            elif (i == 1 and j == len(layers[i])-1 and
                    k == layers[i][j].divisions-1):
                ceiling_node = len(thermal_nodes)
                thermal_nodes.append(
                    node(
                        thermal_inertia=0,
                        resistance_upper=ceiling_resistance,
                        resistance_lower=0,
                        position='C'))  # ceiling thermal node
            else:
                thermal_inertia = (
                    layers[i][j].thickness /
                    layers[i][j].divisions * layers[i][j].density *
                    layers[i][j].specific_heat)
                resistance_upper = (layers[i][j].thickness / (
                    2*layers[i][j].divisions *
                    layers[i][j].thermal_conductivity))
                resistance_lower = (layers[i][j].thickness / (
                    2*layers[i][j].divisions *
                    layers[i][j].thermal_conductivity))
                thermal_nodes.append(
                    node(
                        thermal_inertia=thermal_inertia,
                        resistance_upper=resistance_upper,
                        resistance_lower=resistance_lower,
                        position='I'))  # internal thermal node
```

```
# wall surface thermal node
wall_node = len(thermal_nodes)
thermal_nodes.append(
    node(
        thermal_inertia=0,
        resistance_upper=0,
        resistance_lower=wall_resistance,
        position='S'))

# inner wall thermal node
thermal_nodes.append(
    node(
        thermal_inertia=c_walls,
        resistance_upper=0,
        resistance_lower=0,
        position='K'))

# air thermal node
air_node = len(thermal_nodes)
thermal_nodes.append(
    node(
        thermal_inertia=0,
        resistance_upper=0,
        resistance_lower=0,
        position='A'))

num_thermal_nodes = range(len(thermal_nodes))

for i in num_thermal_nodes:
    if thermal_nodes[i].position == 'F':
        thermal_nodes[i].air_coeff = h_air_to_floor*floor_area
        thermal_nodes[i].wall_coeff = h_floor_to_ceiling*floor_area
        thermal_nodes[i].floor_coeff = 0
        thermal_nodes[i].ceiling_coeff = h_slab_to_walls*floor_area
        thermal_nodes[i].rad_coeff = floor_area/(2*floor_area+wall_area)
        thermal_nodes[i].conv_coeff = 0
        thermal_nodes[i].cond_upper_coeff = 0
        thermal_nodes[i].cond_lower_coeff = (1/(
            thermal_nodes[i].resistance_lower +
            thermal_nodes[i+1].resistance_upper)*floor_area)
        thermal_nodes[i].inertia_coeff = 0
        thermal_nodes[i].circuit_coeff = 0
    if thermal_nodes[i].position == 'I':
        thermal_nodes[i].air_coeff = 0
        thermal_nodes[i].wall_coeff = 0
        thermal_nodes[i].floor_coeff = 0
        thermal_nodes[i].ceiling_coeff = 0
        thermal_nodes[i].rad_coeff = 0
        thermal_nodes[i].conv_coeff = 0
        thermal_nodes[i].cond_upper_coeff = (1/(
            thermal_nodes[i-1].resistance_lower +
            thermal_nodes[i].resistance_upper)*floor_area)
        thermal_nodes[i].cond_lower_coeff = (1/(
            thermal_nodes[i].resistance_lower +
            thermal_nodes[i+1].resistance_upper)*floor_area)
        thermal_nodes[i].inertia_coeff = (
```

```
        thermal_nodes[i].thermal_inertia*floor_area/time_step)
    thermal_nodes[i].circuit_coeff = 0
if thermal_nodes[i].position == 'P':
    thermal_nodes[i].air_coeff = 0
    thermal_nodes[i].wall_coeff = 0
    thermal_nodes[i].floor_coeff = 0
    thermal_nodes[i].ceiling_coeff = 0
    thermal_nodes[i].rad_coeff = 0
    thermal_nodes[i].conv_coeff = 0
    thermal_nodes[i].cond_upper_coeff = (1/(
        thermal_nodes[i-1].resistance_lower +
        thermal_nodes[i].resistance_upper)*floor_area)
    thermal_nodes[i].cond_lower_coeff = (1/(
        thermal_nodes[i].resistance_lower +
        thermal_nodes[i+1].resistance_upper)*floor_area)
    thermal_nodes[i].inertia_coeff = 0
    thermal_nodes[i].circuit_coeff = 1/total_resistance * floor_area
if thermal_nodes[i].position == 'C':
    thermal_nodes[i].air_coeff = h_air_to_ceiling*floor_area
    thermal_nodes[i].wall_coeff = h_floor_to_ceiling*floor_area
    thermal_nodes[i].floor_coeff = h_slab_to_walls*floor_area
    thermal_nodes[i].ceiling_coeff = 0
    thermal_nodes[i].rad_coeff = floor_area/(2*floor_area+wall_area)
    thermal_nodes[i].conv_coeff = 0
    thermal_nodes[i].cond_upper_coeff = (1/(
        thermal_nodes[i-1].resistance_lower +
        thermal_nodes[i].resistance_upper)*floor_area)
    thermal_nodes[i].cond_lower_coeff = 0
    thermal_nodes[i].inertia_coeff = 0
    thermal_nodes[i].circuit_coeff = 0
if thermal_nodes[i].position == 'S':
    thermal_nodes[i].air_coeff = h_air_to_walls*wall_area
    thermal_nodes[i].wall_coeff = 0
    thermal_nodes[i].floor_coeff = h_floor_to_ceiling*floor_area
    thermal_nodes[i].ceiling_coeff = h_floor_to_ceiling*floor_area
    thermal_nodes[i].rad_coeff = wall_area/(2*floor_area+wall_area)
    thermal_nodes[i].conv_coeff = 0
    thermal_nodes[i].cond_upper_coeff = 0
    thermal_nodes[i].cond_lower_coeff = (1/(
        thermal_nodes[i].resistance_lower +
        thermal_nodes[i+1].resistance_upper)*wall_area)
    thermal_nodes[i].inertia_coeff = 0
    thermal_nodes[i].circuit_coeff = 0
if thermal_nodes[i].position == 'K':
    thermal_nodes[i].air_coeff = 0
    thermal_nodes[i].wall_coeff = 0
    thermal_nodes[i].floor_coeff = 0
    thermal_nodes[i].ceiling_coeff = 0
    thermal_nodes[i].rad_coeff = 0
    thermal_nodes[i].conv_coeff = 0
    thermal_nodes[i].cond_upper_coeff = (1/(
        thermal_nodes[i-1].resistance_lower +
        thermal_nodes[i].resistance_upper)*wall_area)
    thermal_nodes[i].cond_lower_coeff = 0
    thermal_nodes[i].inertia_coeff = (
        thermal_nodes[i].thermal_inertia*wall_area/time_step)
    thermal_nodes[i].circuit_coeff = 0
```

```
    if thermal_nodes[i].position == 'A':
        thermal_nodes[i].air_coeff = 0
        thermal_nodes[i].wall_coeff = h_air_to_walls*wall_area
        thermal_nodes[i].floor_coeff = h_air_to_floor*floor_area
        thermal_nodes[i].ceiling_coeff = h_air_to_ceiling*floor_area
        thermal_nodes[i].rad_coeff = 0
        thermal_nodes[i].conv_coeff = 1
        thermal_nodes[i].cond_upper_coeff = 0
        thermal_nodes[i].cond_lower_coeff = 0
        thermal_nodes[i].inertia_coeff = 0
        thermal_nodes[i].circuit_coeff = 0

max_daily_tolerance = 0.0001
max_daily_iterations = 500
max_hourly_tolerance = 0.00001
max_hourly_iterations = 1000
daily_tolenace = 100000
daily_iterations = 0
sum_of_temps = 0

for i in num_thermal_nodes:
    thermal_nodes[i].temp = 22
    sum_of_temps += 24*thermal_nodes[i].temp

water_temp = None
while (daily_iterations < max_daily_iterations and
       daily_tolenace > max_daily_tolerance):
    daily_iterations += 1
    sum_of_temps_prev = sum_of_temps
    sum_of_temps = 0
    daily_tolenace = 0

    for hour in range(24):
        hourly_iteration = 0
        hourly_tolerance = 100000

        for i in num_thermal_nodes:
            thermal_nodes[i].previous_temp = thermal_nodes[i].temp

        while (hourly_iteration < max_hourly_iterations and
               hourly_tolerance > max_hourly_tolerance):
            hourly_tolerance = 0
            hourly_iteration += 1
            circuit_heat_flow = 0

            # loop to try to determine supply temp in the hour
            for i in num_thermal_nodes:
                air_temp = thermal_nodes[air_node].temp
                floor_temp = thermal_nodes[floor_node].temp
                ceiling_temp = thermal_nodes[ceiling_node].temp
                wall_temp = thermal_nodes[wall_node].temp
                pipe_level_temp = thermal_nodes[pipe_level_node].temp

                if boundary[hour].mass_flow > 0 and water_temp is not None:
                    water_temp = max(
                        boundary[hour].water_temp,
                        water_temp + (
```

```
                (circuit_heat_flow -
                 boundary[hour].max_cooling_power) /
                (boundary[hour].mass_flow*fluid_specific_heat)))
    else:
        water_temp = boundary[hour].water_temp

    A = (
        (thermal_nodes[i].air_coeff * air_temp) +
        (thermal_nodes[i].wall_coeff * wall_temp) +
        (thermal_nodes[i].floor_coeff * floor_temp) +
        (thermal_nodes[i].ceiling_coeff * ceiling_temp) +
        (thermal_nodes[i].rad_coeff *
         boundary[hour].rad_heat_flux) +
        (thermal_nodes[i].conv_coeff *
         boundary[hour].conv_heat_flux) +
        (thermal_nodes[i].inertia_coeff *
         thermal_nodes[i].previous_temp) +
        (thermal_nodes[i].circuit_coeff *
         boundary[hour].running_mode * water_temp))

    B = (
        thermal_nodes[i].air_coeff +
        thermal_nodes[i].wall_coeff +
        thermal_nodes[i].floor_coeff +
        thermal_nodes[i].ceiling_coeff +
        thermal_nodes[i].inertia_coeff +
        (thermal_nodes[i].circuit_coeff *
         boundary[hour].running_mode))

    if thermal_nodes[i].position != 'F':
        A += (thermal_nodes[i].cond_upper_coeff *
              thermal_nodes[i-1].temp)
        B += thermal_nodes[i].cond_upper_coeff
    if thermal_nodes[i].position != 'A':
        A += (thermal_nodes[i].cond_lower_coeff *
              thermal_nodes[i+1].temp)
        B += thermal_nodes[i].cond_lower_coeff

    supply_temp = A/B
    hourly_tolerance += abs(supply_temp-thermal_nodes[i].temp)
    thermal_nodes[i].temp = supply_temp

    circuit_heat_flow = (
        thermal_nodes[pipe_level_node].circuit_coeff *
        boundary[hour].running_mode *
        (pipe_level_temp - water_temp))

boundary[hour].air_temp = thermal_nodes[air_node].temp
boundary[hour].floor_temp = thermal_nodes[floor_node].temp
boundary[hour].pipe_level_temp = thermal_nodes[pipe_level_node].temp
boundary[hour].ceiling_temp = thermal_nodes[ceiling_node].temp
boundary[hour].wall_temp = thermal_nodes[wall_node].temp
boundary[hour].water_temp = water_temp
boundary[hour].floor_heat_flow = (
    (thermal_nodes[floor_node].air_coeff *
     boundary[hour].air_temp) +
    (thermal_nodes[floor_node].wall_coeff *
```

```
             boundary[hour].wall_temp) +
            (thermal_nodes[floor_node].ceiling_coeff *
             boundary[hour].ceiling_temp) +
            (thermal_nodes[floor_node].rad_coeff *
             boundary[hour].rad_heat_flux) - (
                thermal_nodes[floor_node].air_coeff +
                thermal_nodes[floor_node].wall_coeff +
                thermal_nodes[floor_node].ceiling_coeff) *
            boundary[hour].floor_temp)
        boundary[hour].ceiling_heat_flow = (
            (thermal_nodes[ceiling_node].air_coeff *
             boundary[hour].air_temp) +
            (thermal_nodes[ceiling_node].wall_coeff *
             boundary[hour].wall_temp) +
            (thermal_nodes[ceiling_node].floor_coeff *
             boundary[hour].floor_temp) +
            (thermal_nodes[ceiling_node].rad_coeff *
                boundary[hour].rad_heat_flux) - (
                    thermal_nodes[ceiling_node].air_coeff +
                    thermal_nodes[ceiling_node].wall_coeff +
                    thermal_nodes[ceiling_node].floor_coeff) *
            boundary[hour].ceiling_temp)
        boundary[hour].wall_heat_flow = (
            (thermal_nodes[wall_node].air_coeff *
             boundary[hour].air_temp) +
            (thermal_nodes[wall_node].floor_coeff *
             boundary[hour].floor_temp) +
            (thermal_nodes[wall_node].ceiling_coeff *
                boundary[hour].ceiling_temp) +
            (thermal_nodes[wall_node].rad_coeff *
                boundary[hour].rad_heat_flux) - (
                    thermal_nodes[wall_node].air_coeff +
                    thermal_nodes[wall_node].floor_coeff +
                    thermal_nodes[wall_node].ceiling_coeff) *
            boundary[hour].wall_temp)
        boundary[hour].circuit_heat_flow = (
            thermal_nodes[pipe_level_node].circuit_coeff *
            boundary[hour].running_mode * (
                boundary[hour].pipe_level_temp -
                boundary[hour].water_temp))
        boundary[hour].water_temp_out = (
            boundary[hour].water_temp + (
                boundary[hour].circuit_heat_flow / (
                    boundary[hour].mass_flow*fluid_specific_heat)))
        boundary[hour].mean_rad_temp = (
            (floor_area*boundary[hour].floor_temp +
            floor_area*boundary[hour].ceiling_temp +
            wall_area*boundary[hour].wall_temp) / (
                2*floor_area+wall_area))
        boundary[hour].operating_temp = (
            boundary[hour].air_temp +
            boundary[hour].mean_rad_temp) / 2

    for i in num_thermal_nodes:
        sum_of_temps += abs(thermal_nodes[air_node].temp)

daily_tolenace = abs(sum_of_temps_prev - sum_of_temps)
```

```
sum_of_conv_flux = 0
sum_of_rad_flux = 0
sum_of_floor_heat_flow = 0
sum_of_ceiling_heat_flow = 0
sum_of_wall_heat_flow = 0
sum_of_circuit_heat_flow = 0

pt = PrettyTable(['Time', 'rad', 'conv', 'running_mode', 'max_power',
                  'm_sp', 'water_temp', 'water_temp_out', 'θ_air', 'θ_mr',
                  'θ_op', 'θ_floor', 'θ_ceiling', 'θ_wall', 'θ_pipe_level',
                  'Q_floor', 'Q_ceiling', 'Q_wall', 'Q_circuit'])
for hour in range(24):
    pt.add_row([
        hour,
        round(boundary[hour].rad_heat_flux),
        round(boundary[hour].conv_heat_flux),
        round(boundary[hour].running_mode),
        round(boundary[hour].max_cooling_power),
        round(boundary[hour].mass_flow, 2),
        round(boundary[hour].water_temp, 1),
        round(boundary[hour].water_temp_out, 1),
        round(boundary[hour].air_temp, 1),
        round(boundary[hour].mean_rad_temp, 1),
        round(boundary[hour].operating_temp, 1),
        round(boundary[hour].floor_temp, 1),
        round(boundary[hour].ceiling_temp, 1),
        round(boundary[hour].wall_temp, 1),
        round(boundary[hour].pipe_level_temp, 1),
        round(boundary[hour].floor_heat_flow),
        round(boundary[hour].ceiling_heat_flow),
        round(boundary[hour].wall_heat_flow),
        round(boundary[hour].circuit_heat_flow)])
    sum_of_conv_flux += boundary[hour].conv_heat_flux
    sum_of_rad_flux += boundary[hour].rad_heat_flux
    sum_of_floor_heat_flow += boundary[hour].floor_heat_flow
    sum_of_ceiling_heat_flow += boundary[hour].ceiling_heat_flow
    sum_of_wall_heat_flow += boundary[hour].wall_heat_flow
    sum_of_circuit_heat_flow += boundary[hour].circuit_heat_flow

print(pt)
print('Sum of convective heat flux: ' + str(sum_of_conv_flux))
print('Sum of radiant heat flux: ' + str(sum_of_rad_flux))
print('Sum of floor surface heat flow: ' + str(sum_of_floor_heat_flow))
print('Sum of ceiling surface heat flow: ' + str(sum_of_ceiling_heat_flow))
print('Sum of wall surface heat flow: ' + str(sum_of_wall_heat_flow))
print('Sum of water circuit heat flow: ' + str(sum_of_circuit_heat_flow))
```

Appendix C-5: Hourly Boundary Conditions and Results

Time	Convective Heat Gain [W]	Radiant Heat Gain [W]	Floor Surface Temp, θ_{floor} [°C]		Ceiling Temp, $\theta_{ceiling}$ [°C]		Air Temp, θ_{air} [°C]		Floor Heat Flow, Q_{floor} [W]		Ceiling Heat Flow, $Q_{ceiling}$ [W]		Internal Wall Surface, Q_{IWS} [W]		Heat Flow Extracted by Circuit, $Q_{circuit}$ [W]	
			ISO	Sim	ISO	Sim	ISO	Sim	ISO	Sim	ISO	Sim	ISO	Sim	ISO	Sim
00:00	30	10	22.7	22.7	22.3	22.3	22.7	22.6	-1	-1	109	113	-68	-72	770	805
01:00	30	10	22.5	22.4	22.1	22.1	22.4	22.4	-8	-7	94	98	-46	-50	716	734
02:00	30	10	22.3	22.2	22	21.9	22.2	22.2	-11	-10	85	88	-34	-38	666	670
03:00	30	10	22.2	22	21.8	21.7	22.1	22	-12	-10	79	81	-27	-31	620	612
04:00	30	10	22	21.9	21.7	21.6	21.9	21.8	-12	-10	75	76	-23	-26	577	559
05:00	30	10	21.9	21.7	21.6	21.4	21.8	21.7	-12	-8	71	71	-20	-23	537	511
06:00	30	10	21.8	21.6	21.5	21.3	21.7	21.5	-11	-7	68	67	-18	-20	501	468
07:00	30	10	21.6	21.4	21.4	21.2	21.6	21.4	-10	-6	66	64	-16	-18	467	429
08:00	400	300	22.5	22.2	21.8	21.7	23.4	23.3	124	134	442	433	134	133	0	0
09:00	400	300	22.7	22.5	22.1	22	23.8	23.7	147	159	472	460	81	81	0	0
10:00	400	300	22.9	22.7	22.3	22.2	24.1	23.9	161	173	485	472	54	55	0	0
11:00	400	300	23.1	22.9	22.5	22.5	24.3	24.2	170	181	490	477	39	42	0	0
12:00	400	300	23.3	23.1	22.7	22.7	24.5	24.4	176	185	492	480	32	36	0	0
13:00	400	300	23.5	23.3	22.9	22.9	24.7	24.6	179	187	493	481	28	32	0	0
14:00	400	300	23.6	23.6	23.1	23.1	24.9	24.9	181	188	493	481	26	31	0	0
15:00	400	300	23.8	23.8	23.3	23.3	25	25.1	182	189	493	481	25	30	0	0
16:00	400	300	24	24	23.4	23.5	25.2	25.3	183	189	493	482	24	29	0	0
17:00	400	300	24.1	24.2	23.6	23.7	25.4	25.5	184	189	493	482	24	29	0	0
18:00	400	300	24.3	24.4	23.8	23.9	25.5	25.7	184	189	492	482	23	29	0	0
19:00	150	100	23.8	23.9	23.5	23.6	24.3	24.4	89	88	246	246	-85	-84	871	863
20:00	150	100	23.6	23.7	23.2	23.3	24	24.1	69	66	236	240	-55	-56	915	903
21:00	150	100	23.4	23.5	23	23	23.8	23.9	55	53	234	239	-40	-43	926	914
22:00	150	100	23.3	23.3	22.8	22.8	23.6	23.6	47	46	234	239	-32	-36	878	919
23:00	150	100	23.1	23.1	22.6	22.6	23.4	23.4	42	42	234	239	-26	-31	826	882
	5390	**3880**	-	-	-	-	-	-	**2096**	2199	**7169**	7072	**0**	-1	**9270**	9269
	9270															

15 Appendix D: Pipe Details and Circuit Diagrams

Appendix D-1: Technical Details of Pexal Multilayer Pipe (Valsir-Uneeq, 2013)

Description	Value	Unit
External Diameter	20	mm
Total thickness	2.5	mm
Coil length	100 – 600	m
Water volume content	0.176	l/m
Operating temperature	0-80	°C
Maximum operating temperature	95	°C
Maximum operating pressure (temp 95°C)	10	bar
Coefficient of heat expansion	0.026	mm/mK
Internal heat conductivity	0.43	W/mK
Internal roughness	0.007	mm
Oxygen diffusion	0.000	mg/l
Bending radius without a pipe bender	100	mm
Bending radius with a pipe bender	80	mm
Colour	White (9003)	RAL

Appendix D-2: Pipe Details and Circuit Diagrams

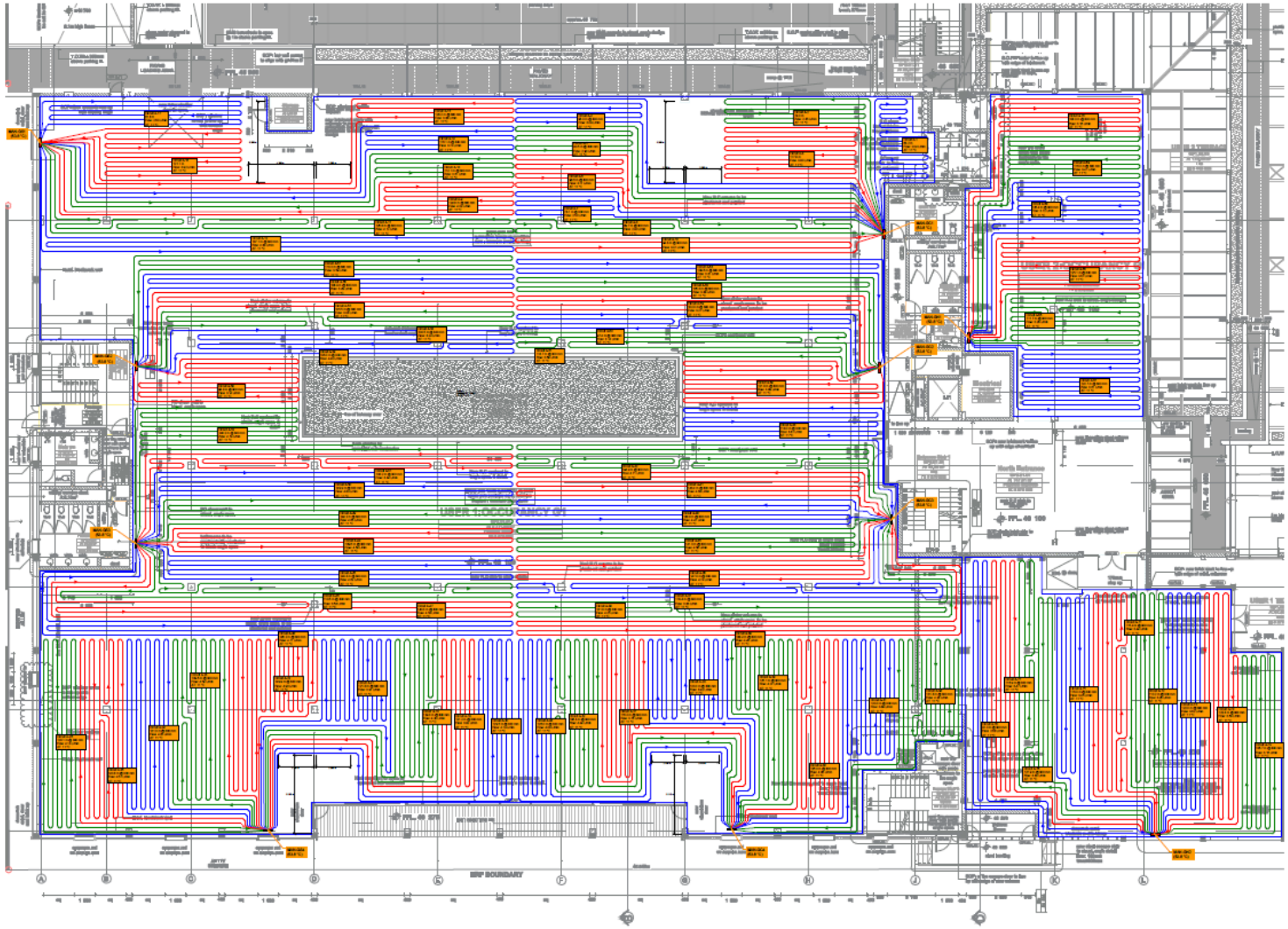

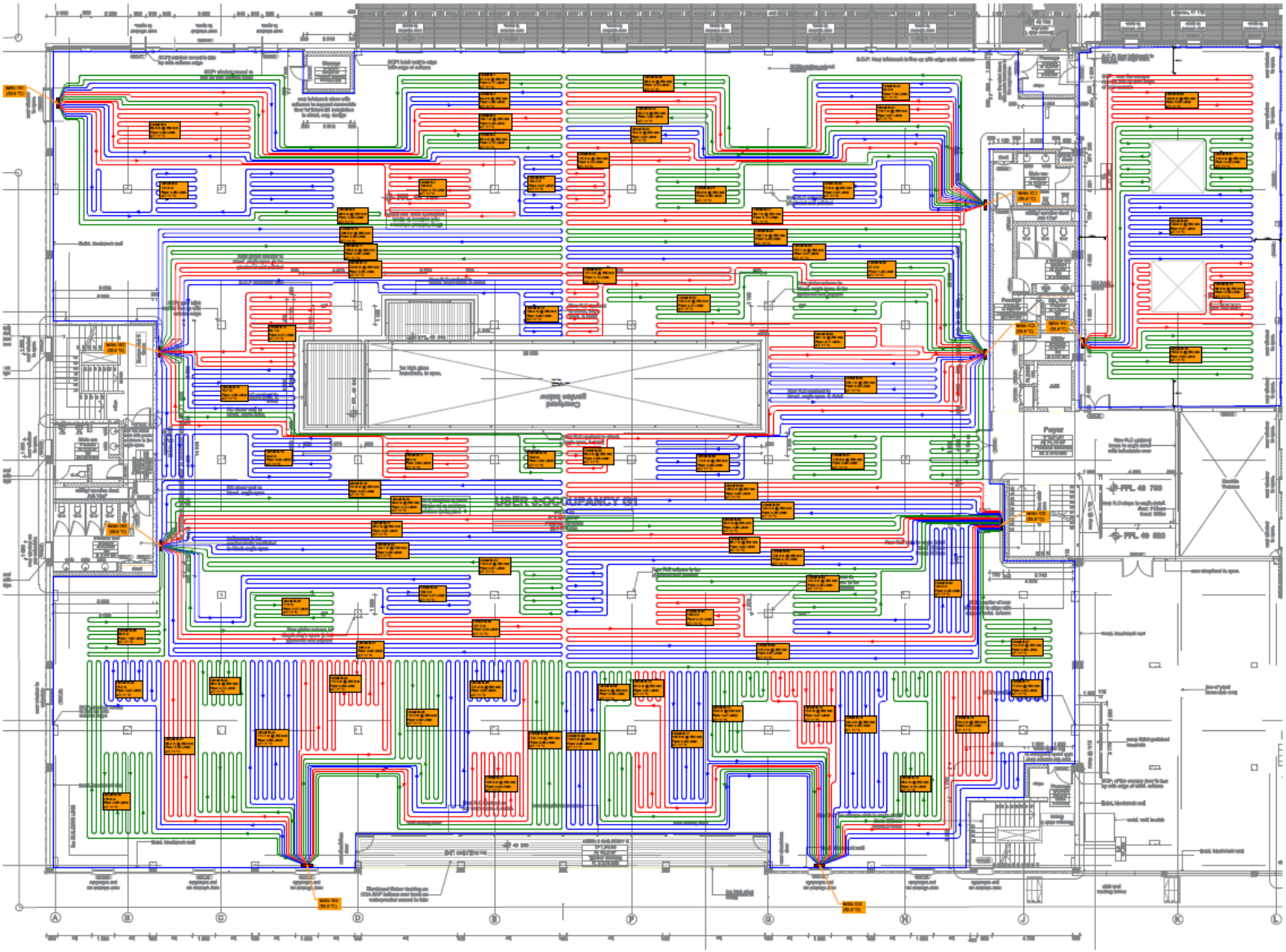
USER 3:OCCUPANCY 01

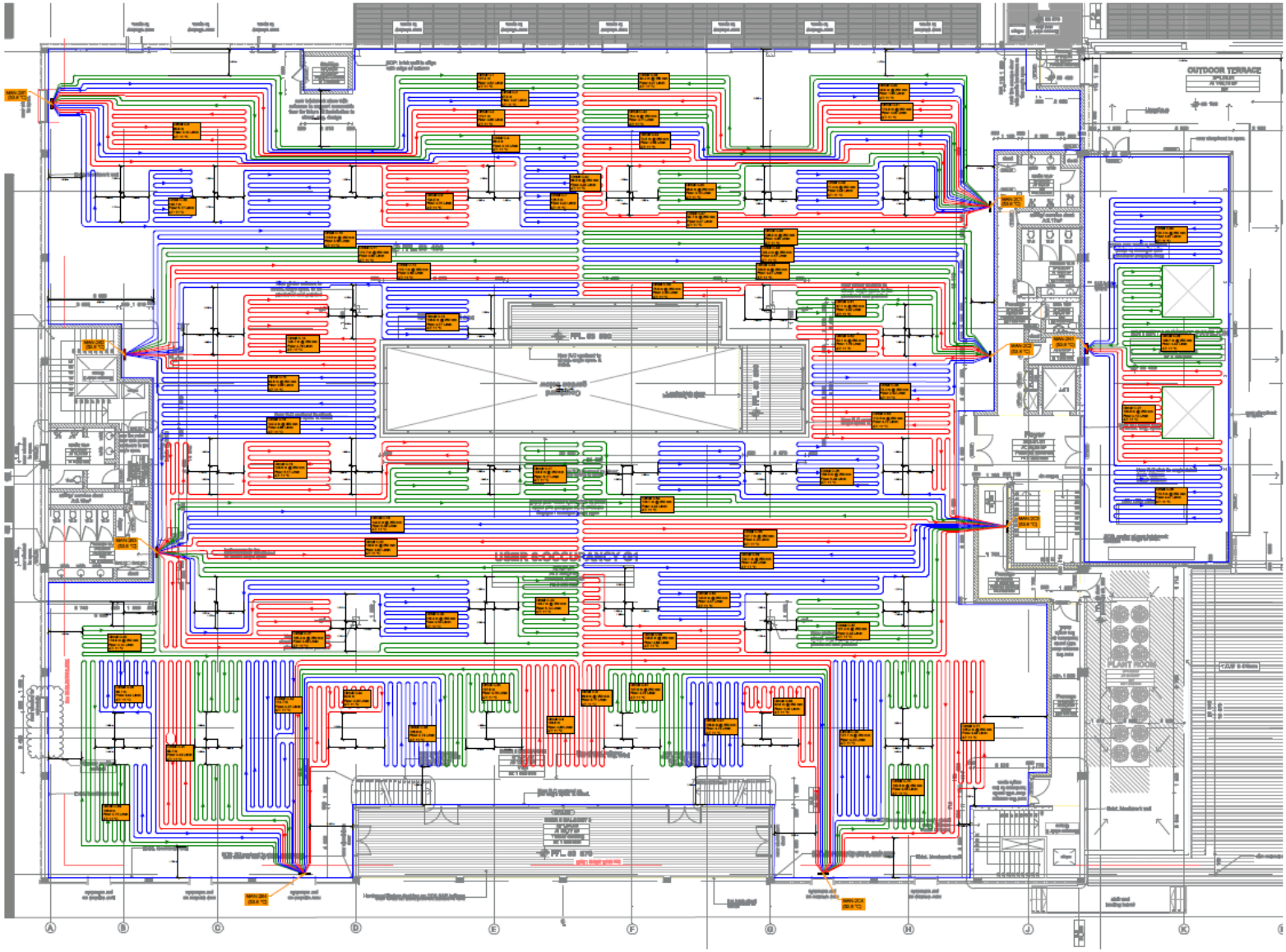
OUTDOOR TERRACE
PLANT ROOM

16 Appendix E: Heat Pump Specifications

Specification for NECS-N/CA 2416

Power supply		V/ph/Hz	400/3/50
PERFORMANCE			
COOLING ONLY (GROSS VALUE)			
Cooling capacity	(1)	kW	625
Total power input	(1)	kW	215
EER	(1)	kW/kW	2.91
ESEER	(1)	kW/kW	4.09
COOLING ONLY (EN14511 VALUE)			
Cooling capacity	(1)(2)	kW	622
EER	(1)(2)	kW/kW	2.87
ESEER	(1)(2)	kW/kW	3.92
Cooling energy class			C
HEATING ONLY (GROSS VALUE)			
Total heating capacity	(3)	kW	674
Total power input	(3)	kW	210
COP	(3)	kW/kW	3.21
HEATING ONLY (EN14511 VALUE)			
Total heating capacity	(3)(2)	kW	676
COP	(3)(2)	kW/kW	3.18
Cooling energy class			B
SEASONAL EFFICIENCY IN HEATING (EN14825 VALUE)			
PDesign	(4)	kW	-
SCOP	(4)		-
Performance ηs (Reg. 811/2013 UE)	(4)	%	-
Seasonal efficiency class (Regulation (UE) 811/2013)	(4)		-
EXCHANGERS			
HEAT EXCHANGER USER SIDE IN REFRIGERATION			
Water flow	(1)	m³/h	108
Pressure drop	(1)	kPa	47.4
HEAT EXCHANGER USER SIDE IN HEATING			
Water flow	(3)	m³/h	117
Pressure drop	(3)	kPa	56.2
COMPRESSORS			
Compressors nr.		N°	6
No. Circuits		N°	3
NOISE LEVEL			
Noise Pressure	(5)	dB(A)	78
Sound power level in cooling	(6)(7)	dB(A)	99
Sound power level in heating	(6)(8)	dB(A)	0
SIZE AND WEIGHT			
Operating weight	(9)	kg	5400
A	(9)	mm	7430
B	(9)	mm	2260
H	(9)	mm	2450

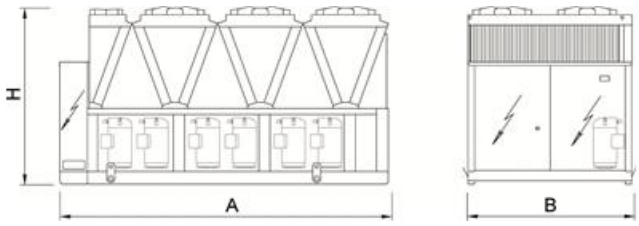

Notes:

1. Plant (side) cooling exchanger water (in/out) 12°C/7°C; Source (side) heat exchanger air (in) 35°C.
2. Values in compliance with EN14511-3:2013.
3. Plant (side) heat exchanger water (in/out) 40°C/45°C; Source (side) heat exchanger air (in) 7°C - 87% R.H.
4. Seasonal space heating energy efficiency class LOW TEMPERATURE in AVERAGE climate conditions [REGULATION (UE) N. 811/2013]
5. Average sound pressure level at 1m distance, unit in a free field on a reflective surface; non-binding value calculated from the sound power level.
6. Sound power on the basis of measurements made in compliance with ISO 9614.
7. Sound power level in cooling, outdoors.
8. Sound power level in heating, outdoors.
9. Unit in standard configuration/execution, without optional accessories.

17 Appendix F: Results of the Case Study of Office Building with TABS

	Oct-20			Nov-20		
Time	**Average of Actual Chiller Demand [kW]**	**Average of Simulated Chiller Demand [kW]**	**Diff**	**Average of Actual Chiller Demand [kW]**	**Average of Simulated Chiller Demand [kW]**	**Diff**
00:00	0.90	0.00	0.90	0.85	0.00	0.85
01:00	0.90	0.00	0.90	0.85	0.00	0.85
02:00	11.76	15.29	-3.53	13.05	25.74	-12.70
03:00	20.26	15.29	4.96	19.83	25.74	-5.91
04:00	21.88	15.29	6.59	20.65	25.74	-5.09
05:00	22.17	15.29	6.88	21.94	25.74	-3.80
06:00	11.23	0.00	11.23	11.34	0.00	11.34
07:00	0.89	0.00	0.89	0.84	0.00	0.84
08:00	0.88	0.00	0.88	0.83	0.00	0.83
09:00	0.88	0.00	0.88	0.84	0.00	0.84
10:00	10.37	15.35	-4.98	16.89	25.94	-9.05
11:00	17.52	15.39	2.13	29.23	26.02	3.21
12:00	16.98	15.41	1.57	32.81	26.06	6.75
13:00	18.54	15.43	3.11	33.93	26.09	7.83
14:00	18.27	15.44	2.83	34.72	26.11	8.60
15:00	18.61	15.43	3.18	33.79	26.12	7.67
16:00	19.18	15.41	3.78	32.64	26.08	6.56
17:00	19.31	0.00	19.31	31.54	0.00	31.54
18:00	10.37	0.00	10.37	14.51	0.00	14.51
19:00	0.89	0.00	0.89	0.84	0.00	0.84
20:00	9.26	0.00	9.26	11.38	0.00	11.38
21:00	0.93	0.00	0.93	0.85	0.00	0.85
22:00	0.90	0.00	0.90	0.84	0.00	0.84
23:00	0.90	0.00	0.90	0.84	0.00	0.84

	Dec-20			Jan-21		
Time	**Average of Actual Chiller Demand [kW]**	**Average of Simulated Chiller Demand [kW]**	**Diff**	**Average of Actual Chiller Demand [kW]**	**Average of Simulated Chiller Demand [kW]**	**Diff**
00:00	0.84	0.00	0.84	0.83	0.00	0.83
01:00	0.84	0.00	0.84	0.83	0.00	0.83
02:00	14.09	31.01	-16.93	9.48	58.11	-48.63
03:00	21.24	31.01	-9.77	12.98	58.11	-45.13
04:00	23.03	31.01	-7.98	14.06	58.11	-44.05
05:00	23.01	31.01	-8.01	13.35	58.11	-44.76
06:00	11.44	0.00	11.44	31.51	0.00	31.51
07:00	0.84	0.00	0.84	35.67	0.00	35.67
08:00	0.83	0.00	0.83	38.05	0.00	38.05
09:00	0.83	0.00	0.83	40.26	0.00	40.26
10:00	17.06	31.32	-14.25	47.82	59.26	-11.44
11:00	29.93	31.40	-1.48	55.22	59.55	-4.33
12:00	33.58	31.48	2.10	56.86	59.74	-2.88
13:00	35.41	31.52	3.89	54.37	59.85	-5.48
14:00	34.61	31.54	3.07	58.33	59.87	-1.53
15:00	35.33	31.54	3.78	60.97	59.81	1.17
16:00	32.32	31.48	0.84	62.94	59.73	3.21
17:00	32.32	0.00	32.32	58.50	0.00	58.50
18:00	15.41	0.00	15.41	24.86	0.00	24.86
19:00	0.84	0.00	0.84	0.82	0.00	0.82
20:00	12.80	0.00	12.80	7.31	0.00	7.31
21:00	0.84	0.00	0.84	0.82	0.00	0.82
22:00	0.84	0.00	0.84	0.82	0.00	0.82
23:00	0.84	0.00	0.84	0.82	0.00	0.82

	Feb-21			Mar-21		
Time	**Average of Actual Chiller Demand [kW]**	**Average of Simulated Chiller Demand [kW]**	**Diff**	**Average of Actual Chiller Demand [kW]**	**Average of Simulated Chiller Demand [kW]**	**Diff**
00:00	0.73	0.00	0.73	0.73	0.00	0.73
01:00	0.73	0.00	0.73	0.73	0.00	0.73
02:00	11.07	58.05	-46.98	17.64	29.63	-11.99
03:00	20.68	58.05	-37.37	26.74	29.63	-2.89
04:00	22.58	58.05	-35.46	26.58	29.63	-3.05
05:00	22.25	58.05	-35.80	27.13	29.63	-2.50
06:00	24.99	0.00	24.99	12.21	0.00	12.21
07:00	24.41	0.00	24.41	0.72	0.00	0.72
08:00	24.96	0.00	24.96	0.72	0.00	0.72
09:00	25.92	0.00	25.92	0.72	0.00	0.72
10:00	44.94	59.24	-14.30	22.55	29.85	-7.30
11:00	58.24	59.43	-1.19	35.23	29.91	5.33
12:00	60.17	59.56	0.61	37.13	30.01	7.12
13:00	61.11	59.70	1.41	39.68	30.09	9.59
14:00	62.02	59.82	2.20	41.68	30.14	11.54
15:00	61.73	59.81	1.92	40.89	30.15	10.73
16:00	60.19	59.71	0.48	39.77	30.09	9.68
17:00	39.26	0.00	39.26	18.22	0.00	18.22
18:00	11.48	0.00	11.48	0.72	0.00	0.72
19:00	0.73	0.00	0.73	0.73	0.00	0.73
20:00	25.37	0.00	25.37	36.25	0.00	36.25
21:00	0.73	0.00	0.73	0.73	0.00	0.73
22:00	0.73	0.00	0.73	0.73	0.00	0.73
23:00	0.73	0.00	0.73	0.73	0.00	0.73

	Apr-21			May-21		
Time	**Average of Actual Chiller Demand [kW]**	**Average of Simulated Chiller Demand [kW]**	**Diff**	**Average of Actual Chiller Demand [kW]**	**Average of Simulated Chiller Demand [kW]**	**Diff**
00:00	0.73	0.00	0.73	0.74	0.00	0.74
01:00	0.73	0.00	0.73	0.74	0.00	0.74
02:00	6.44	19.99	-13.55	7.44	12.42	-4.98
03:00	11.69	19.99	-8.29	7.89	12.42	-4.53
04:00	10.88	19.99	-9.11	9.03	12.42	-3.39
05:00	11.28	19.99	-8.71	8.37	12.42	-4.05
06:00	6.32	0.00	6.32	4.74	0.00	4.74
07:00	0.73	0.00	0.73	0.73	0.00	0.73
08:00	0.72	0.00	0.72	0.73	0.00	0.73
09:00	0.72	0.00	0.72	0.72	0.00	0.72
10:00	14.47	20.09	-5.62	10.05	12.47	-2.43
11:00	23.40	20.09	3.32	15.38	12.46	2.91
12:00	26.15	20.14	6.01	15.13	12.47	2.66
13:00	27.55	20.19	7.37	17.25	12.48	4.77
14:00	28.25	20.19	8.06	18.69	12.48	6.21
15:00	27.98	20.18	7.80	18.73	12.48	6.25
16:00	27.26	20.15	7.11	18.53	12.47	6.06
17:00	12.20	0.00	12.20	9.53	0.00	9.53
18:00	0.73	0.00	0.73	0.73	0.00	0.73
19:00	0.73	0.00	0.73	0.73	0.00	0.73
20:00	23.82	0.00	23.82	17.19	0.00	17.19
21:00	0.74	0.00	0.74	0.81	0.00	0.81
22:00	0.73	0.00	0.73	0.74	0.00	0.74
23:00	0.73	0.00	0.73	0.74	0.00	0.74

	Jun-21		
Time	**Average of Actual Chiller Demand [kW]**	**Average of Simulated Chiller Demand [kW]**	**Diff**
00:00	0.77	0.00	0.77
01:00	0.77	0.00	0.77
02:00	10.80	15.75	-4.96
03:00	11.91	15.75	-3.84
04:00	11.20	15.75	-4.55
05:00	11.01	15.75	-4.75
06:00	5.75	0.00	5.75
07:00	0.76	0.00	0.76
08:00	0.76	0.00	0.76
09:00	0.76	0.00	0.76
10:00	12.45	15.82	-3.37
11:00	16.09	15.82	0.27
12:00	14.96	15.83	-0.87
13:00	13.45	15.85	-2.40
14:00	12.36	15.86	-3.50
15:00	12.73	15.86	-3.12
16:00	12.51	15.85	-3.33
17:00	7.07	0.00	7.07
18:00	1.06	0.00	1.06
19:00	1.06	0.00	1.06
20:00	10.94	0.00	10.94
21:00	0.84	0.00	0.84
22:00	0.77	0.00	0.77
23:00	0.77	0.00	0.77

18 Appendix G: Results of the Case Study of the Conventional HVAC System

	Jan			Feb		
Time	**Average of Actual Chiller Demand [kW]**	**Average of Simulated Chiller Demand [kW]**	**Diff**	**Average of Actual Chiller Demand [kW]**	**Average of Simulated Chiller Demand [kW]**	**Diff**
00:00	0.04	0.00	0.04	4.09	0.00	4.09
01:00	0.04	0.00	0.04	3.11	0.00	3.11
02:00	0.04	0.00	0.04	3.06	0.00	3.06
03:00	0.04	0.00	0.04	2.83	0.00	2.83
04:00	0.04	0.00	0.04	2.74	0.00	2.74
05:00	0.04	0.00	0.04	2.61	0.00	2.61
06:00	100.88	68.60	32.28	79.82	52.79	27.03
07:00	109.96	75.50	34.47	76.99	59.22	17.78
08:00	103.35	82.81	20.53	71.25	63.98	7.28
09:00	110.17	97.26	12.91	81.74	69.14	12.61
10:00	111.73	111.07	0.66	85.93	76.74	9.19
11:00	124.90	119.93	4.97	88.59	82.66	5.93
12:00	119.46	127.84	-8.37	91.04	87.25	3.79
13:00	126.31	132.17	-5.86	95.17	89.99	5.17
14:00	129.67	135.31	-5.64	97.71	91.64	6.07
15:00	124.70	138.23	-13.52	97.05	92.57	4.48
16:00	128.09	138.59	-10.50	97.73	93.38	4.36
17:00	118.36	138.58	-20.23	89.74	91.73	-1.99
18:00	79.89	100.23	-20.34	65.33	61.69	3.64
19:00	0.19	0.00	0.19	4.24	0.00	4.24
20:00	0.48	0.00	0.48	4.74	0.00	4.74
21:00	0.05	0.00	0.05	4.76	0.00	4.76
22:00	0.05	0.00	0.05	4.26	0.00	4.26
23:00	0.05	0.00	0.05	4.06	0.00	4.06

	Mar			Apr		
Time	**Average of Actual Chiller Demand [kW]**	**Average of Simulated Chiller Demand [kW]**	**Diff**	**Average of Actual Chiller Demand [kW]**	**Average of Simulated Chiller Demand [kW]**	**Diff**
00:00	0.02	0.00	0.02	0.04	0.00	0.04
01:00	0.02	0.00	0.02	0.04	0.00	0.04
02:00	0.02	0.00	0.02	0.04	0.00	0.04
03:00	0.02	0.00	0.02	0.04	0.00	0.04
04:00	0.02	0.00	0.02	0.04	0.00	0.04
05:00	0.02	0.00	0.02	0.04	0.00	0.04
06:00	52.22	31.15	21.08	38.30	19.64	18.66
07:00	50.79	33.19	17.59	36.91	22.92	13.99
08:00	44.04	36.77	7.27	33.87	31.85	2.02
09:00	51.04	39.44	11.60	38.31	37.72	0.59
10:00	55.25	42.96	12.29	42.39	42.01	0.38
11:00	58.83	46.76	12.07	45.64	46.90	-1.26
12:00	62.93	50.15	12.78	50.93	49.90	1.03
13:00	63.61	53.92	9.69	52.87	51.40	1.47
14:00	65.41	55.77	9.64	54.15	52.93	1.23
15:00	63.90	57.11	6.80	54.89	54.34	0.54
16:00	60.32	57.99	2.33	54.93	54.02	0.91
17:00	57.33	49.65	7.68	48.92	43.86	5.06
18:00	40.41	37.59	2.82	30.30	34.72	-4.42
19:00	0.02	0.00	0.02	0.03	0.00	0.03
20:00	0.02	0.00	0.02	0.04	0.00	0.04
21:00	0.02	0.00	0.02	0.04	0.00	0.04
22:00	0.02	0.00	0.02	0.04	0.00	0.04
23:00	0.02	0.00	0.02	0.04	0.00	0.04

	May			Jun		
Time	**Average of Actual Chiller Demand [kW]**	**Average of Simulated Chiller Demand [kW]**	**Diff**	**Average of Actual Chiller Demand [kW]**	**Average of Simulated Chiller Demand [kW]**	**Diff**
00:00	0.04	0.00	0.04	0.04	0.00	0.04
01:00	0.04	0.00	0.04	0.04	0.00	0.04
02:00	0.03	0.00	0.03	0.03	0.00	0.03
03:00	0.04	0.00	0.04	0.04	0.00	0.04
04:00	0.03	0.00	0.03	0.03	0.00	0.03
05:00	0.04	0.00	0.04	0.04	0.00	0.04
06:00	20.27	8.68	11.59	8.18	11.35	-3.16
07:00	24.72	9.83	14.88	28.01	13.06	14.94
08:00	24.00	14.25	9.75	20.96	14.26	6.70
09:00	27.11	25.31	1.80	23.36	20.85	2.50
10:00	29.01	33.60	-4.58	26.39	30.37	-3.98
11:00	30.16	37.53	-7.36	27.60	34.74	-7.14
12:00	30.78	40.41	-9.63	28.33	37.42	-9.09
13:00	36.83	41.58	-4.75	28.79	40.15	-11.36
14:00	35.49	43.58	-8.09	30.21	40.90	-10.69
15:00	35.06	44.68	-9.62	29.63	42.50	-12.86
16:00	34.74	44.12	-9.38	29.58	42.16	-12.58
17:00	32.84	36.58	-3.74	28.06	35.81	-7.75
18:00	20.26	24.16	-3.89	17.48	23.32	-5.84
19:00	0.02	0.00	0.02	0.02	0.00	0.02
20:00	0.03	0.00	0.03	0.04	0.00	0.04
21:00	0.04	0.00	0.04	0.04	0.00	0.04
22:00	0.04	0.00	0.04	0.04	0.00	0.04
23:00	0.04	0.00	0.04	0.04	0.00	0.04

	Jul			Aug		
Time	**Average of Actual Chiller Demand [kW]**	**Average of Simulated Chiller Demand [kW]**	**Diff**	**Average of Actual Chiller Demand [kW]**	**Average of Simulated Chiller Demand [kW]**	**Diff**
00:00	0.04	0.00	0.04	0.04	0.00	0.04
01:00	0.04	0.00	0.04	0.04	0.00	0.04
02:00	0.03	0.00	0.03	0.03	0.00	0.03
03:00	0.03	0.00	0.03	0.03	0.00	0.03
04:00	0.03	0.00	0.03	0.03	0.00	0.03
05:00	0.04	0.00	0.04	0.04	0.00	0.04
06:00	7.35	3.44	3.91	5.33	1.47	3.86
07:00	32.32	2.90	29.41	24.13	1.41	22.73
08:00	18.21	4.90	13.31	12.54	3.30	9.24
09:00	19.79	11.06	8.73	17.27	8.98	8.28
10:00	22.35	22.33	0.02	19.01	17.18	1.83
11:00	23.94	29.22	-5.29	19.62	20.17	-0.55
12:00	28.46	30.98	-2.51	20.59	23.67	-3.07
13:00	26.46	33.21	-6.75	21.36	25.10	-3.74
14:00	26.51	35.85	-9.34	22.83	25.55	-2.72
15:00	27.02	36.49	-9.46	22.93	25.21	-2.28
16:00	28.19	35.55	-7.36	23.96	25.09	-1.13
17:00	26.05	28.51	-2.46	20.06	20.12	-0.06
18:00	14.98	17.07	-2.10	13.75	11.88	1.87
19:00	0.03	0.00	0.03	0.03	0.00	0.03
20:00	0.04	0.00	0.04	0.04	0.00	0.04
21:00	0.04	0.00	0.04	0.04	0.00	0.04
22:00	0.04	0.00	0.04	0.04	0.00	0.04
23:00	0.04	0.00	0.04	0.04	0.00	0.04

	Sep			Oct		
Time	**Average of Actual Chiller Demand [kW]**	**Average of Simulated Chiller Demand [kW]**	**Diff**	**Average of Actual Chiller Demand [kW]**	**Average of Simulated Chiller Demand [kW]**	**Diff**
00:00	0.03	0.00	0.03	0.04	0.00	0.04
01:00	0.03	0.00	0.03	0.03	0.00	0.03
02:00	0.03	0.00	0.03	0.03	0.00	0.03
03:00	0.03	0.00	0.03	0.03	0.00	0.03
04:00	0.02	0.00	0.02	0.03	0.00	0.03
05:00	0.04	0.00	0.04	0.06	0.00	0.06
06:00	7.07	1.56	5.51	9.11	12.74	-3.63
07:00	33.54	1.59	31.95	31.55	21.01	10.54
08:00	21.45	11.18	10.27	28.13	30.05	-1.92
09:00	25.70	21.86	3.84	29.80	33.67	-3.88
10:00	27.11	25.29	1.81	32.30	35.73	-3.43
11:00	28.42	28.46	-0.04	34.21	37.17	-2.96
12:00	31.22	31.23	-0.01	35.11	38.74	-3.63
13:00	30.06	30.99	-0.93	36.42	40.10	-3.68
14:00	29.98	31.54	-1.56	37.38	40.99	-3.61
15:00	30.96	33.26	-2.30	37.99	41.39	-3.40
16:00	30.15	32.07	-1.92	36.92	42.05	-5.13
17:00	28.73	25.91	2.81	34.05	38.10	-4.05
18:00	16.87	17.15	-0.28	23.00	32.29	-9.29
19:00	0.01	0.00	0.01	0.03	0.00	0.03
20:00	0.02	0.00	0.02	0.03	0.00	0.03
21:00	0.03	0.00	0.03	0.04	0.00	0.04
22:00	0.03	0.00	0.03	0.03	0.00	0.03
23:00	0.03	0.00	0.03	0.04	0.00	0.04

	Nov			Dec		
Time	**Average of Actual Chiller Demand [kW]**	**Average of Simulated Chiller Demand [kW]**	**Diff**	**Average of Actual Chiller Demand [kW]**	**Average of Simulated Chiller Demand [kW]**	**Diff**
00:00	0.04	0.00	0.04	0.04	0.00	0.04
01:00	0.04	0.00	0.04	0.03	0.00	0.03
02:00	0.04	0.00	0.04	0.03	0.00	0.03
03:00	0.04	0.00	0.04	0.03	0.00	0.03
04:00	0.04	0.00	0.04	0.03	0.00	0.03
05:00	0.04	0.00	0.04	0.03	0.00	0.03
06:00	27.86	45.33	-17.46	46.13	60.70	-14.57
07:00	39.57	53.84	-14.28	66.51	63.71	2.80
08:00	37.99	56.85	-18.86	65.00	65.35	-0.35
09:00	42.64	58.27	-15.63	71.28	67.72	3.57
10:00	45.68	59.51	-13.83	76.60	71.71	4.89
11:00	49.27	61.15	-11.88	82.08	76.06	6.02
12:00	51.91	61.62	-9.72	84.65	80.64	4.01
13:00	54.69	61.33	-6.63	85.94	83.20	2.74
14:00	57.04	62.65	-5.62	86.74	87.69	-0.94
15:00	58.06	64.58	-6.53	84.48	90.56	-6.08
16:00	56.05	64.12	-8.07	78.38	93.98	-15.60
17:00	51.83	60.47	-8.64	78.87	92.08	-13.21
18:00	45.38	56.61	-11.24	68.16	76.79	-8.63
19:00	0.03	0.00	0.03	0.04	0.00	0.04
20:00	0.04	0.00	0.04	0.04	0.00	0.04
21:00	0.04	0.00	0.04	0.04	0.00	0.04
22:00	0.04	0.00	0.04	0.05	0.00	0.05
23:00	0.04	0.00	0.04	0.04	0.00	0.04